ABSTRACT

Title of thesis: EVALUATION OF THERMAL IMAGING CAMERA SPOT TEMPERATURE MEASUREMENTS IN STRUCTURE FIRES

Julie Bryant
Masters of Science, 2019

Thesis directed by: Dr. James A Milke
Department of Fire Protection Engineering

Fire service thermal imaging cameras (TICs) are utilized to provide an image of the environment when visibility is limited or impaired by absorbing infrared radiation (IR) emitted from solid objects within its field of view (FOV). This image is often accompanied by a temperature output that may mislead firefighters who do not have proper training of the limitations associated with such quantitative measurements.

An evaluation of TIC spot temperature measurements was conducted to determine the TICs ability to quantify thermal hazards within an ambient and smoke-filled fire environment. During ambient conditions spot temperature measurements are a function of focal length. During fire experiments participating media (i.e., smoke) impact the IR received by TICs therefore affecting the temperature outputs. This research explores the impact of participating media on solid object temperature measurements from fire service TICs.

EVALUATION OF THERMAL IMAGING CAMERA SPOT TEMPERATURE MEASUREMENTS IN STRUCTURE FIRES

by

Julie Bryant

Thesis submitted to the Faculty of the Graduate School of the
University of Maryland, College Park in partial fulfillment
of the requirements for the degree of
Masters of Science
2019

Advisory Committee:
Dr. James A Milke, Chair/Advisor
Dr. Michael Gollner, Professor/Defense Committee
Dr. Daniel Madrzykowski, UL FSRI/Defense Committee

Acknowledgments

I owe my gratitude to all the people who have made this thesis possible and because of whom my graduate experience has been one that I will cherish forever.

First and foremost I'd like to thank Dr. James A Milke, my departmental advisor, for your support during both my undergraduate and graduate careers.

I would also like to thank Robin Zevotek, my UL FSRI advisor, for your guidance through this process and for answering my questions about Python and LaTeX.

All of my colleagues both at the University of Maryland and UL FSRI, for your encouragement and companionship.

I would also like to acknowledge the never endless support from Nicole Hollywood, my undergraduate academic advisor and dear friend.

I owe my deepest thanks to my mother and father.

I would like to acknowledge UL FSRI for financial support, without this fellowship I would not have had the opportunity to further my education.

It is impossible to remember all, and I apologize to those I've inadvertently left out.

Table of Contents

List of Tables

List of Figures

List of Abbreviations

ACH	Air changes per hour
AFG	Assistance to Firefighters Grant
ANSI	American National Standards Institute
ARFF	Aircraft rescue and fire fighting (applications)
ASTM	American Section of the International Association for Testing Materials
CECOM	Communications - Electronics Command
CV	Coefficient of variation
DARPA	Defense Advanced Research Projects Agency
DelCo	Delaware County Emergency Services Training Center
DHS	U.S Department of Homeland Security
EM	Electromagnetic
Exp.	Experiment
FEMA	Federal Emergency Management Agency
FOV	Field of view
FPA	Focal plane array
FSRI	UL Firefighter Safety Research Institute
IDLH	Immediately dangerous to life and health
IFSI	Illinois Fire Service Institute
IR	Infrared radiation
ISFSI	International Society of Fire Service Instructors
IR	Infrared
LWIR	Long-wavelength infrared radiation
NETD	Noise equivalent temperature difference
NFPA	National Fire Protection Association
NIOSH	The National Institute for Occupational Safety and Health
NIST	National Institute Standards and Technology
OCR	Optical character recognition
PD	Percent difference
RIC	Rapid intervention crew
ROIC	Read-out integrated circuit
SCBA	Self-contained breathing apparatus
TC(s)	Thermocouple(s)
TCR	Temperature coefficient of resistance
TI(s)	Thermal imager(s)
TIC(s)	Thermal imaging camera(s)
UL	Underwriters Laboratories

List of Symbols

α	Spectral Absorbance
τ	Spectral Tranmitance
ρ	Spectral Reflectance
M	Excitance $[\frac{\mathrm{W}}{\mathrm{m}^2}]$
σ	Stefan Boltzmann Constant $[\frac{\mathrm{W}}{\mathrm{m}^2\mathrm{K}^4}]$
T	Temperature [K]
E	Electromagnetic Radiation $[\frac{\mathrm{J}}{\mathrm{m}^2\mathrm{s}}]$
ω	Relative Humidity [%]
d	Distance [m]
ϵ	Emissivity
c	Thermal Capacity $[\frac{\mathrm{J}}{\mathrm{K}}]$
t	Time [s]
I	Biased Current [A]
V	Biased Voltage [V]
P	Radiation [W]
g	Thermal Conductance $[\frac{\mathrm{W}}{\mathrm{K}}]$
A	Area $[\mathrm{m}^2]$

List of Subscripts

λ	Wavelength
tot	Total
obj	Object
refl	Reflectance
atm	Atmosphere
t	Target Source
s	Surroundings

Definition List

Accuracy

: A measurement of trueness or a degree of closeness between the measurement and known true value, including a description of systematic errors.

: Also referred to as bias, or an amount of inaccuracy.

Ambient

: Conditions similar to air at standard temperature (273 K) and pressure (101 kPa) without the presence of combustion products.

Error

: An evaluation of the execution of a statistical experiment design, further defined into three types: human, systematic, and random.

Nonparticipating Medium

: A transparent material or substances predominately in a gaseous state containing symmetric molecules that emit or absorb negligible amounts of radiation. Examples include vacuums or air at ambient conditions.

Participating Medium

: A material or substance predominately in a gaseous state containing aerosolized particulates of non symmetrical molecules that can emit, absorb, and/or scattering radiation.

Precision

: Refinement within a measurement, representing the closeness between measurements, including a description of random errors.

: Also referred to as variability, or an amount of imprecision.

Repeatability

: A component of precision expressing the variation between measurements. A measure of agreement of measurements on replicate specimens by the same methodology carried out with a single instrument or person.

Reproducibility

: A component of precision expressing whether a measurement or test method can be reproduced. A measure of closeness of the agreement between results of measurements of the same measurand carried out with the same methodology by differing instruments or people.

Smoke

A medium composed of a combination of solid, liquid, and gaseous particulates produced when a material undergoes pyrolysis or combustion, along with a quantity of air entrained or otherwise mixed into the medium.

Thermal Imager (TI)

An instrument that renders a thermogram of an environment by detecting infrared radiant energy emitted, transmitted, or reflected within environment.

Thermal Imaging Camera (TIC)

An instrument that renders and records a thermogram of an environment by detecting infrared radiant energy emitted, transmitted, or reflected within environment.

Thermogram

A visual record of the infrared radiant energy present within an environment.

Uncertainty

A quantitative measurement of precision and accuracy representing a range of possible values within which the true value of the measurement lies.

Chapter 1: Introduction

The history surrounding thermal imaging technology dates back to the 19th century when William Herschel first discovered what he called "calorific rays" of light. These invisible rays are now known as infrared wavelengths of light and are the basis of thermal imaging technology [1]. The development of the first thermal imager (TI) in the 1970's was contributed to a combination of various scientific developments occurring across multiple centuries. This TI was intended for use in limited visibility combat situations by militaries [2]. Since the declassification of thermal imaging technology in the 1990's, TIs have been incorporated into various civilian occupations such as medical research, private security, and firefighting [2,3].

Fire service TIs typically provide three pieces of vital information to firefighters. The first piece is to provide a working image of an environment during low visibility. Smoke, a medium composed of gaseous, liquid, and solid particulates produced during pyrolysis or combustion, lowers the ambient light levels within an environment. When low light prohibits the human eye from perceiving information, the working image rendered by a TI allows firefighters to distinguish between floors and walls while interpreting environment details. The working image allows firefighters the ability to theoretically 'see through smoke' [4].

The second piece is to provide a thermal observation of the environment. TIs depict thermal contrasts, heat signatures, and convective flows resulting from the production of smoke. The working image presents this information as a change in contrast or by false coloring the image. This information allows firefighters to use a TIC for search and rescue of victims, investigate hidden fire located within walls and / or ceilings, and monitor the environment for unsafe conditions.

The final piece is a thermal quantification of the environment. TIC spot temperature measurements are determined by the amount of radiant energy present within an environment. This apparent temperature allows firefighters to quantify the heat associated with an enclosure fire and infer the perceived danger resulting from such temperatures. Although NFPA produces two standards regarding TI, NFPA 1408 and NFPA 1801, neither specifies a requirement for spot temperature measurements at non-ambient conditions. Ambient conditions mimic environmental air at standard temperature (273 K) and pressure (101 kPa) without the presence of smoke.

The TIC has proven to be a versatile tool to the modern firefighter, aiding firefighters on fire grounds, during hazardous materials incidents, and during motor vehicle collisions and electrical emergencies. On a fire ground the TIC has been used in scene size-up, interior / exterior suppression, search and rescue, ventilation, over-haul, and rapid intervention crew (RIC) operations [5].

The National Institute for Occupational Safety and Health (NIOSH) first suggested exploring the use of thermal imaging cameras (TICs) during search and rescue operations during their investigation of the 1999 Cold-Storage and Warehouse Build-

ing Fire in Worcester, Massachusetts [6]. Since then, NIOSH has often incorporated TIC use, value, and limitations into their Fire Fighter Fatality Investigation and Prevention recommendations [7–10]. A 2014 investigation report, recommends TIC use during firefighting operations to accomplish the primary mission of saving lives. It also recommends that personnel be properly trained in TIC use and understand limitations [9]. A 2015 investigation report, expands on TIC limitations by warning readers of the misconception that TIC temperature measurements estimate air temperatures [10].

Underwriters Laboratories (UL), has utilized TICs determine surface temperatures of floors and ceilings [11] and to document thermal conditions within otherwise visually obscured environments [12]. TICs provide both a quantification of thermal energy, an image of the environment's configuration and hazards (furnishings and / or obstacles), and a distinction between the hot and cool gas layers. TICs continue to provide such information when ambient light levels are to low for the human eye to perceive information [12].

1.1 Problem Statement

While the benefits of TIC use during firefighting operations is well documented, limitations of such devices have not fully been investigated in realistic fire conditions. This report aims to quantify the TIC's ability to represent hazards within an environment affected by heat, smoke, and flames. To establish the limitations of this study, a preliminary evaluation comparing TIC spot temperature measure-

ments to TC measurements was conducted utilizing data from two UL FSRI investigations [12,13]. The information and conclusions from this preliminary evaluation were incorporated into a new series of experiments that explored TIC spot temperature measurements in both an ambient and combustion environments. Data was collected and is presented to further the understanding of spot temperature measurements in realistic smoke environments.

Chapter 2: Literature Review & Background Information

2.1 Literature Review

A literature review was conducted to identify current tactics and knowledge gaps as it relates to the fire service's use and understanding of TICs in structure fires. This review also identifies previous research related to TIC. This section outlines a selection of various articles found in fire service publications, governing codes and standards, and previous research works. This is not intended to be an all-encompassing review, only to highlight some of the current literature available on the use and fire service understanding of TICs.

2.1.1 Fire Service Publications

Turenne states TIC usage on fire ground operations, hazardous materials incident response, and motor vehicle collision response aides company officers, incident commanders, and incident safety officers to make more informed decisions by providing additional information about the scene despite limited visibility. Turenne states that information obtained from the TIC in addition to a firefighter's "understanding and comprehension of the conditions presented" could positively influence

decisions made during an incident in his *Fire Engineering* article [5].

Jakubowski [4] states TICs detect emitted heat through "smoke and dust", "a door or wall", and "reflected off water or mirrors" [4]. Turenne suggests a three-part scan of a structure aids in accurately understanding the obvious indicators presented by the scene. This three-part scan is composed of a high, medium, and low level scan to identify heat extension, fire spread, viable victim locations, etc. [14].

Both authors warn firefighters of the limitations associated thermal imaging technology. Jakubowski warns that although TICs provide valuable information, they should not replace a firefighter's senses [4]. Turene advises the TIC can readily help firefighters "see through smoke" but advises to "remember that glass and shiny objects could potentially give false readings such as reflections [14]."

Training with TICs should be conducted in environments similar to actual use to avoid complacency and an overconfident attitude towards the TIC. Nix warns firefighters to "never make the mistake of using the TIC in place of their basic firefighting skills [15]." Nix stresses that a TIC can trick firefighters into forgetting basic skills such as staying low and crawling or remaining with their team when navigating a structure. He states, "[TICs] cannot see ... a hole in the floor or furniture in a temperature-stable room [15]." The article also stresses the three-pass technique of a high, middle, and low level scan of the room. It elaborates that the high scan should focus on heat accumulation, potential vent points, and structural integrity, the middle scan should focus on the physical layout and contents of the room in addition to secondary egress points, and the low scan should focus on potential victims and special hazards [15].

2.1.2 Codes and Standards

The National Fire Protection Association (NFPA) released the first edition of *NFPA 1801 - Standard on Thermal Imagers for the Fire Service* in 2010. The standard is now in its third edition as of the time of this reports publication. This standard specifies design and performance requirements for fire service TICs. Design requirements include specifics regarding visual / temperature outputs and audio, video, and data recording / transmission. The fourth edition is currently proposing the removal of temperature outputs, including temperature bar and numeric temperature measurement indicator [16]. Two performance requirements evaluate the TICS ability to perform under super heated conditions. These requirements include a Heat Resistance Test and a Heat and Flame Test. The Heat Resistance Test specifies the spatial resolution of the camera must be unaffected by heat. The Heat and Flame Test specifies the housing of the camera must remain in-tact when exposed to direct flame contact. Two additional performance requirements evaluate the TICs ability to detect temperature differences at ambient conditions. These requirements include an Effective Temperature Range and Thermal Sensitivity Test. The TICs ability to detect temperatures during an immediately dangerous to life and health (IDLH) environment is not explored [17].

NFPA released *NFPA 1408 - Standard for Training Fire Service Personnel in the Operation, Care, Use, and Maintenance of Thermal Imagers* in 2015. The second edition of this document is proposed to be released in 2020. This document outlines the intended goals and proficiency expected from students and instructors who wish

to train with TICs. Training should consist of lecture education as well as hands-on education of practical evaluations in IDLH environments with proper self-contained breathing apparatus (SCBA) use. Students should be proficient in interpreting temperature or temperature range color output from the TIC they are using, how the temperature gauge specific to their device measures these temperatures, as well as understand TIC image interpretation / misinterpretation for multiple reasons including: false readings and differences in emissivity values for two or more different materials in the TIC field of vision [18].

2.1.3 Previous Research

Several reports, published by the National Institute of Standards and Technology (NIST), investigate varying aspects of TICs in the fire service. In a 2008 study, NIST proposed performance metrics for fire service TICs by conducting small- and full- scale experiments [19]. The development of test conditions representative of fire service operations was established. To define meaningful bounds on test conditions, activities in which TICs are used by the fire service were presented as Thermal Classes, see Table 2.1.3. It was determined that no particular detector technology or model excelled in the performance metrics analyzed: image contrast, effective temperature range, spatial resolution, image non-uniformity, and thermal sensitivity.

In a report produced in 2009, NIST investigated image quality of fire service TICs on human perception [20]. Five fire service TICs were selected and tested according to the requirements of NFPA 1801 for the following metrics: FOV, non-

Table 2.1: Metrics for defining thermal class associated with the environment in which the TIC is located [19].

Thermal Class	Maximum Time (min)	Maximum Temperature
I	25	100 ° C
II	15	160 ° C
III	5	260 ° C
IV	¡1	>260 ° C

uniformity, spatial resolution, effective temperature range, and thermal sensitivity. For each metric, it was determined that fire service TICs respond differently regardless of sensing material and detector array size.

In another 2009 study, NIST and the University of Maryland attempted to re-quantify if TIC display quality had an effect on firefighter task performance [21]. The effects of thermal imaging display contrast, brightness, spatial resolution, and noise on a firefighter's ability to identify a fire hazard were observed. It was determined that the combined interaction between contrast, brightness, spatial resolution, and noise influenced human perception greater than variation in any one effect alone.

2.2 Background Information

A background investigation was conducted to understand the general theory associated with thermal imaging technologies. This section first outlines the overarching theory associated with TICs, with no specificity to fire service TICs, then outlines specific requirements associated with microbolometers, the classification of TIC utilized by the fire service. This is not intended to be an all-encompassing review; but, rather it is intended to provide information necessary to understand

how TICs operate and produce temperature outputs.

2.2.1 TIC Technology

The desire to see in limited visibility environments, such as complete or partial darkness and environments affected by dust, fog / mist, and / or smoke, has led to the development of thermal imaging technology. Infrared radiation (IR) is less susceptible than visible light to absorption from small particulates of matter present within a typical environment, due to their longer wavelengths. Thermal radiation, in the IR range, is the ideal measurable quantity when imaging an environment with low ambient light. Thermal imaging is the process of interpreting thermal energy emitted by solid objects to visually quantify an environment that is otherwise imperceivable to the human eye. To quantify a scene / room in an visually obscured environment, IR radiation must be focused into an array of infrared detectors, pixels, before being processed into a thermogram, an image composed entirely from detecting temperatures of objects within the field of view [2].

From a limited market review, most, if not all fire service TICs employ a resistive microbolometer array composed of vanadium oxide or amorphous silicon sensing materials. Resistive bolometers operate by detecting a change in electrical resistance of the sensing material due to induced temperature increase from absorbed incident IR. The resistance of the sensing material will either increase (metallic materials) or decrease (semi-conducting materials) when the temperature is increased and vice versa when the temperature is decreased. The resistance of the material is obtained

by applying a bias voltage or current through the sensing material and measuring the resulting current or voltage [3, 22].

2.2.2 Theoretical Overview

The exact algorithms employed by fire service TIC manufacturers to determine temperature from received thermal radiation are considered proprietary information. The following theoretical overview is compiled from several sources and is aimed to give the reader a general understanding of how TICs function and approximate spot temperatures from thermal radiation, with limited specificity to fire service TICs. It is assumed that fire service TICs operate in a similar manner to non-fire service TICs; with a constant value for target object emissivity as this is typically disclosed information. The exact process for determining target object reflectivity, atmospheric relative humidity, atmospheric temperature, atmospheric attenuation, and propagation distance are unknown.

The Electromagnetic (EM) Spectrum encompasses all frequencies of electromagnetic radiation quantified by differing wavelengths and photon energy levels. The spectrum is divided into 'bands', most notably for this report are visible light and infrared radiation. Visible light, 0.40 - 0.70 μm, is the only class of the EM spectrum that is perceivable to the human eye. The visible light spectrum contains relatively short wavelengths; which, can be absorbed by small particulates of dust, fog / mist, and / or smoke present in the atmosphere, creating a semi-opaque environment to the human eye. Particulates compromised of two or more atomic species

can absorb short wavelengths of radiation: absorption is reliant on electron energy levels of both the particulate and the visible light wavelength. Infrared radiation, 0.7 - 30.0 μm, is located just beyond the visible spectrum with longer wavelengths; which, allows energy to transmit through or reflect off small particulates of dust, fog / mist, and / or smoke. IR radiation when compared to visible light is not as affected by small particulates present in the atmosphere. The infrared spectrum is divided into several regions, or bands, according to wavelength. The boundaries of these regions vary by scientific discipline and therefore are not sharply defined. For this report the infrared spectrum band of interest includes wavelengths of 8.0 - 14.0 μm, referred to as long-wavelength infrared (LWIR).

All solid objects with an absolute temperature greater than 0 K emit radiation. In addition, these objects also absorb, transmit, or reflect a certain amount of incidental radiation produced by surrounding objects and environment. Energy transmitted within the LWIR is representative of emitted energy. The total amount of incident radiation that is absorbed, transmitted, or reflected is wavelength dependent and can be quantified by Equation 2.1, where α is the spectral absorbance, τ is the spectral transmittance, and ρ is the spectral reflectance [23].

$$\alpha_\lambda + \tau_\lambda + \rho_\lambda = 1 \tag{2.1}$$

Conservation of energy dictates that the amount of radiation absorbed, transmitted, and reflected has to be equal to the total amount of energy emitted, 100 % or 1. The amount of energy emitted is dependent on object temperature and emis-

sivity. Emissivity, ϵ, is the ratio of the energy radiated from an object's surface to that of a blackbody at the same temperature. A blackbody is theoretically a perfect emitter of energy, $\epsilon = 1$, and theoretically a perfect absorber of incidental radiant energy, $\alpha = 1$. Blackbodies are quantified in realistic scenarios by opaque, flat black objects with a rough texture [19]. Stefan's Law relates the excitance, emitted power per unit area, E_b, measured in $\frac{W}{m^2}$, emitted by a black body as a function of its thermodynamic temperature, measured in K. Excitance is represented by Equation 2.2, where σ is the Stefan-Boltzmann constant, 5.67×10^{-8} $\frac{W}{m^2K^4}$.

$$E_b = \sigma T^4 \tag{2.2}$$

Most objects however are not considered to be blackbodies but rather gray bodies. Gray bodies reflect some amount of incident radiation emitted by their surroundings. Emitted radiation originates from the surfaces of the object and transmits in all directions into the surrounding environment, creating a hemisphere of radiative wavelengths. While not all objects radiate uniformly into this hemisphere, TICs assume solid objects are Lambertian Radiators or emit constant radiant energy in all directions; eliminating the need for solid angle corrections. TICs will perceive a constant radiance for an object, resulting in a potential variance in temperature dependent on viewing angle.

The intensity of this emitted radiation is wavelength dependent; therefore, a peak emission exists at a certain wavelength. The peak wavelength for objects at a temperature of 300 K in an ambient environment, is 10.0 μ m [3, 22].

To create a thermogram and / or a temperature readout, TICs must interpret the total radiation, E_{total}, received from the environment. The total radiation received by the TIC is composed of the energy emitted by the target object, E_{obj}, incidental radiation reflected by the target object, E_{refl}, and the emitted radiation from the atmosphere, E_{atm}. Conservation of energy dictates the relationship presented in Equation 2.3 [23].

$$E_{total} = E_{obj} + E_{refl} + E_{atm} \tag{2.3}$$

Not all of the energy emitted or reflected by a target object will be absorbed by the TIC due to atmospheric attenuation; therefore, energy loss to the surrounding atmosphere must be accounted for. Atmospheric attenuation determines how much radiation is absorbed by the atmosphere before reaching another object. Molecules consisting of a single elemental species do not absorb IR radiation; however, molecules consisting of compounds do absorb IR radiation. Gaseous materials such as nitrous oxide, carbon monoxide, and methane are considered absorbers of radiation and commonly found within earth's atmosphere; but, are ignored as their concentrations at ambient conditions are typically too low to affect atmospheric attenuation. Atmospheric attenuation is dependent on wavelength; Figure 2.1 represents the atmospheric transmittance as a function of wavelength.

From Figure 2.1, atmospheric attenuation of IR is most constant for the SWIR band, peaking around 80 % transmittance. The regions of lower percent attenuation are dependent on the presence of two compounds within the atmosphere: water va-

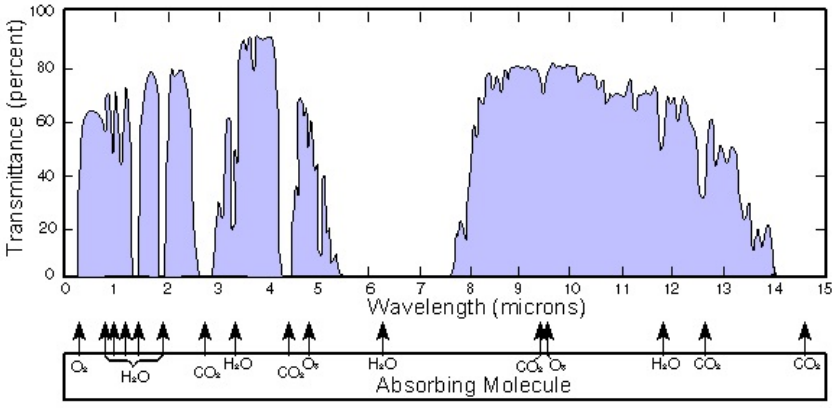

Figure 2.1: Atmospheric transmittance over a distance of 1852 m at sea level for an ambient environment [24].

por and carbon dioxide. Carbon dioxide is ignored in most atmospheric attenuation calculations as its concentration is constant and its transmittance over wavelengths between 7.5 - 14 μm is unitary for a distance less than 200 m. Relative humidity, measurement of water vapor relative to temperature of the atmosphere, is considered in attenuation calculations and is represented by ω %. Propagation distance, distance between the camera and the object, d, measured in meters, and the temperature of the atmosphere, T_{atm}, measured in °C, are also needed to calculate the attenuation of the propagation atmosphere. The exact formula to determine atmospheric attenuation is propriety information: Equation 2.4 states that atmospheric attenuation is a function of the aforementioned variables [25].

$$\tau_{atm} = f(\omega\ \%, d, T_{atm}) \tag{2.4}$$

The IR emitted by the target object is dependent on atmospheric transmit-

tance as well as the emissivity of the object. Equation 2.5 expresses the emitted IR produced by the target object [23].

$$E_{obj} = \epsilon_{obj}\tau_{atm}\sigma T_{obj}^4 \tag{2.5}$$

The incidental IR reflected by the target object, originally emitted from the surroundings, is also a function of atmospheric transmittance. The camera assumes the object is a gray body and therefore is also dependent on the objects reflectivity. Equation 2.6 expresses the emission reflected from the target object [23].

$$E_{refl} = \rho_{obj}\tau_{atm}\sigma T_{refl}^4 \tag{2.6}$$

The IR emitted by the atmosphere is dependent on the emissivity of the environment which can be rewritten in terms of attenuation. Equation 2.7 expresses the emission produced from the atmosphere [23].

$$E_{atm} = (1 - \epsilon_{atm})\sigma T_{atm}^4 \tag{2.7}$$

When equations 2.5 - 2.7 are substituted into 2.3 and rearranged, the temperature of the object can be determined. Equation 2.8 expresses the temperature of the target object [23].

$$T_{obj} = \sqrt[4]{\frac{E_{total} - (1 - \epsilon_{obj})\tau_{atm}\sigma T_{refl}^4 - (1 - \tau_{atm})\sigma T_{atm}^4}{\epsilon_{obj}\tau_{atm}\sigma}} \tag{2.8}$$

It is assumed that the following process is followed: relative humidity and

atmospheric temperature variables are used to calculate absolute humidity of the propagating medium (atmosphere), propagation distance is used to calculate perceptible water within the propagating medium, internal transmittance of the propagating medium is calculated, emissivity and temperature are used to calculate the power radiated by the object in question, the emissivity and temperature of objects within the environment are used to calculate the power reflected by the object in question, finally the power received by the TIC is calculated [26].

The following variables are observed from the environment: relative humidity, atmospheric temperature, propagation distance, emissivity of target object and surroundings, and temperature of target object and surroundings. Fire service TICs only publish emissivity values; while, the remaining variables are not mentioned in published specifications and manuals [19, 27–29].

The total emission received by the TIC is determined from the resistance change within the sensing material. The sensing material absorbs energy emitted from and reflected by the target object as well as emitted from the surrounding environment, this results in an increase in temperature of the material. The increase in temperature causes a resistance change in the material; which, is measured by applying a bias voltage or current to the sensing material and observing the resultant current or voltage. The overarching heat balance equation for thermal imagers is presented by Equation 2.9. The following variables are specific to the microbolometer: c is thermal capacity of the sensing material measured in $\frac{\mathrm{J}}{\mathrm{K}}$, T is the temperature of the microbolometer measured in K, I is the biased current across the microbolometer measured in A, V is the biased voltage across the microbolometer measured in

V, and g is the thermal conductance measured in $\frac{\mathrm{W}}{\mathrm{K}}$.

$$c\frac{dT}{dt} = IV + \epsilon P_t + \epsilon P_s \ - \ g(T - T_s) \ - \ (2A)\epsilon\sigma T^4 \tag{2.9}$$

The following variables are also present in Equation 2.9, time, t, measured in s, P_t is the radiation from the target source measured in W, P_s is the radiation from the reservoir measured in W, T_s is the temperature of the reservoir measured in K, and the final term is Stefan's Law or the power created from the bias current. Stefan's Law is characterized by area from the microbolometer, A, measured in m^2. As the joule heating, temperature increase from the applied bias, is considerably greater than the thermal heating, temperature increase from received IR produced by the target object, the first term characterized by IV must be accounted for in Equation 2.9 [3].

2.2.3 Microbolometer Sensor and Pixel Arrays

Microbolometer sensors are only one integral part of a TIC. The exact structure is undisclosed, propriety information dependent on manufacturer: the following information is supplied to ensure the reader has a general understanding of the structure of monolithic pixels. The sensor is encased in a vacuum package and sandwiched between the camera lens, which will allow for penetration of IR, and the back-end electronics, which produce the visible image, see Figure 2.2. Microbolometer sensors are extremely complex due to the need to both thermally isolate while simultaneously conduct electricity between the sensing material and electrical components.

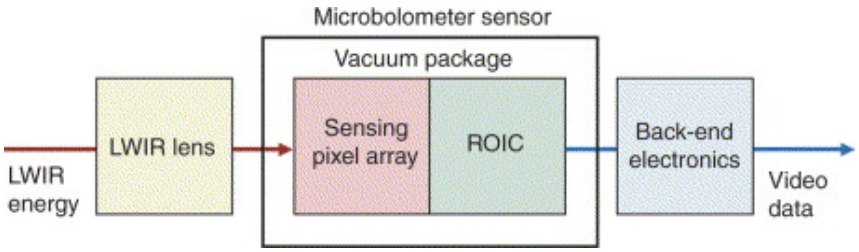

Figure 2.2: General overview of the internal structure of a microbolometer engine block [30].

The general structure of a microbolometer sensor consists of two parts: a radiation sensing pixel array and a read-out integrated circuit (ROIC), as illustrated in Figure 2.3. This sensor is contained within a vacuum to ensure the high thermal isolation needed to process data. This vacuum eliminates the need for cryogenic cooling and limits the thermal heat transfer between components. Although this vacuum eliminates any convective heat transfer between components, the main mode of heat loss in this small space is dominated by conduction.

The pixel component is shaped like a table top with two legs that elevate it off the silicon substrate ROIC. These legs provide the thermal insulation necessary to isolate the components while also completing the circuit between the sensing material and the ROIC. The pixel is made of electrically conductive material, typically a silicon nitride compound, encapsulating the temperature sensitive resistor material, resistive bolometry typically uses Vanadium Oxide; although, Amorphous Silicon is also common. It is responsible for absorbing light and consequently increasing in temperature [32].

The ROIC consists of a silicon substrate that contains integrated electrical con-

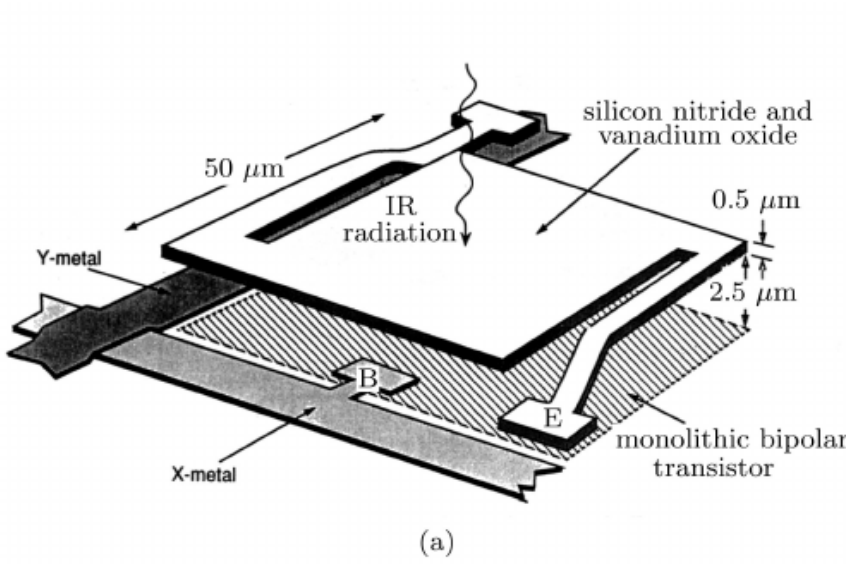

Figure 2.3: General overview of the internal structure of a microbolometer pixel [31].

tacts. This combination of materials forms a monolithic bipolar transistor responsible for measuring the change in electrical resistance present within the temperature sensitive pixel.

In addition to the microbolometer sensor, another important feature of a microbolometer engine block is the reflector. A reflector is located on top of the ROIC and marks the end of the vacuumed enclosure. This layer is designed to reflect back any light that may transmit through the absorption layer to maximize the absorption through this layer [30, 32].

The following information regarding specific specifications are published by fire service TIC manufactures and specific to fire service TICs.

Lens Specifications

In order for IR to be processed it must first pass through the camera lens. The material used for these lens must be relatively durable while also allowing IR to pass through its composition. Most lens are made of germanium (Ge). Germanium is a high density, relatively hard, IR transmitting material. It is known to block ultra-violet and visible wavelengths of light while transmitting up to 45 % of infrared wavelengths between 2.0 - 14.0 μm. As this material increases in temperature its efficiency in transmitting radiation decreases, rapidly decreasing above 200 °C. It is not recommended to use this material in environments where the ambient temperature exceeds 200 °C [33, 34].

Microbolometer Specifications

After the IR has passed through the lens, it must be processed by the microbolometer detector. In order to be processed, it must first be absorbed by an IR sensing material and the resultant increase in temperature must affect some quantifiable physical property of the sensing material. Two materials are commonly used in fire service TICs, Vanadium Oxide (metallic) and Amorphous Silicon (semi-conducting). These two materials are ideal sensing materials as their electrical resistance are dependent on temperature. Vanadium Oxide (VOx) changes its structural form around 68 °C, causing electrons in previously unbroken bonds to become free increasing the electrical conductivity of the material. In addition, this material can change from being IR transparent to nearly a perfect IR absorber. The

resultant effect is the ability to act as a high speed shutter for use in TICs [35, 36]. Amorphous Silicon (a-Si) microbolometers surpass VOx in performance: offering an increased temperature coefficient of resistance (TCR) and more efficient thermal isolation. A-Si microbolometers can achieve a TCR in excess of $\frac{5\%}{^{\circ}C}$, efficiently increasing the sensitivity of the detector [37].

The resolution of the microbolometer refers to the number of pixels present within the sensor. The higher the resolution, the more pixels are present and an increase in clarity is achieved. This resolution is ultimately dependent on the pixel and sensor size. Original microbolometer pixels were 50.0 μm while today most microbolometer pixels are approximately 17.0 μm [3, 19, 22, 38].

The spectral response of the microbolometer quantifies the range of EM wavelengths the sensor will operate within. This range is typically within the LWIR band as this region of the EM spectrum maximizes the IR attenuation through the atmosphere. Fire service TICs typically operate between 8.0 - 14.0 μm; while, some models include the 7.0 - 8.0 μm region [3, 22].

The dynamic range of a TIC refers to two aspects: the temperature range the camera is calibrated to detect and the maximum temperature a TIC can display. The variance within the dynamic range allows for more contrast within the gray-scale image, adding definition and detail to the working image produced. The maximum temperature within the dynamic range is the maximum temperature the TIC can display before the camera becomes saturated, creating a 'white out' screen. Most TICs produced today have temperature indicating colors associated with extreme temperature ranges so the 'white out' may in fact be of another color, typically red

for extreme temperatures. This 'white out' effect is typically associated with flash over. There is great variance between TICs but most operate at 537 - 1093 °C [3, 22, 38].

Back-End Electronics

The circuitry used to convert the electrical information produced by the ROIC is not readily available from published specifications. This information is typically considered proprietary information and not disclosed for public consumption. The overarching theory to process IR as an image is discussed in Section 2.2.2.

Chapter 3: Instrumentation & Equipment

Throughout the various chapters of this report measurements of temperature (acquired from TICs and TCs) and opacity are discussed. This section is intended to summarize the instrumentation used to collect these measurements. To avoid repetitiveness each instrument is described in detail and the potential uncertainty associated with each measurement is presented below. While the use of TICs and TCs are consistent throughout Sections 4 - 5, the use of the remaining instrumentation is specific to Section 5.

3.1 Fire Service TICs

The demands placed on fire service TICs by the environment and operation require that such devices be portable, operable with a single hand, reliable, able to determine the difference between a hot object and a cold object, and rugged enough to withstand high working temperatures, dirty environments, and potential external stressors. Uncooled microbolometers are best suited to fit these requirements as they are small and lightweight, do not need to be constantly cooled or re-calibrated for accuracy, and can be outfitted with protective measures. There are two leading types of bolometry, pyroelectric / ferroelectric and resistive. From a brief market review

of available fire service TICs it appears that resistive microbolometers, specifically Vanadium Oxide, are commonly used by fire service TIC manufacturers.

NFPA 1801 - Standard on Thermal Imagers for the Fire Service dictates the design requirements for fire service specific TICs. Specific design requirements outlined in this standard include the minimum working time of 120 min at 22 °C ± 3 °C, spectral range of 8 - 14 μm, a minimum display resolution of 76,800 pixels, and a minimum frame rate of 25 frames per second. Display specifications include a gray-scale image display with 'hot white' polarity and informational indicators of power source, overheated conditions, and power on. The location of informational indicators are also specified by this standard. The standard considers heat indicating color, temperature bar, numeric temperature indicator, and audio, visual, and data recording / transmission capabilities optional.

While a spot temperature measurement is not a basic required functionality of fire service TICs, requirements specific to this feature are discussed in NFPA 1801. If a spot temperature measurement is an included feature it must be accompanied by a measurement zone to better help firefighters aim and control the TIC, as the temperature measurement will only be calculated for the objects located within this area. This measurement zone is to be indicated in the center third of the viewing area by a transparent green box or by box corners indicated by a green border. Related to the spot measurement, the viewing area must contain a numeric temperature indicator, a temperature bar, or both. If a numeric temperature indicator is utilized, it must be represented in the bottom right corner in green superimposed on a black background. If a temperature bar is utilized, it must be represented in the right

third of the viewing area by a green range divided into at least four incremented sections.

NFPA 1801 does not dictate the programed emissivity value for fire service TICs. In several tests described throughout the standard, objects with an emissivity values of 0.95 ± 0.03 are often used. To minimize set up time and ease usability the emissivity value is typically fixed. By fixing this value, firefighters do not have to complete an additional step prior to using the camera. These values range around 0.85 - 0.95. Typically fire service TICs are used to evaluate the temperature of common building materials. The emissivity values associated with such materials are within the previously stated range [39].

3.1.1 TICs Investigated

Three manufacturers of TICs were investigated in various sections of this report, referred to as TIC # 1, TIC # 2, and TIC # 3. Although three manufacturers of TICs were investigated, only one model per manufacturer was considered. Readily available product specifications for these TICs are listed in Tables 3.1 - **??**. While the specifications vary dependent on the manufacturer, each TIC utilizes a resistive microbolometer sensor.

TIC # 1 was a hand held TIC; which, allowed for external recording, capturing video at 30 frames per second. TIC # 2 was a hand held TIC; which, allowed for external recording, capturing video at roughly 30 frames per second. Both TIC # 1 and TIC # 2 were employed in the initial spot temperature evaluation and the

experiments specifically conducted for this report. TIC # 3 was a hand-held TIC; which, did not allow for real time external monitoring. Rather this TIC offered an internal recording feature capturing video at 10 frames per second.

Product specifications of concern for this report are presented in Table 3.1. For instances where product information was not readily available, commonly seen for TIC # 1, a blank box is depicted.

Table 3.1: TIC Microbolometer Specifications

Attribute	TIC # 1	TIC # 2	TIC # 3
Sensing Material	Vanadium Oxide	Vanadium Oxide	Amorphous Silicon
Emissivity	0.95	Un-published	Un-published
Spectral Response	8.0 - 14.0 μm	7.0 - 14.0 μm	7.5 - 14.0 μm
Pixel Size		17.0 μm	25.0 μm
Pixel Count	320 x 240	320 x 240	384 x 288
Update Rate		60 Hz	60 Hz
NETD	50 mK (0.05 °C)	>50 mK (>0.05 °C)	>50 mK (>0.05 °C)
Dynamic Range	1100 °C	593 °C	-40 - 1100 °C

Fire service TICs operate under proprietary algorithms to determine temperatures of solid objects. Without knowledge of these algorithms and input information, the analysis conducted within this report was dependent on the spot temperature measurements obtained from the TICs investigated. This output information was not presented in a format conducive to analysis; therefore, a series of computer programs were created to translate this information into a usable format. The conclusions presented within this report therefore are not definitive. A working relationship with manufacturers to provide proprietary information is needed to support

research and claims presented within this report.

Visual Output

Two versions of the TIC # 1 type exist. The difference being in the visual output, seen in Figure 3.1. Both TICS are white hot polarity and provide a spot temperature measurement with a numeric readout and temperature bar.

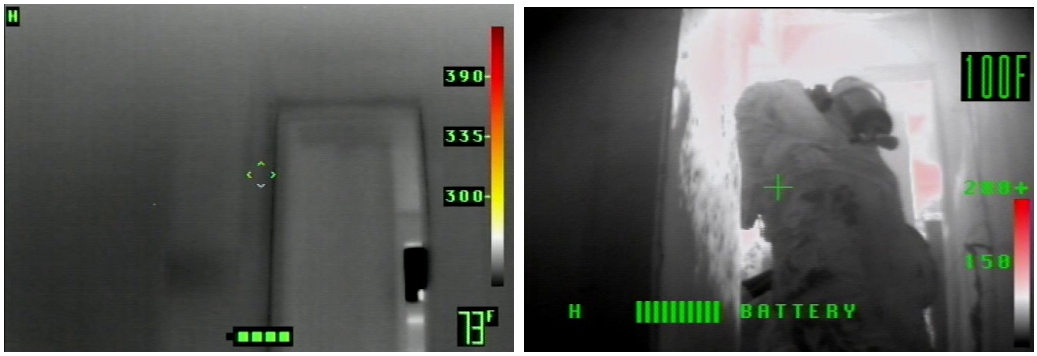

(a) Camera Type 1 (b) Camera Type 2

Figure 3.1: TIC # 1 visual output comparison.

Figure 3.1(a) is an example of the visual output produced from the first version of TIC # 1, referred to as Camera Type 1. This TIC has a measurement zone indicated by a transparent set of arrows, colored in green. The numeric temperature readout is colored in green superimposed onto a black background and the temperature bar is colored in green with three defined segments. The temperature bar provides a tricolor visual for the heat indicating colors upon initial startup. Heat indicating colors visually depict different temperature ranges within the FOV. Figure 3.2 represents the heat indicating color range offered by this TIC. This TIC

does not meet the current requirements of 2018 edition of NFPA 1801.

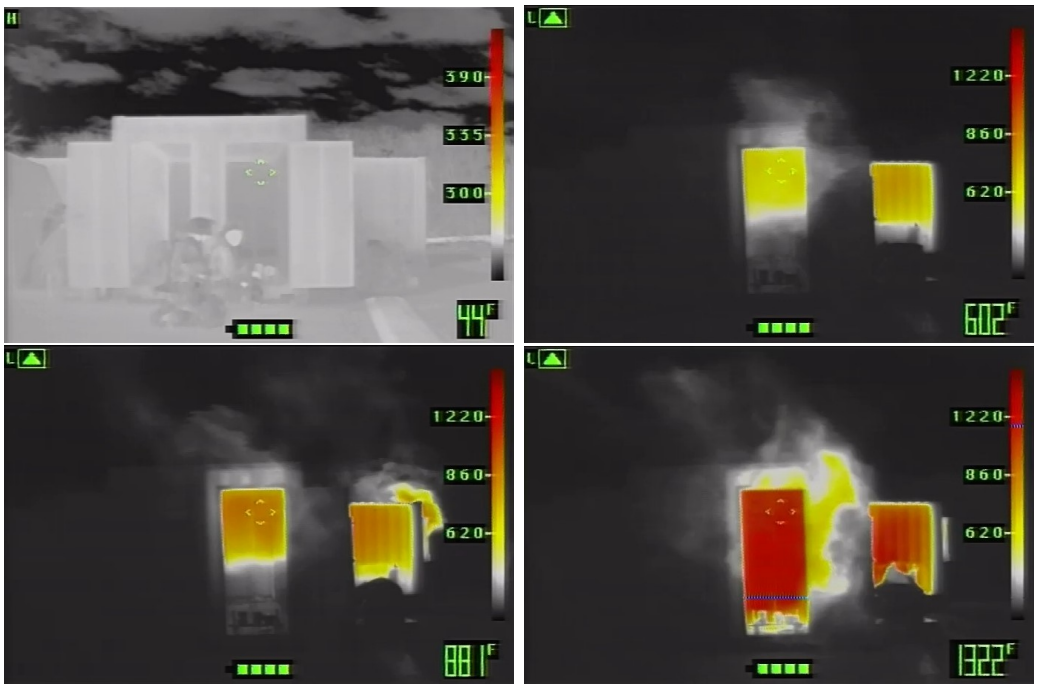

Figure 3.2: TIC # 1 Camera Type 1 visual output including heat indicating colors.

Figure 3.1(b) is an example of the visual output produced from the second version of TIC # 2, referred to as Camera Type 2. This TIC has a measurement zone indicated by a set of cross-hairs. The numeric temperature readout is colored in green and is superimposed on a black background and the temperature bar is colored in green with two defined segments. The temperature bar provides a dual color visual for heat indicating colors upon initial startup, this changes to a tricolor visual when temperatures within the FOV increase substantially. These heat indicating colors are employed to visualize the temperature gradient of objects within the FOV. Figure 3.3 represents the dual color range offered by this TIC. Figure 3.4 represents

the tri-color color range offered by this TIC. This TIC does not meet the current requirements of 2018 edition of NFPA 1801.

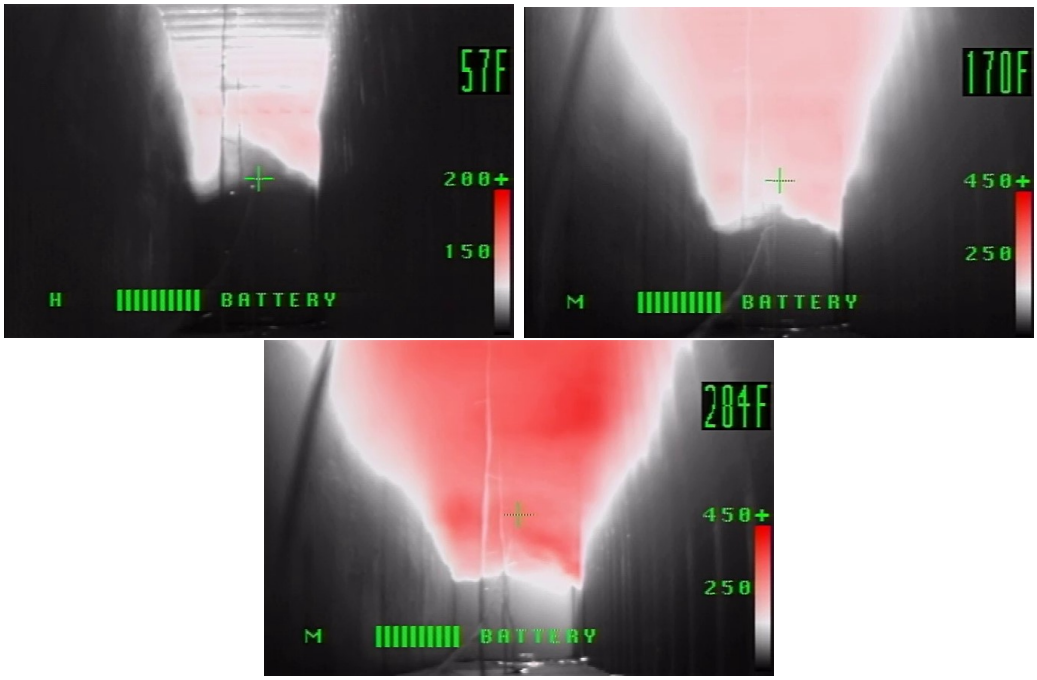

Figure 3.3: TIC # 1 Camera Type 2 visual output including dual color heat indicating display.

Other differences in visual output are apparent between the two TICs, including battery status and font type. It is assumed that the both TICs have a fixed emissivity value 0.95. Both TICS have an approximate frame rate of 30 frames per second.

TIC # 2 was used during the Fire Attack study as well as this studies experimental design. Figure 3.5 depicts the visual output produced from this TIC.

The visual output of this TIC has a white hot polarity and includes a spot temperature measurement accompanied by a numeric readout and temperature bar. The

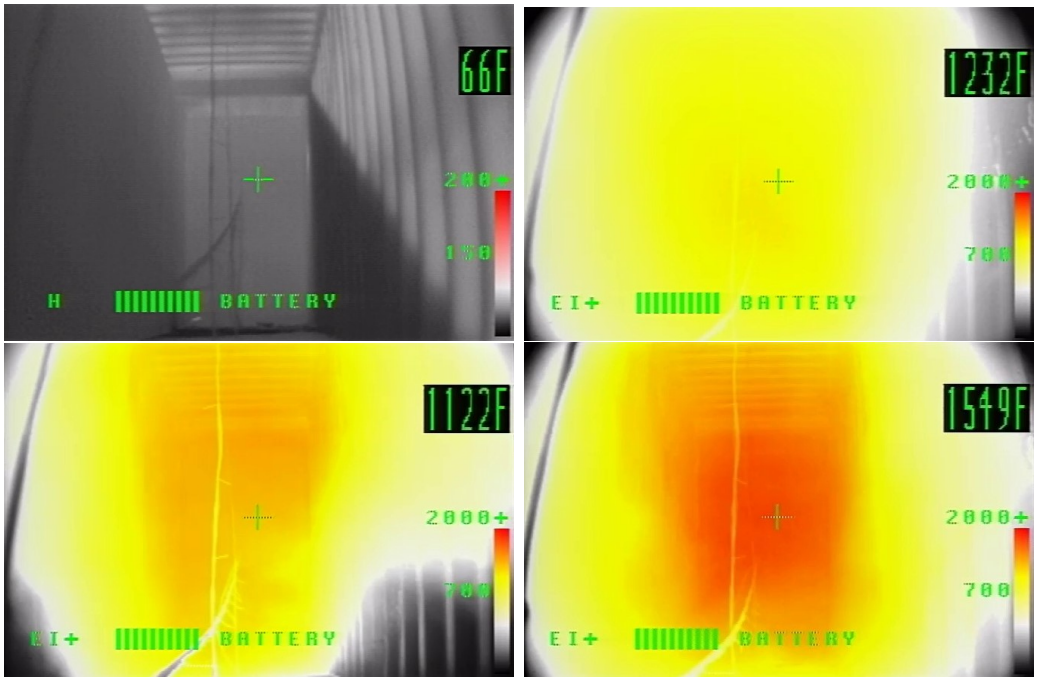

Figure 3.4: TIC # 1 Camera Type 2 visual output including tricolor heat indicating display.

measurement zone is indicated by a transparent box, colored in green, the numeric temperature readout is colored in green superimposed onto a black background, and the temperature bar is colored in green with four defined segments. This TIC model employs heat indicating colors to better visualize the thermal gradients within the FOV: yellow for temperatures in the range of 260 - 426 °C (500 - 799 °F), orange for temperatures in the range of 427 - 537 °C (800 - 999 °F), and red for temperatures greater than 538 °C (1000 °F) [40]. Figure 3.8 represents the heat indicating color range offered by this TIC. This TIC meets the current requirements of 2018 edition of NFPA 1801.

TIC # 3 was implemented in the experiments specifically conducted for this

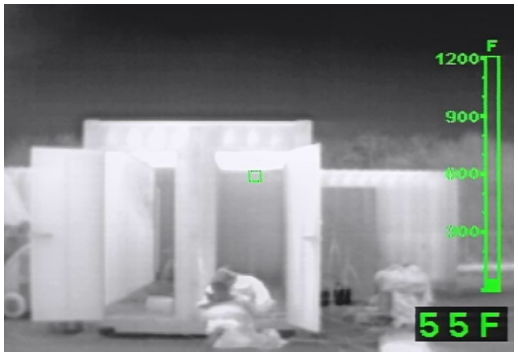

Figure 3.5: TIC # 2 visual output.

report. Figure 3.7 depicts the visual output produced from this TIC.

The visual output of this TIC has a white hot polarity and includes a spot temperature measurement accompanied by a numeric readout. The measurement zone is indicated by transparent box corners, colored in green, while the numeric temperature readout is colored in green superimposed onto a black background. This TIC model offers heat indicating colors for better visualization of temperature ranges within the FOV: yellow for temperatures in the range of 150 - 500 °C, orange for temperatures in the range of 500 - 600 °C, and red for temperatures in the range of 600 - 1100 °C [41]. Figure 3.8 represents the heat indicating color range offered by this TIC. This TIC meets the current requirements of 2018 edition of NFPA 1801.

3.1.2 Image to Text Video Processing

The TICs evaluated by this report could not convert or export spot temperature measurements from video to text format, i.e. a data file containing only text, characters, or digits. However, all three cameras offered video recording of the visual

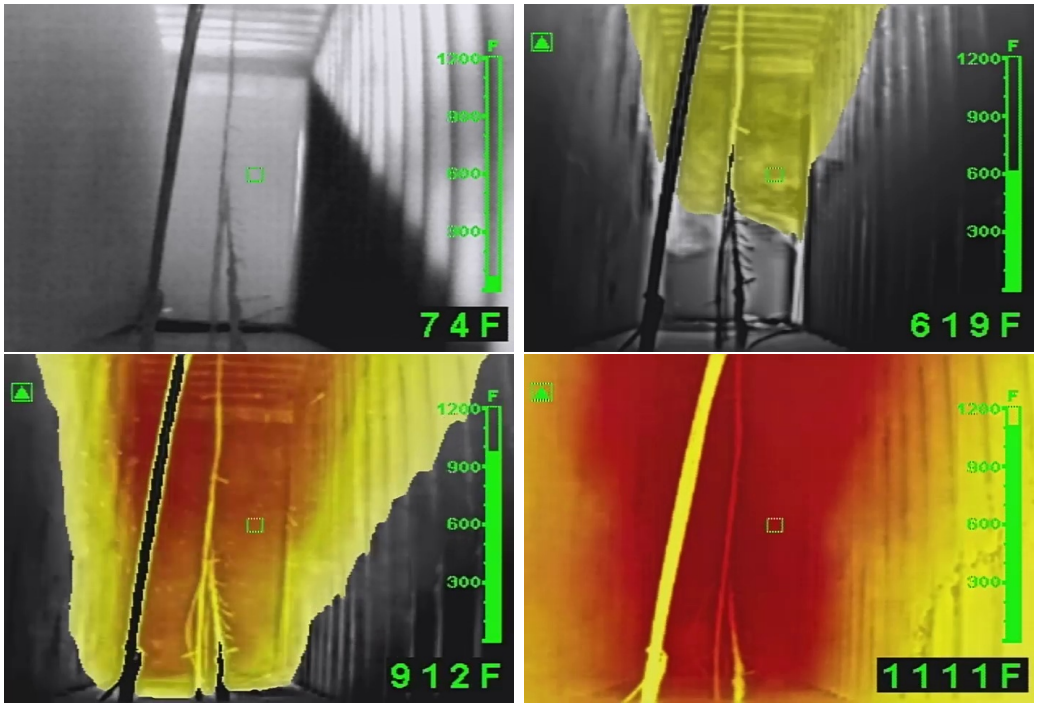

Figure 3.6: TIC # 2 visual output including heat indicating colors.

output produced during use. TIC # 1 and TIC # 2 allowed for real time monitoring from an external location via a BNC (Bayonet Neill-Concelman) connection; the external location recorded data in a .mp4 format. TIC # 3 did not allow for real time monitoring but rather recorded visual output internally in a .avi format; which, at a later time could be downloaded from the TIC to a computer via a micro USB connection. To obtain the spot temperature in text format, a series of processing scripts were created to recognize the temperature text from each video file and record it into a .csv (Comma Separated Values) file.

Each TIC's visual output is unique despite the requirements specified in NFPA 1801. The temperature text style and location within the visual output presented unique challenges for each of the TICs investigated. This resulted in the need for multiple

Figure 3.7: TIC # 3 visual output. An ambient environment is depicted.

techniques to covert the temperature output from a video format into a text format. Each technique is summarized below and further detailed in Appendix A. The raw data produced from the following scripts were manually inspected. Any outlying temperature measurements were manually compared to TIC video and updated if needed.

Seven-Segment

The temperature text style produced from TIC # 1 Camera Type 1 is similar to a seven-segment display. Seven-segment displays are a type of electronic format commonly used in light-generating or controlling displays, digital clocks and calculators [42]. The script developed to read this temperature text style, evaluated each digit within the temperature output to identify the 'on' or 'off' status of the seven-segments. First, the video was converted into a series of images, taken at each second or every 30 frames. Second, each image was cropped to include only the temperature text and converted into binary color, black and white. Third, the im-

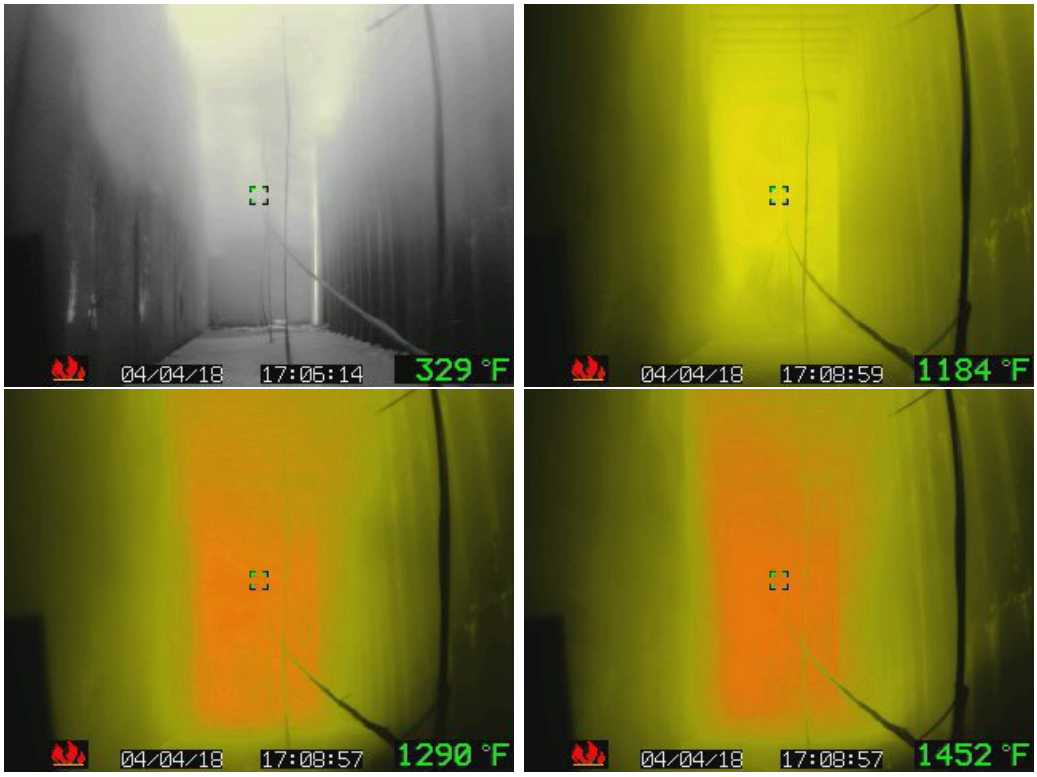

Figure 3.8: TIC # 3 visual output including heat indicating colors.

age was further cropped to include only one numbers place within the measurement, ones, tens, hundreds, thousands. Fourth, the color of each segment was determined to be either white ('on') or black ('off') and recorded into an array of values specific to that digit, 1 representing white and 0 representing black. Fifth, the array was referenced against a master array representing the status of each of the desired digits 0 - 9 to reconstruct the individual number. Finally, the individual numbers were combined to assemble the whole spot temperature measurement.

Figure 3.9 is a representation of the temperature text style produced by Camera Type 1.

A seven-segment indicator consists of seven components (equal in size and

Figure 3.9: Sample TIC temperature text produced from TIC # 1 Camera Type 1.

shape) to represent digits or characters. To represent a digit, each of these seven components can be considered 'on' or 'off'. Many possible combinations of 'on' and 'off' segments exist; but, only 10 are desired for this code. These combinations correspond to the digits 0 - 9. Figure 3.10 represents a seven-segment indicator with each segment numbered.

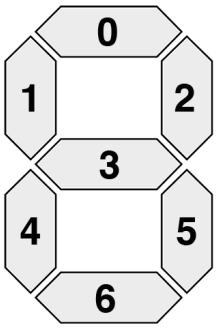

Figure 3.10: Breakdown of each segment in a seven-segment display [42].

Image Comparison

The script developed to read the temperature output produced by Camera Type 2, compared each digit within the temperature output to a reference set of digits [43]. The reference set of images created manually by assessing the TIC videos for each of the 10 digits (0 - 9) needed to reconstruct the temperature measurement. First, the video was converted into a series of images, taken at each second or every 30 frames. Second, each image was cropped to only include the temperature text and converted into binary color, black and white. Third, the image was further cropped to include only one numbers place within the measurement, ones, tens, hundreds, and thousands. Third, the image was compared to the reference set analyzed. The mean squared error and structural similarly index was calculated for each image in the reference set. The temperature output was properly identified when the calculated values for a single reference image has simultaneously the lowest mean squared error and the highest structural similarly index. Fourth, the individual numbers were combined to assemble the whole spot temperature measurement. Figure 3.11 is a representation of the temperature text style produced by Camera Type 2.

Optical Character Recognition

An Optical Character Recognition (OCR) engine designed to recognize and 'read' text embedded in images was utilized to covert the spot temperature measurements from TIC # 2 and TIC # 3 [44, 45]. The most recent version of this

Figure 3.11: Sample text produced from the camera used only in the combustion environment series, located inside the structure.

OCR was released June 1, 2017 and is maintained by on GitHub. First, the video was converted into a series of images, taken at each second or every 30 frames or 10 frames, respectively. Second, each image was cropped to only include the temperature text and converted into a binary color, black and white. Third, the image was ran through the OCR engine and the temperature output was determined.

Figure 3.12 is a representation of the temperature text styles from each TICs visual output.

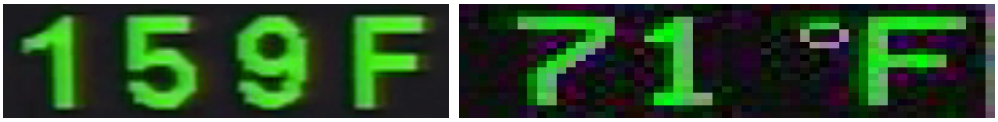

(a) TIC # 2 Temperature Text Style (b) TIC # 3 Temperature Text STyle

Figure 3.12: Sample TIC temperature text from both TIC # 2 and TIC # 3.

3.2 Thermocouples

To monitor gas temperatures, UL FSRI utilizes individual bare-bead, chromel-alumel thermocouples (TCs). The K-Type TCs have a nominal diameter of 0.5 mm. These TCs were strung together into an array to measure temperatures at varying elevations. There were two types of trees employed, with the difference being the distance between each TC bead. The first TC array configuration measured temperatures at 0.61 m intervals. The second TC array configuration measured temperatures at 0.30 m intervals. The highest TC was placed 0.03 cm from the ceiling resulting in two configurations: 0.30, 0.91, 1.52, and 2.13 m or 0.30, 0.61, 0.91, 1.22, 1.52, 1.83, 2.13, and 2.44 m below the ceiling, respective of interval distance.

Due to radiation exchanges within the surrounding environment, walls, gases, soot, and ambient environment, gas temperatures measured from bare bead TCs are not always representative of the actual gas temperature. For TCs within the hot gas layer, temperatures produced from TCs are typically lower than the actual gas temperatures. Conversely, temperatures measured from TC arrays in the lower layer are higher than actual gas temperatures. The percent error is most noticeable for the TC located in the lower layer when true temperatures are close to ambient temperature while, the upper layer is at an elevated temperature. An expanded uncertainty, based on the findings from two NIST reports [46,47], has been calculated and applied to all temperature measurements to account for these losses. Due to the effect of radiative heat transfer to the TCs, the expanded uncertainty is

approximately ± 15 %.

3.3 Opacity Sensors

To determine the opacity of the smoke produced during experimentation, an ambient oil mist system was utilized. Opacity was determined using the theory of light attenuation. Data was obtained by utilizing a 'green laser light beam', reflector, and receiver. According to the manufacturers information, the relative uncertainty of the system is ± 2 %.

The system determined opacity of the environment by employing the theory of light attenuation. This process included focusing a light array through the semi- or opaque environment onto a reflector. The light must then bounce off the reflector and travel back through the semi- or opaque environment onto the receiver. The process calculated opacity from the amount of light received, lower attenuation indicates higher opacity and higher attenuation indicates lower opacity. The manufacturers specifications indicated that a 'green laser light beam' was employed for this process to occur. The specifications indicate that this light beam has 'special spectral characteristics' that allowed for particles of 'oil, smoke, and dust' to be detected. The manufacturer provided additional information about these characteristics, specifically the wavelength of 550 nm. This measurement therefore was indicative of opacity as perceived by the human eye. A 0 % opacity indicated full visibility; while, 100 % opacity indicated the saturation of the sensor.

A TIC is capable of receiving wavelengths within the IR spectrum, roughly

8 - 14 μm for fire service TICs. The measurements from the oil mist system cannot be employed to determine when IR was obscured within the environment, adversely affecting the TIC spot temperature measurement. For example, 100 % opacity does not correlate to when radiant energy was fully or partially blocked or obscured.

Chapter 4: Initial TIC Spot Temperature Evaluation

To develop a more comprehensive understanding of the limitations associated with TIC spot temperature measurements, experimental data obtained during Cardiovascular and Chemical exposure Risks in Modern Firefighting [13] and Impact of Fire Attack Utilizing Interior and Exterior Streams on Firefighter Safety and Occupant Survival: Full Scale Experiments [12] were evaluated. Instrumentation was employed during both projects to monitor hazards, conditions, and operations associated with a fire event.

This report aims to quantify the TIC's ability to capture hazards within a fire environment. Instrumentation was not initially employed for this type of analysis; therefore, was best accomplished for these two experiments by evaluating TIC spot temperature measurements against TC temperature measurements from the TC array closest to the location of the TIC measurement zone at appropriate heights. This approach was fundamentally limited as TICs are designed to capture radiant energy from solid surfaces and participating media; while, TCs are designed to measure gas temperatures.

4.1 Cardiovascular and Chemical Exposure Risks in Modern Firefighting

UL FSRI partnered with the Illinois Fire Service Institute (IFSI) to conduct a series of twelve experiments designed to investigate the thermal and cardiovascular strain placed on firefighters while during forcible entry, search and rescue, and fire attack in realistic fire environments. The effects of fire size, firefighting tactics, and fire ground assignment on physiological responses and markers of toxic exposure of firefighters were explored. The experiments referenced in this section are summarized in the Interim Report, *Cardiovascular & Chemical Exposure Risks in Modern Firefighting* [13].

Inspired by homes built during the mid-twentieth century, a ranch-style structure was built specifically for this experimental study. To maximize the use of the structure and minimize downtime between individual experiments, two internal configurations were designed. Interior structure walls and ceiling were finished with Type X gypsum board. During each individual experiment, a fire was set in both bedrooms located at the end of the hallway. Suppression tactics varied between interior and exterior attacks. Instrumentation deployed throughout the structure included thermocouples to monitor gas temperatures and TICs to monitor internal conditions during combustion. TIC # 1 was employed in two locations to document thermal gas flows within the structure. This instrumentation was used to monitor firefighters and the progress of various fire-ground operations. A depiction of the

structure layout and instrumentation location is presented in Figure 4.1.

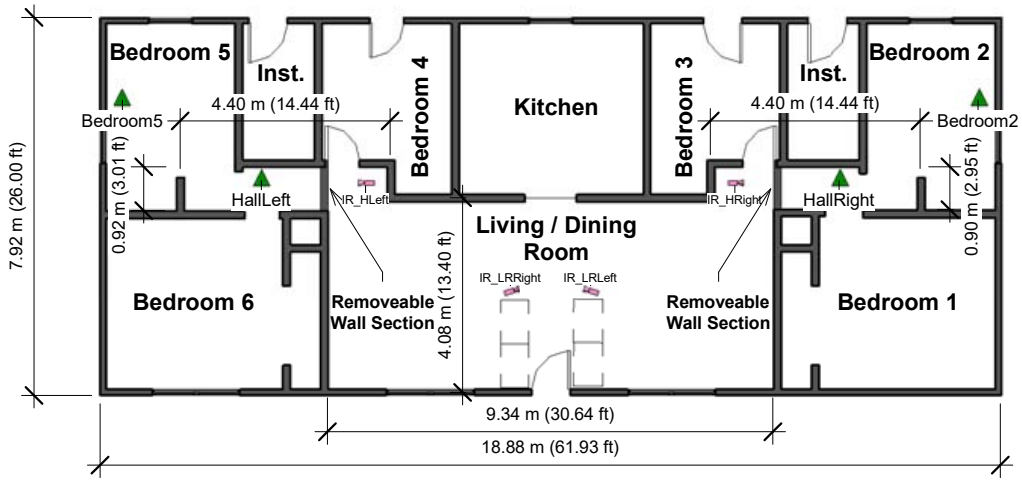

Figure 4.1: Ranch-style structure built for the IFSI Experiments [13]. Two internal configurations were created by the addition or removal of temporary walls. Green triangles represent TC arrays which measure at 0.61 m intervals. Pink symbols represent the two TIC locations.

Experiment # 9 utilized the left internal configuration of the ranch-style structure. Both bedroom windows were framed open; however, bedroom 5's second window was initially simulated closed with a sheet of gypsum board. A fire was ignited in bedroom 6 followed by ignition in bedroom 5 two minutes later. Both fires were allowed to grow and burn for five minutes. At such time the front door was opened and interior suppression efforts began shortly after. Bedroom 5's second window was opened roughly a two minutes after.

At ambient conditions, TIC # 1 produced an image of both the hallway and living room with little contrast. Figure 4.2(a) depicts the Hallway TIC's FOV. This location near bedroom 4 allowed for visualization the hallway and bedroom 5's door-

way and window. Figure 4.2(c) depicts the Living Room TIC's FOV. This location near the front door visualized the contents of the living room. While the general structure and associated hazards of both spaces were distinguishable, details were limited. This was expected as all objects within the FOV were at ambient temperature. As seen in Figure 4.2(b) and 4.2(d), the visual output remained unchanged 10 s post ignition in bedroom 6.

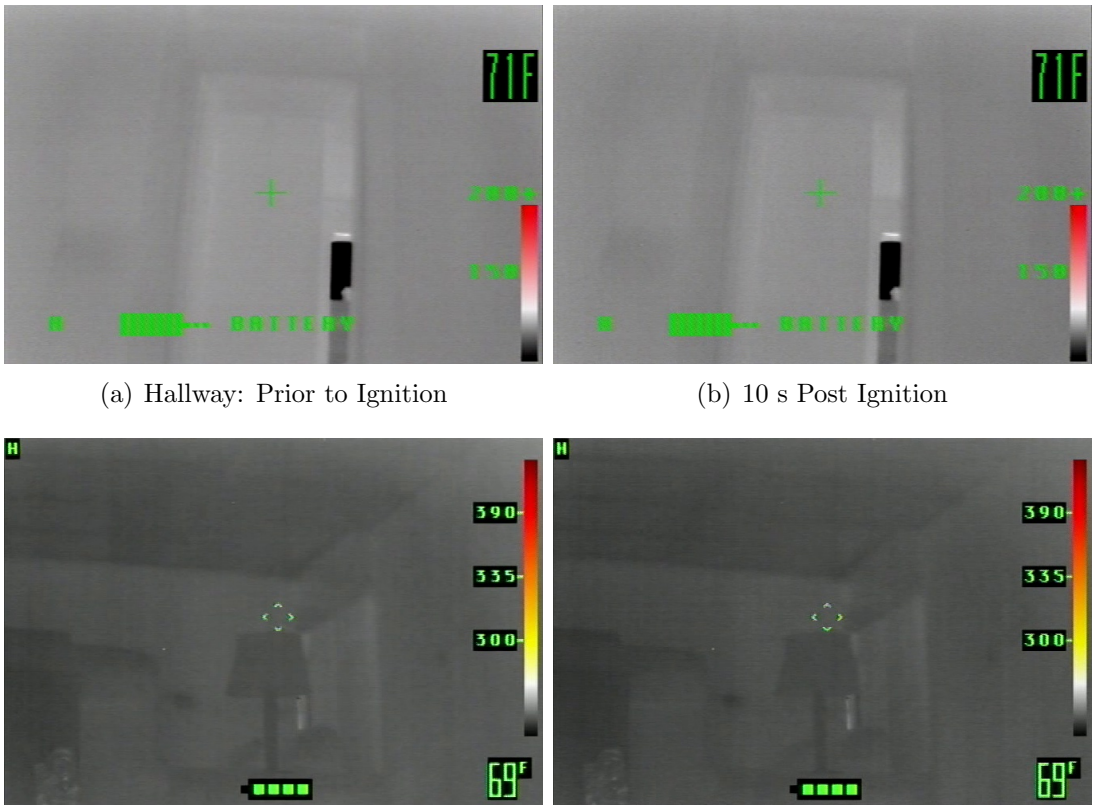

(a) Hallway: Prior to Ignition

(b) 10 s Post Ignition

(c) Living Room: Prior to Ignition

(d) 10 s Post Ignition

Figure 4.2: TIC visual output during ambient conditions, obtained during Experiment # 9.

As the fire grew, heat was transfered to the surrounding environment. This was documented by the TIC as an overall increase in contrast. As such, more

details of the space became apparent. As the fire entrained air from all directions, a bi-directional flow through the windows and doors within the room enclosure was established. Cool air was entrained through the bottom of openings; while, hot gases were expelled through the top. Figure 4.3(a) and 4.3(c) indicate this flow an increase in contrast from the top of bedroom 6's doorway. As the fire continued to grow in size, more energy was transfered to the surroundings. The TIC documented the thermal flow by false coloring the image with various heat indicating colors, as seen in Figure 4.3(b) and 4.3(d). Heat indicating colors are specific to certain temperature ranges and are utilized to visualize temperature hazards within the FOV, see Section 3.1.1 for further detail.

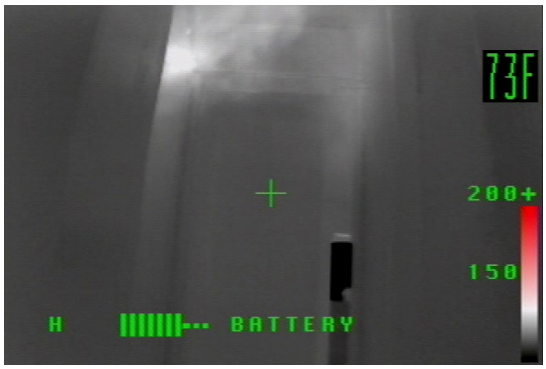

(a) Hallway: 100 s Post Ignition

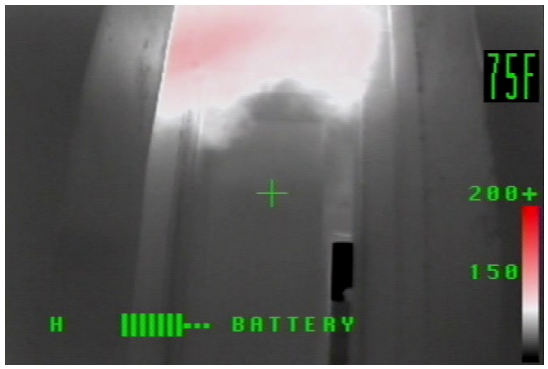

(b) Hallway: 125 s Post Ignition

(c) Living Room: 100 s Post Ignition

(d) Living Room: 125 s Post Ignition

Figure 4.3: TIC # 1 visual output 100 s after bedroom 6 ignition during Experiment # 9.

Similar fire development was experienced from the ignition in bedroom 5. Due to the designed two minute gap in ignition times, the flow from bedroom 6 dominated the image produced from the TIC. The initial stages of thermal flow from bedroom 5 are not visible by the TIC. Once the flow from bedroom 5 was large enough it began to mix with the flow from bedroom 6. This was documented by the TIC as a larger false colored area, as seen in Figure 4.4.

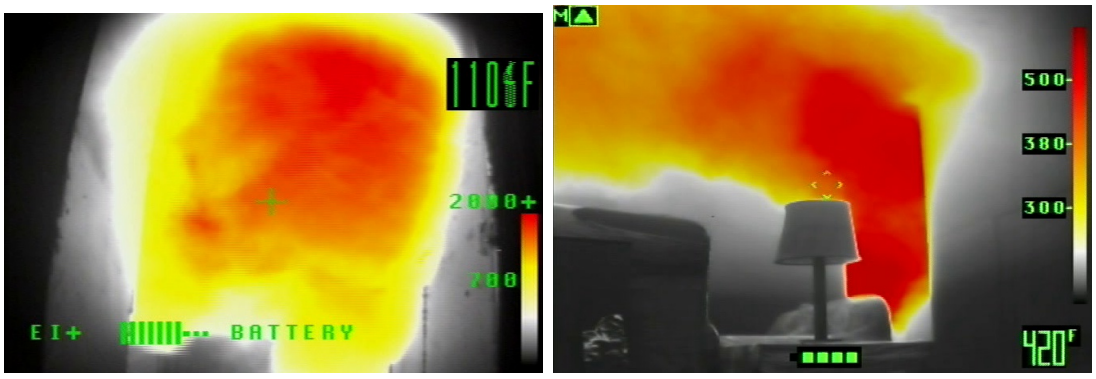

(a) Hallway: 230 s Post Ignition (b) Living Room: 230 s Post Ignition

Figure 4.4: TIC # 1 visual output of both thermal flows during Experiment # 9.

The fire grew continued to grow until suppression occurred. The TIC documented an increase in flow and maximum temperature, followed by an immediate decrease prior to door ventilation and suppression efforts. Figure 4.5 and 4.6 represent this behavior, respectively.

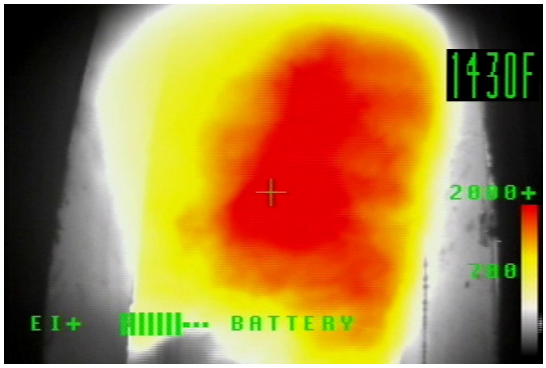

(a) Hallway: 232 s Post Ignition

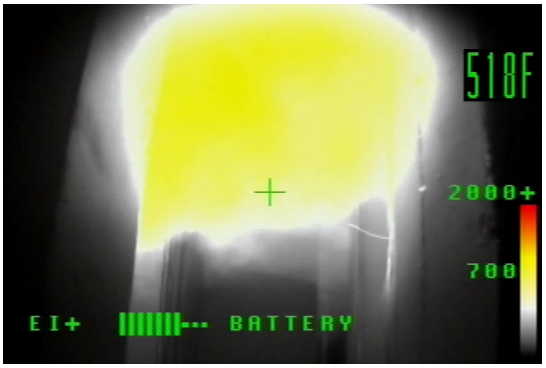

(b) Hallway: 242 s Post Ignition

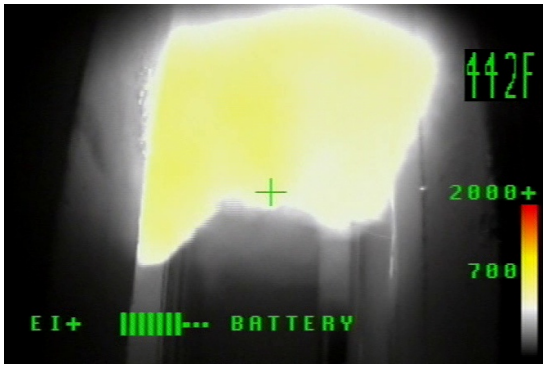

(c) Hallway: 252 s Post Ignition

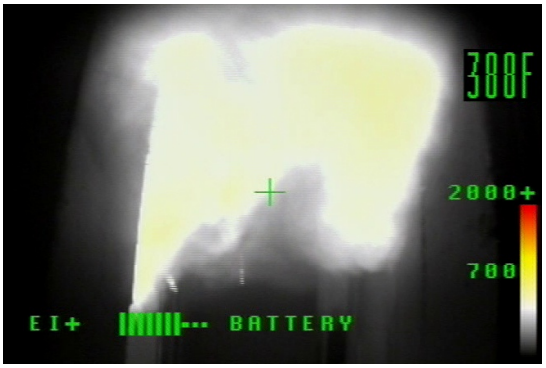

(d) Hallway: 262 s Post Ignition

Figure 4.5: TIC # 1 Camera Type 2 visual output during Experiment # 9 for the Hallway TIC. Images represent time of peak temperature and 10 s, 20 s, and 30 s after peak temperature occurs, respectively.

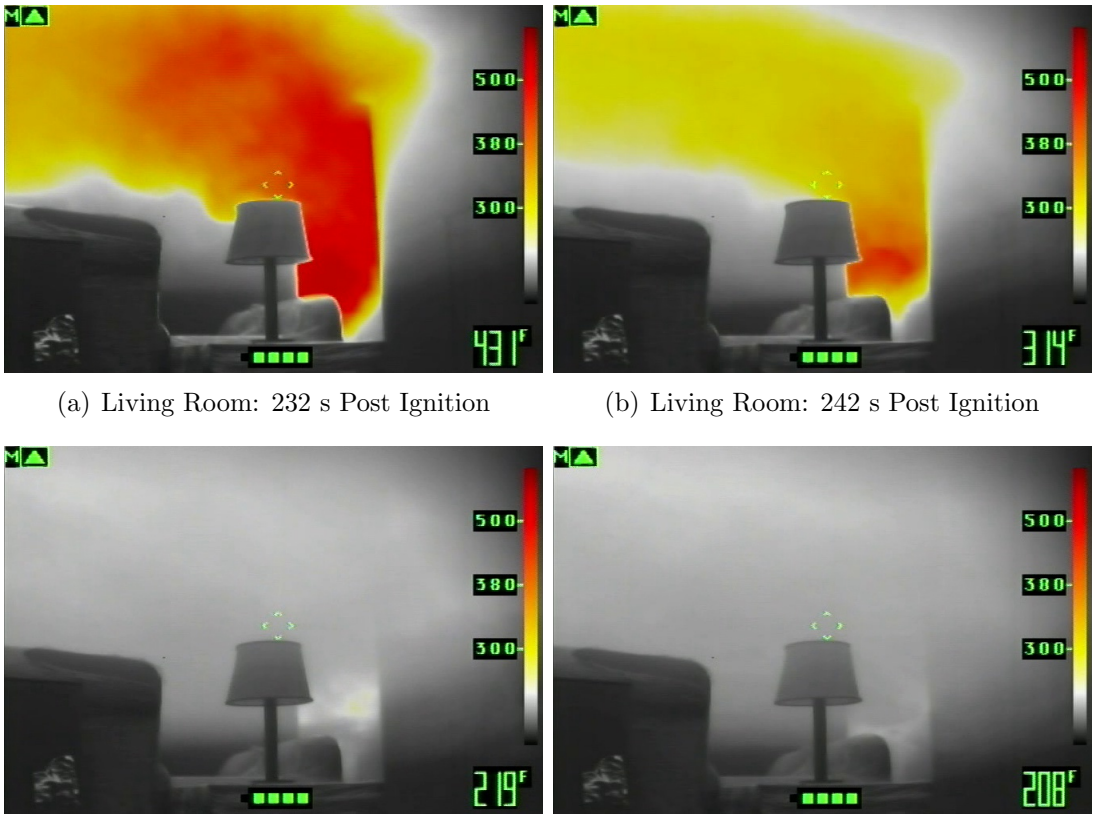

(a) Living Room: 232 s Post Ignition

(b) Living Room: 242 s Post Ignition

(c) Living Room: 252 s Post Ignition

(d) Living Room: 262 s Post Ignition

Figure 4.6: TIC # 1 Camera Type 2 visual output during Experiment # 9 for the Hallway TIC. Images represent time of peak temperature and 10 s, 20 s, and 30 s after peak temperature occurs, respectively.

The structure door was opened allowing for the thermal flow within the structure to grow. This was documented by the TIC with increase in false coloring of the thermal area, as seen in Figure 4.7.

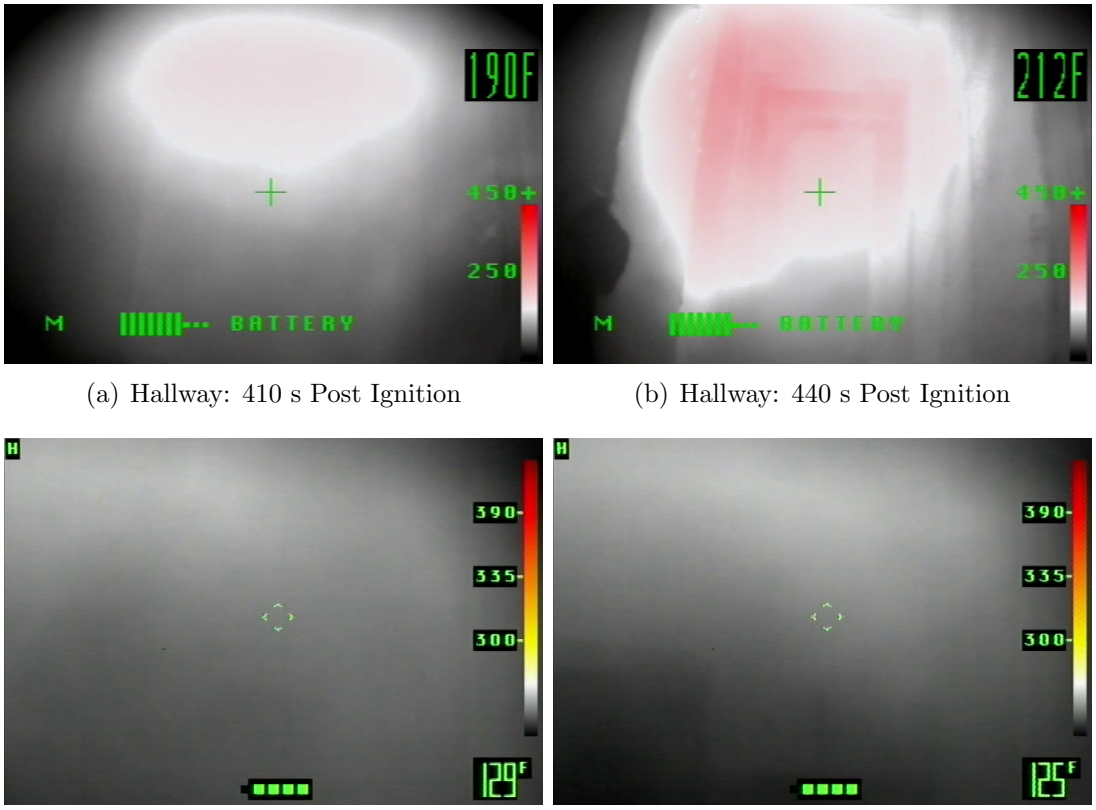

(a) Hallway: 410 s Post Ignition

(b) Hallway: 440 s Post Ignition

(c) Living Room: 410 s Post Ignition

(d) Living Room: 440 s Post Ignition

Figure 4.7: TIC # 1 visual output of both thermal flows during Experiment # 9.

Shortly after ventilation, suppression efforts began to extinguish the fire. The thermal flow depicted by the TIC decreased in size after the application of water. The TIC depicted in Figure 4.8, portrayed details of the scene with various contrasts.

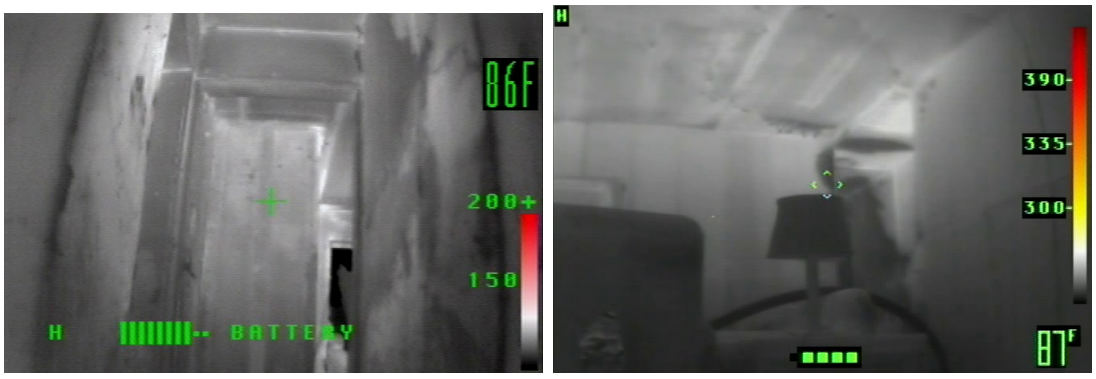

(a) Hallway: Test Conclusion (b) Living Room: Test Conclusion

Figure 4.8: TIC # 1 visual output of both thermal flows during Experiment # 9.

To analyze the TIC's ability to quantify the temperature hazard within the space, a comparison between TIC spot temperature and TC measurements was conducted. This required the TIC's spot temperature measurement to be converted into a text file. The methodology outlined in Appendix A was followed. The location of each TIC's measurement zone location was determined from inspection of visual output following the methodology outlined in Appendix B. The hallway TIC's measurement zone was located on the divider wall within bedroom 5 at an elevation of 1.52 m. The closest TC array to this location was located within bedroom 5. The temperature output produced from the TIC was compared to the temperatures measured from the TC array, 'Bedroom5'. The location of the living room TIC's measurement zone was on the living room wall to the left of the hallway entrance at an elevation of 2.13 m. The closest TC array was located within the hallway, between bedroom 5 and bedroom 4. The temperature output produced form this TIC was compared to the temperatures measured from the TC array, 'HallLeft'. Tem-

perature measurements obtained from each TIC and associated TC is presented in Figures 4.9 - 4.10.

Figure 4.9(a) and Figure 4.10(a) indicate that for both TIC locations, the spot temperature measurement produced an initial ambient temperature until ignition occurred. After which, an increase in temperature terminated into a peak maximum temperature. Before ventilation or suppression efforts began, a decrease in temperature was observed. These temperatures remained relatively stable until the experiment concluded. For both TC locations, the temperature measurements also remained at a steady ambient temperature until ignition. After which, an increase in temperature occurred which remained steady until ventilation and suppression efforts began. Following suppression efforts, temperatures returned to ambient conditions and remained throughout the conclusion of the experiment.

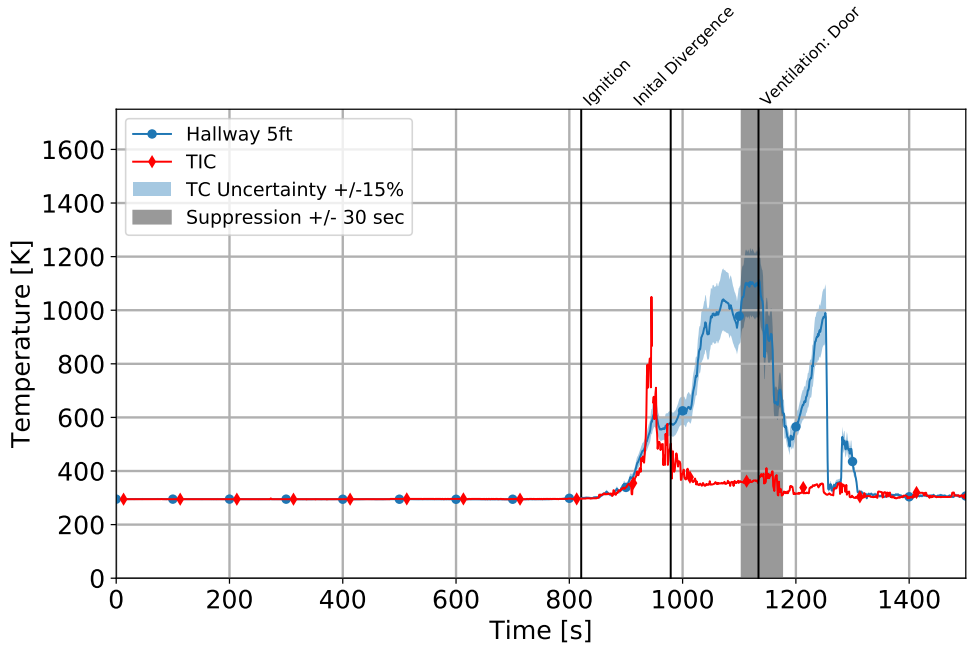

(a) Hallway: Temperature Comparison

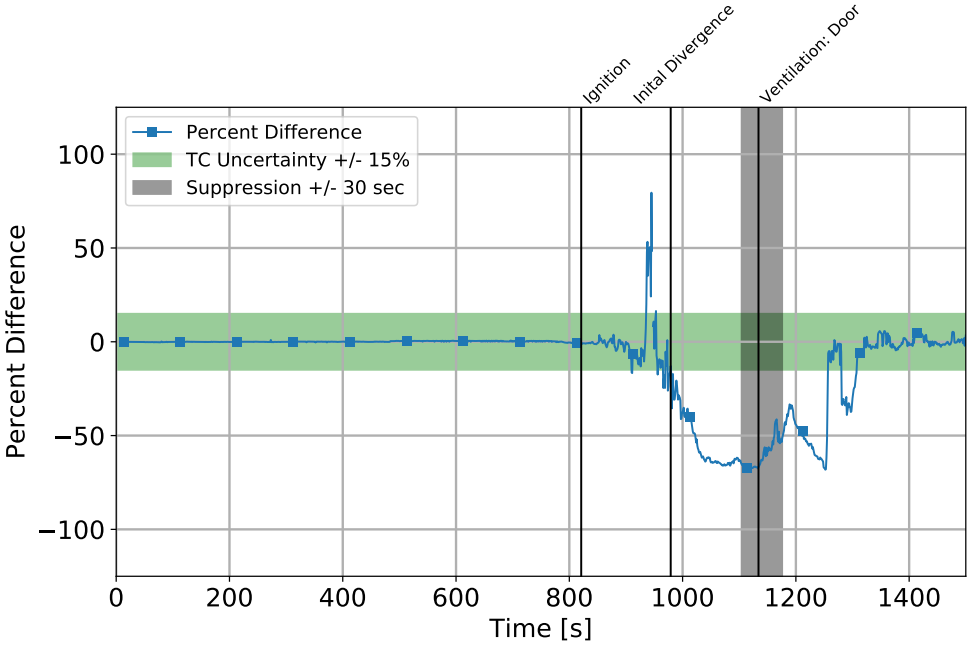

(b) Hallway: Percent Difference

Figure 4.9: Temperature data obtained from TIC # 1 and 'Bedroom5' TC array obtained from Experiment # 9. TC expanded uncertainty of ± 15 % is depicted on 4.9(a) by a light blue region.

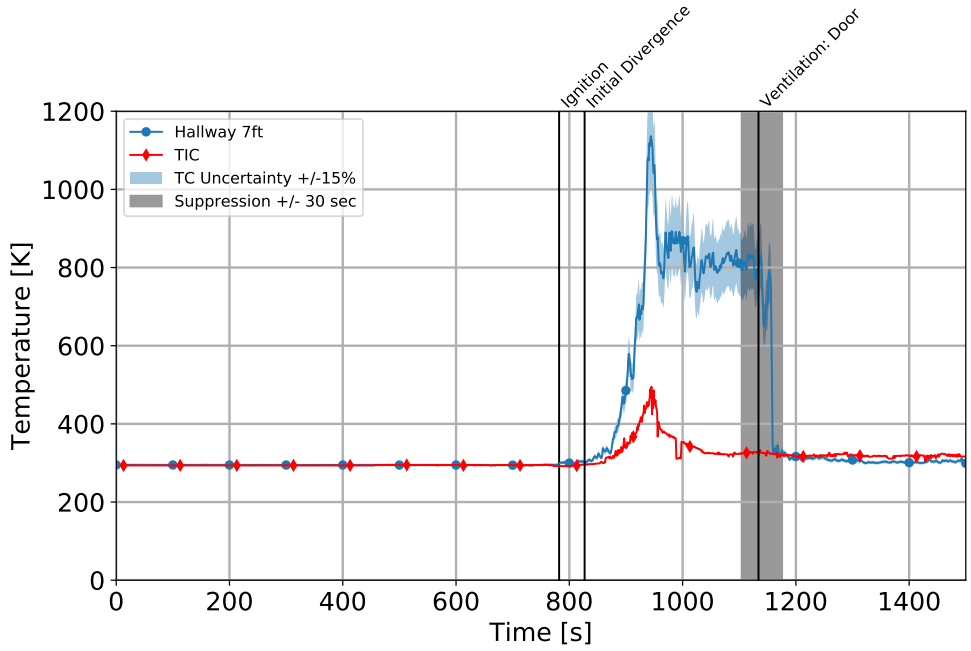

(a) Living Room: Temperature Comparison

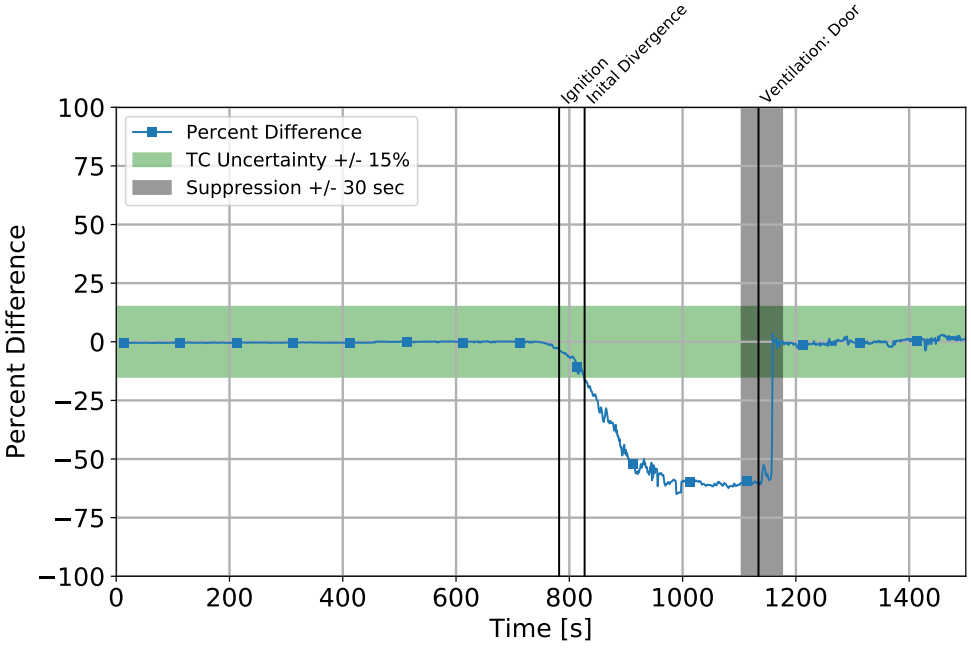

(b) Living Room: Percent Difference

Figure 4.10: Temperature data obtained from TIC # 1 and 'HallLeft' TC array obtained from Experiment # 9. TC expanded uncertainty of ± 15 % is depicted on 4.10(a) by a light blue region and 4.10(b) as a light green region.

Figure 4.9(b) and Figure 4.10(b) depict the TC uncertainty, indicating when the two temperature methods produce indistinguishable temperatures. For both TIC locations, the comparison between TIC spot temperatures and TC measurements produced similar results. It was determined that the two temperature measurement methods were comparative for pre-ignition and post-suppression conditions. The average percent difference was 1 % and 16 %, respectively. The post-suppression average percent difference is higher than ± 15 %, indicating that the two methods are not comparable. However, this is due to the increase in temperature observed from the TC array after suppression. If this time is excluded, the percent differences is less than the expanded uncertainty associated with the TC measurement. The two temperature measurements are not comparable for combustion conditions. The percent difference is 53 %.

After comparing both methods, it was established that the TIC temperature measurements indicated a peak and decay. Simultaneously the TC indicated gas temperatures were steady at an elevated magnitude. It was expected that wall temperatures should continue to increase while gas temperatures are elevated. The temperatures from the TIC suggested otherwise indicating that the radiation received by the TIC was impacted. This was verified by visually analyzing the TIC video feed, Figures 4.5 - 4.6. The thermal flow, indicated by yellow, orange, and red, grew in size till a peak temperature occurred, then the flow quickly diminished. This should indicate that the fire intensity was decaying; however, TC measurements indicate the opposite, suggesting that the radiation received by the TIC was impacted.

After evaluating both TIC locations for each experiment within this series, the limitations and obstacles associated with this type of analysis were determined. The measurement zone location influenced the behavior of the TIC spot temperature measurements. The Hallway TIC in Experiments # 2, 6, 8, and 10 had measurement zone locations below 0.91 m. This height was typically below the hot gas layer throughout the duration of the experiment. During these experiments the TIC temperatures gradually increased. The remaining experiments had measurement zone locations above 0.91 m. The measurement zone was located within the smoke layer once ignition occurred. During these experiments the TIC temperatures increased into a peak temperature. This emphasized the need for repeatable measurement zone locations near TC arrays. Figure 4.11 indicates the TIC spot temperature measurements when the measurement zone was below 0.91 m.

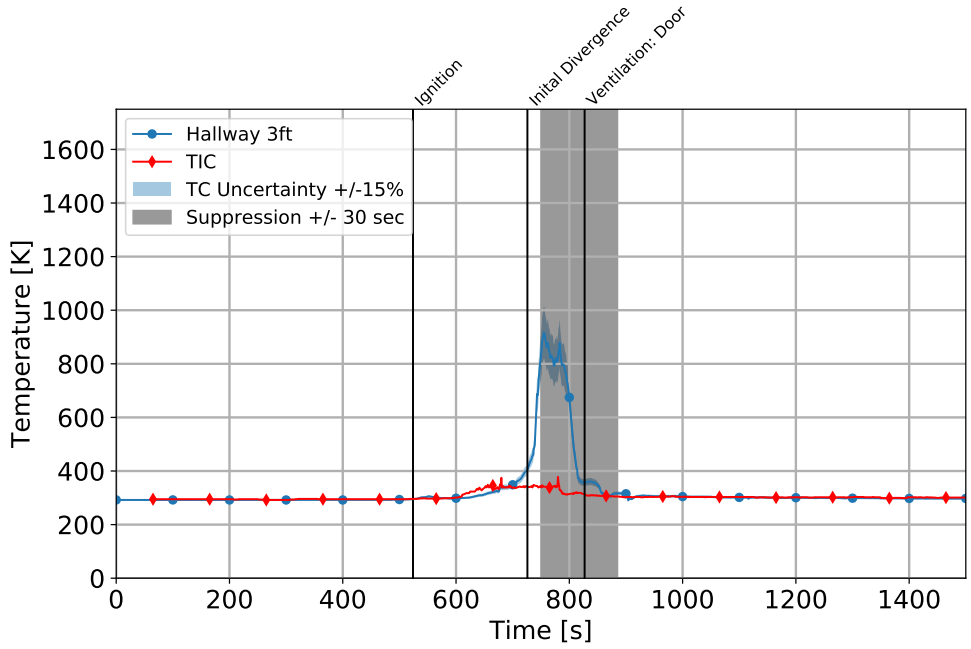

(a) Experiment # 8 Temperature Comparison

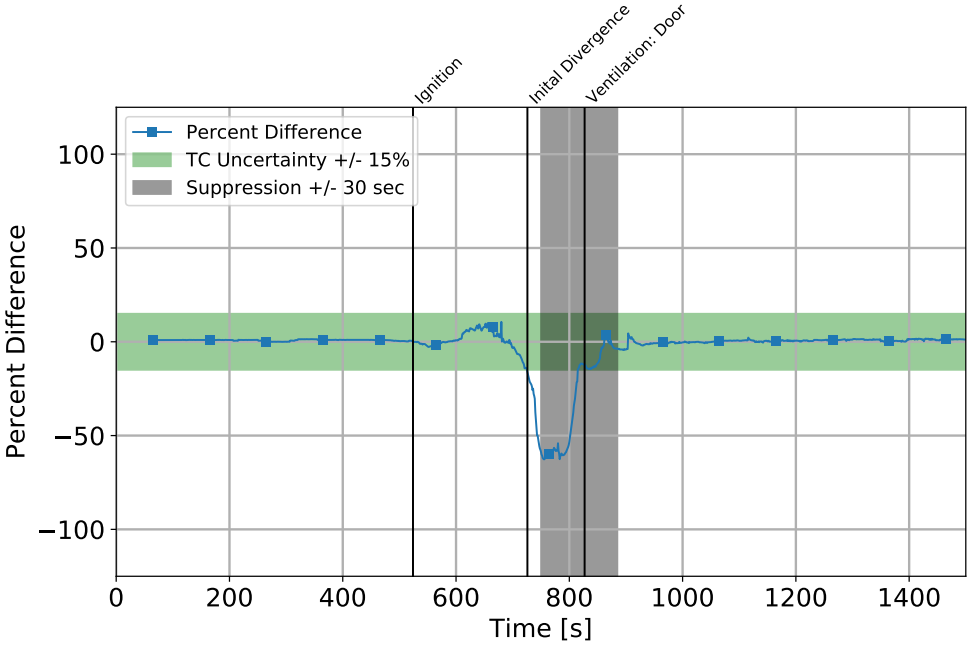

(b) Experiment # 8 Percent Difference

Figure 4.11: Temperature data obtained from TIC # 1 and Bedroom2 TC array obtained from Experiment # 8. TC expanded uncertainty of ± 15 % is depicted on 4.11(a) by a light blue region and 4.11(b) as a light green region.

This TIC spot temperature behavior from Figure 4.11(a) is different than from Figures 4.9 - 4.10. The TIC spot temperature measurement minimally responded to the increase in heat produced from the fire. The response from the TIC spot temperature measurement was to be expected as its measurement zone was within the lower cool thermal layer. The cool thermal layer was less affected by smoke. It was assumed the TIC was determining the temperature of the wall without influence from the smoke layer. As the wall was not isothermal, upper portions are hotter than lower portions. The temperature gradient of the wall was reflected by the TIC spot temperature measurement when the measurement zone was below the smoke layer.

The evaluation of the measurement zone location only considered the distance off the floor, it does not account for the distance between the TIC and the target object. This distance was not investigated by this analysis as there were not multiple TC arrays located in series throughout the structure. However, it was determined that at shorter distances between the TIC and target object, TIC temperature outputs become more representative of true object temperatures. During the tactical evolutions this study included, it was necessary for firefighters to enter the FOV for both camera locations. Although the firefighters' presence in the FOV only amounted to a short duration, both TIC types were able to display the temperature difference between the firefighters and the surrounding environment, when firefighters were present in the foreground of the TIC FOV. See Figure 4.12 for visual representation of the TIC view with and without firefighter presence.

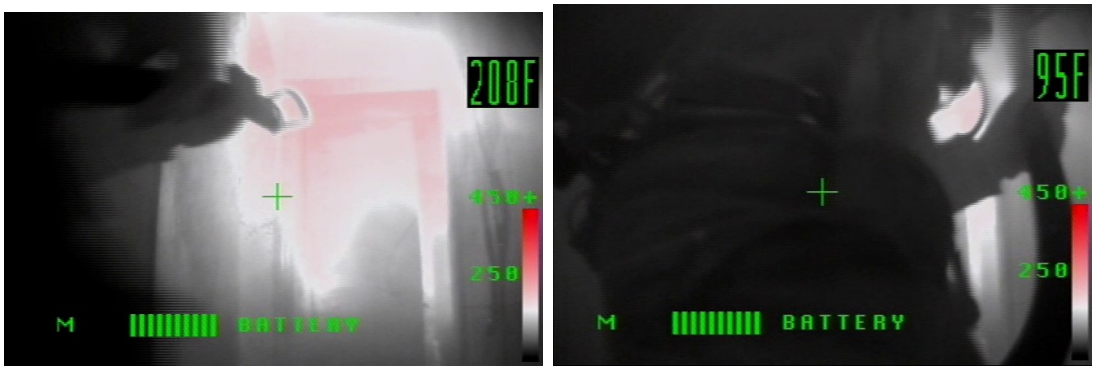

Figure 4.12: Typical FOV without (left) and with (right) firefighters present the measurement zone for the hallway Type 2 TIC. The time difference between the two images was roughly 2 seconds.

Although the temperature of the firefighters gear was not recorded it can be assumed to be some temperature between the firefighter's body temperature and the ambient (before combustion) temperature, resulting in a temperature less than the heated environment. As seen in Figure 4.12, the TIC was able to determine this temperature difference. This suggests that at short distances the emitted energy IR wavelengths can penetrate the semi-opaque atmosphere to be absorbed by the TIC measure temperatures.

The living room TIC was accompanied by a standard video camera, which allowed for visual observation of the living room and hallway during experimentation. The smoke obscuration of the environment was observed. The living room retained visual clarity longer than the hallway, which is expected as the seat of the fire was located in the bedroom at the end of the hall and smoke follows general physic principles, flowing from areas of high concentration to areas of low concentration. This additional time did not appear to have a substantial effect on the TIC spot

temperature measurements as the data obtained from both TIC locations produced similar results, when compared to the TC locations.

For complete documentation of experimental results, including all plots, see Appendix B.

4.2 Impact of Fire Attack Utilizing Interior and Exterior Streams on Firefighter Safety and Occupant Survival: Full Scale Experiments

UL FSRI conducted a series of twenty-four experiments to investigate the effects of various ventilation configurations and suppression tactics on interior conditions during a structure fire. Ventilation configurations included none, single window, or double window. Each ventilation configuration investigated the combined effects when coupled with both interior and exterior suppression tactics. The findings from this investigation are summarized in the report, *Impact of Fire Attack Utilizing Interior and Exterior Streams on Firefighter Safety and Occupant Survival: Full Scale Experiments* [12].

A ranch-style structure was built specifically for this series of experiments. After each individual experiment was conducted, the structure was outfitted with new materials to ensure repeatability. In some experiments, the turn around rate between burns did not allow enough time for drywall mud to be completely dry. This caused increased moisture within the gypsum walls. During these cases the TIC produced cooler ambient temperatures than the TC. A fire was set in either bedroom 1, no or single ventilation, or simultaneously in both bedroom 1 and bedroom 2, double ventilation. Suppression tactics varied between interior and exterior attacks with various nozzles types and moment techniques. Instrumentation was deployed throughout the structure to monitor interior conditions during experiments. This

included thermocouples to monitor gas temperatures and TICs to monitor thermal flows during combustion. TIC # 2 TIC was employed in two locations within the structure. The structure layout and instrumentation locations are depicted by Figure 4.13.

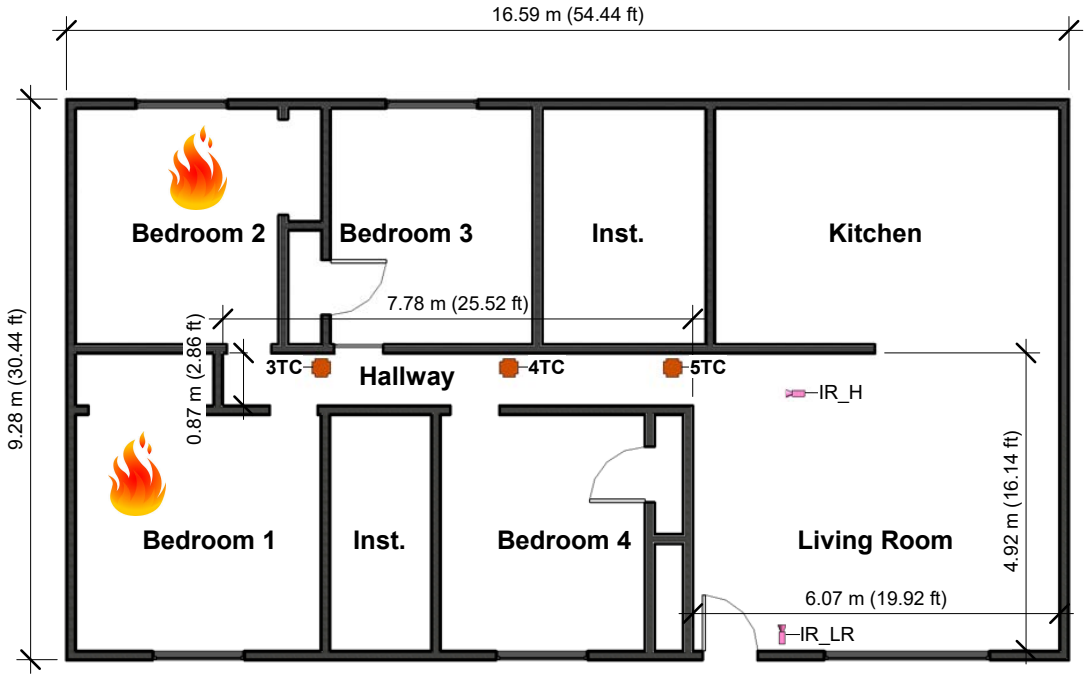

Figure 4.13: Ranch-style structure built for the Fire Attack Experiments [12]. Orange crosses represent TC arrays which measure at 0.30 m intervals. Pink symbols represent the two TIC locations.

Experiment # 13 and Experiment # 15 explored the combined effects of double ventilation with interior suppression efforts. During both experiments bedroom 1 and bedroom 2's windows were framed open; while, all other openings were simulated closed at the beginning of the experiment. Following a similar time-line of events and interventions, a fire was ignited in both bedroom 1 and bedroom 2 si-

multaneously. The fire was allowed to grow and burn uninterrupted for roughly five and half minutes until the front door was opened. At which time, firefighters entered the structure and began suppression efforts. The remaining openings within the structure were ventilated some time after: four and a half minutes later, Experiment # 13, and four minutes later, Experiment # 15.

Before ignition of bedrooms 1 and 2 during Experiment # 13, TIC # 2 produced an image of the hallway and living room with little contrast. The lack of varying contrast was expected, as the space and solid objects were assumed to all be at ambient temperatures. Figure 4.14(a) depicts that although the details of the space were difficult to determine, the length of the hallway, bedroom entrances, and additional instrumentation were apparent. Figure 4.14(c) depicts the part of the living room, including the back of the couch and bookcase. As heat generated from the fire transfer to the surrounding environment, the TIC produced an image with varying contrasts. Figure 4.14(b) and Figure 4.14(d) represents this change in visual output, as boundaries of the space and details become more distinct.

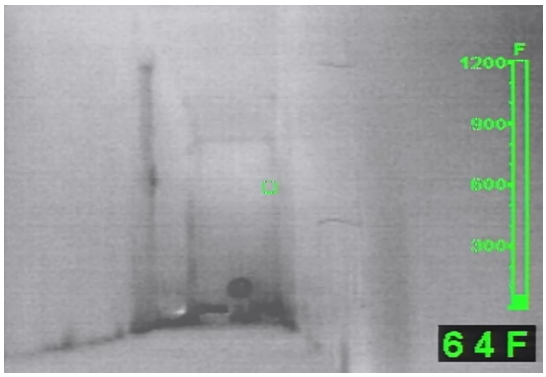

(a) Experiment # 13: Prior to Ignition

(b) Experiment # 13: 90 s Post Ignition

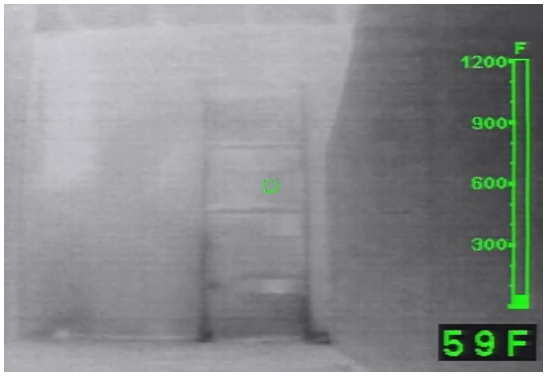

(c) Experiment # 15: Prior to Ignition

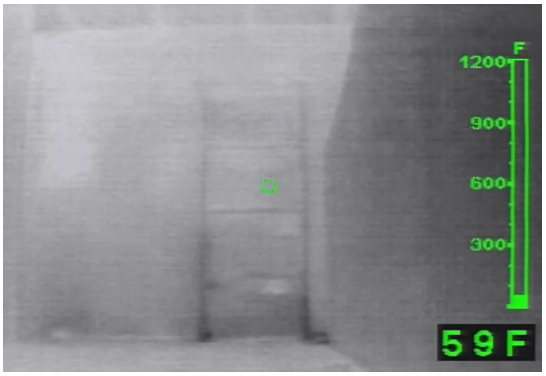

(d) Experiment # 15: 83 s Post Ignition

Figure 4.14: TIC # 2 visual output at ambient conditions during Experiment # 13 and Experiment # 15.

As the fire continued to grow and burn, air entrainment through windows and doors within bedroom 1 and 2 increased. This created a bi-directional flow through these openings. Hot thermal gases exited the room from the top of these openings; while, cool air entered the room from the bottom of these openings. Figure 4.15(a) depicts these thermal flows by an increase in contrast at the end of the hallway. This flow increased in temperature as the fire continued to burn. Figure 4.15(b) indicated this growth by false coloring the image yellow, orange, and red.

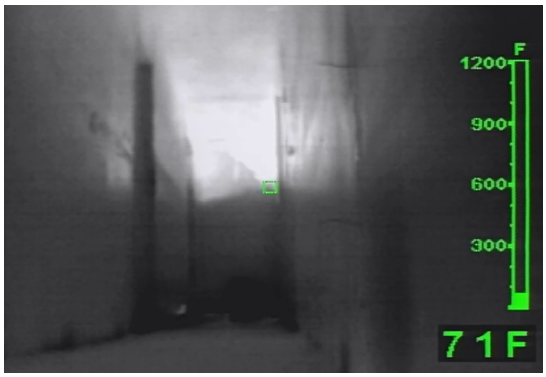

(a) Experiment # 13: 120 s Post Ignition

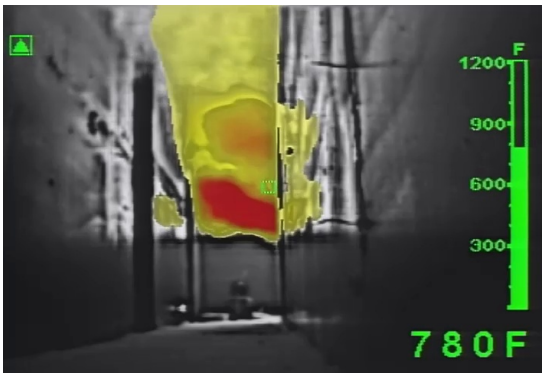

(b) Experiment # 13: 190 s Post Ignition

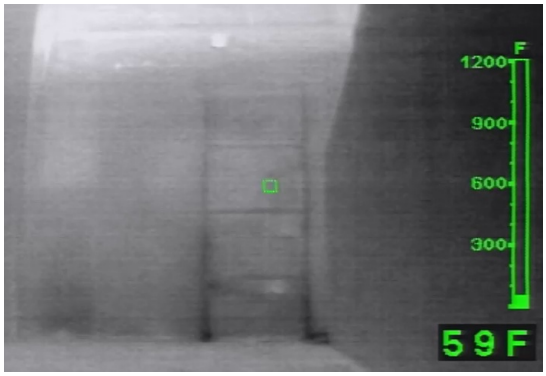

(c) Experiment # 15: 113 s Post Ignition

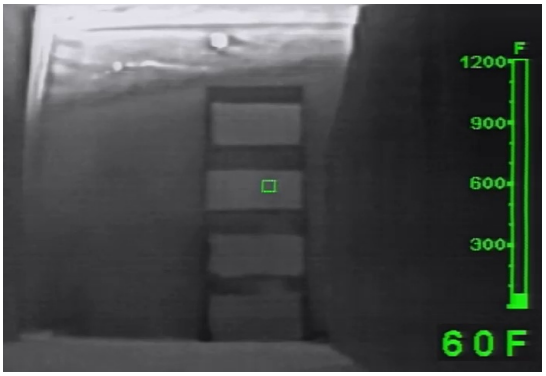

(d) Experiment # 15: 173 s Post Ignition

Figure 4.15: TIC # 2 visual output at ambient conditions during Experiment # 13 and Experiment # 15.

The fire continued to grow until interior suppression efforts began. The TIC documented this growth with increased false colored areas. Immediately following this growth the TIC displayed a indicated a decay in fire size without ventilation or suppression interventions. Figures 4.16 - 4.17 indicates this decay.

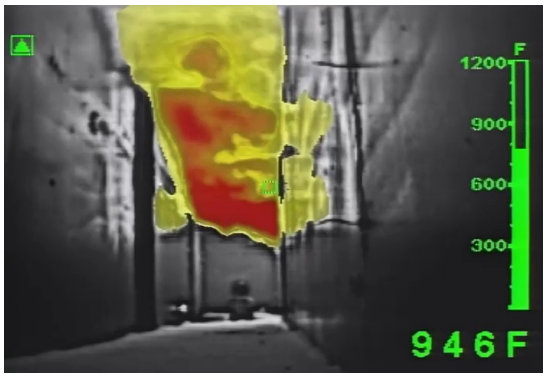

(a) Experiment # 13: 198 s Post Ignition

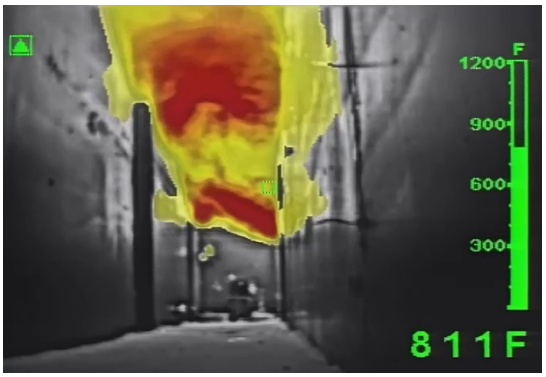

(b) Experiment # 13: 208 s Post Ignition

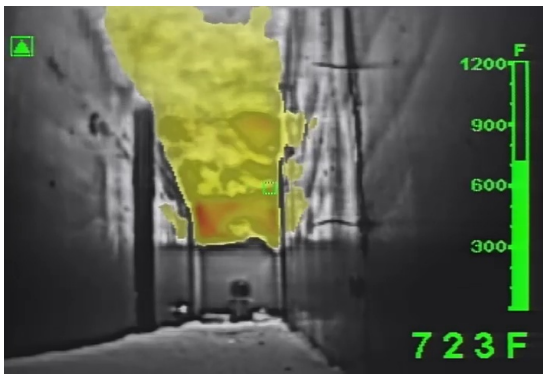

(c) Experiment # 13: 218 s Post Ignition

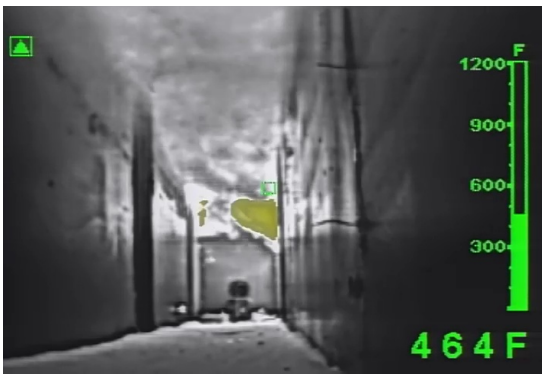

(d) Experiment # 13: 228 s Post Ignition

Figure 4.16: TIC # 2 visual output during Experiment # 13 for the Hallway TIC. Images represent time of peak temperature and 10 s, 20 s, and 30 s after peak temperature occurs, respectively.

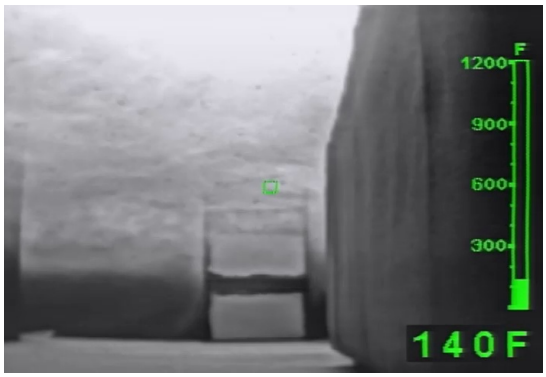

(a) Experiment # 15: 285 s Post Ignition

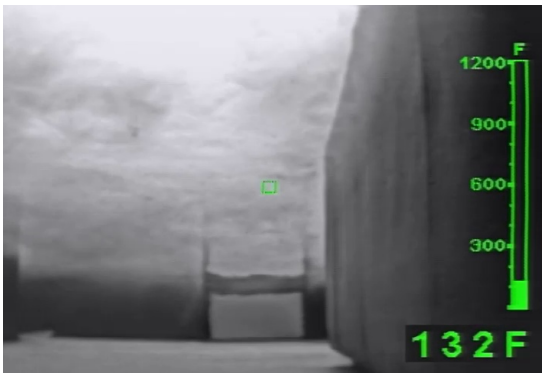

(b) Experiment # 15: 295 s Post Ignition

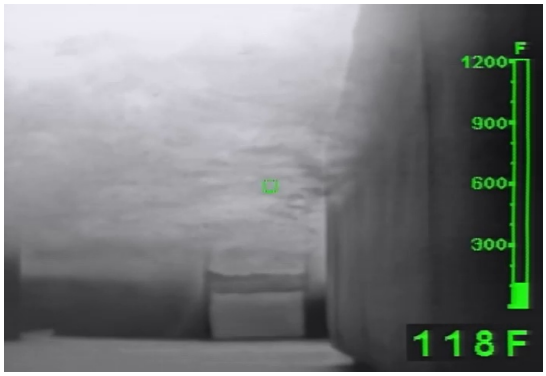

(c) Experiment # 15: 305 s Post Ignition

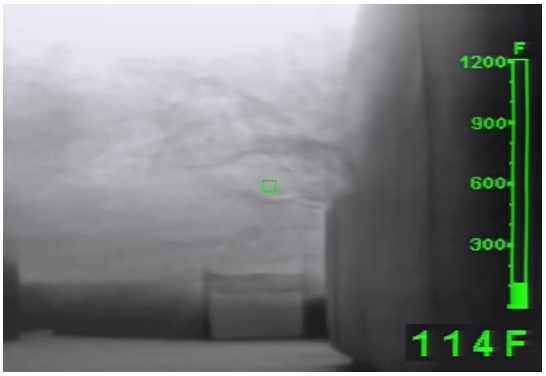

(d) Experiment # 15: 315 s Post Ignition

Figure 4.17: TIC # 2 visual output during Experiment # 15 for the Living Room TIC. Images represent time of peak temperature and 10 s, 20 s, and 30 s after peak temperature occurs, respectively.

After the front door was opened firefighters made their way to the hallway and began suppression efforts. A short burst of water was introduced to the hallway to cool the environment before advancing closer to the fire. Firefighters than moved to the end of the hallway to extinguish the fires in both rooms. Figure 4.18(a) represents the TIC visual output shortly after the front door was opened. Figure 4.18(b) indicates the decrease in temperature after burst suppression began. After suppression efforts the environment returned to a quasi ambient conditions.

(a) Experiment # 13: 345 s Post Ignition

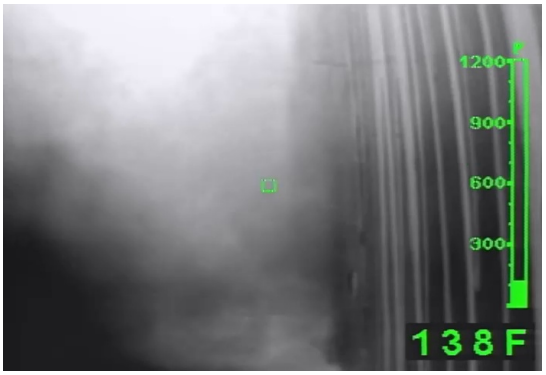

(b) Experiment # 13: 360 s Post Ignition

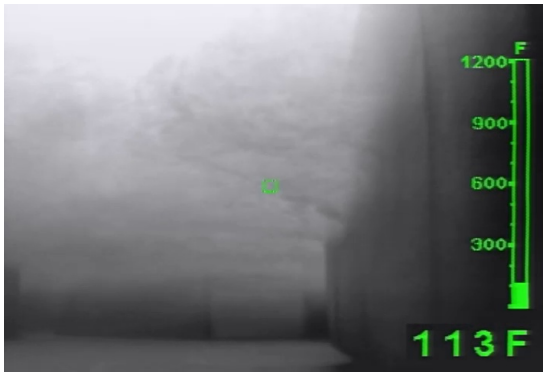

(c) Experiment # 15: 339 s Post Ignition

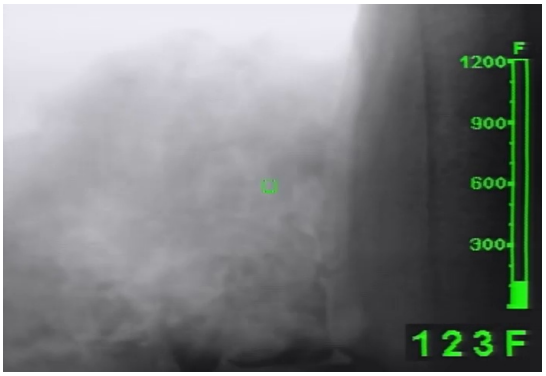

(d) Experiment # 15: 353 s Post Ignition

Figure 4.18: TIC # 2 visual output at ambient conditions during Experiment # 13.

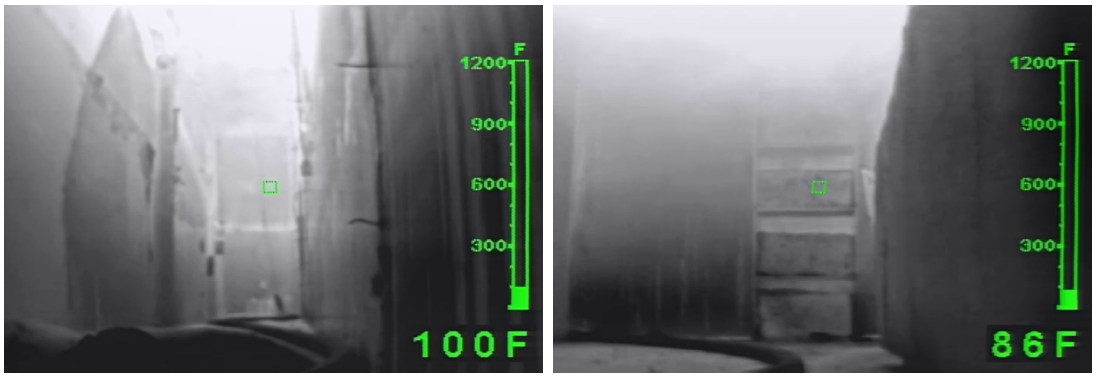

(a) Experiment # 13: Test Conclusion (b) Experiment # 15: Text Conclusion

Figure 4.19: TIC # 2 visual output at ambient conditions during Experiment # 13.

In order to evaluate the evaluate TIC # 2's ability to quantify the thermal hazards within the environment, the TIC spot temperatures were compared to TC temperature measurements. The TIC's spot temperature measurement was converted into a text file following the methodology outlined in Appendix A. To Determine the location of the measurement zone a two-dimensional analysis was preformed. First, the height was determined by following the methodology presented in Appendix B. Second the depth within the FOV was determined by correlating the distance between the TIC lens and target object to one of several TC arrays located within the hallway. The Hallway TIC measurement zone height during Experiment # 13 was approximated to an elevation of 1.52 m and depth was determined to be far, or residing at the end of the hallway. This depth correlated to the TC array located at the end of the hallway, labeled '3TC'. The Living Room TIC measurement zone height during Experiment # 15 was approximated to an elevation of 0.91 m. Only one TC array was located in the living room, labeled '5TC'. The temperature

measurements obtained from both instruments are presented in Figure 4.20

Figure 4.20(a) indicates that the Hallway TIC spot temperature output remained at a steady ambient temperature until ignition occurred. At which time, an increase in temperature occurred terminating into a peak temperature. Immediately afterwards, a decrease in temperature was witnessed. This lesser temperature remained fairly constant throughout the remainder of the experiment. The TIC spot temperatures appeared to be unaffected from ventilation and suppression tactics. This behavior differs from the measurements obtained from the TC array. Figure 4.20(a) indicates that the TC initial ambient temperature remained steady until ignition. After which, an increase in temperature occurred terminating into elevated temperature. This temperature remained constant until ventilation and suppression tactics occurred. These tactics resulted in a steady lesser temperature throughout the duration of the experiment. To visually quantify the agreement between the TIC spot temperature and the TC measurements, the percent difference between the two methods was determined and plotted on Figure 4.20(b). When both temperature method outputs overlap the $\pm$ 15 % TC uncertainty region, it can be assumed that the two are producing indistinguishable results. Figure 4.20(b) indicates that the comparison between these two methods produced similar results during during pre-ignition and post-suppression conditions. The average percent difference is 1 % and 5 %, respectively. The comparison produced vastly different results during combustion conditions with an average percent difference of 34 %.

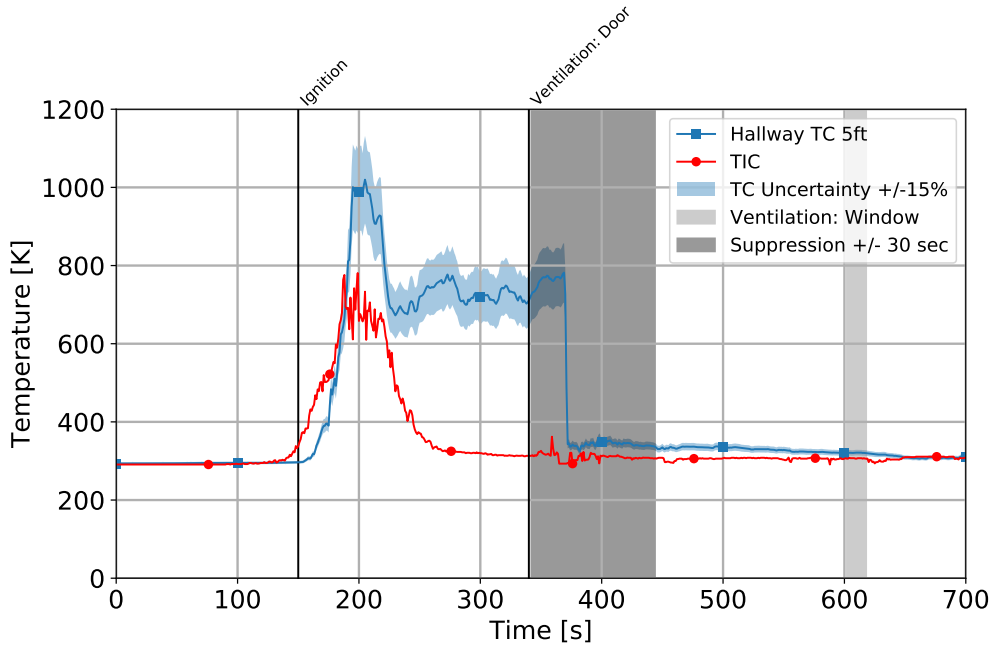

(a) Experiment # 13: Temperature Comparison

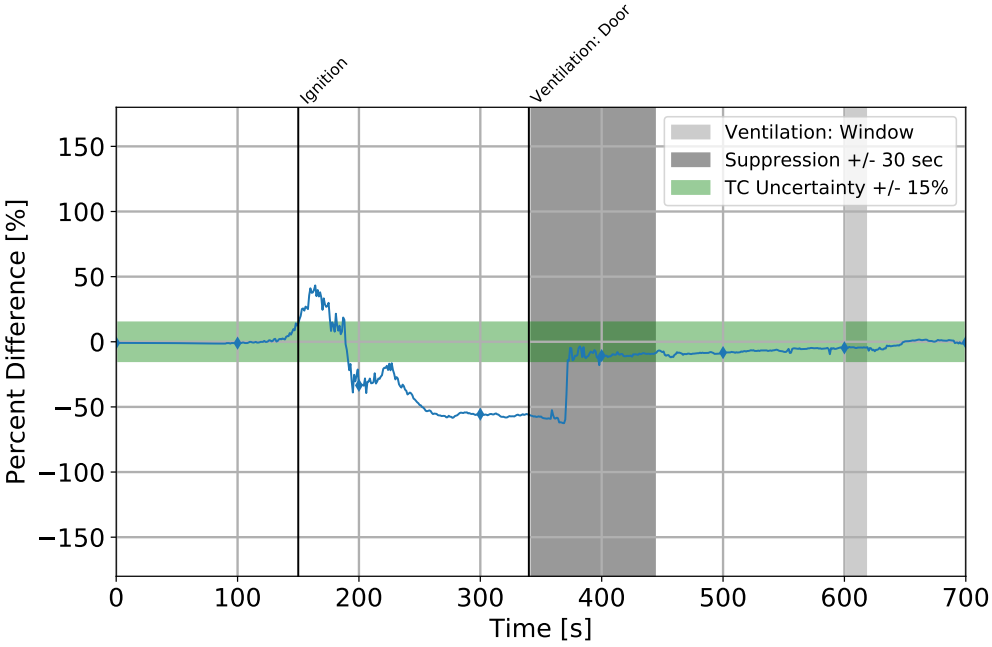

(b) Experiment # 13: Percent Difference

Figure 4.20: Temperature data obtained from TIC # 2 and 3TC TC array during Experiment # 13. TC uncertainty of ± 15 % is depicted on 4.20(a) as a light blue region and on 4.20(b) by a light green region.

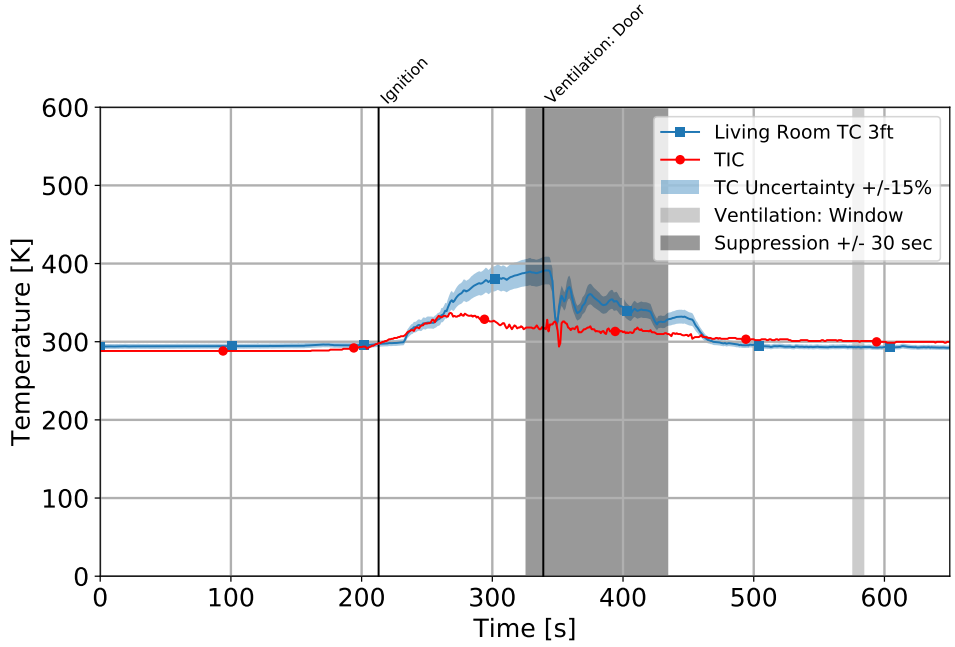

(a) Experiment # 15: Temperature Comparison

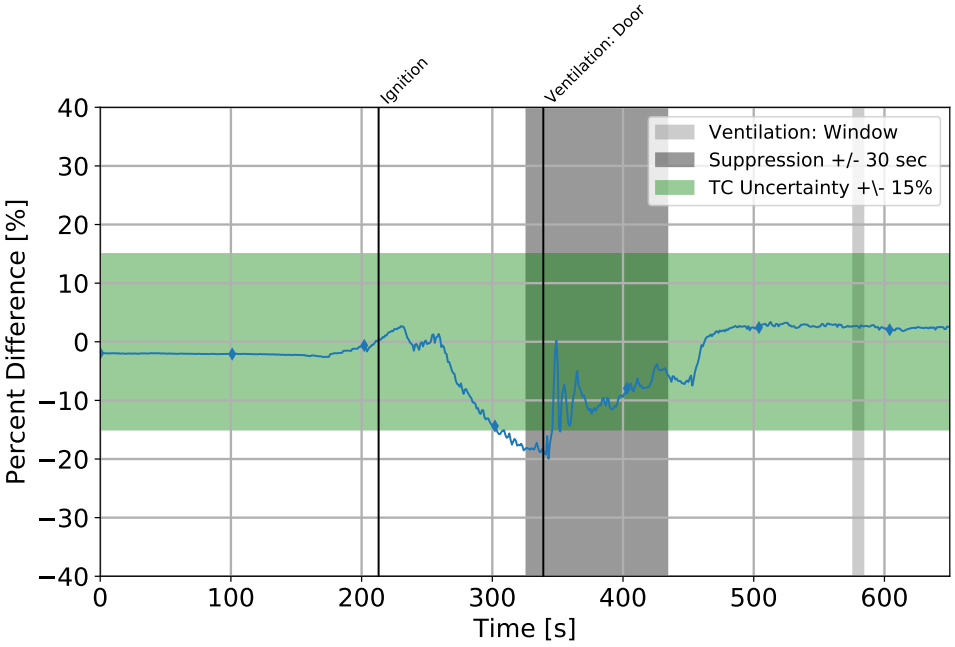

(b) Experiment # 15: Percent Difference

Figure 4.21: Temperature data obtained from TIC # 2 and 5TC during Experiment # 15. TC uncertainty of ± 15 % is depicted on 4.21(a) as a light blue region and on 4.21(b) by a light green region.

Figure 4.21(a) indicates the Living Room TIC spot temperature measurement remained at an initial ambient temperature until ignition. After which, an increase in temperature gradually occurred terminating into an elevated steady temperature. These steady temperatures gradually decrease prior to suppression tactics. Temperatures continue to decrease, with little or no impact from suppression efforts, for the remainder of the experiment. The TC produces measurements of steady ambient temperatures until ignition. After which temperates increase to a elevated magnitude. These elevated temperatures remain steady until ventilation and suppression tactics are introduced. After which temperatures return to a lower magnitude for the remained of the experiment. Figure 4.21(b) depicts the percent difference between the two temperature methods during Experiment # 14. The two temperature methods produce indistinguishable results throughout the majority of the experiment. The average percent difference for pre-ignition, combustion, and post suppression are as follows: -2 %, 17 %, 2 %, respectively.

After a comparison, it was determined that the Hallway TIC indicated a decrease in temperature while the TC indicated a growing/constant temperature. It is expected that wall temperatures would continue to increase as long as air temperatures increase or remained at a greater magnitude than the wall. As the TIC indicates otherwise, it was concluded that the radiation received by the TIC was impacted. This was verified by visually analyzing the TIC video feed. The thermal flow, indicated by areas of higher contrast, grew in size till a peak temperature was recorded shortly afterward 'white out' (thermal overload, saturation of false color or contrast) was achieved. The Living Room TIC indicated steady temperatures

similar to TC temperatures but at a lesser magnitude. This suggests that the radiation received by the TIC was not impacted during combustion conditions as the wall would continued to increase/hold steady.

During Experiments # 1, 12, and 17 the time to suppression was extended. This extended time-line did not affect the comparison between the two temperature methods, as similar observations to the above example analysis were determined. The TIC's with a FOV of the hallway, produced temperature outputs comparative to TC measurements for pre-ignition, the initial temperature increase during combustion, and post-suppression. During combustion the two temperature methods suddenly diverged, without correlation to any ventilation or suppression tactic. The TIC's with a FOV of the living room, produced temperature outputs comparative to TC measurements during the entire experiment. During combustion the two temperature methods gradually diverged. This indicates that radiant energy absorbed by the TIC in the Hallway locations was impacted while the TIC in the living room was representative of the actual wall temperature.

Agreement between the two temperature methods was observed during the initial combustion temperature growth for the TIC with a FOV of the hallway, regardless of ventilation type. While, agreement was observed throughout the entire combustion time-frame for the TIC with a FOV of the living room, regardless of ventilation type. Evaluating each TIC location, it was apparent the TIC located in the hallway produces a higher percent difference for combustion conditions than the TIC located in the living room. It again appeared that something was impacting the radiant energy absorption of the TIC, which affected the TIC closer to the

fire origin more quickly and more severely than the TIC located remotely from the fire origin. The average percent difference for each time period is represented by Tables B.8 - B.10.

The evaluation of the measurement zone location considered the height of the measurement zone location for both TIC locations. Specifically, the distance between the TIC and the target object was evaluated for the TIC with a hallway FOV. During this series of experiments there were three TC arrays located throughout the hallway, 3TC, 4TC, and 5TC. The temperature comparison for each TIC with a hallway FOV was between the TIC and the TC closest to the measurement zone location. The temperature behavior recorded in Experiment # 3 is different than the remaining experiments, as its measurement zone was at the start of the hallway. The temperatures behave more similarly to the temperatures recorded from the TC located in the living room. During this experiment the percent difference was low throughout all time-frames, indicating that for this location the TICs spot temperature measurement was similar to the TC temperature measurement. The temperatures in Experiments # 2 & 3, experience lower peak temperatures than the remaining experiments, as their measurement zone locations were in the middle of the hallway. The percent difference during combustion for these two experiments were similar to the percent difference for the experiments with a measurement zone at the end of the hallway; indicating distance did not affect TIC spot temperature measurements.

While the evaluation of the measurement zone location did not evaluate the distance between the TIC and target object for the TIC with a living room FOV, it

was determined that at shorter distances the TIC spot temperature measurement more resembles the TC temperature measurements. It was necessary for firefighters to enter the living room FOV throughout experimentation; specifically, between time of initial entry to time at the beginning of the hallway. Although firefighter presence in the TIC FOV amounted to a short duration in most instances, the TIC was able to determine the temperature difference between the firefighters and the surrounding heated environment. Figure 4.22 depicts this temperature difference with two images taken roughly 2 seconds apart.

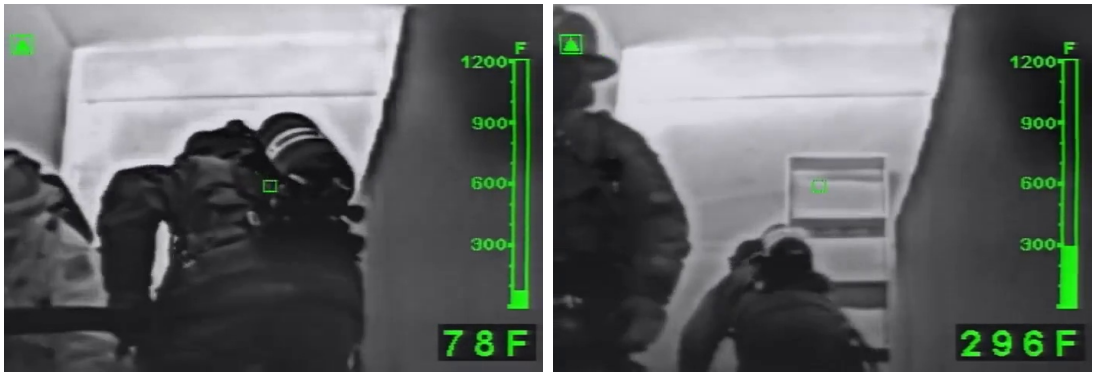

Figure 4.22: Typical FOV with (left) and without (right) firefighters present the measurement zone for the front door IR camera.

The temperature of the firefighters gear was not recorded; but, can be assumed to be between the firefighter's body temperature and the ambient environment temperature, resulting in a temperature less than the heated environment. As seen in Figure 4.22, the TIC was able to detect the difference in temperature between the firefighter and the surrounding environment. This suggests that at short distances the emitted energy IR wavelengths can penetrate the semi-opaque atmosphere.

Chapter 5: Study Design & Methods

The second phase of this report was to design and conduct experiments with the goal of assessing the TIC's spot temperature measurement. These experiments were conducted at room-scale and leveraged information and knowledge obtained during initial evaluation summarized in Section 4. The initial evaluation compared spot temperature measurements to gas phase TC measurements. This comparison produced large percent differences. In an attempt to better quantify spot temperature measurements, the effects of smoke opacity and distance between TIC and target object were investigated.

To further investigate how smoke opacity affects the TIC spot temperature measurements, each TIC was evaluated in two different environments: an ambient environment and a combustion environment. During the baseline experiments, the ambient environment was not altered in any way. During the room-scale fire experiments, the environment was affected by heat, smoke, and flames produced by the fuel load described in Section 5.2.1. Three manufactures of fire service TICs were investigated by this report; Table 5.1 lists the relevant product information for these TICs [27–29].

Each experimental series was conducted in a room-scale fire training prop

Table 5.1: Fire Service TICs used in both series of experiments.

TIC	Microbolometer Material	Spectral Response	Emissivity
# 1	VOx	8.0 - 14 μm	0.95
# 2	VOx	7.0 - 14 μm	Un-published
# 3	A-Si	7.5 - 14 μm	Un-published

located at the Delaware County Emergency Service Training Center (DelCo). The prop was constructed from a modified metal shipping container, represented by Figure 5.1. This specific training prop was previously used in the FEMA/DHS2014 - Training Fires Experiment [48]. The prop consisted of a 7.0 m x 1.22 m long hallway terminating into roughly a 2.44 m x 4.6 m room. A layer of 13.00 mm thick cement board was installed on top of the subfloor producing a consistent height of 2.36 m. The walls of the prop consisted of 6.00 mm thick corrugated steel. The burn room window and hallway door were framed open. To allow for the manipulation of ventilation openings, a window and door were created from steel with latching mechanisms. The prop was mirrored across the length of the hallway, producing two identical configurations in one structure; the right configuration was used for both experimental series.

The room-scale fire training prop was created out of two metal shipping containers. While this structure allowed for quick turn-around between tests, it was not representative of typical residential or commercial structures. The training prop had 6 mm thick metal walls. Residential or commercial structure walls typically consist of several layers of exterior finishing materials (siding), rigid structure framing, insulation, and interior finishing materials (gypsum) with various air-gaps to fur-

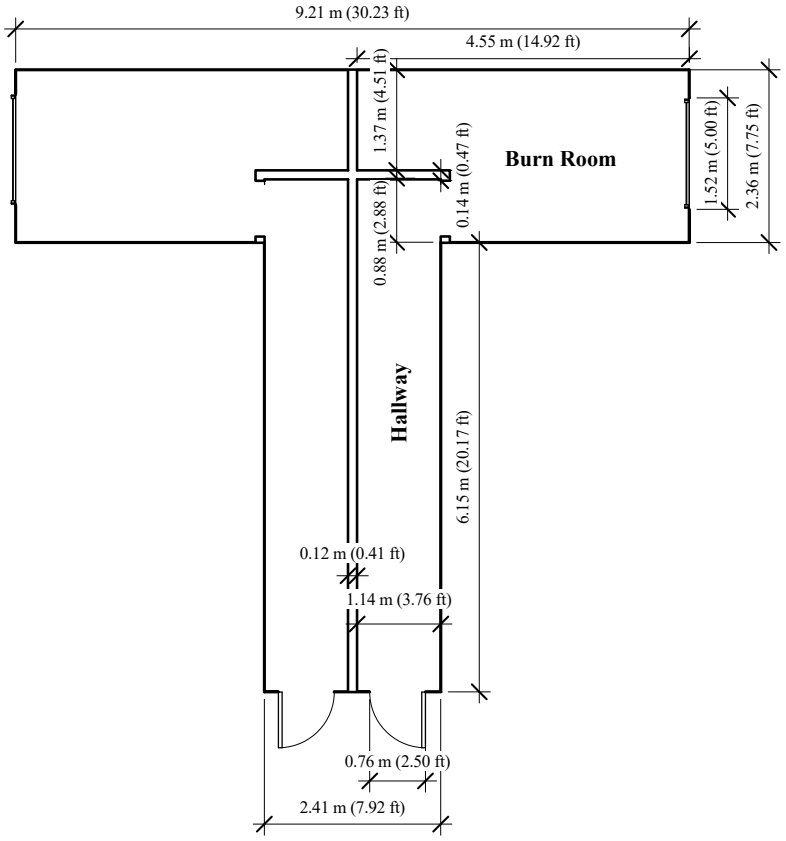

Figure 5.1: Schematic drawing of the modified metal shipping container located at Deco. The structure is mirrored across the hallway to produce two training props.

ther insulate the structure. This layering of materials results in a wall thickness much greater than of the metal prop. This difference in thickness and material composition affects the heat transfer through the walls. The metal structure aides in heat losses to the surrounding environment. Metal has a high thermal conductivity and conducts heat in two-dimensions allowing for transfer of heat to the outside air quickly. A typical residential or commercial structure, would prevent heat losses to the surrounding environment. The various material and air layers leads to one-

dimensional conduction of heat slowing the transfer of heat to the outside air. The metal walls will not radiate as much energy back into the structure as residential or commercial structures would. This indicates that the temperature measurements obtained during the baseline and room-scale fire experiments would be lower than witnessed in a residential or commercial structures.

The difference in material composition also implies a difference in material emissivity. The measurement zone location on the wall encompassed an area that had been scrubbed to expose a surface viable for welding and an area that had been repeatedly exposed to flames and soot. The emissivity for the metal used in shipping containers is roughly 0.88 when 'new'. The emissivity of soot varies on wavelength and thickness, but is assumed to be 0.95 [49]. The emissivity for the metal container can be assumed between 0.88 - 0.95 at ambient conditions. Fire service TICs emissivity values are preset to 0.95 suggesting agreement in emissivity between the TIC and target object at ambient temperatures. At elevated temperatures an objects emissivity can change suggesting during combustion conditions a disagreement between TIC and target object emissivity. It cannot be determined how much this disagreement between TIC and target object emissivity values affects spot temperature measurements obtained from TICs.

5.1 Baseline Experiments

Experiments were designed to investigate TIC spot temperature measurements under ambient conditions as a function of distance and orientation. Two TIC orientations (off-plane and on-plane) and five focal lengths (1.5 m, 3.1 m, 4.6 m, 6.1 m, and 7.2 m), distance between the TIC lens and target object, were investigated. All locations of the TICs for both the off-plane and on-plane experiments can be seen in Figure 5.2.

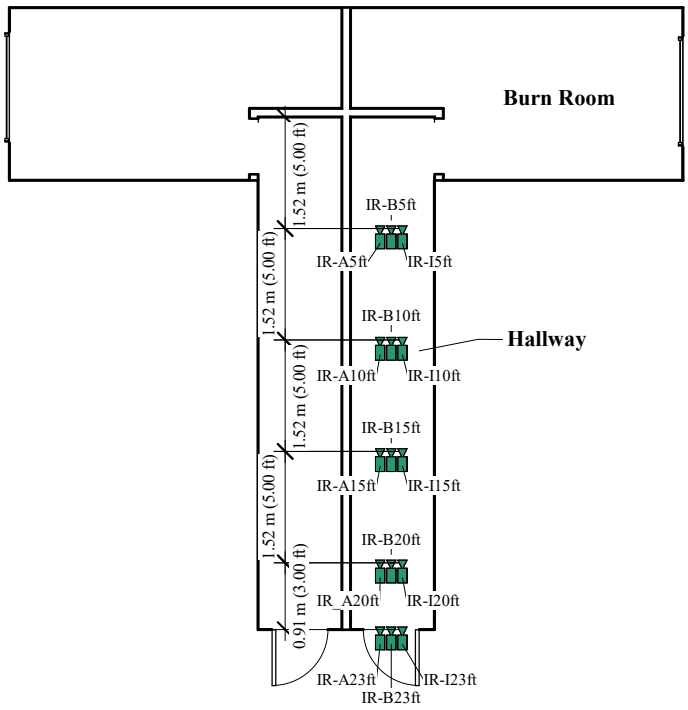

Figure 5.2: The TICs location within the structure for both the off-plane and on-plane experiments.

The off-plane experiments explored any potential effect shape factor might

have on the TIC temperature outputs. The target object consisted of the corrugated steel that composed the structure walls. Specifically the target object was the wall at the end of the hallway. The distance between the TIC and target object was determined from the length of the hallway, 7.0 m. This distance mimicked the distance in the room-scale fire experiments. During these experiments each TIC was placed in a custom stand on the hallway floor located roughly 89 cm from the door opening. This orientation placed the measurement zone on the wall at the end of the hallway. The measurement zone was adjusted to be 1.5 m off the floor. This created an angled line of sight, approximately 14 °, between the TIC and the wall target, see Figure 5.3. The focal length between the TIC lens and target object was 7.2 m. The off-plane experiments only explores the spot temperature measurements at this one distance. Figure 5.4 indicates the location of the TICs.

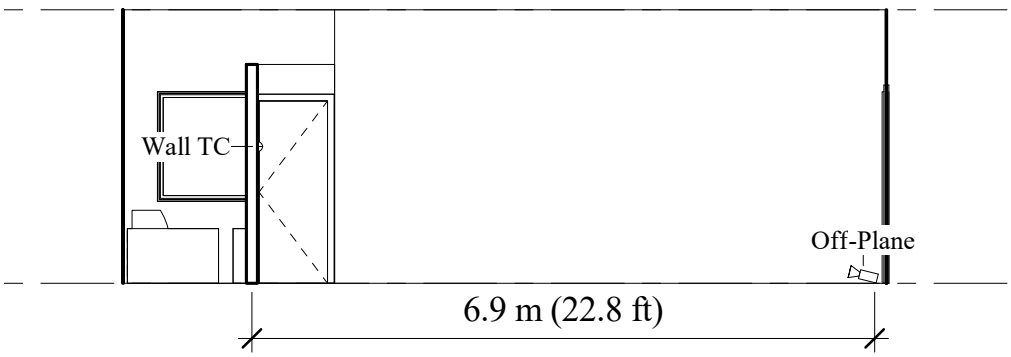

Figure 5.3: Off-Plane TIC orientation

Figure 5.4: Typical set up for the off-plane orientation

The on-plane experiments investigated if distance has any affect on TIC spot temperature outputs. The target object consisted of the corrugated steel that composed the structure walls. Specifically the target object was the wall at the end of the hallway. The distance between the TIC and target object varied in increments of 1.5 m. During the on-plane experiments each TIC was placed in a tripod and adjusted such that the TIC measurement zone was centered on the wall target at an elevation of 1.5 m above the finished floor. This created a level line of sight between the TIC and wall target, see Figure 5.5. Each TIC was evaluated separately for this orientation and evaluated at distances of 1.5, 3.1, 4.6, and 6.1 m. Figure 5.6 visually represents the on-plane TIC set-up.

For each experiment in the baseline experimental series, a TC was tack-welded to the corrugated metal wall located at the end of the hallway. This tack-weld was placed 1.5 m above the finished floor and was replaced after each experiment. This location corresponded to the measurement zone location during each experiment. The signals produced from the TC were recorded with a digital data acquisition

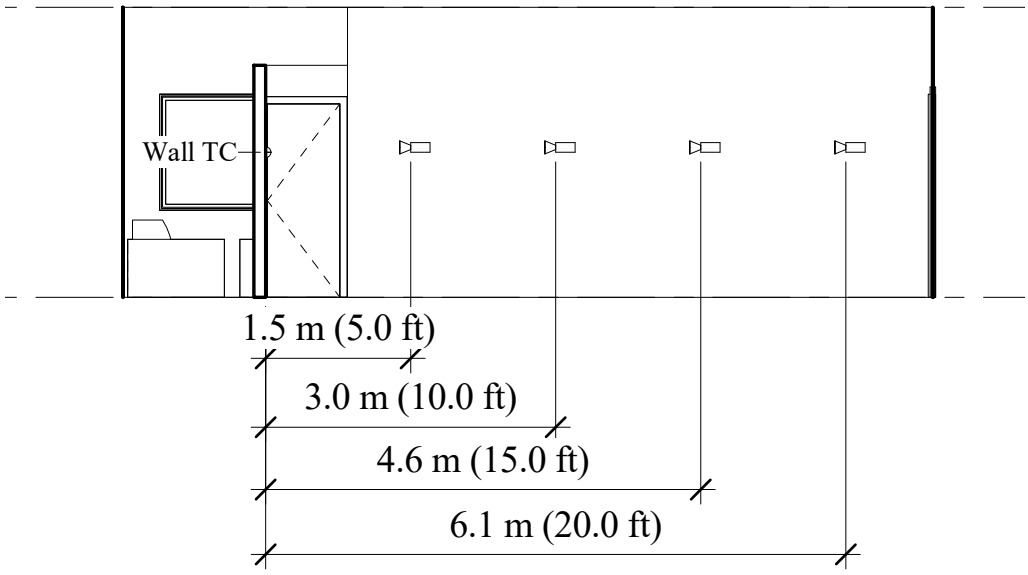

Figure 5.5: On-Plane TIC orientation

system. The data acquisition system and video feed were synced to record at the same time. The location of the wall mounted TC for both the off-plane and on-plane experiments can be seen in Figure 5.7; while, an example of the weld can be seen in Figure 5.8.

The weld was created with chromel-alumel TC wire. Due to the law of intermediate metals the signal produced from this Type-K TC is representative of the wall temperature [50].

In total, five experiments were conducted for each fire service TIC listed in Table 5.1. Table 5.2 summarizes the five experiments conducted for each TIC.

To evaluate the spot temperature measurement at various temperatures, the

Figure 5.6: Typical set up for each TIC evaluated in the baseline experimental series.

target object, corrugated steel, was repeatedly heated and allowed to naturally cool. First, the steel was exposed to high heat from a propane torch. Direct flame impingement was ensured for 15 s. The heated area was confirmed to fill the entire measurement zone box for each test. Second, the steel was allowed to cool for 45 s. This process was repeated five times per experiment. Table 5.3 displays the general time-line of events.

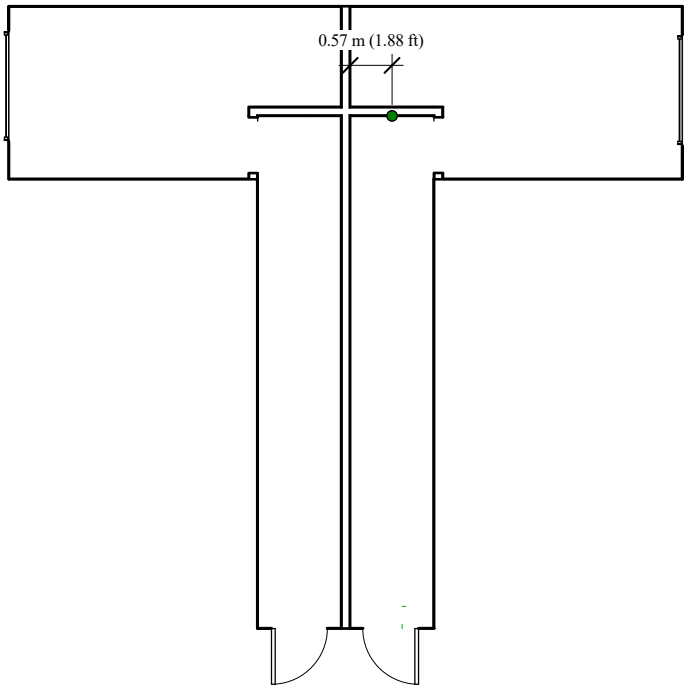

Figure 5.7: The wall mounted TC located on the back hallway wall within the structure for both the baseline experiments.

Figure 5.8: Wall-Mounted TC located on the target object (metal wall). TC was affixed to the target object by a tack-weld.

Table 5.2: Baseline Experiments: Overview
Overview of Baseline Experiments.

TIC	Orientation	Distance (between TIC and target object)
# 1	Off-plane	7.0 m
	On-plane	6.1 m
	On-plane	4.6 m
	On-plane	3.1 m
	On-plane	1.5 m
# 2	Off-plane	7.0 m
	On-plane	6.1 m
	On-plane	4.6 m
	On-plane	3.1 m
	On-plane	1.5 m
# 3	Off-plane	7.0 m
	On-plane	6.1 m
	On-plane	4.6 m
	On-plane	3.1 m
	On-plane	1.5 m

Table 5.3: Baseline Experiments: Time-line

Time [s]	Associated Event
0	Experiment Begin
1 - 60	Ambient Conditions
61 - 75	Heat Applied
76 - 120	Cool Down
121 - 125	Heat Applied
126 - 180	Cool Down
181 - 195	Heat Applied
196 - 240	Cool Down
241 - 255	Heat Applied
256 - 300	Cool Down
301 - 315	Heat Applied
316 - 400	Cool Down
401 - 430	Ambient Conditions
431	Experiment End

5.2 Room-Scale Fire Experiments

Within this series of experiments, four full scale experiments were conducted. Each test was similar in time-line, fire-size, and TIC location / orientation. To investigate the affect of different building materials on TIC spot temperature measurements, two different target object material compositions were investigated (metal and drywall). The two materials investigated by this experimental series have similar emissivity values. Each test is summarized in Table 5.4 [39, 51, 52].

Table 5.4: Room-Scale Fire Experiments: Overview

Exp. #	Building Material	Emissivity Value
1	Metal (Cor-Ten AZP)	0.85 *
2	Metal (Cor-Ten AZP)	0.85 *
3	Metal (Cor-Ten AZP)	0.85 *
4	Dry Wall (Gypsum Wallboard)	0.90 *

* Indicates emissivity value associated with new building materials.

The experimental time-line was designed to mimic firefighter evolutions and typical fire growth within an enclosed structure. At time of ignition all windows and doors to the structure were closed. The fire grew, peaked, and began to decay. Before complete extinction was reached, the structure was ventilated. The fire then regrew, re-peaked, and reached a quasi-steady state. Finally, the fire was suppressed. This time-line allowed for an analysis of the TIC's spot temperature measurement during all fire stages (ignition, growth, steady state, and decay) as well as during the effect of firefighter tactics, ventilation and suppression. Table 5.5 represents the typical time-line of events for the room-scale fire experiments.

Table 5.5: Room-Scale Fire Experiments: Time-line

Time [s]	Actions	Fire Stage
0	Ignition	Initial growth, peak, and decay
240	Open Hallway Door	Secondary growth and peak
540	Open Windows	Steady State
660	Suppression	Extinction

5.2.1 Fuel Load

A fire was ignited in the room portion of this structure, referred to as 'burn room'. Fuel loads were representative of typical fuels found in residential structures. This included two sofas and carpet with associated padding (installed in the burn room only). The sofa was described as having faux wood finished feet with 100 % polyester upholstery [53]. The carpet and padding was described as 100 % Olefin fiber with a Polypropylene backing and recycled foam, respectively [54]. Item descriptions and average initial weights are listed in Table 5.6. Fuels were consistent across the experimental series so that replicates can be compared. Figure 5.9 illustrates the location of the fuel load within the structure; while, 5.10 depicts the actual fuel load used throughout this series of experiments.

Table 5.6: Room-Scale Fire Experiments: Fuel Load

Item	Quantity per Experiment	Description	Average Initial Weight
Sofa	2	2.26 x 0.99 x 1.02 m	49.50 kg
Carpet	9.75 m^2	Thickness 0.26 cm	12.90 kg
Carpet Padding	9.75 m^2	Thickness 0.95 cm	8.10 kg

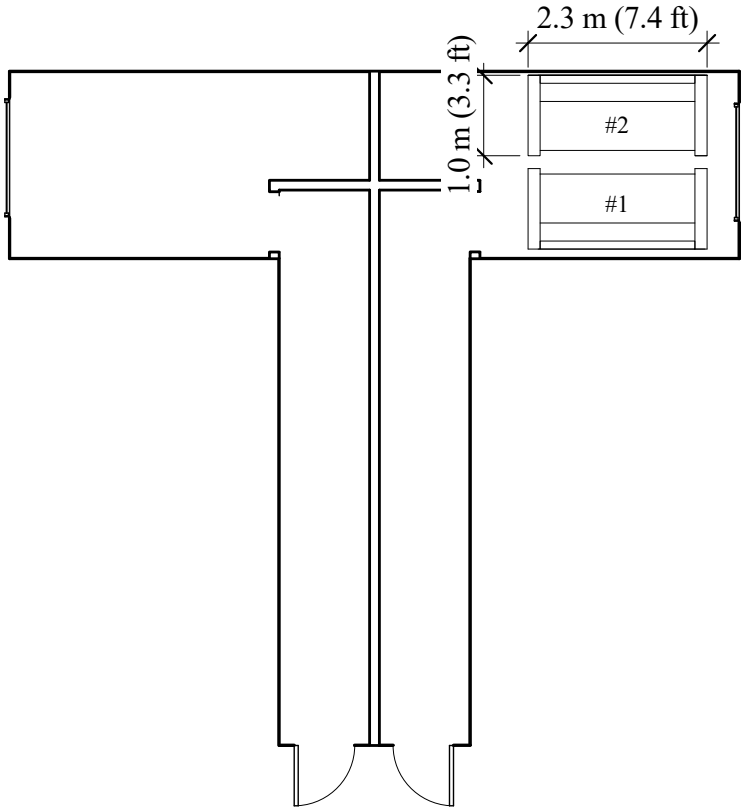

Figure 5.9: Burn room fuel load configuration consisting of two sofas and associated flooring.

5.2.1.1 Fuel Load Heat Release Characterization

UL FSRI quantified the magnitude and repeatably energy release of the fuel load sofa in the report, *Impact of Flashover Fire Conditions on Exposed Energized Electrical Cords and Cables* [55]. The sofa was quantified by oxygen consumption calorimetry for three ignition locations by electric matchbook and allowed to burn in the absence of a compartment. During each experiment the sofa produced similar heat and smoke conditions. The peak heat release between the three experiments

Figure 5.10: Burn room fuel load configuration with two sofas and floor covering. Photo from Experiment # 4.

varied representing the natural variability of the fuel. The total energy release between the three experiments were similar, 10 % difference. Table 5.7 documents the peak heat release rate and total energy released for each ignition location. Figure 5.11 visually represents the heat release results for each ignition location along with a picture of the sofa during experimentation.

Table 5.7: Fuel Load Heat Release Characterization

Ignition Location	Peak HRR (MW)	Total Energy Released (MJ)
Left	4.2	639
Center	2.5	655
Right	4.1	649

5.2.2 Video Documentation

Two TIC locations, exterior and interior, were investigated for each TIC listed in Table 5.1. Each TIC location was accompanied by a standard video camera. Figure 5.12 shows the location for the thermal and standard video camera locations

within and surrounding the structure.

The exterior location remained constant throughout experimentation, this location was located 7.62 m away from the exterior side of the hallway door. The TICs were placed in tripods and adjusted so the lens was 1.5 m above the ground.

The interior location remained constant throughout experimentation, this location was located at the entry end of the hallway, roughly 89 cm inside from the door opening. This location corresponded to a distance of 7.0 m between the TIC and the target object. The TICs were placed approximately 15 cm above the ground and angled upwards. This created an angled line of sight between the TIC lens and target object, resulting in focal length of 7.2 m. To keep the TICs in this specific location a custom metal stand was created. The interior TIC location is presented in Figure 5.4.

The exterior FOV was oriented such that a full view of the exterior of the structure was available and the measurement zone was aimed 0.30 m from the top of the hallway door. For all four experiments, a propane torch was applied to the exterior side of the metal door to verify the location of the measurement zone. The torch was applied in the center of the door approximately 0.30 m below the top edge. All three TICs were adjusted so the measurement zone was directly in the center of the heated area. Figure 5.13 represents the typical FOV for the both the interior (left) and exterior (right) TIC locations.

The interior FOV was oriented such that the entire length of the hallway was present and the measurement zone was aimed 1.5 m above the finished floor on the back wall. The measurement zone location was verified with heat for all three TICs.

For Experiments 1 - 3, a propane torch was applied to the metal container wall to heat a location in the center of the back wall, 1.5 m above the finished floor. All three TICs were adjusted so the measurement zone was directly in the center of the heated area. For Experiment 4 a similar method was used; however, the hallway target wall was covered with drywall.

The video from all three TICs was analyzed following the same procedure outlined in Section 3.1.2.

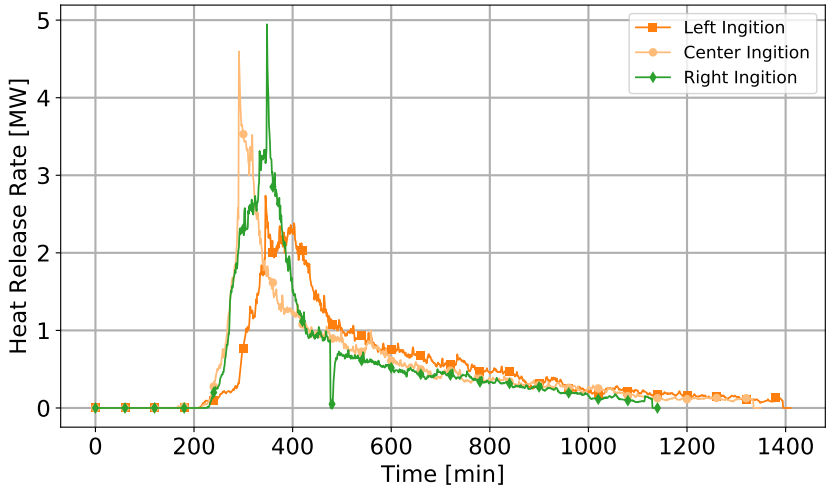

(a) Heat Release Rate

(b) Sofa

Figure 5.11: Figure 5.11(a) represents the heat release rate results for each ignition location. Figure 5.11(b) was taken during experimentation, the column of black smoke it seen above the fuel package [55]

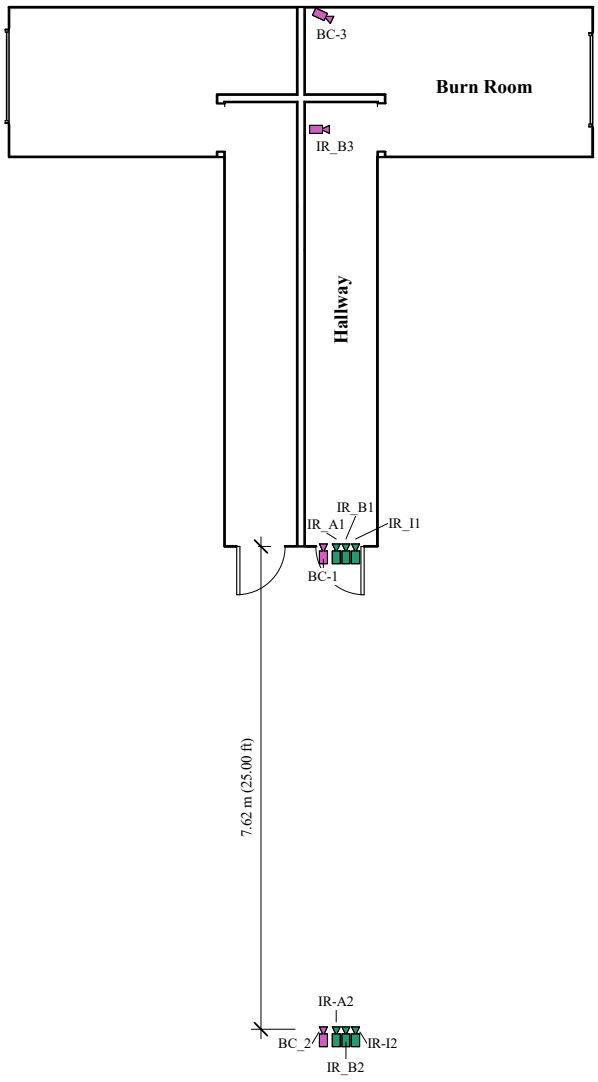

Figure 5.12: Schematic drawing depicting the location of the thermal imaging and standard video cameras. TICs are depicted by green symbols; while, standard video cameras are depicted by pink symbols.

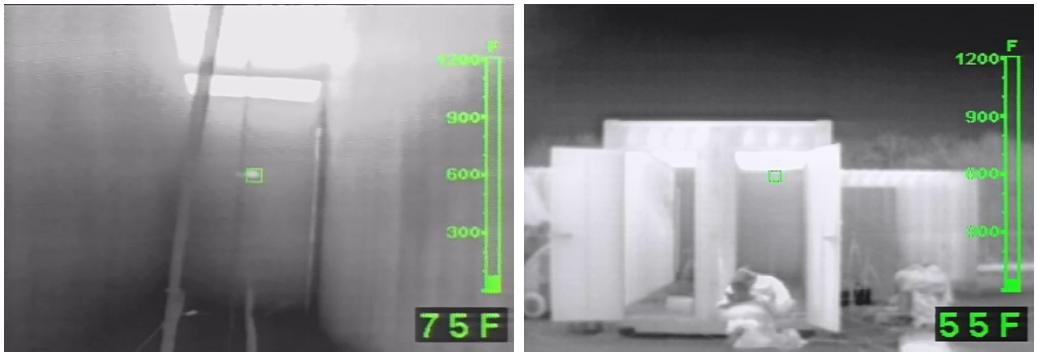

(a) Interior FOV (b) Exterior FOV

Figure 5.13: The typical FOV for the interior and exterior TIC locations. Figure 5.13(a) indicates the length of the hallway. Within its FOV two vertical TC arrays and one angled TC array are seen. Figure 5.13(b) indicates the exterior of the structure. The doorway and associated exterior of the burn room are seen.

5.2.3 Instrumentation

The structure was outfitted with sensors to measure wall temperatures, gas temperatures, and optical density. The instrumentation locations remained constant throughout the four individual experiments. Figure 5.14 depicts the instrumentation locations.

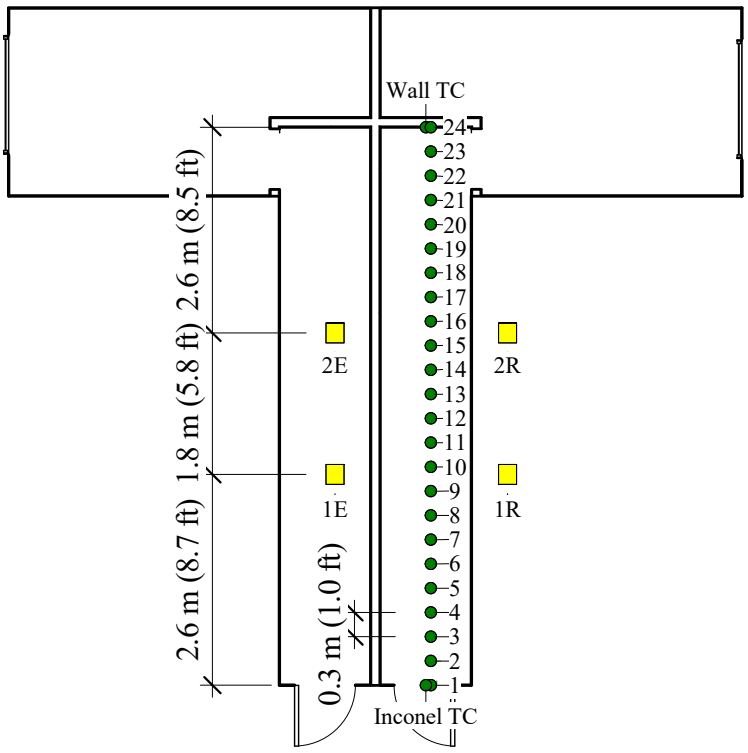

Figure 5.14: Schematic drawing depicting the location of all instrumentation. Yellow squares labeled 'OD' are representative of opacity sensors (the emitter, E, or receiver, R). Green circles labeled with a number are representative of a TC measuring gas temperatures along the TIC line of sight. Green circle labeled 'Wall TC' is representative of the wall mounted TC. Green circle labeled 'Inconel' is representative of the Inconel TC.

K-type TCs were used to measure both solid object and gas temperatures.

Wall temperatures were measured by a TC either tack-welded to the metal shipping container wall or implanted in dry wall used to line the target wall of the structure, see Figure 5.15. The wall TC was located on the far hallway wall roughly 1.22 m above the finished floor. This location remained constant regardless of the wall material. Each interior TIC was oriented such that the measurement zone was aimed on this TC location. The TC height and location were used to calibrate the measurement zone of the interior TICs mentioned above.

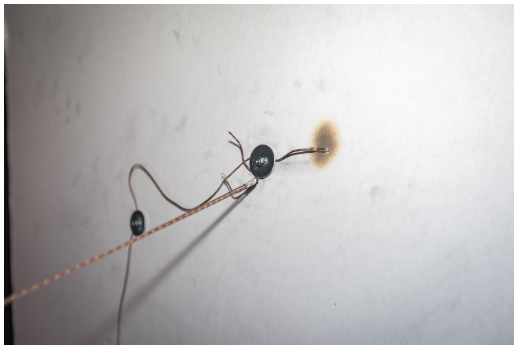

Figure 5.15: Typical set up for the wall-mounted TC. TC was implanted in the drywall during room-scale fire experiment # 4.

Gas temperatures were measured in the upper gas layer and along the TIC line of sight. An Inconel TC was used to measure temperatures at a single location within the structure. The Inconel TC was located in the doorway roughly 0.30 m from the top of the door. Each exterior TIC was oriented such that the measurement zone was aimed at this location. The TC height and location were used to calibrate the measurement zone of the exterior TICs mentioned above. Gas temperatures along the TIC line of sight were measured by a TC array. This TC array measured temperatures at a 0.3 m interval from the TIC lens to the target object. A resulting

7.32 m array was oriented at the same angle created by the TIC lens and the wall mounted TC, roughly 14 °.

Optical density was measured at two different locations in the hallway. These two monitoring locations were placed at heights associated with the TIC measurement zone path, 0.69 m and 1.12 m. Due to the thermal sensitivity of these sensors, the receiver and emitter were placed on the exterior of the structure; therefore, holes were drilled into the metal container to allow for the light beam to pass through the combustion environment. Two locations were positioned at the following distances: 2.67 m and 4.44 m from the hallway door.

Chapter 6: Experimental Results, Analysis, & Discussion

The TIC temperature outputs acquired during this process and the TC temperatures acquired during the experiment were compared and analyzed statistically. The temperatures measured by the TCs were outfitted with its expanded uncertainty, to indicate if / when the TIC was calculating comparable temperatures.

For the baseline experiment analysis the experimental time-line and time periods of direct flame impingement are indicated on the temperature graph. During flame impingement the TC was measuring flame temperatures rather than wall temperatures. Temperatures recorded during this time period are excluded from the following analyses.

For the room-scale fire experimental analysis, suppression and ventilation efforts were indicated on the temperature graph. Temperatures recorded during this time period are excluded from the following analyses.

6.1 Repeatability Discussion

Repeatability is regarded as the measure of closeness between results of successive measurements of the same measured argument obtained under similar conditions. The result of a measurement is only an approximation or estimate of the

true value of the measured argument; therefore, the result is incomplete without an accompanied quantitative statement of uncertainty [56].

The methods documented by NIST [56] were implemented in this report to accurately quantify the associated uncertainty of measurements taken throughout experimentation. The NIST report states there are two basic methods to evaluate the uncertainty of a measurement: Type A and Type B. Type A evaluates measurement components of uncertainty arising by statistical methods. Type B evaluates measurement components of uncertainty arising from a systematic effect, or an evaluation of uncertainty based on scientific judgment utilizing all relevant information available: including previous measurement data, experience, reference data, and manufacturer's specifications.

By definition, the uncertainties associated with the TC measurements discussed throughout this report were estimated using a Type B evaluation. These measurements were expressed with an expanded uncertainty including a coverage factor of two. This coverage factor dictates that the values within the uncertainty interval have a confidence level of 95 %. To further clarify, if the measured temperature was reported as 300 °C, there is a 95 % certainty that a similar measured temperature would be within the range of 255 - 345 °C.

To ensure a consistent baseline between experiment it was desired to create fires, or experimental environments, that generated repeatable smoke and temperature conditions. This allowed for data obtained over several iterations of the same experiment to be analyzed and compared. A repeatability analysis was performed on both the baseline and room-scale fire experiments before analysis of raw data

was conducted.

6.1.1 Baseline Experiments

To ensure similar heating techniques between baseline experiments a repeatability analysis was conducted on data obtained from the wall thermocouple. Temperature data was grouped by orientation, on-plane and off-plane, and distance between the TIC and target object: off-plane 7.0 m, on-plane - 6.1 m, on-plane - 4.6 m, on-plane - 3.0 m, and on-plane - 1.5 m. As each TIC was evaluated separately there are three sets of TC data for each grouping mentioned above. The methodology presented in Appendix D can only compare two sets of data. Therefore, three analyzes

were conducted for each grouping to ensure the heating conditions were similar between all three TIC tested. The intraclass correlation coefficient (ICC) and bias factor (δ) was determined for each coupled group of data. The intraclass correlation coefficient is an indication of reliability and can be used to express reproducibility and repeatability between paired data. It represents the variance of paired data expressed as a proportion of the total variance. The bias factor is a measure of accuracy that describes the relationship between the paired experiential data and idealized data.

After analyzing the results produced from the repeatability analysis, it was determined that the TC heating was agreeable or highly agreeable between all tests. The overall bias for each comparison was within the highly agreeable category for all

experiments. The overall ICC for each comparison was within the highly agreeable category for all but three comparisons. These three comparisons were within the agreeable category. This indicates that in these three comparisons the TC temperatures collected presented with a higher variance than the overall variance. These results suggest that repeatable heat exposure conditions were achieved throughout the baseline experiments.

6.1.2 Room-Scale Fire Experiments

To definitively quantify the repeatability of the room-scale fire experiments, the temperature measurements obtained from the wall mounted TC during each experiment were plotted on the same graph. The wall mounted TC was chosen for the repeatability verification because it was least affected by uncontrollable environmental wind. Figure 6.1 visually represents the data obtained the wall mounted TC.

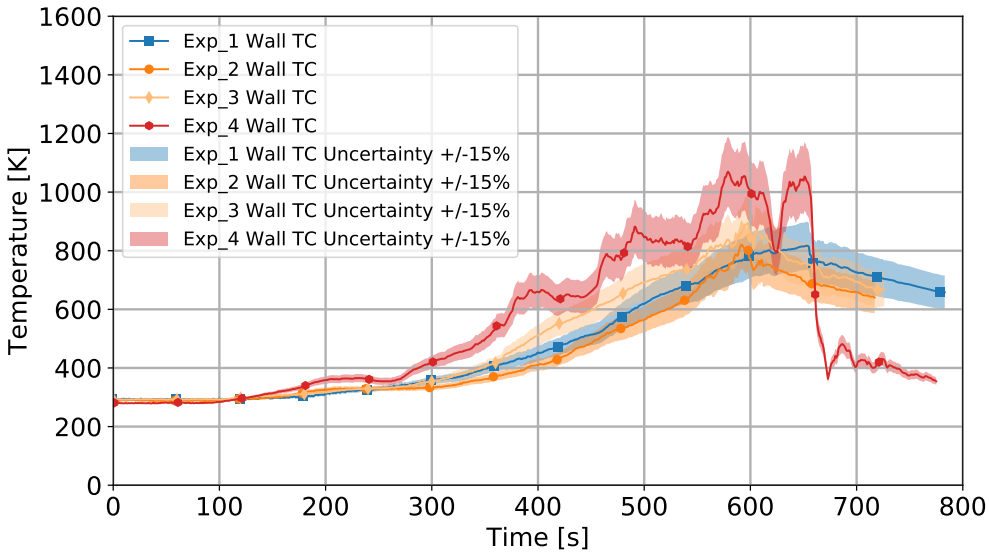

Figure 6.1: Temperature measurements for the wall mounted TC with associated Type B expanded uncertainty for all room-scale fire experiments.

From visual observation of Figure 6.1, the increase in wall temperatures for Experiments # 1 - 3 were similar. The gypsum target object during Experiment # 4 produced different temperature behavior than the metal target object during Experiments # 1 - 3. The gypsum target object produced higher wall temperatures at a quicker rate. Metal has a high thermal conductivity causing increased heat transfer through the wall. Gypsum has a lower thermal conductivity resulting in fewer heat losses through the wall.

A Type A analysis was then conducted on the data presented in Figure 6.1 to quantify the level of reproduction. The coefficient of variation (CV) is a measure of dispersion from the mean and calculated using Equation 6.1.

$$CV = \frac{\sigma}{\mu} \tag{6.1}$$

Where σ is the standard deviation and μ is the mean of the data collected during each of the four experiments. Figure 6.2 represents this calculation at each time-step.

Figure 6.2(a) indicates that the variation between metal wall temperatures remained below 10 % until shortly after ventilation of the hallway door, occurring at roughly 240 seconds. Figure 6.2(b) indicates that the variation in wall temperatures between all experiments occurred after ignition, roughly 150 seconds. It was determined that similar heating environments were created and variation occurred due to the dissimilar nature of the target wall material.

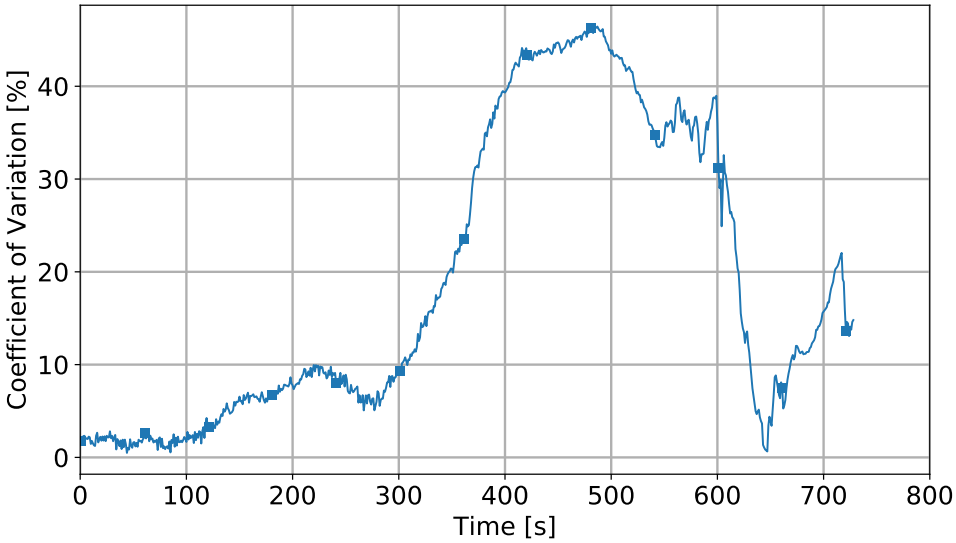

(a) Experiments # 1 - 3

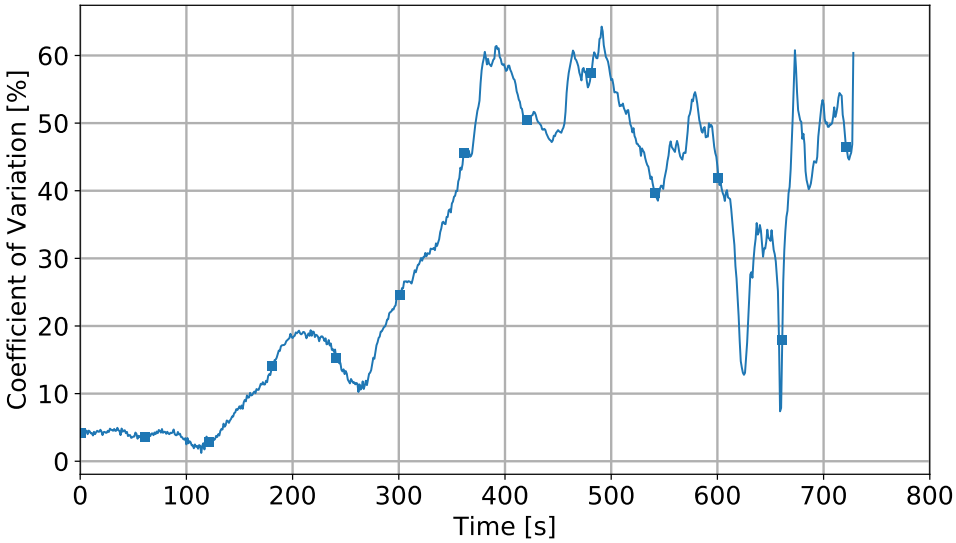

(b) Experiments # 1 - 4

Figure 6.2: Type A analysis, coefficient of variation, for wall temperatures obtained during Experiments # 1 - 3 and Experiments # 1 - 4.

6.2 Impact of TIC Proximity and Orientation to Target Object

To evaluate the effect of TIC proximity and orientation to the target object on the spot temperature measurements, the baseline experiments were conducted. This series of experiments explored the affects of optimal distance, between the TIC and the target object, and focal length. The focal length is the minimum distance needed between the TIC and the target object to ensure the target object's critical dimension subtends the required number of pixels to be detected, recognized, or identified. The focal length was a commonly published value in fire service TIC specifications; typically reported as 1.00 m to infinity. Fire service TIC standards to not dictate a requirement for focal length. TIC # 3's focal length is optimized at 4.00 m. Focal length indicates that the target object must be at least 1.00 m, 4.00 m in the case of TIC # 3, away from the TIC for the temperature of the object to be optimally determined.

The optimum focal length was investigated in two orientations, or two solid angles. A solid angle is the surface area of a unit sphere covered by the surface's projection onto the sphere, or a measure of the surface area of the projection from a surface onto a singular point. The solid angle, ω subtended by a surface at a singular point is calculated from Equation 6.2.

$$\omega = \int \int \sin(\phi) d\theta d\phi \tag{6.2}$$

Where ϕ is the colatitude and θ is the longitude. These two angles describe

the cone created by the surfaces projection onto the point in two dimensions. Solid angles are important when calculating the irradiance emitted from an object. TIC temperature calculation theory assumes that objects are Lambertian emitters, or that all objects emit radiation equally in all directions. This assumption therefore eliminates the need for solid angles when calculating irradance. Therefore, the angle and distance from the target object should not negatively affect the spot temperature measurements.

The first experiment evaluated an off-plane orientation, identical to the interior TIC location in the combustion series of events. The second experiment evaluated a on-plane orientation at differing distances. This series of experiments aims to solidify the assumption that TIC orientation does not affect spot temperature measurements and to discover an optimized focal length for each model of TIC.

6.2.1 Off-Plane

A total of three off-plane experiments were conducted. Each experiment evaluated spot temperature measurements from single TIC with a focal distance of 7.2 m. The focal distance was determined as the angle between the TIC lens and measurement zone location on the target wall.

The spot temperature measurements determined from an ambient temperature target object were analyzed first. The percent difference between TIC spot temperatures and TC temperature measurements during the first 60 s of experimentation is presented in Table 6.1. During ambient temperature conditions, the

percent difference between the two temperature methods was within ± 15 %, uncertainty associated with the TC measurement. This indicates that the TIC and TC are producing statistically similar results.

Table 6.1: Baseline Off-Plane Experiments: Percent Difference during ambient conditions, 0 - 60 s

TIC	Focal Length	Percent Difference
# 1	7.2 m	-1
# 2	7.2 m	3
# 3	7.2 m	-1

The TIC temperature outputs determined from a target object at elevated temperatures was analyzed second. The percent difference between TIC temperature measurements and TC temperatures was evaluated for each time-period without direct flame impingement, 75 - 120, 135 - 180, 195 - 240, 255 - 300, and 315 - 360 seconds. It was determined that after the initial application of heat to the target object, the two temperature measurement methods began to measure different temperatures.

The TIC # 3 spot temperature measurements drop around 225 s and 300 s. This error is caused when the TC weld becomes temporarily un-joined from the wall. This happens when the weld at the joint becomes hot enough to melt during direct flame impingement of the torch. The connection becomes stable once the torch is removed and the weld cools creating the joint. TIC # 3 temperature output responded to the increase in temperature of the shipping container wall. The magnitude of the TIC temperature was less than recorded by the TC. Figure 6.3 represents the TC and TIC # 3's temperature measurement.

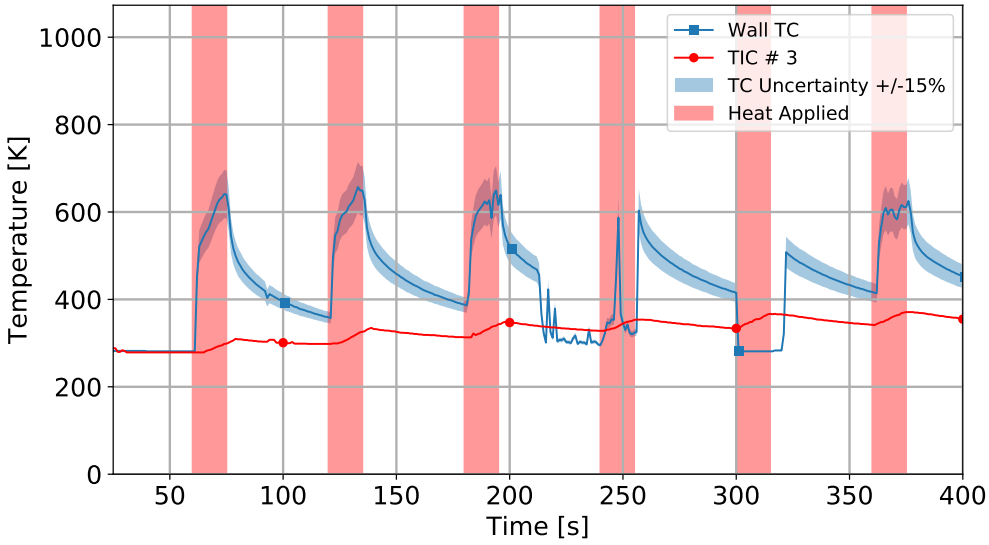

Figure 6.3: Temperature output from TIC # 3 and tack-welded TC for the angled baseline experiments.

TIC # 1 and TIC # 2 TIC temperature outputs did not respond instantaneously to the increase in temperature of the shipping container wall; rather, they responded gradually, as seen by the overall increase in temperature throughout the two experiments. The increase in temperature calculated by the TICs were less than the temperatures recorded by the TC. The TIC did not respond to the cooling period as the temperatures did not decrease over this time-period. The temperatures recorded during the cooling period were fairly stable with a decreasing trend observed during the last cool down period, which lasted two minutes rather than the one minute. The TC and TIC temperature measurements for TIC # 1 and TIC # 2 cameras can be seen in Figure 6.4.

To quantify the visual trends observed from Figures 6.3 - 6.4, the percent difference between the two temperature measurements was calculated for each time-step during experimentation. These values were then averaged together for each time-period and each experiment as a whole. The data is presented for TIC evaluated in Table 6.2.

Table 6.2: Baseline Off-Plane Experiments: Percent Difference during non-ambient conditions.

TIC	75 - 120 s	135 - 180 s	195 - 240 s	255 - 300 s	315 - 360 s	Avg.
# 1	-26	-27	-31	-32	-29	-29
# 2	-26	-31	-31	-33	-33	-31
# 3	-27	-28	-10	-26	-16	-24

The out-lier witnessed during 195 - 240 s during the TIC # 3 evaluation was not included in the final averaged percent difference value. This time-period produced inconsistent results due to a fault connection at the TC join. All three TICs performed poorly when compared to the temperature measurements from the wall-mounted TC, as all percent difference values were outside of the $\pm$ 15 % expanded uncertainty. The TICs produced temperatures roughly 24 - 31% lower than measured from TCs.

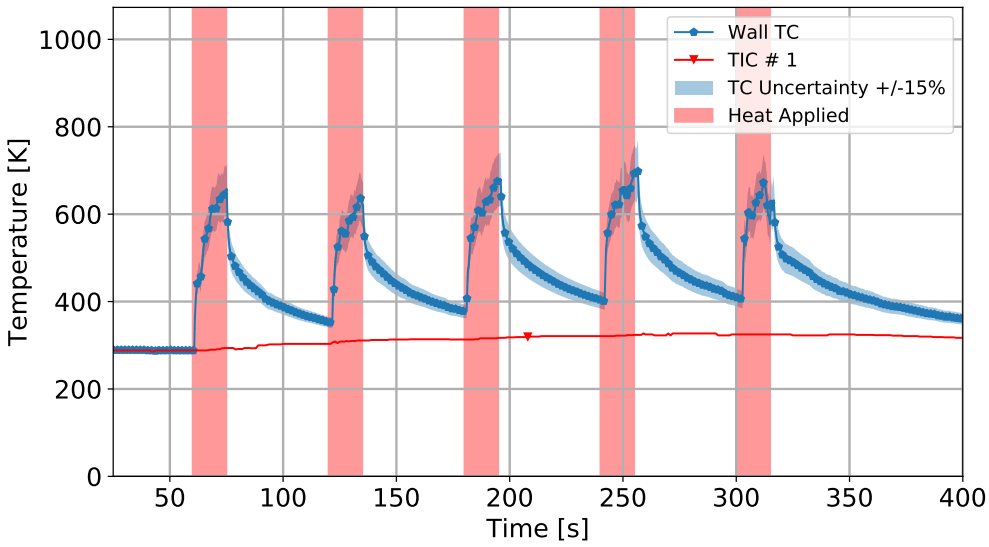

(a) TIC # 1

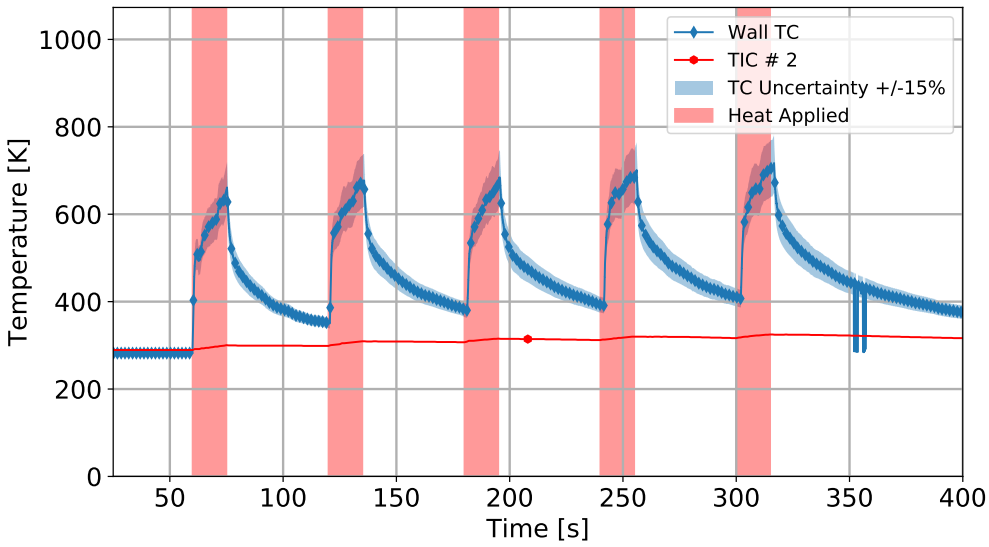

(b) TIC # 2

Figure 6.4: Temperature output from the TIC # 1 and TIC # 2 TICs and tack-wielded TC for the off-plane baseline experiments.

6.2.2 On-Plane

Each TIC was evaluated for an on-plane orientation a total of four times, varying the distance between the TIC and the target object at the following distances: 1.5, 3.0, 4.6, and 6.1 m. The TICs were placed in camera tripods that allowed for the line of site between TIC and target object to be level with the floor, as both the TIC and measurement zone were placed 1.5 m above the finished floor. The target object's temperature was monitored by a wall-mounted TC.

The spot temperature measurements with a target object at ambient conditions was analyzed first. The percent difference between each TIC and TC for the first 60 s of experimentation is presented in Table 6.3. Similarly to the off-plane experiments the percent difference between the two temperature methods was within $\pm$ 15 %, expanded uncertainty of the TC temperature measurements. This indicates that the TIC and TC are measuring similar temperatures.

The spot temperature measurements with a target object at elevated temperatures was analyzed second for each distance evaluated. Figure 6.5 documents the TIC and TC temperatures for each distance for TIC # 1.

Table 6.3: Baseline On-Plane Experiments: Percent Difference during ambient conditions, 0 - 60 s

TIC	Focal Length	Percent Difference
# 1	6.1 m	2
	4.6 m	1
	3.0 m	-3
	1.5 m	-1
# 2	6.1 m	1
	4.6 m	3
	3.0 m	-1
	1.5 m	-1
# 3	6.1 m	-1
	4.6 m	1
	3.0 m	-1
	1.5 m	-1

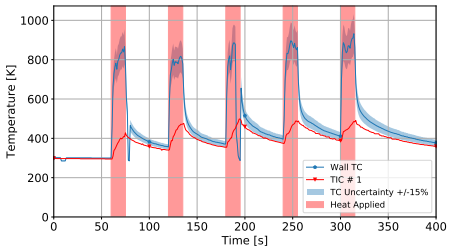

(a) TIC # 1 1.5 m

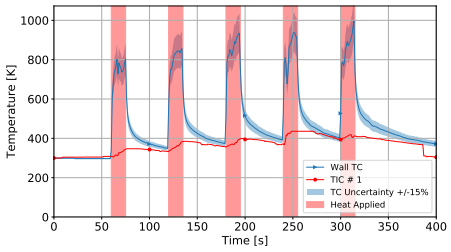

(b) TIC # 1 3.0 m

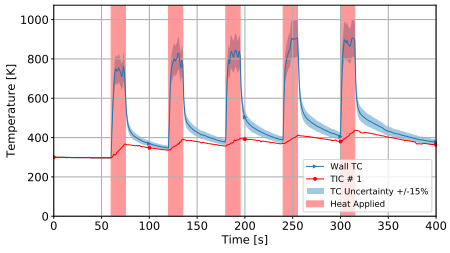

(c) TIC # 1 4.6 m

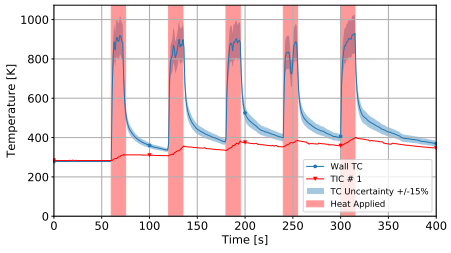

(d) TIC # 1 6.1 m

Figure 6.5: Temperature output measured for each distance evaluated for TIC # 1 during the on-plane baseline experiments.

TIC # 1 did not recognize the increase in wall temperature during times of direct flame impingement. Once the flame was removed the TIC responded to the increase in wall temperature. This created a delay before TIC temperatures became indistinguishable from the TC temperatures. TIC # 2 recognized the increase in wall temperature during times of direct flame impingement. TIC temperature was similar to TC temperatures but not indistinguishable. TIC # 3 responded to the increase in wall temperature during times of direct flame impingement during the first, second, and third heating time-period. The temperature output measured similar temperatures as the TC only when the wall cooled to temperatures near 400 K.

The percent difference for each time-period not affected by direct flame impingement was evaluated. Figure 6.6 represents the percent difference produced from TIC # 1 for all distances evaluated.

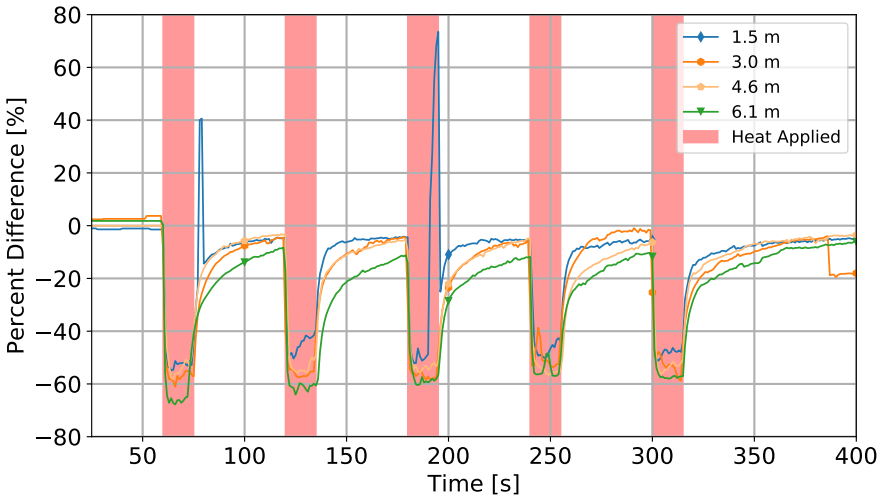

Figure 6.6: Percent difference evaluated for TIC # 1 during the on-plane baseline experiments.

Figure 6.6 indicates that as the TIC is moved closer to the target object the percent difference between the two temperature measurement methods becomes lower. To investigate this the average percent difference was determined get a percent difference associated with each TIC at each distance. This information allows for an assessment of focal length on spot temperature measurements. These values are presented in Table 6.4, all graphical representation of data is presented in Appendix D. TIC # 1, TIC # 2, and TIC # 3's temperature outputs were most representative to TC temperature measurements at a focal length of 1.5 m, determined from the experiment with the lowest average percent difference. The TIC temperature output improved as a function of distance between TIC and target object during ambient conditions.

Table 6.4: Baseline On-Plane Experiments: Percent Difference during non-ambient conditions.

TIC	Distance	Percent Difference
# 1	6.1 m	-20
	4.6 m	-13
	3.0 m	-13
	1.5 m	-9
# 2	6.1 m	-17
	4.6 m	-18
	3.0 m	-18
	1.5 m	-15
# 3	6.1 m	-23
	4.6 m	-26
	3.0 m	-18
	1.5 m	-5

6.2.3 Conclusions

The baseline, on-plane and off-plane, experiments determined that during ambient conditions TIC proximity had a greater affect TIC spot temperature measurements than orientation. During the off-plane orientation or distances greater than 6.1 m, the spot temperature outputs were 16 - 30 % lower than TC temperatures. The off-plane orientation was not evaluated at various lengths (thusly at various angles). It can not be determined if at closer distances the TIC temperature outputs would become more similar to TC temperature measurements. During the on-plane orientation at short distances, TIC temperature outputs became indistinguishable from TC temperature measurements. It was determined that TIC temperature outputs are a function of distance. As the TIC and target object become closer, the target object accounts for a greater percentage of the TICs FOV. Although the

TIC produces a spot temperature measurement for the objects within the measurement zone, the pixels within this zone are also receiving IR from all objects within the room. Therefore the agreement between temperature measurement methods at shorter distances can be explained by the increase in target object percentage of the FOV or decrease of addition sources of incidental IR within the FOV.

6.3 Impact of Environmental Smoke Obscuration

To evaluate the effect of smoke obscuration on TIC spot temperature measurements, the room-scale fire experiments were conducted. These experiments explored the effects of smoke opacity on the TICs ability to accurately determine temperatures.

The first TIC location was interior of the structure. The TIC and target object were both affected by smoke and heat. The interior TIC temperature outputs were compared to wall mounted and gas TC temperature measurements. The wall TC was used to assess the TICs ability to measure wall temperatures through the smoke. The gas TCs were used to determine the smoke's, participating media's, impact on temperatures.

The second TIC location was exterior of the structure. The TIC was removed to a distance where it would not be affected by smoke or heat. The target object was affected by smoke and heat. The exterior TIC temperature outputs were compared to wall and gas TC temperature measurements. An analysis of gas and wall TC measurements were used to determine if a TIC could determine the temperature of

smoke exiting the structure. For complete results from this series of experiments, see Appendix D.

During each experiment the smoke obscuration was evaluated at two locations within the structure. The percent opacity recorded from the instrumentation discussed in Section 3.3 is presented in Figures 6.7 - 6.8.

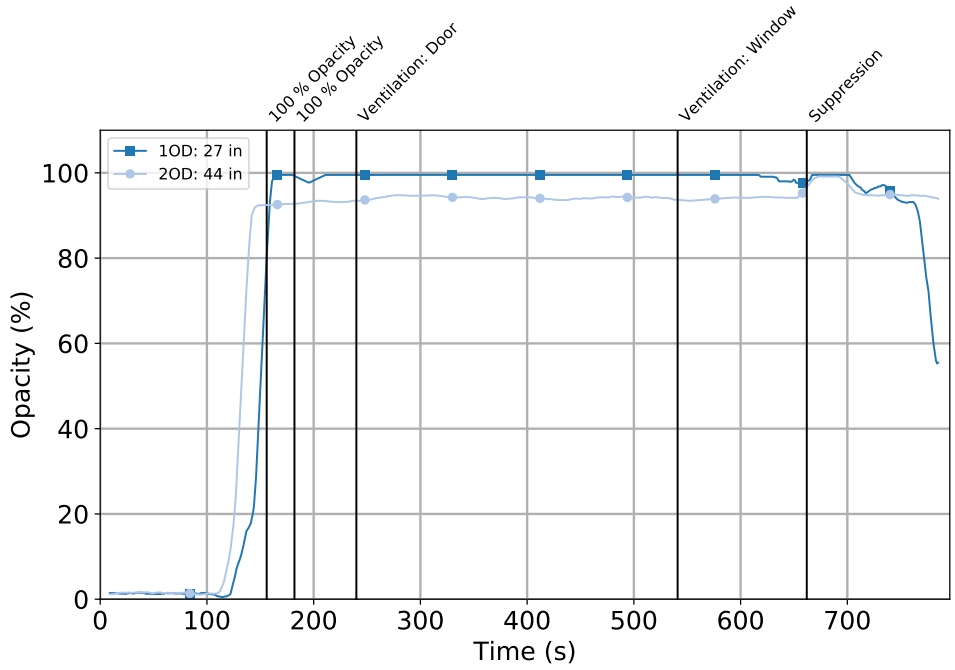

(a) Experiment # 1

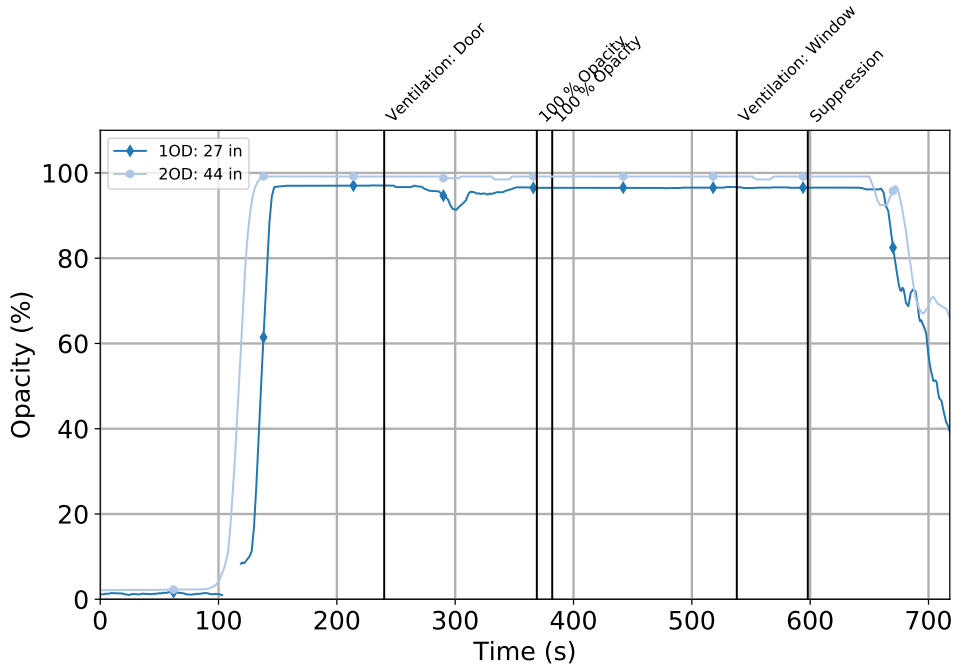

(b) Experiment # 2

Figure 6.7: Percent Opacity during each room-scale fire experiment. Opacity at 2.7 m from the front door at a height of 68.6 cm in dark blue. Opacity at 4.4 m at a height of 111.8 cm in light blue.

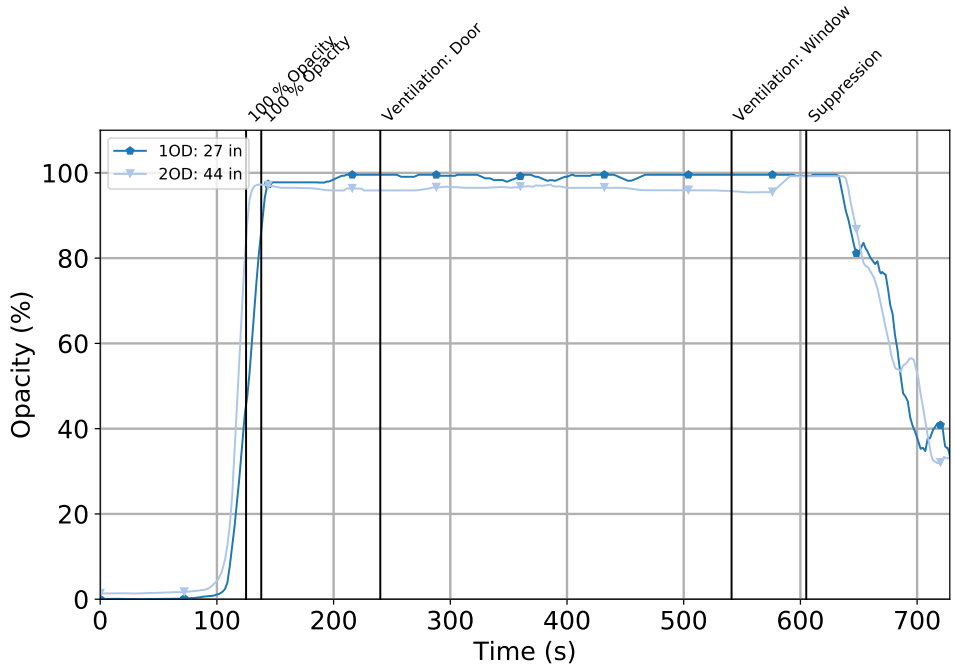

(a) Experiment # 3

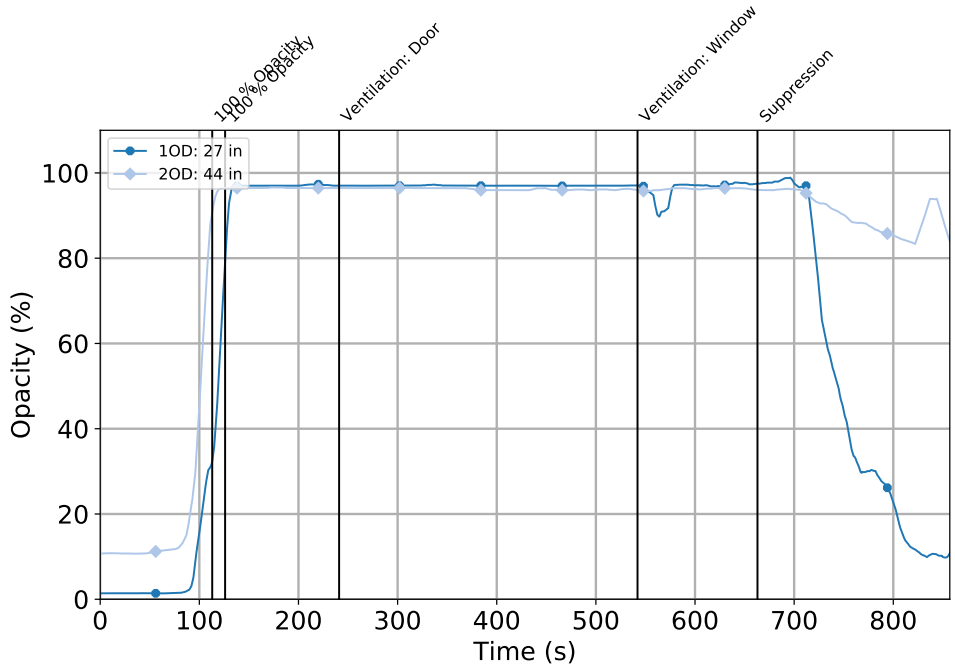

(b) Experiment # 4

Figure 6.8: Percent Opacity during each room-scale fire experiment. Opacity at 2.7 m from the front door at a height of 68.6 cm in dark blue. Opacity at 4.4 m at a height of 111.8 cm in light blue.

In all experiments, the smoke opacity reached 100 % before ventilation of the door occurred. The smoke opacity remained near 100 % till after suppression occurred. 100 % obscuration indicated that the atmosphere was so optically thick that the light beams of the instrumentation were unable to penetrate through the smoke.

6.3.1 Exterior TIC Location

The exterior location was monitored by a standard camera as well as each TIC evaluated by this report. The measurement zone for each TIC was located 0.03 m below the top of the door. This location corresponded to a TC placed inside the structure, due the temperatures expected in the upper gas layer an Inconel TC was employed. From the initial evaluation of prior data in Section 4, it was determined that TIC did not capture and display the full hazard associated with the environment. It was suggested that the radiant energy received by the TIC was impaired by the smoke, participating media. This may indicate that the TIC was calculating temperatures for the optically thick smoke rather than the solid objects present within the measurement zone. To try to capture the impact of the presence of sooty smoke during the first 240 s of experimentation, hallway door remained closed.

The data obtained from the TICs located exterior of the structure and TC located within the door way were graphed together and are presented in Figure 6.9. To quantify the relationship between TIC temperature outputs and TC temper-

ature measurements, the percent difference was calculated for three time-periods: door ventilation to window ventilation, window ventilation to suppression, and suppression to test conclusion. Similarly to previous analyses 30 s before and after suppression efforts begin were ignored. This information is presented in Tables 6.5 - 6.10.

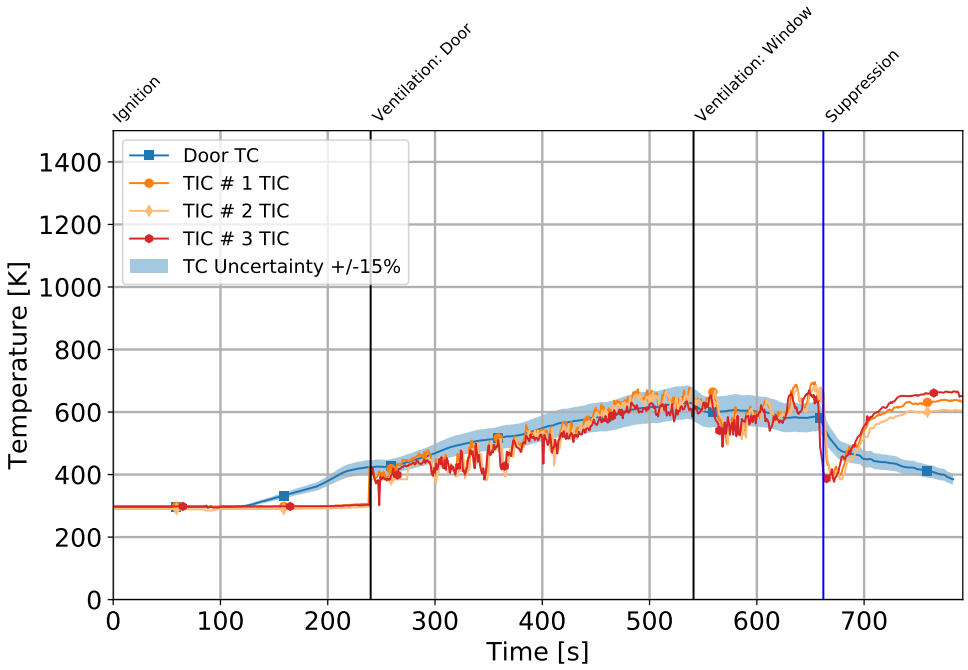

(a) Experiment # 1

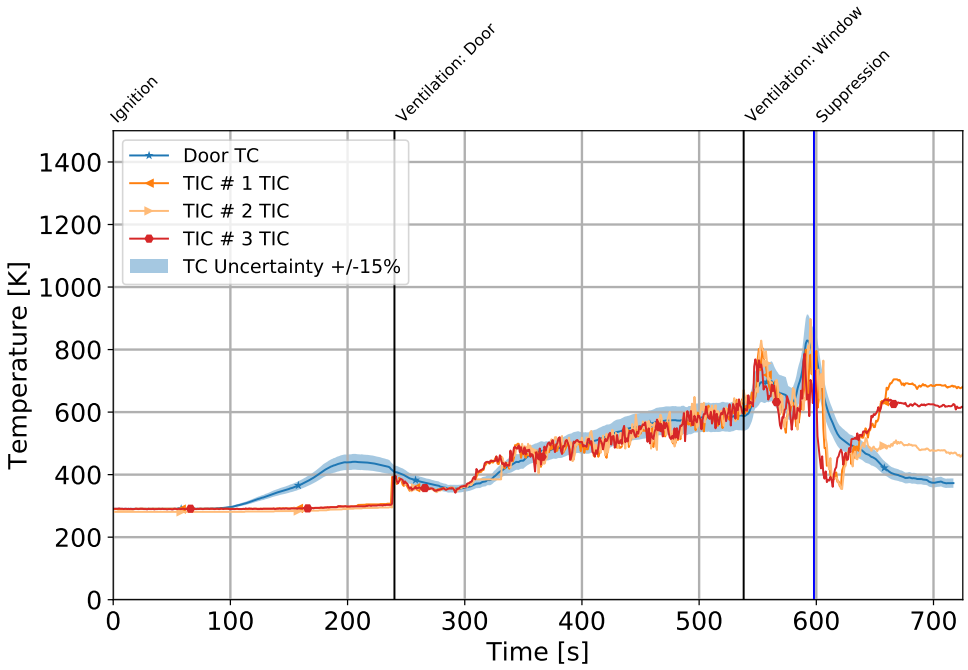

(b) Experiment # 2

Figure 6.9: Exterior TIC # 1, TIC # 2, and TIC # 3 vs. Inconel TC

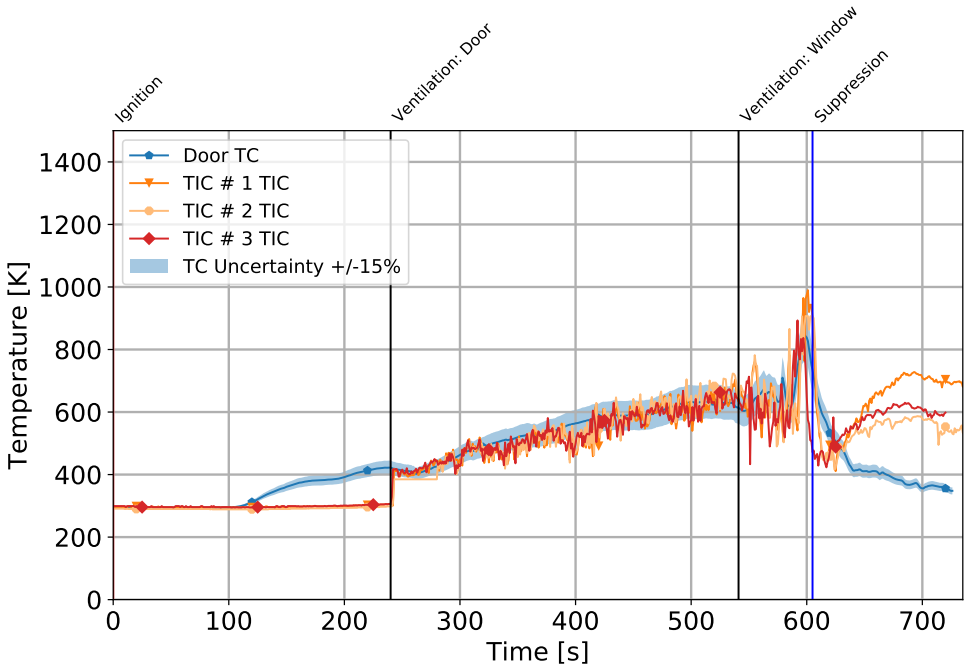

(a) Experiment # 3

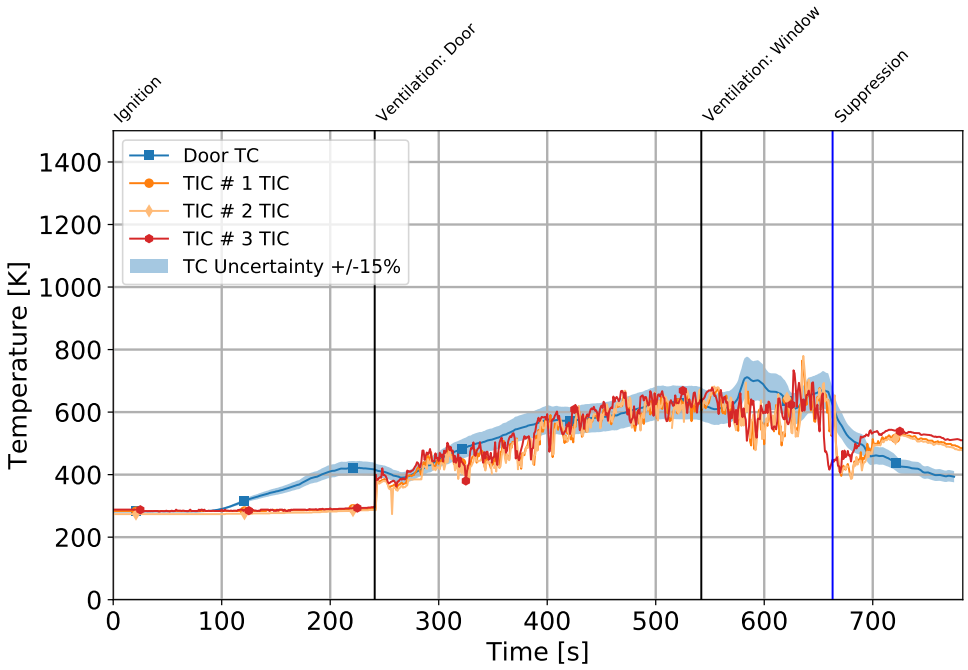

(b) Experiment # 4

Figure 6.10: Exterior TIC # 1, TIC # 2, and TIC # 3 vs. Inconel TC

Table 6.5: Room-Scale Fire Experiments - Exterior TIC vs. Inconel TC: Percent Difference

TIC	Exp. #	PC (Door - Window)	PC (Window - Prior to Suppression)	PC (Post Suppression - End)
# 1	1	-3	-1	43
	2	-2	4	57
	3	-3	1	73
	4	-5	-9	20
# 2	1	-6	-2	37
	2	-1	6	19
	3	-3	3	45
	4	-6	-8	18
# 3	1	-6	-3	51
	2	2	2	50
	3	-2	-6	55
	4	-1	-5	25

The temperature measurements from door ventilation to suppression were within the ± 15 % expanded uncertainty of the TC. It was determined the two temperature methods were measuring indistinguishable temperatures. This suggests that the particulates within the smoke layer are in a sufficient enough quantity to impact radiant energy received by the TIC. Recall Section 2.2.2, TICs are designed to absorb IR in the LWIR range. This wavelength range is indicative of radiant energy emitted from solid objects. There is not enough information to exclude the contribution of the metal structure wall in this measurement. The temperatures produced by the TIC are indicative of the contributions from both the solid object and smoke particulate.

The third section the percent difference indicates that the two temperature

methods were producing distinguishably different results. The TIC was producing larger temperatures than the TC. There was little to no smoke present within the structure during this time resulting of a TIC temperature measurement of the structure wall. The measurement zone location did not correspond directly with the location of the wall-mounted TC. The measurement zone was located fully on the hallway wall at a higher elevation than the TC. The hallway way was not isothermal during experimentation; however, as multiple wall mounted TC were not installed this analysis compares TIC data to the wall mounted TC at 1.5 m. Figure 6.6 - 6.12 visually represents the temperature outputs of the TICs and the wall-mounted TC while Table 6.6 indicates the percent difference between each TIC and the wall-mounted TC on the hallway back wall.

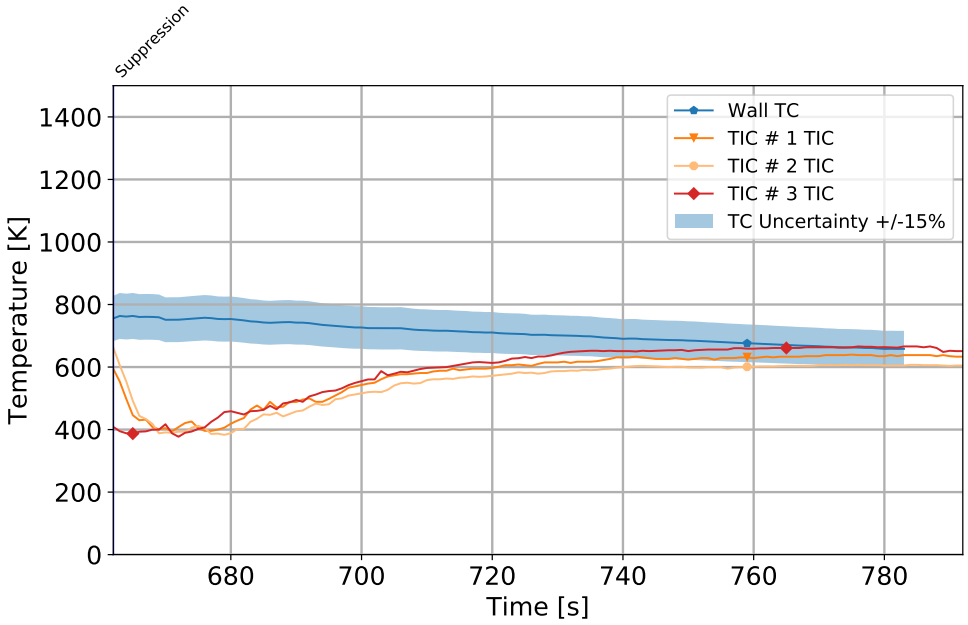

(a) Experiment # 1

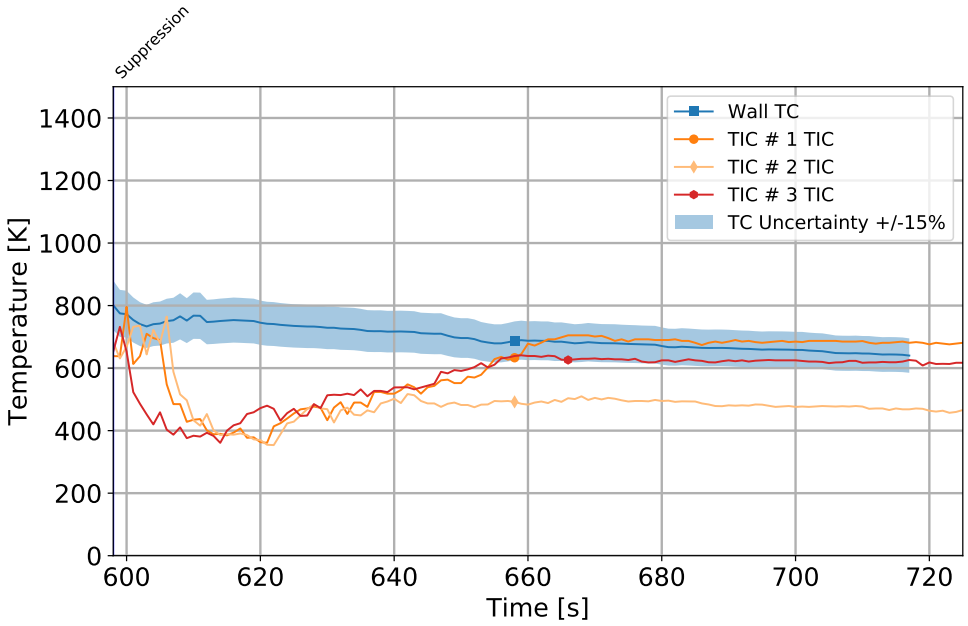

(b) Experiment # 2

Figure 6.11: Exterior TIC # 1, TIC # 2, and TIC # 3 vs. Wall-Mounted TC

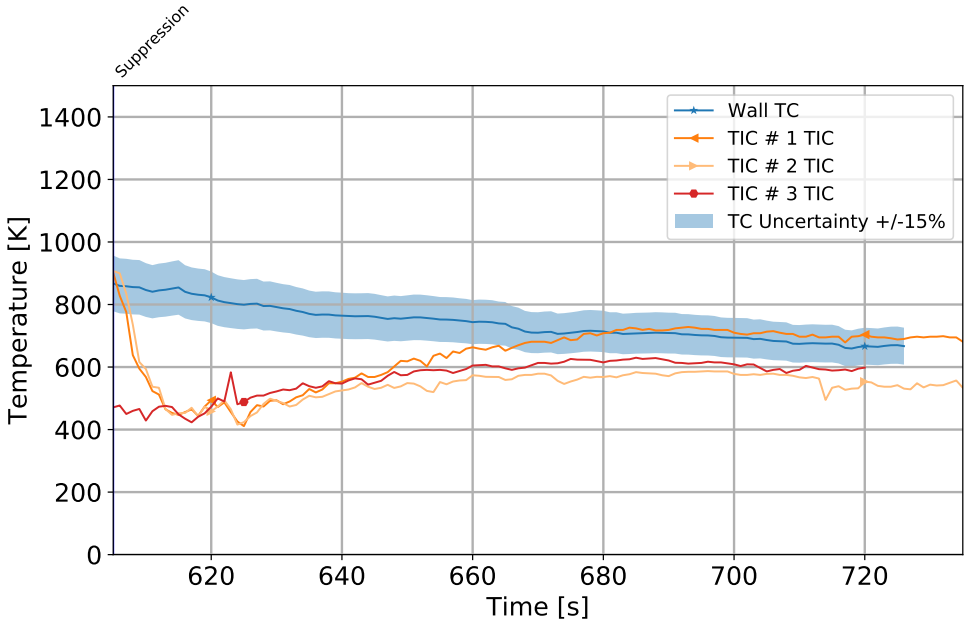

(a) Experiment # 3

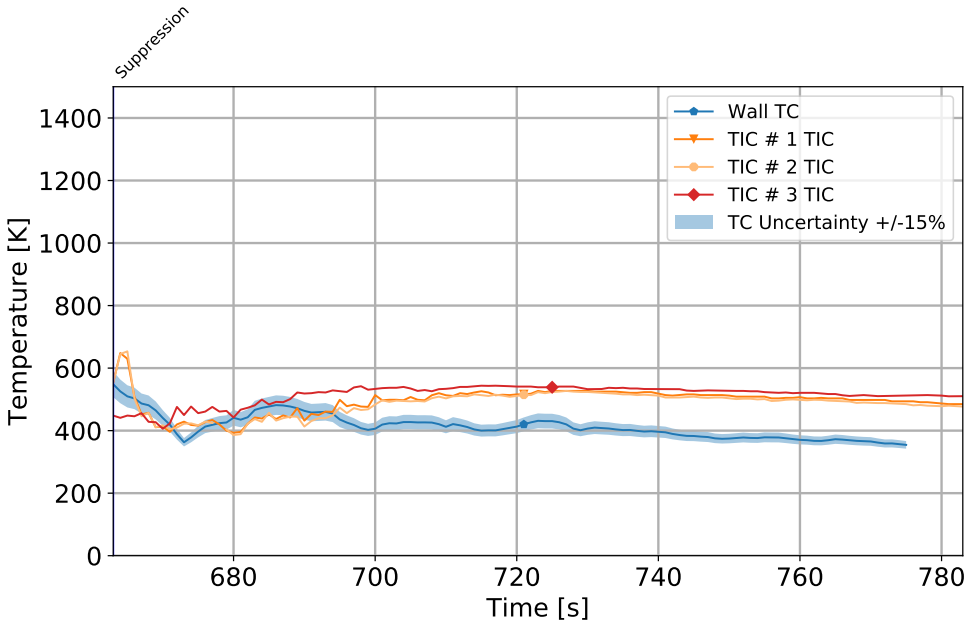

(b) Experiment # 4

Figure 6.12: Exterior TIC # 1, TIC # 2, and TIC # 3 vs. Wall-Mounted TC

Table 6.6: Room-Scale Fire Experiments - Exterior TIC vs. Wall TC: Percent Difference

TIC	Exp. #	PC (Post Suppression-End)
# 1	1	-13
	2	7
	3	-8
	4	29
# 2	1	-17
	2	-29
	3	-23
	4	27
# 3	1	-9
	2	-11
	3	-17
	4	34

The results presented in Table 6.6 are not within the expanded uncertainty of ± 15 %, indicating distinguishably different results. However, these results are are more similar than those presented in Table 6.5. This indicates that the TIC was reading the hallway wall rather than the gas temperatures when smoke concentration was low. The percent differences were between 8 - 34%. This percent difference range can be explained by the behavior of the TIC temperature outputs. The TIC calculates temperatures at a lower magnitude than the TC for the first 60 s, than increases in magnitude similarly to that of the TC temperatures. During this first 60 s, the opacity of the structure is still high, low visibility, as seen in Figure 6.7. The opacity of the structure gradually decreased, increasing visibility; which, corresponded to more consistent temperatures between the TIC and TC. This trend affected the average percent difference during this time-frame causing the wide range of values witnessed.

6.3.2 Interior TIC Location

The measurement zone associated with the interior TIC location was directed on the far wall of the hallway, nearest the fire room. The target object was monitored by a wall mounted TC; while, the focal length between the TIC and TC were monitored by several gas TC arrays. This location is near the fire room and likely to be affected by radiative energy originating flames; however, the temperatures were not corrected for these effects. Rather the analysis includes an expanded uncertainty of ± 15 %. The TIC temperature outputs were first analyzed against the wall-mounted TC. The temperature outputs from both measurement methods are visually represented by Figure 6.13 - 6.14.

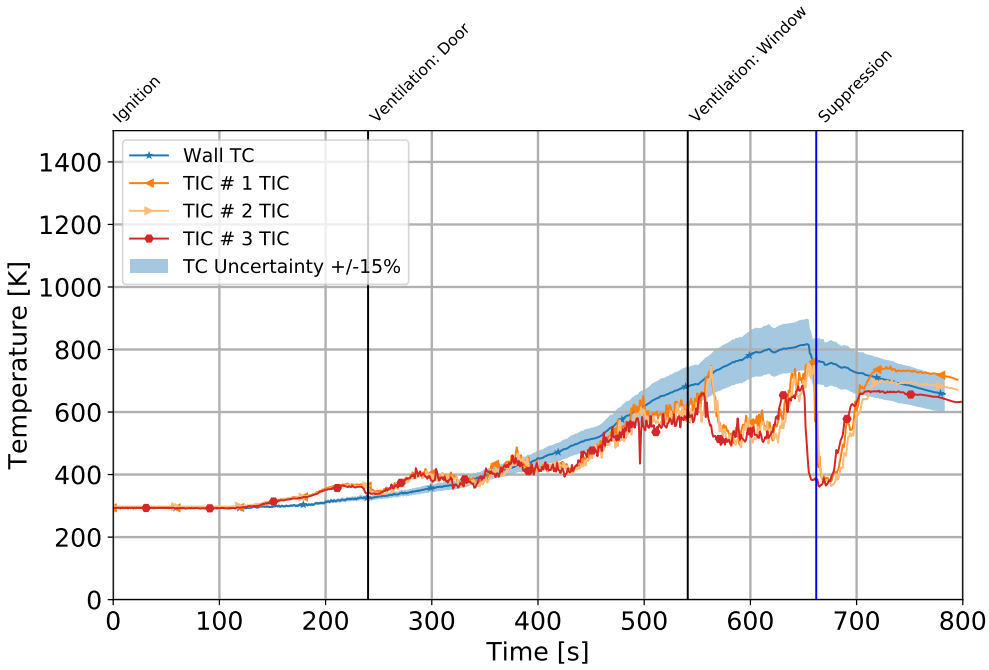

(a) Experiment # 1

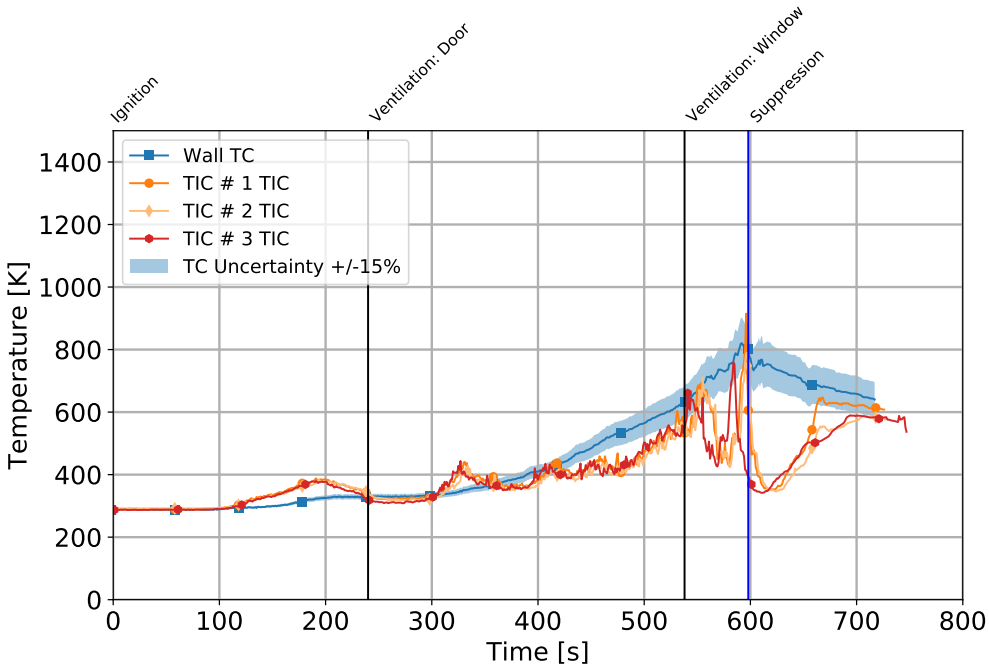

(b) Experiment # 2

Figure 6.13: Interior TIC # 1, TIC # 2, and TIC # 3 vs. Wall-Mounted TC

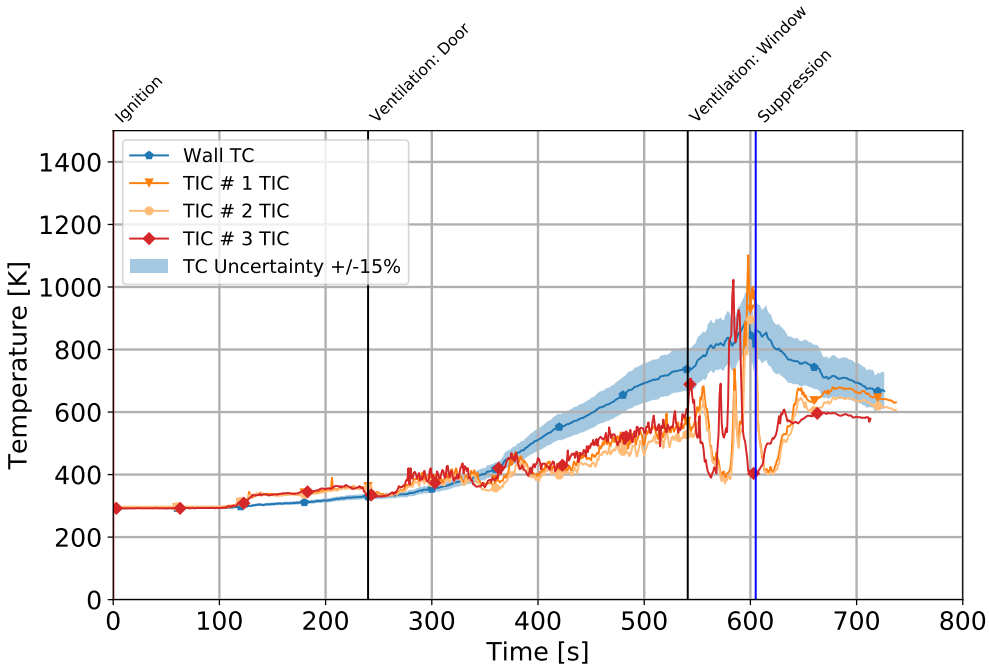

(a) Experiment # 3

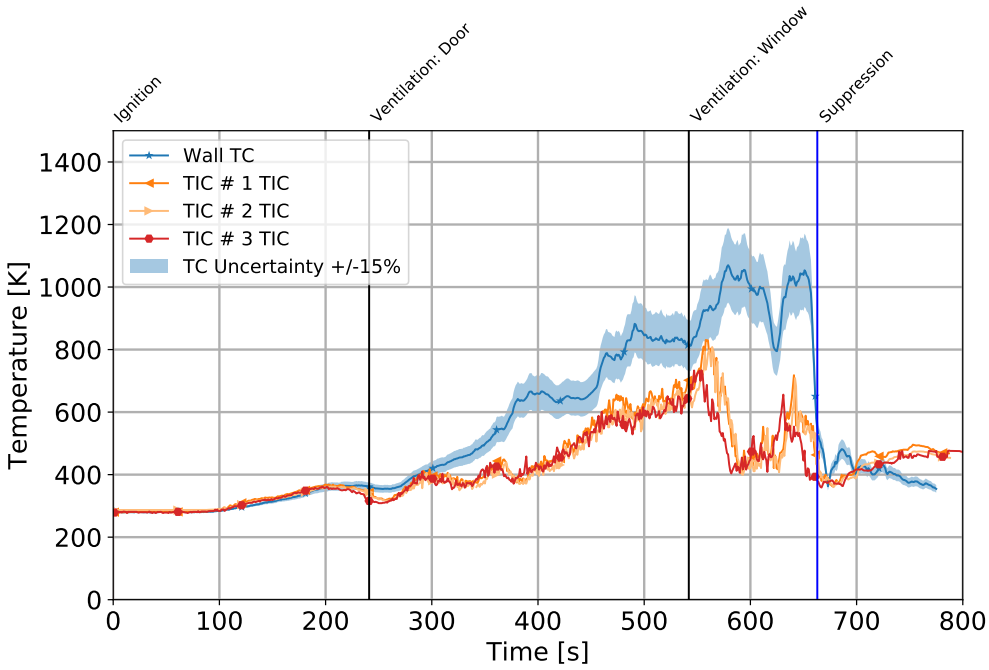

(b) Experiment # 4

Figure 6.14: Interior TIC # 1, TIC # 2, and TIC # 3 vs. Wall-Mounted TC

The percent difference between the two measurement methods was calculated for each time-step and averaged over the following time-periods: door to window ventilation, window ventilation to suppression, and suppression to test end. This information is presented in Table 6.7.

Table 6.7: Room-Scale Fire Experiments - Interior TIC vs. Wall TC: Percent Difference

TIC	Exp. #	PC (Door - Window)	PC (Window - Prior to Suppression)	PC (Post Suppression - End)
# 1	1	-1	-22	2
	2	-5	-11	-17
	3	-11	-31	-10
	4	-20	-39	19
# 2	1	-3	-25	-5
	2	-8	-12	-25
	3	-15	-35	-15
	4	-23	-41	14
# 3	1	3	-28	-7
	2	-6	-20	-23
	3	-9	-35	-20
	4	-23	-43	12

Experiment # 4, shows a larger percent difference for the time-frame from door ventilation to window ventilation. The target object material composition varied during this experiment. There is not enough information to determine if this solely impacts the percent difference during this time. It should be noted that Experiment # 4 experienced considerably higher wind speeds. The difference in temperature method outputs could be explained by a combination of effects from both material composition and wind.

Between window ventilation to prior to suppression, the TIC produced differ-

ent temperatures from the wall TC. During this time the radiant energy emitted from the wall was impacted by the optically thick thermal gases. The participating media can absorb IR radiation produced from the wall, transmit / scatter IR from the wall, or emits its own IR energy similarly to that of a solid object. To explore if the effects of participating media on TIC spot temperatures, the temperature measurements obtained from the TC array representing the focal length between the TIC and target object was graphed along with the TIC temperature outputs. Figures 6.15 - 6.16 represents the TIC temperature output and the three TCs that produced the most similar temperatures.

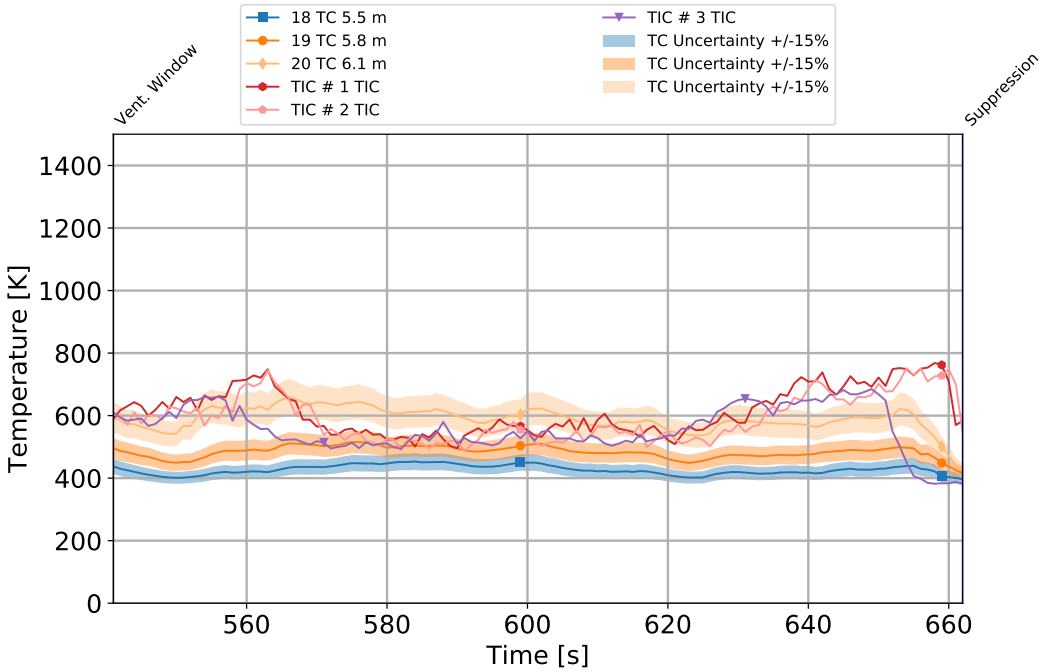

(a) Experiment # 1

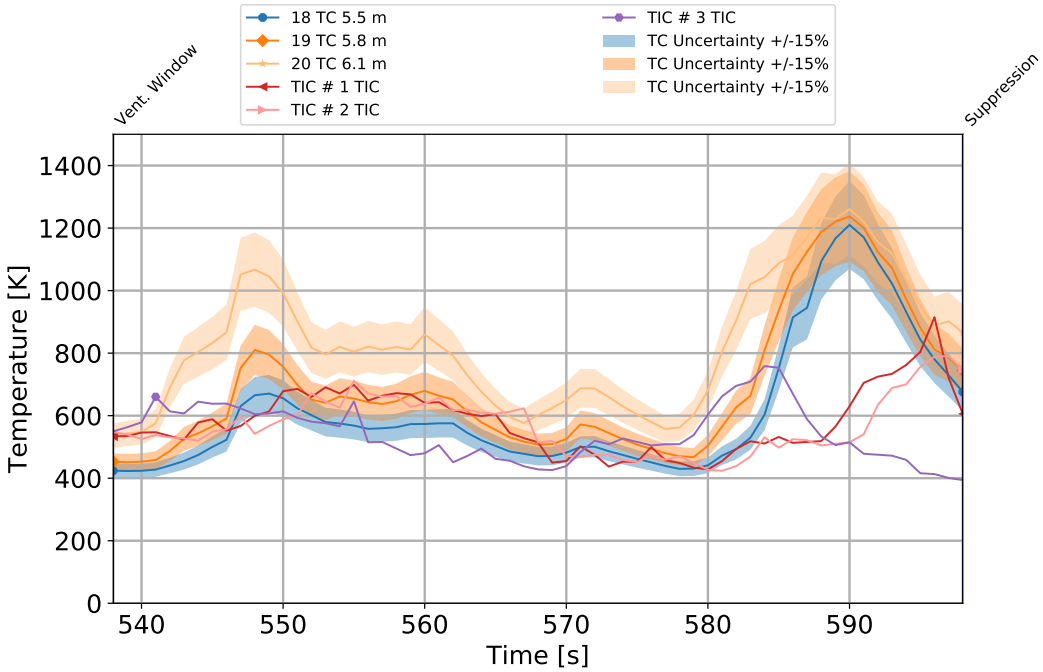

(b) Experiment # 2

Figure 6.15: Interior TIC # 1, TIC # 2, and TIC # 3 vs. Gas TC. The TC labels indicate the distance between the TIC lens and the target object, e.g. 18T was located 5.5 m (18 ft) from the TIC lens along the focal length.

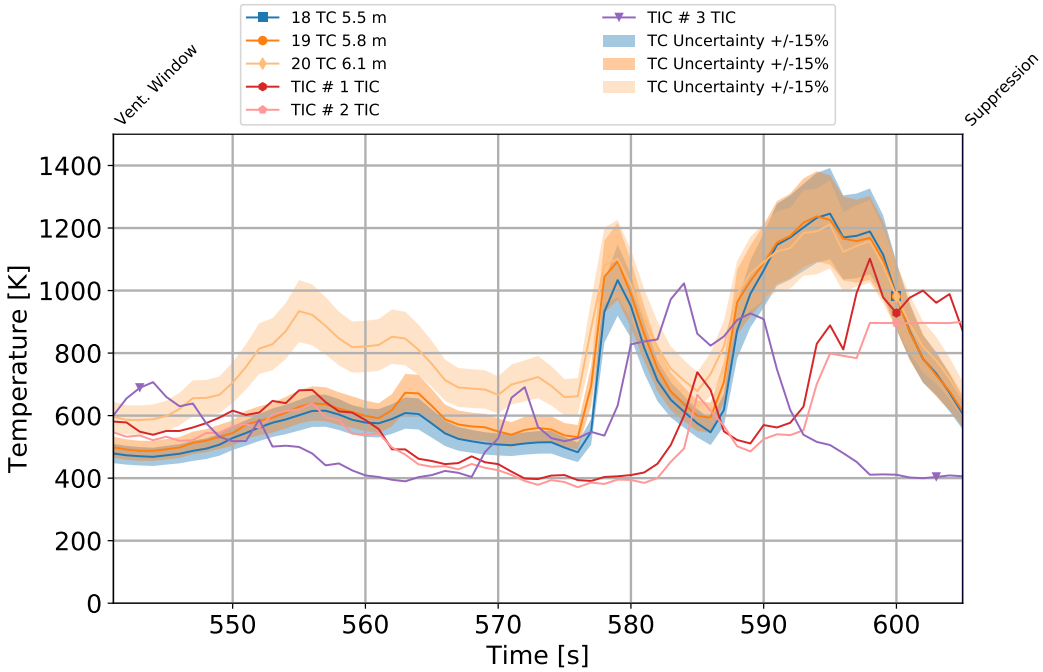

(a) Experiment # 3

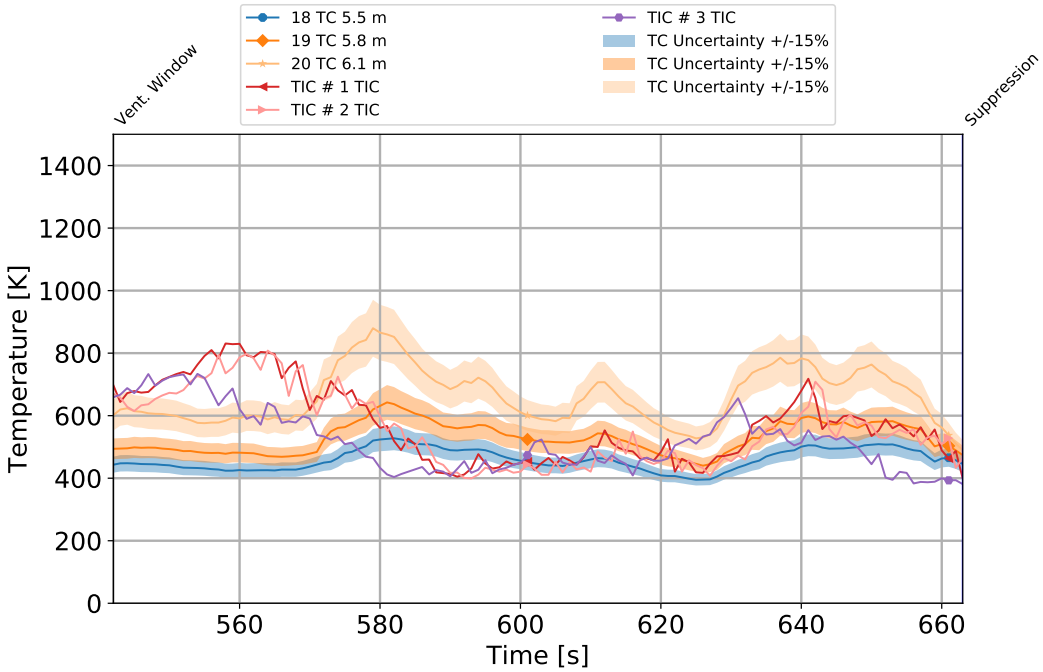

(b) Experiment # 4

Figure 6.16: Interior TIC # 1, TIC # 2, and TIC # 3 vs. Gas TC. The TC labels indicate the distance between the TIC lens and the target object, e.g. 18T was located 5.5 m (18 ft) from the TIC lens along the focal length.

The TIC measured temperatures comparable to those obtained from gas TCs at various distanced within the focal length. The focal lengths producing the lowest percent difference are summarized in Table 6.8. It was determined that TIC temperature was approximately the same as the gas TC temperature at distances of 5.5 - 6.1 m. The affect of participating media on solid surface radiant energy transmission influences TIC spot temperature measurements.

Table 6.8: Room-Scale Fire Experiments - Focal Length

TIC	Exp. # 1	Exp. # 2	Exp. # 3	Exp. # 4
# 1	6.1 m	5.8 m	5.5 m	6.1 m
# 2	6.1 m	5.8 m	5.5 m	5.8 m
# 3	6.1 m	5.5 m	5.5 m	5.8 m

The optimal focal lengths, that of which produced the lowest percent difference between TIC and TC temperature measurements, between the interior TIC and the gas TC was investigated for the remaining time frames: ignition to door ventilation, door ventilation to window ventilation, and suppression to test end. This resulted in similar focal lengths as presented in Table 6.8, distances between 4.89 - 6.1 m for times characterized by the presence of smoke, ignition to suppression. During the time period of suppression to test end, there was not an optimal focal length, percent difference below ± 15 %. This suggests that during times without smoke presence, the TIC could determine the temperature solid target objects. This suggestion is validated by the agreement of interior TIC temperature outputs against the wall mounted TC in Figure 6.13.

6.3.3 Conclusions

The room-scale fire experiments determined that TICs are affected by smoke obscuration. Radiant energy emitted from solid objects can be impacted by participating media. The exterior TIC was able to determine the temperature of smoke leaving the structure but there is not sufficient enough data to determine the IR contribution from solid wall within the smoke layer. The interior TIC was able to determine the temperature of the target object during ambient conditions. There is not sufficient enough data to determine the affects of IR absorption, transmission/scatter, and emission from participating media. It was determined TIC spot temperatures are most similar to gas temperatures roughly 5.5 - 6.1 m away.

Chapter 7: Future Research

TIC spot temperature measurements were evaluated in two different environments. The effect of distance and orientation were explored during ambient conditions. TIC spot temperatures were influenced by distance between the TIC and target object. Further research is needed to determine how TICs determine temperatures of solid objects. Future experiments should include an isothermal target object with a known emissivity value, at or near the pre-defined emissivity value of fire service TICs. These experiments should include iterations at varying distances to investigate how the percentage of the target object within the FOV affects spot temperature measurements.

The effect of participating media was explored during a smoke-filled environment. Further research is needed to understand the influence of participating media on solid object IR. Future experiments should explore how participating media absorbs, transmits/scatters, and emits IR radiation. After it is established how participating media affects IR, a new series of experiments evaluating a TICs ability to quantify thermal hazards should be conducted. It is suggested that an isothermal object with known emissivity similar to a black body should be utilized. Black bodies are known as perfect emitters as they absorb all radiation that comes it comes

in contact with. Utilizing a black body as the target object would reduce any unknowns associated with emissivity. It is also suggested that smoke be introduced to the test environment without the presence of flames. This will eliminate any interaction of IR beyond the smoke or target object.

Chapter 8: Summary

Two sets of experiments were conducted on three fire service TICs to evaluate the TICs ability to quantify hazards within an environment. The first set of experiments evaluated the effect of distance and orientation on TIC spot temperature measurements during ambient conditions. The target object was heated to above ambient temperatures with a torch. Spot temperatures were compared to wall mounted TC measurements for the target object. Spot temperatures were determined to be a function of distance between the TIC and target object during ambient conditions.

The second set of experiments evaluated the effect of participating media on TIC spot temperature measurements during combustion conditions. Two sofas were ignited in a metal training structure, creating repeatable heating conditions for the target object. Spot temperatures were compared to gas and wall mounted TC measurements. It was determined that participating media affects spot temperature measurements during smoke-filled environments.

Chapter A: Image Post Processing Techniques

Three separate scripts utilizing different image processing techniques were created to evaluate the TIC visual outputs. While each script operates independently of each other, all three techniques share similarities in initial endeavors to convert video into a string of images. The overarching common structure and commands is introduced in this section. Architecture and commands specific to each script is summarized in the following technique specific sections.

The preamble, or introductory statement, defines the required Python packages and commands needed to properly execute the script. There are five common packages between the three techniques. The first is Pillow, or PIL, and is a fork of Python Image Library; which, allows for easy manipulation of images specifically when opening, editing, and saving in different file formats. The second is OpenCV, or cv2, and is an open source computer vision library; which, allows for computational efficiency when writing computer vision scripts. The third is Python's Miscellaneous Operating System Interface, or os; which, allows the script to interface with a computers operating system to complete various tasks. The fourth is NumPY, or np, and is the fundamental scientific computing package with Python; which, adds additional functionality. The fifth is Pandas, Python Data Analysis Library or pd;

which, aids in analyzing data, in formats such as a CSV, in Python.

```
# Preamble
from PIL import Image, ImageFilter, ImageEnhance
import cv2
import numpy as np
import pandas as pd
```

After the preamble is defined, the specific experiment information is defined. This information includes an initial list of all experiments to be analyzed by the specific code. A second list, corresponding to the first, includes information needed to successfully define the raw videos location path.

```
# Specify experimental information ['Video Name']
Video = ['video_1']

# Specify path Location information ['Folder Name', 'File Name']
Location = {'video_1':['Combust_Exp_1', 'Bullard_Ext_TIC']}
```

Now that all necessary information regarding packages, functions, and experiment specific information has been defined, the script can begin to compute. The first step is to loop over the initial list of experiments, 'Video', to define that all following commands be applied to each video specified. This condenses the length of the code considerably and avoids unnecessary redundancy.

The first step within the analysis of each video is to specifically define the input, raw videos, location path by combing the information previously specified with general path information and video format. The second step is to specifically define the output, .csv file, location path for the post processed information the script is designed to produce.

```
# Begin program
for exp in Video:

    # Specify the input video location and file type
    input_location = '../path/' + Location[exp][0] + '/'
    video_format = '.avi'

    # Specify the output CSV location
    output_location = '../path/' + Location[exp][0] + '_TIC/'
```

After specifying the input and output information locations, analysis of the raw experimental data, videos, can commence. This is typically accomplished by utilizing the cv2 python package to manipulate the video files. First, the script opens and 'reads' each video. Second, the script determines the total video length, in terms of total frames. Third, the script determines the approximate frame rate, number of frames per second. This determination is approximate, as the frame rate is not typically a whole number per second; but rather, the frame rate varies by a fraction of a frame per second.

```
    # Read the video
    vid = cv2.VideoCapture(input_location + exp + video_format)

    # Determine the total number of frames and display it on the screen
    frames = (vid.get(cv2.CAP_PROP_FRAME_COUNT))
    print (frames)

    # Determine the frame rate and display it on the screen
    frame_rate = float(vid.get(cv2.CAP_PROP_FPS))
    print (frame_rate)
```

Finally, the last common step between each script is to create a data frame or array of values, using the Pandas python package. This data frame stores the post processed temperature output indexed to the respective frame it was determined from. This data frame is initially specified to be empty for each experiment; this allows the script to auto populate the data frame as it complies.

```
36      # Define a data frame for frame number and temperature
37      values = pd.DataFrame({'Frame':[],'Temp':[]}).set_index('frame')
```

A.1 Seven-Segment

To analyze TIC # 1 Camera Type 1 temperature text style, this script evaluates each digit in the TIC temperature output, ones, tens, and hundreds, separately [42]. This scripts preamble includes one additional Python package, Imutils, and one specific function from this package. The python package Imutils, is a series of functions that make image editing easier. The specific function, contours, is used to find outlines within the image. This function is defined here so it may be 'called' later within the code.

```
1 # Preamble
2 from PIL import Image, ImageFilter, ImageEnhance
3 import cv2
4 import numpy as np
5 import pandas as pd
6 import imutils
7 from imutils import contours
```

Lines 9 - 37 are identical to the aforementioned common commands (Lines 9 - 37). This script continues after the creation of the data frame (Line 37) for the temperature and frame by specifying additional information. First, a second data frame is created for each individual numbers place, ones, tens, and hundreds. The thousands number place was not needed for these videos. Second, the location of each numbers place (in the x direction) within visual output of the video is defined. Third, a reference table of values 0 - 9 is created. Each value is defined according to the corresponding 'on' and 'off' segments, assuming a seven-segment display.

The script continues by looping over every frame within the video, at an inter-

```
39    # Define a Data Frame for each numbers place
40    number_value = {'Ones':'', 'Tens':'', 'Hundreds':''}
41
42    # Define the location of each numbers place in the TIC temperature output
43    number_location = {'Ones':[641,659], 'Tens':[623,641], 'Hundreds':[605,623]}
44
45    # Define the reference table for the seven-segment display
46    DIGITS_LOOKUP = {
47    (0, 0, 0, 0, 0, 0, 0): '',
48    (1, 1, 1, 0, 1, 1, 1): 0,
49    (0, 0, 1, 0, 0, 1, 0): 1,
50    (1, 0, 1, 1, 1, 0, 1): 2,
51    (1, 0, 1, 1, 0, 1, 1): 3,
52    (0, 1, 1, 0, 0, 1, 0): 4,
53    (1, 1, 1, 0, 0, 1, 0): 4,
54    (1, 1, 0, 1, 0, 1, 1): 5,
55    (1, 1, 0, 1, 1, 1, 1): 6,
56    (1, 0, 1, 0, 0, 1, 0): 7,
57    (1, 1, 1, 1, 1, 1, 1): 8,
58    (1, 1, 1, 1, 0, 1, 1): 9}
```

val equal to the frame rate, and 'reads' or interprets the video. This specifies that the following commands be executed for a single frame every second for the total length of the video.

```
60    # Read a single frame per second
61    for frame in range(0, frames, int(round(frame_rate))):
62        ret, im = vid.read()
```

First, if the script can interpret the video, the script loops over each numbers place. This specifies that the following commands be executed for each numbers place within the TIC temperature output. Second, it converts the video frame to an image, cropped to only include the TIC temperature output corresponding to the specific numbers place. Third, the image is saved to the output location

The script again loops over each numbers place and a series of morphological processes are applied to the image. These morphological processes utilize both CV2 and NumPY to increase the accuracy of the seven-digit post processing technique; however, these languages are not always compatible resulting in saving and reopen-

```
64        if ret:
65
66            # Crop video frame to display one digit at a time
67            for num in number_location:
68                im_crop = im[405:455, number_location[num][0]:number_location[num][1]].copy()
69
70                # Save video frame as an image
71                cv2.imwrite(output_location + num + '.jpg', im_crop)
```

ing the image several times. The ideal image is in a binary, black and white, color space with minimal noise and increased smoothness/blur.

```
73            # Manipulate the image one digit at a time
74            for num in number_location:
75                im = Image.open(output_location + num + '.jpg')
76
77                # Resize the image with specific DPI
78                size = (140, 145)
79                im = im.resize(size)
80                width, height = im.size
81                im.save(num + '.jpg', dpi=(300, 300))
82
83                # Resize the cropped image
84                image = cv2.imread(num + '.jpg')
85                nx , ny, channels = image.shape
86                im_crop = cv2.resize(image, (int(ny*2), int(nx*2)))
87
88                # Convolve (smooth) the image with a square kernel
89                s_kernel = np.ones((7,7), np.float32)/25
90                smooth = cv2.filter2D(im_crop, -1, s_kernel)
91
92                # Convert the color space from RGB to grayscale
93                grayscale = cv2.cvtColor(smooth, cv2.COLOR_BGR2GRAY)
94
95                # Determine the color of each pixel (black or white)
96                pixel = cv2.threshold(gray, 0, 255,
97                cv2.THRESH_BINARY_INV | cv2.THRESH_OTSU)[1]
98
99                # Convolve (remove noise)  with a non-square kernel
100               ns_kernel = cv2.getStructuringElement(cv2.MORPH_ELLIPSE, (1, 5))
101               noise = cv2.morphologyEx(pixel, cv2.MORPH_OPEN, ns_kernel)
102
103               # Resize the image to a specific height
104               image = imutils.resize(noise, height=410)
105
106               # Convolve (blur) the image with a Gaussian kernel
107               blurred = cv2.GaussianBlur(image, (5, 5), 0)
```

After manipulating the image, the script determines the ‘on’ or ‘off’ status of each of the seven-segments for each numbers place TIC temperature output.

Once the ‘on’ and ‘off’ status of each segment is determined, the reference table is used to identify the digit. The digit is saved to the corresponding data

```
109             # Find the contours of the TIC temperature output
110             cnts = cv2.findContours(blurred, cv2.RETR_EXTERNAL,
111                 cv2.CHAIN_APPROX_SIMPLE)
112             cnts = cnts[0] if imutils.is_cv2() else cnts[1]
113             digitCnts = []
114
115             # Create a bounding box over the height of the text
116             for c in cnts:
117                 (x, y, w, h) = cv2.boundingRect(c)
118                 if w >= 18 and (h >= 300 and h <= 410):
119                     digitCnts.append(c)
120
121             digits_num = []
122
123             # Find the shape of each digit
124             for c in digitCnts:
125                 (x, y, w, h) = cv2.boundingRect(c)
126                 roi = thresh[y:y + h, x:x + w]
127                 (roiH, roiW) = roi.shape
128                 (dW, dH) = (int(roiW * 0.25), int(roiH * 0.15))
129                 dHC = int(roiH * 0.05)
130
131             # Define where the 7-segments are located over the image
132             segments = [
133                 ((w // 4, 30 - dHC), (w - (w // 4), 30 + dHC)),                  # top segment
134                 ((0, 10), (dW, h // 2)),                                        # top-left segment
135                 ((w - dW, 10), (w, h // 2)),                                    # top-right segment
136                 ((w // 4, (h // 2) - dHC) , (w - (w // 4), (h // 2) + dHC)),    # center segment
137                 ((0, h // 2), (dW, h)),                                         # bottom-left segment
138                 ((w - dW, h // 2), (w, h)),                                     # bottom-right segment
139                 ((w // 4, 345 - dHC), (w - (w // 4), 345 + dHC))]               # bottom segment
140             on = [0] * len(segments)
141
142             # Compute the total number of pixels in each segment
143             for (i, ((xA, yA), (xB, yB))) in enumerate(segments):
144                 segROI = roi[yA:yB, xA:xB]
145                 cv2.rectangle(thresh, (xA, yA), (xB, yB), (57, 255, 20), 1)
146                 total = cv2.countNonZero(segROI)
147                 area = (xB - xA) * (yB - yA)
148
149                 # Define 'on' when at least 50 percent of pixels are white
150                 if total / float(area) > 0.50:
151                     on[i]= 1
```

frame.

```
153             # Reference 7-digit table to determine number
154             digit = DIGITS_LOOKUP[tuple(on)]
155             digits_num.append(digit)
156
157             # Save post processed 7-Digit output to data frame
158             number_value[num]=digit
```

Lastly the script rearranges the numbers place into a complete number and saved to the corresponding data frame. The data frame is saved as a new entry to the experiment specific csv file.

```
---
160             # Put whole number back together
161             digit = (str(number_value['Hundreds']) + str(number_value['Tens']) + str(number_value['Ones']))
162             print('final number is ' + digit)
163 
164             # Save post processed 7-Digit output to DataFrame
165             values.loc[int(frame)] = digit
166 
167         # Save DataFrame to a CSV File
168         values.to_csv(output_location + exp + '.csv')
```

A.2 Image Comparison

TIC # 1 Camera Type 2 temperature text style evaluates each digit in the TIC temperature output, ones, tens, and hundreds, separately. This scripts preamble includes an additional python package, gc, and a specific function. The Python Package Garbage Collector interface, gc, is a strategy for memory allocation. The specific function compare ssim, computes the mean structural similarity index between two images. This function is defined here so it may be 'called' into use later within the code.

```
# Preamble
from PIL import Image, ImageFilter, ImageEnhance
import cv2
import numpy as np
import pandas as pd
from skimage.measure import compare_ssim
import gc
```

In addition, another function, mse, is defined within the preamble. This function is used to calculate the mean squared error between two images and requires specific information to be defined before it can be 'called' into use [43].

```
# Define Mean Squared Error (MSE) function
def mse(imageA, imageB):
    err = np.sum((imageA.astype("float") - imageB.astype("float")) ** 2)
    err /= float(imageA.shape[0] * imageA.shape[1])
    return err
```

Lastly to maximize the efficiency of this script, the set of 10 reference images, which were obtained by hand, are loaded into the script. This allows the script to reference the images throughout the analysis without the need to reload the image

for every comparison.

```
15 # Load reference image set
16 ISG_Outside_loc = '../path/'
17 Refernce_numbers = [0, 1, 2, 3, 4, 5, 6, 7, 8, 9]
18 reference = {}
19 for ref in Numbers:
20     reference[ref] = cv2.imread(ISG_Outside_loc + str(ref) + '.jpg')
21     print ('read ' + str(ref))
```

Lines 23 - 51 are identical to the aforementioned common commands (Lines 9 - 37). This script continues after the creation of the data frame, (common command Line 37) for the temperature and frame, by specifying additional information. First, a second data frame is created for each individual numbers place, ones, tens, and hundreds. Second, the location of each numbers place (in the x direction) within the visual output of the video is defined.

```
53     # Define a data frame for each numbers place in the TIC temperature output
54     number_value = {'Ones':'', 'Tens':'', 'Hundreds':''}
55
56     # Define the physical location of each numbers place in the TIC visual output
57     number_location = {'Ones':[641,659], 'Tens':[623,641], 'Hundreds':[605,623]}
```

The script continues by looping over every frame within the video, at an interval equal to the frame rate, and 'reads' or interprets the video. This specifies that the following commands be executed for a the first frame within every second for the total length of the video.

```
59     # Read a single frame per second
60     for frame in range(0, frames, int(round(frame_rate))):
61         vid.set(1, frame-1);
62         ret, im = vid.read()
```

First, if the script can interpret the video for the specified frame, the script loops over each numbers place and attempts to determine the digit, otherwise the script records an empty data frame for temperautre for the given frame. This specifies that the following commands be executed for each numbers place for each frame within the length of the video. Second, it converts the video frame into an image, cropped to only include the TIC temperature output corresponding to the specific numbers place. Third, the image is saved to the output location.

```
64        if ret:
65
66            # Crop video frame to display one digit at a time
67            for num in number_location:
68                im_crop = im[405:455, number_location[num][0]:number_location[num][1]].copy()
69
70                # Save video frame as an image
71                cv2.imwrite(output_location + num + '.jpg', im_crop)
```

The script again loops over each numbers place and opens the previously saved image. A series of morphological processes are applied to the image utilizing both CV2 and NumPY, to increase the accuracy of the image comparison post processing technique; however, these languages are not always compatible resulting in saving and reopening the image several times. The ideal image is in a binary, black and white, color space with minimal noise and increased smoothness.

After manipulating the image, the script determines the relative similarity and relative difference of each numbers place to all 10 reference images.

Once the similarities and differences for each reference number is determined, the script identifies which reference number is most similar and least different from the numbers place image.

```
        # Manipulate the image one digit at a time
        for num in number_location:

            # Resize the image with specific DPI
            im = Image.open(output_location + num + '.jpg')
            size = (140, 145)
            im = im.resize(size)
            width, height = im.size
            im.save(num + '.jpg', dpi=(300, 300))

            # Resize the cropped image
            image = cv2.imread(output_location + num + '.jpg')
            nx , ny, channels = image.shape
            im_crop = cv2.resize(image, (int(ny*2), int(nx*2)))

            # Convolve (smooth) the image with a square kernel
            s_kernel = np.ones((7,7), np.float32)/25
            smooth = cv2.filter2D(im_crop, -1, s_kernel)

            # Convert the color space from RGB to grayscale
            grayscale = cv2.cvtColor(smooth, cv2.COLOR_BGR2GRAY)

            # Determine the color of each pixel (black or white)
            pixel = cv2.threshold(grayscale, 0, 255,
            cv2.THRESH_BINARY | cv2.THRESH_OTSU)[1]

            # Convolve (remove noise) with a non-square kernel
            ns_kernel = cv2.getStructuringElement(cv2.MORPH_ELLIPSE, (1, 5))
            noise = cv2.morphologyEx(pixel, cv2.MORPH_OPEN, ns_kernel)

            # Save the manipulated image to the output location
            cv2.imwrite(output_location + num + '.jpg', noise)
```

Once each numbers place value is determined, the script complies the three digits into a single number. The post processed temperature digit is saved to the data frame corresponding to the frame evaluated. After each frame is evaluated the post processed temperature digits per second is saved to a .csv file.

```
                # Create an empty array for each variable
                m = {}
                min_m = {}
                s = {}
                max_s = {}

                # Ensures the arrays are empty
                gc.collect()

                # Compare numbers place images with each reference image
                temperature = cv2.imread(output_location + num + '.jpg')
                for ref in Numbers:

                    # Determine mean squared error (MSE)
                    m[ref] = mse(reference[ref], temperature)

                    # Determine structural similarity index (SSI)
                    s[ref] = compare_ssim(reference[ref], temperature, multichannel=True)

                    max_value_s = max(s.values())
                    min_value_m = min(m.values())

                # Determine the reference image with the highest SSI
                max_s = max(s, key=s.get)
                values.loc[int(frame), num + '_s_ref'] = max_s

                # Determine the reference image with the lowest MSE
                min_m = min(m, key=m.get)
                values.loc[int(frame), num + '_m_ref'] = min_m









                # Determine most likely digit as most similar and least different
                if max_s == min_m:
                    number_value[num] = max_s

                # Otherwise save an empty data frame for this numbers place
                else:
                    number_value[num] = ''









        # Put number back together
        digit = (str(number_value['Hundreds']) + str(number_value['Tens']) + str(number_value['Ones']))
        print('final number is ' + str(digit))

        # Save temperature value to Data Frame
        values.loc[int(frame), 'Temp'] = digit

    # Save Data Frame to a CSV File
    values.to_csv(output_location + exp + '.csv')

    number_value = {'Ones':'', 'Tens':'', 'Hundreds':''}
    max_s = {'Ones':'', 'Tens':'', 'Hundreds':''}
    min_m = {'Ones':'', 'Tens':'', 'Hundreds':''}
```

A.3 Optical Character Recognition

To analyze TIC # 2 and TIC # 3 TIC temperature output, two additional Python packages were needed: Pytesseract and regular expression operations, re. Pytesseract is an OCR engine. Re is a syntax tool which allows for the use of special characters within the given script without invoking their special meaning.

```
1 # Preamble
2 from PIL import Image, ImageFilter, ImageEnhance
3 import cv2
4 import numpy as np
5 import pandas as pd
6 import pytesseract
7 import re
```

Lines 9 - 37 are identical to the aforementioned common commands (Lines 9 - 37). This script continues after the creation of the data frame (Line 37) by looping over every frame within the video, at an interval equal to the frame rate, and 'reading' or interpreting the video. This for loop specifies that the following commands be executed for a single frame every second for the total length of the video.

```
39     # Read a single frame per second
40     for frame in range(0, int(frames), int(frame_rate)):
41         vid.set(1, frame-1);
42         ret, im = vid.read()
```

First, if the script can interpret the video, the script converts the video frame into an image, cropped to only include the text of the TIC temperature output.

Although, Pytesseract can read various types of text in various states of disarray, a series of morphological processes, NumPY and CV2 python packages, are

```
        if ret:
            # Crop image to display only the TIC temperature output
            im_crop = im[416:465, 500:650].copy()
```

applied to the cropped image to increase the accuracy of Pytesseract. The ideal image is in a binary, black and white, color space with minimal noise and increased smoothness/blur. The manipulated image is then saved to the output location.

```
..
            # Manipulate the image

            # Resize the cropped image
            nx , ny, channels = im_crop.shape
            im_crop = cv2.resize(im_crop, (int(ny*3), int(nx*3)))

            # Convolve (smooth) the image with a square kernel
            s_kernel = np.ones((5,5), np.float32)/25
            smooth = cv2.filter2D(im_crop, -1, s_kernel)

            # Convert the color space from RGB to grayscale
            grayscale = cv2.cvtColor(smooth, cv2.COLOR_BGR2GRAY)

            # Determine the color of each pixel (black or white)
            pixel = cv2.threshold(grayscale, 0, 255,
                cv2.THRESH_BINARY | cv2.THRESH_OTSU)[1]

            # Convolve (remove noise) the image with a non-square kernel
            ns_kernel = cv2.getStructuringElement(cv2.MORPH_ELLIPSE, (1, 5))
            noise = cv2.morphologyEx(pixel, cv2.MORPH_OPEN, ns_kernel)

            # Fill background color
            h, w = noise.shape[:2]
            mask = np.zeros((h+2, w+2), np.uint8)
            cv2.floodFill(noise, mask, (0,0), 0);

            # Invert color space to desired black letters on white background
            thresh_floodfill_inv = cv2.bitwise_not(noise)

            # Save the manipulated image
            cv2.imwrite(output_location + exp + '.jpg', thresh_floodfill_inv)
```

Lastly the Pytesseract engine is applied to the new image. The output text produced from the Pytesseract software is then post processed to increase accuracy. The new text is then saved to the data frame indexed to the respective frame number. The data frame is saved as a new entry to the experiment specific csv file.

```
            # Run the image through Pytesseract
            new_img = Image.open(output_location + exp +'.jpg')

            # Save Pytesseract output as 'temp'
            temp = pytesseract.image_to_string(new_img)

            # Redefine misconstrued letters to digits
            temp = temp.replace('U', '0')
            temp = temp.replace('I', '1')
            temp = temp.replace('O', '0')
            temp = temp.replace('B', '8')

            # Eliminate all letters
            temp = re.sub('[^0-9]', '', temp)

            # Save post processed Pytesseract output to data frame
            values.loc[int(int(frame), 'Temp')]=temp

        # Save data frame to a CSV File
        values.to_csv(output_location + exp + '.csv')
```

Chapter B: Initial Evaluation Results

B.1 Percent Difference Analysis Example

To quantify the observed trends between the TIC spot temperature measurement and TC measurements, the percent difference (PD) between the two temperature measurement methods was calculated from Equation B.1.

$$PD = \frac{T_{TIC} - T_{TC}}{T_{TC}} * 100 \tag{B.1}$$

Where T_{TIC} represents the temperature measurements obtained from the TIC and T_{TC} represents the temperature measurements obtained from the TC, both temperature measurements were converted into Kelvin [K]. Kelvin is an absolute thermodynamic temperature scale whose zero point is the temperature of absolute zero, or the temperature at which molecules stop moving. This temperature scale allows the difference between the two temperature methods to be determined and presented as a percentage.

When the temperatures measured from the TC array are greater than calculated by TIC, the graph is represented by a negative percent difference. When the temperatures measured from the TC array are less than calculated by the TIC,

the graph is represented by a positive percent difference. Due to the measurement uncertainty of TC ($\pm$ 15 %), there exists a temperature range for which the two temperature measurement methods produce quantitatively the same temperature. If the percent difference is less than 15 %, the two methods cannot be distinguished from one another. If the percent difference is higher than this number it is determined that the two temperature measurement methods are producing distinguishable measurements.

The time-line of the experimental tests has been bounded into three regions. The first region 'Pre-Ignition' is representative of the ambient conditions observed before combustion occurred, bounded by time 0 s to the first instance of a temperature increase greater than 15 % above ambient conditions. The second region 'Combustion' is representative of the combustion conditions observed during experimentation, bounded by the first instance of a temperature increase greater than 15 % to 30 s before suppression efforts began. This region ends prior to initiation of suppression tactics to avoid interference on the TIC temperature output, from firefighters and water spray present in the FOV. The third region 'Post-Suppression' is representative of the conditions observed after combustion occurred, bounded by 30 s post suppression efforts ended to the last recorded temperature. Figure B.1 represents each comparative technique discussed above, as well as the bounded time-line.

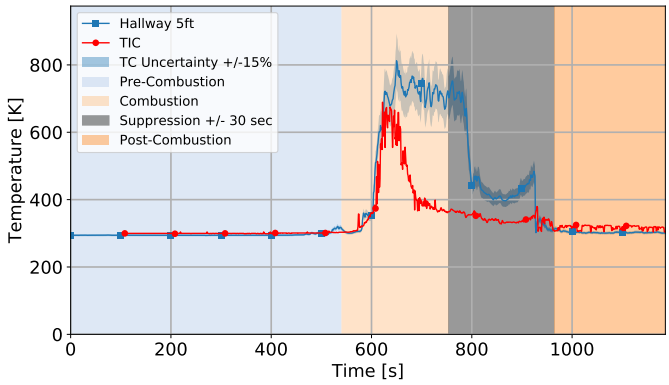

(a) Temperature

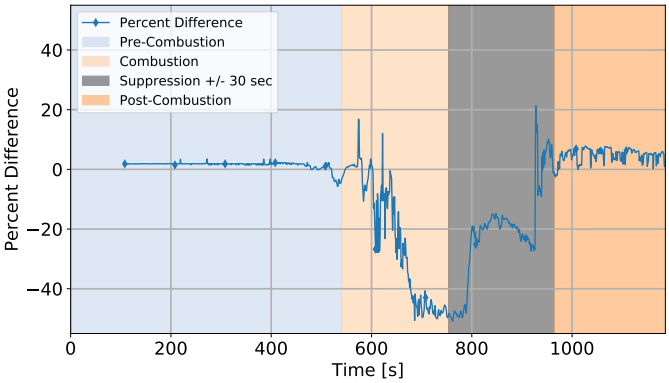

(b) Percent Difference

Figure B.1: Figure B.1(a) contains temperature data obtained from the TC array and TIC bounded into time-periods to quantify similarities observed between the TIC temperature output and the TC measured temperatures. The 'Pre-Ignition' region is colored light blue, the 'Combustion' region is colored light orange, and the 'Post-Suppression' region is colored dark orange. The time excluded from the analysis, indicative of the time in which suppression tactics were conducted, has been colored blue.

In the following analysis, the 'Combustion' region was broken into two sub-regions to further analyze the two temperature measurement methods. The first sub-region was deemed 'Initial Combustion', representing the time-period when the two temperature measurement methods are indistinguishable after ignition. During this time-period, the percent difference between the two temperature methods is nominally less than $\pm$ 15 %. This time-period ends when the percent difference increases beyond $\pm$ 15 % and indicates distinguishable temperatures for the duration of the 'Combustion' region. The second sub-region is 'Combustion', representing the time-period when the two temperature methods produce distinguishable results during combustion conditions. During this region the percent difference between the two temperature methods remains greater than $\pm$ 15 %.

The percent difference between the two temperature methods was calculated at every time-step during the experiment; therefore, the average percent difference for each time-period could be calculated. These averaged values represent the TICs ability to quantify thermal hazards during the various stages of fire growth, burn, and decay. To easily identify if the two temperature methods produced distinguishable or indistinguishable temperatures, the color scale presented in Table B.1 was created. When the average percent difference indicates the two temperature measurement methods produced indistinguishable results, the value was highlighted green. If the average percent difference indicates that the two temperature measurement methods produced distinguishable results, the value was highlighted red.

Table B.1: Levels of Agree-ability: Percent Difference

Level of Agree-ability	Percent Difference	Color Indicator
Agreeable	-15 % > PD < 15 %	
Different	-15 % < PD or PD > 15 %	

B.2 Measurement Zone Height Approximation

The following method was established to quantify the height of the TIC spot temperature measurement zone during the Fire Attack and IFSI experiments. Interior firefighting operations were employed during both projects, causing firefighters to pass within the TIC FOV. The height of measurement zone was normalized by the height of the firefighters. The average height of an adult male in the United States is 1.70 m [57] and standard body proportionality measurements were assumed. The relative scale, shown in Figure B.2 was established.

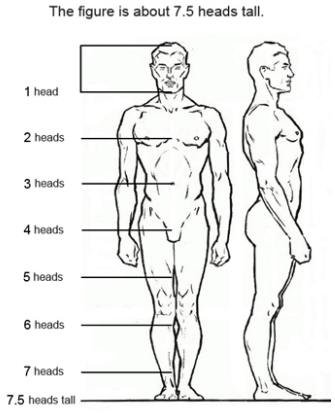

Figure B.2: Modern canons (system of measuring proportions) for expressing the human body are based on the length of the head. Generally, the overall height of an average human is expressed as 7.5 head lengths [58].

Three standing / kneeling firefighter positions were observed. The first position assumed the firefighter was standing, referred to as the standing position. The second position assumed the firefighter was kneeling, with their torso, hips, and quadriceps in alignment; referred to as the kneeling / standing position. The third position assumed the firefighter was kneeling, with their torso and hips in alignment forming a 90 ° with their quadriceps, referred to as the kneeling position. Each position and associated body proportionality is visually represented by Figure B.3.

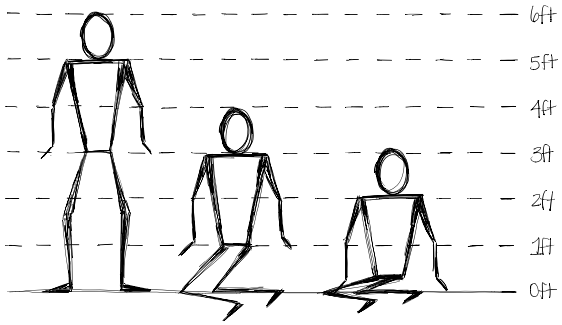

Figure B.3: Assuming the height of the firefighter and standard body proportionality, the height of each position was calculated.

For each position, the height of the firefighter was determined by evaluating the length various body parts. These heights were approximated to the nearest whole foot to mimic the TC array interval distance. The height and length of various body parts associated with each position are presented in Table B.2.

To determine the height of the measurement zone, the TIC video was visually assessed during times of firefighter presence within the FOV. As the firefighters passed within the measurement zone (at a similar depth within the FOV), the height of the measurement zone was compared to the height of the firefighter. This

Table B.2: Assuming the height of the firefighter and standard body proportions, the height of each position was represented numerically.

FF Position	Head	Shoulders	Waist	Hips	Knees
Standing	1.83 m	1.52 m	1.22 m	0.91 m	0.61 m
Standing / Kneeling	1.22 m	0.91 m	0.61 m	0.30 m	-
Kneeling	0.91 m	0.61 m	0.30 m	-	-

process produced a relative height for the TIC spot temperature measurement zone. The following analysis utilized this relative height to determine the TC bead most representative of the measurement zone location.

B.3 Measurement Zone Depth within the FOV Approximation

The following method was established to quantify the depth within the FOV for the TIC spot temperature measurement zone during the Fire Attack experiments. During this experimental series three TC arrays were employed in the hallway. To determine which TC array to use for the following analysis the TIC video was visually assessed to determine the location of the measurement zone location. Three distances were determined (near, middle, and far). For a near distance, the measurement zone was located in the living room or in the hallway nearest the living room. For a middle distance, the measurement zone was located equidistant between both the beginning and end of the hallway. For an end distance, the measurement zone was located at the end of the hallway.

B.4 Cardiovascular and Chemical Exposure Risks in Modern Firefighting

B.4.1 Hallway TIC

Table B.3: Measurement Zone Location: IFSI Hallway TIC

Exp. #	Camera Type	Zone Approx. Location	Zone Height	Associated TC Tree
2	Type 1	Far Bedroom Door, Half Open	0.91 m	Bedroom2
3	Type 1	Far Bedroom Door, Half Open	1.52 m	Bedroom5
4	Type 1	Far Bedroom Door, Half Open	1.52 m	Bedroom2
6	Type 1	Far Bedroom Door, Half Open	0.91 m	Bedroom2
8	Type 1	Far Bedroom Door, Half Open	0.91 m	Bedroom2
9	Type 2	Far Bedroom Door, Half Open	1.52 m	Bedroom5
10	Type 2	Far Bedroom Wall with Window	0.91 m	Bedroom2
11	Type 2	Far Bedroom Door, Half Open	2.13 m	Bedroom5
12	Type 2	Far Bedroom Door, Half Open	1.52 m	Bedroom2

Conclusions

Table B.4: Average Percent Difference: IFSI Hallway TIC

Exp. #	Pre-Ignition	Initial Combustion	Combustion	Post-Suppression
2	3	5	-48	-3
3	2	-7	-46	3
4	2	-3	-49	-1
6	2	-2	-50	1
8	1	1	-36	1
9	1	-2	-54	-16
10	1	9	-57	2
11	1	-7	-61	-3
12	2	-5	-53	-18

When the average percent difference indicates the two temperature methods are indistinguishable, the cell is colored green. When the average percent difference indicates the two temperature method are significantly different, the cell is colored red.

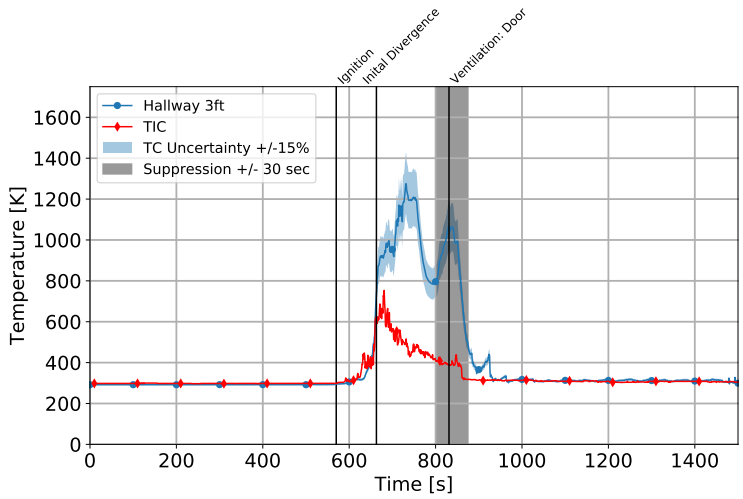

(a) Temperature

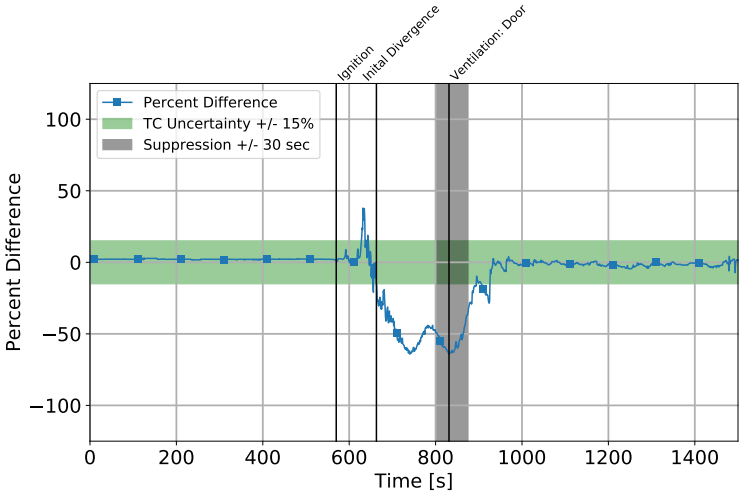

(b) Percent Difference

Figure B.4: Experiment #2 Hallway TIC vs. TC

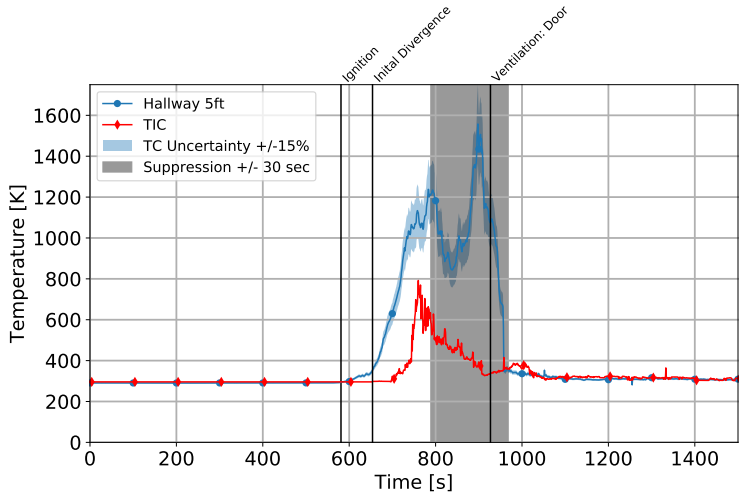

(a) Temperature

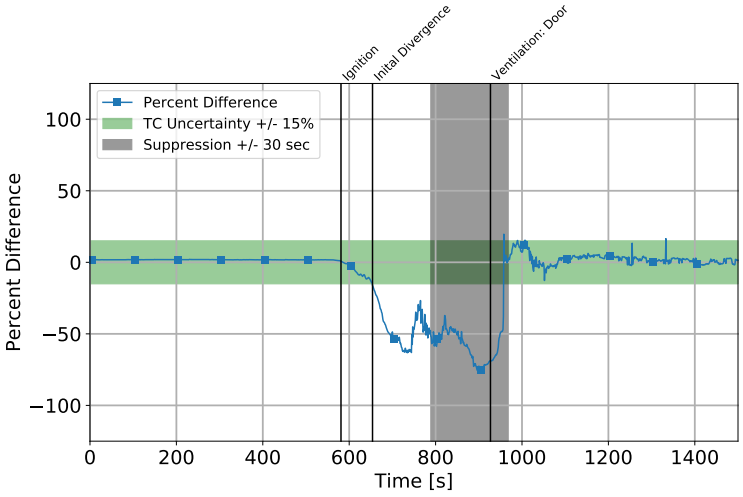

(b) Percent Difference

Figure B.5: Experiment # 3 Hallway TIC vs. TC

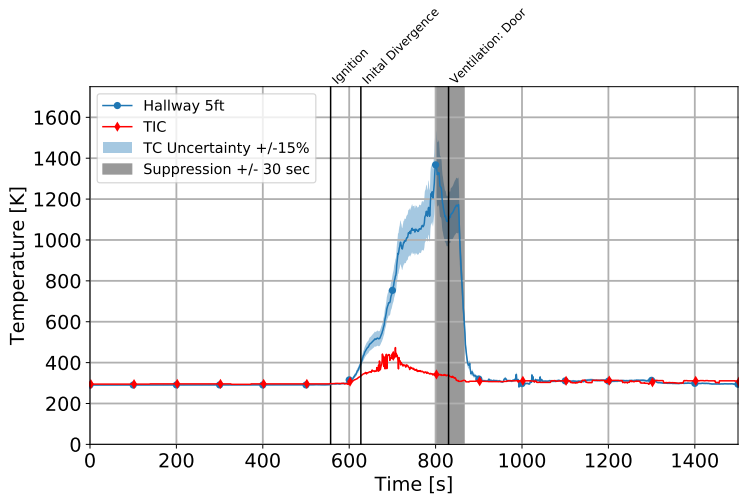

(a) Temperature

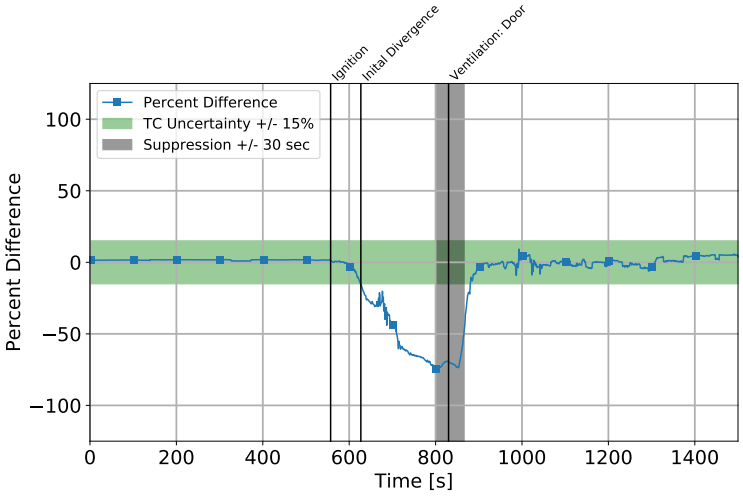

(b) Percent Difference

Figure B.6: Experiment # 4 Hallway TIC vs. TC

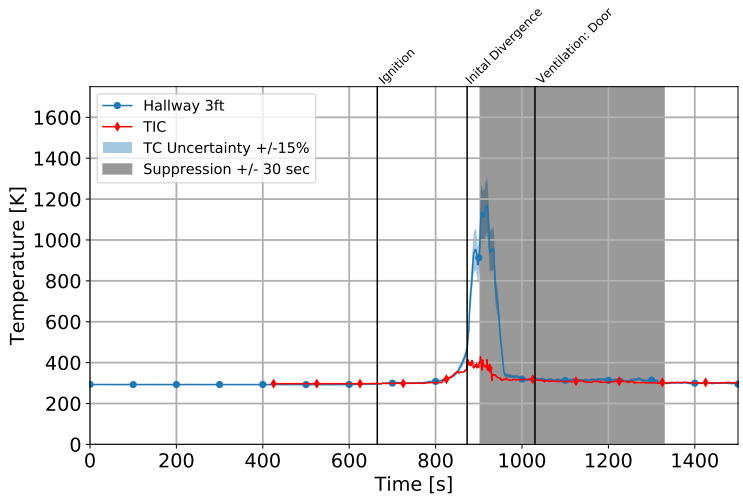

(a) Temperature

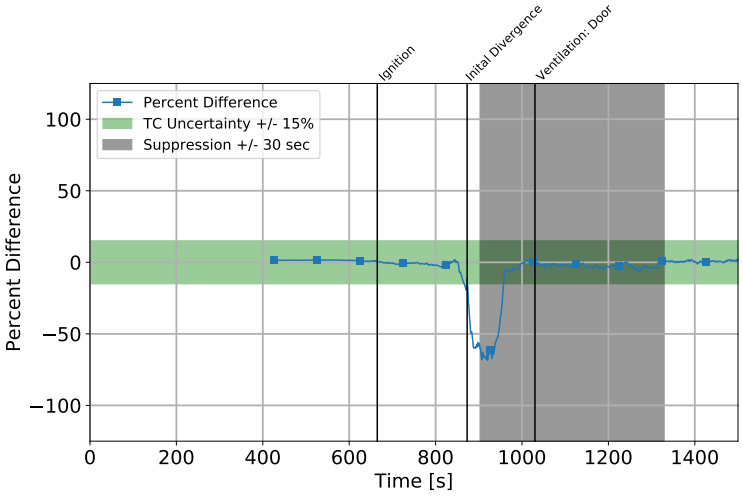

(b) Percent Difference

Figure B.7: Experiment # 6 Hallway TIC vs. TC

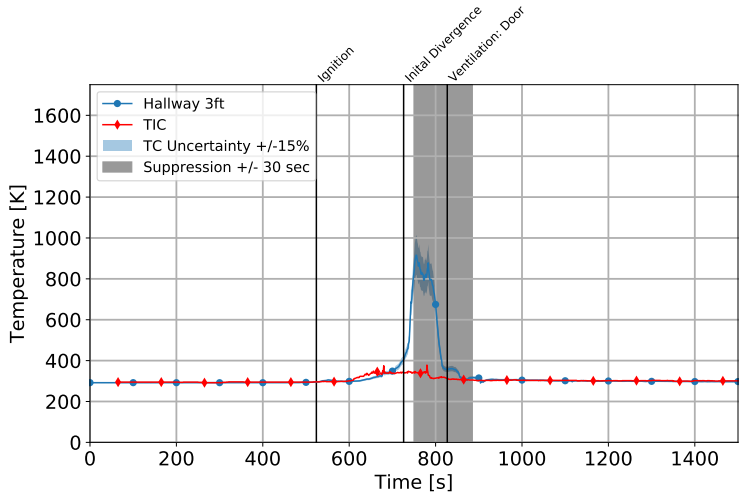

(a) Temperature

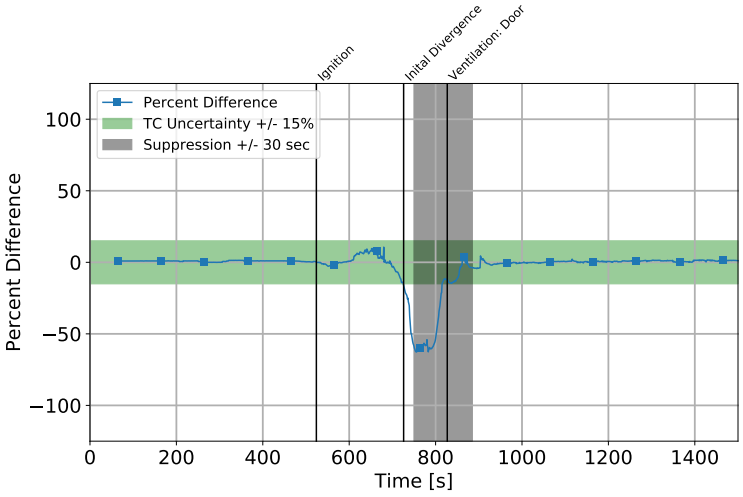

(b) Percent Difference

Figure B.8: Experiment # 8 Hallway TIC vs. TC .

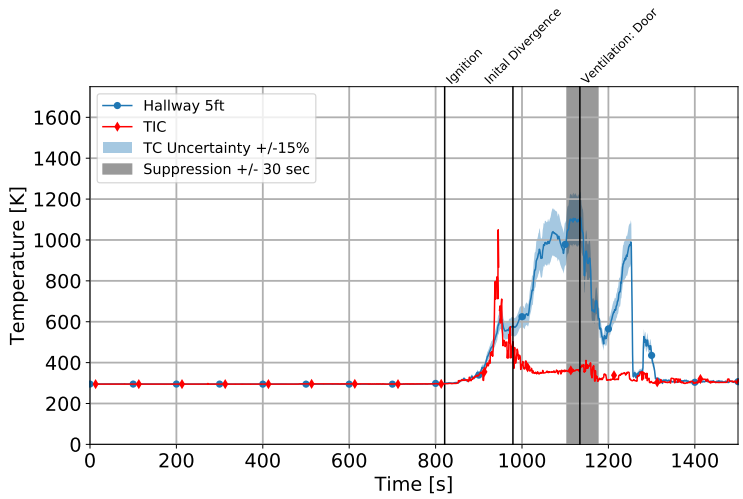

(a) Temperature

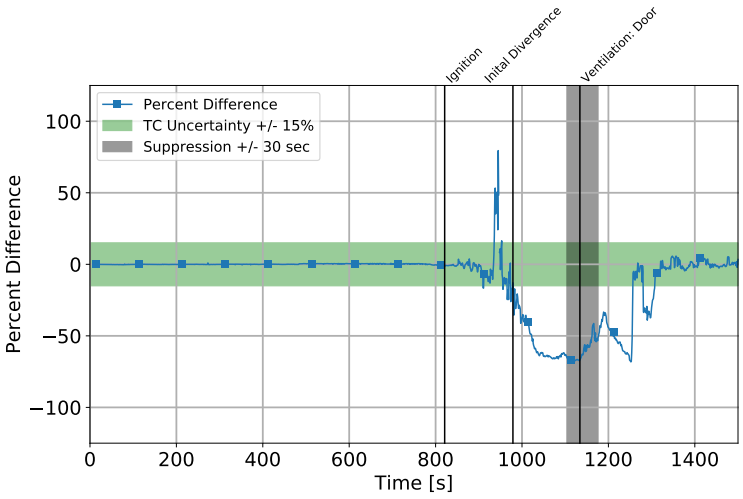

(b) Percent Difference

Figure B.9: Experiment # 9 Hallway TIC vs. TC

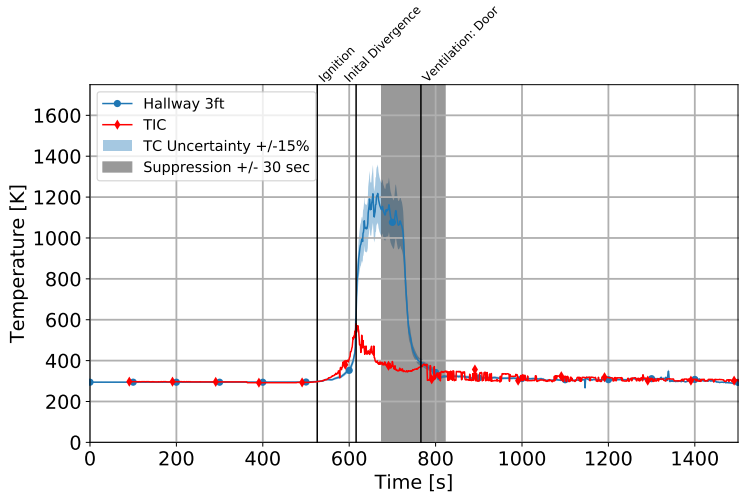

(a) Temperature

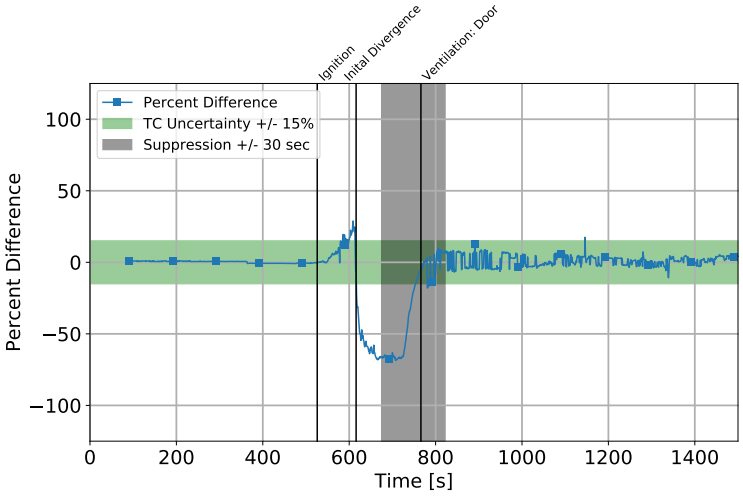

(b) Percent Difference

Figure B.10: Experiment # 10 Hallway TIC vs. TC

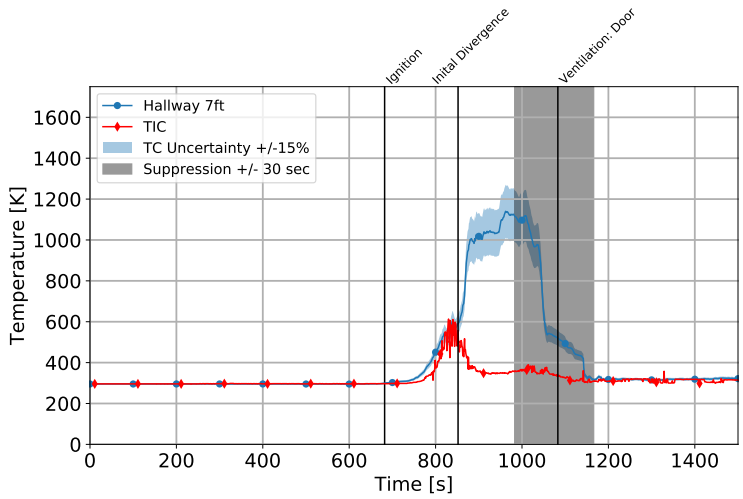

(a) Temperature

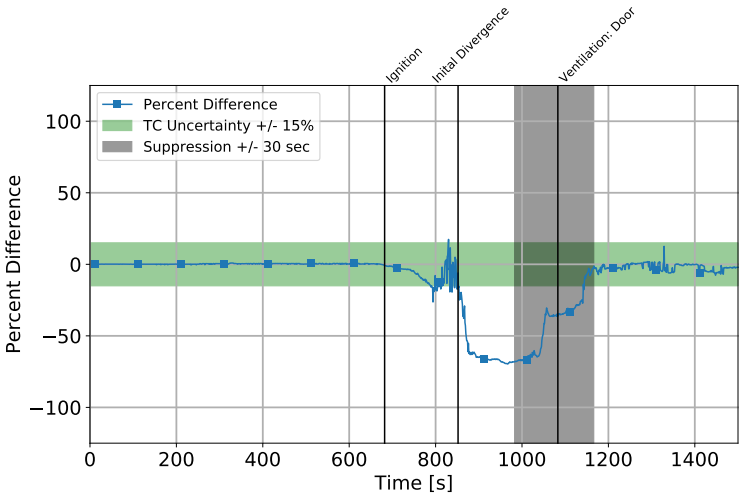

(b) Percent Difference

Figure B.11: Experiment # 11 Hallway TIC vs. TC

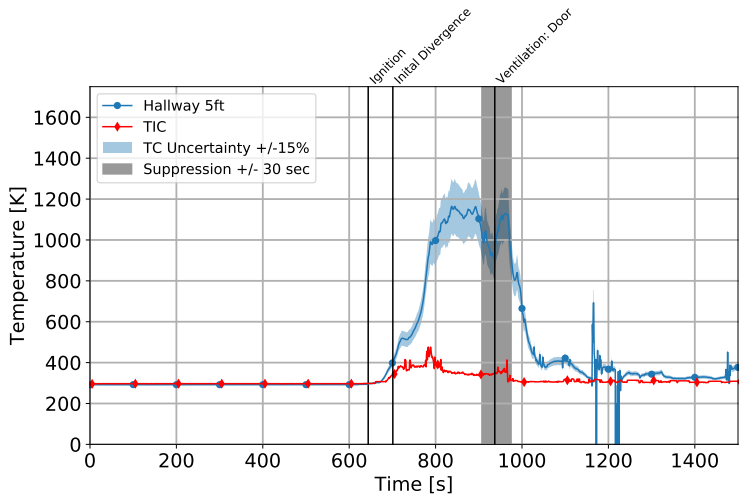

(a) Temperature

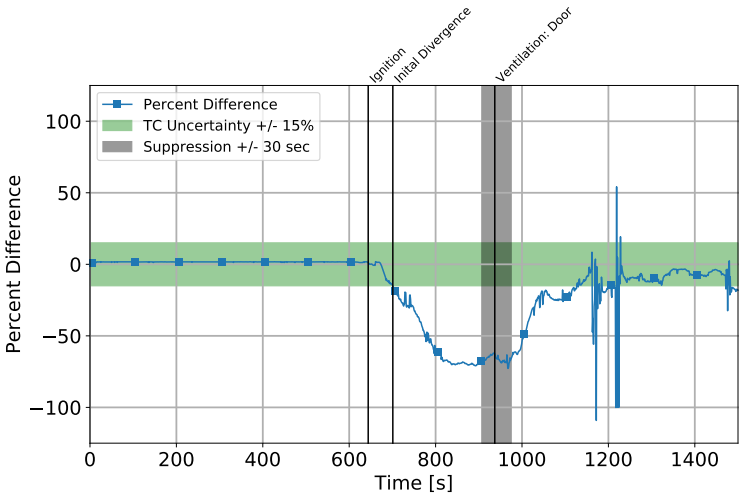

(b) Percent Difference

Figure B.12: Experiment # 12 Hallway TIC vs. TC

B.4.2 Living Room TIC

Table B.5: Measurement Zone Location: IFSI Living Room TIC

Exp. #	Camera Type	Zone Approx. Location	Zone Height	Associated TC Tree
1	Type 1	Bedroom 4 / Hallway Shared Wall	1.52 m	HallLeft
7	Type 2	Bedroom 6 / Living Room Shared Wall	1.52 m	LRRearLeft
9	Type 1	Bedroom 6 / Living Room Shared Wall	2.13 m	LRRearLeft
11	Type 1	Bedroom 4 / Hallway Shared Wall	2.13 m	HallLeft

Conclusions

Table B.6: Average Percent Difference: IFSI Living Room TIC

Exp. #	Pre-Ignition	Initial Combustion	Combustion	Post-Suppression
1	2	4	-43	7
7	2	-5	-50	1
9	-1	-9	-52	1
11	-1	-9	-49	-11

When the average percent difference indicates the two temperature methods are indistinguishable, the cell is colored green. When the average percent difference indicates the two temperature method are significantly different, the cell is colored red.

B.5 Impact of Fire Attack Utilizing Interior and Exterior Streams on Firefighter SAfety and Occupant Survival: Full Scale Experiments

B.5.1 Hallway TIC

Table B.7: Measurement Zone Location: FA Hallway TIC

Exp. #	Approx. Height	Associated TC Tree	Approx. Distance	Zone Additional Info.
1	2.13 m	4TC	Middle	Hallway ceiling
2	2.13 m	4TC	Middle	Hallway Ceiling
3	0.61 m	5TC	Start	Living Room west wall
4	1.22 m	5TC	End	Hallway north wall
5	1.22 m	3TC	End	Hallway west wall
6	1.22 m	3TC	End	Hallway west wall
7	1.52 m	3TC	End	Hallway west wall
8	1.52 m	3TC	End	Hallway west wall
9	1.52 m	3TC	End	Hallway west / north wall
10	1.52 m	3TC	End	Hallway west wall
11	1.52 m	3TC	End	Hallway west wall
12	1.52 m	3TC	End	Hallway west wall
13	1.52 m	3TC	End	Hallway west wall
15	1.83 m	3TC	End	Hallway west wall
16	1.52 m	3TC	End	Hallway west wall
17	1.83 m	3TC	End	Hallway west wall
18	1.83 m	3TC	End	Hallway west wall
19	1.52 m	3TC	End	Hallway west wall
20	1.52 m	4TC	End	Hallway north wall
21	1.83 m	3TC	End	Hallway south wall
22	2.13 m	3TC	End	Hallway ceiling
24	1.52 m	3TC	End	Hallway west / south wall

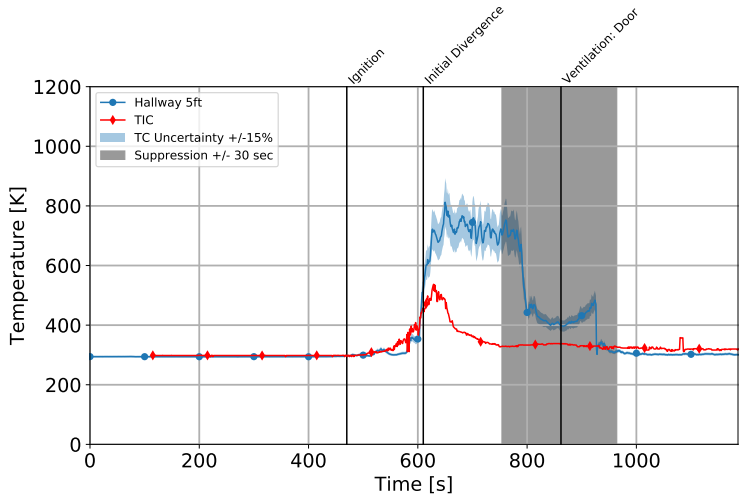

(a) Temperature

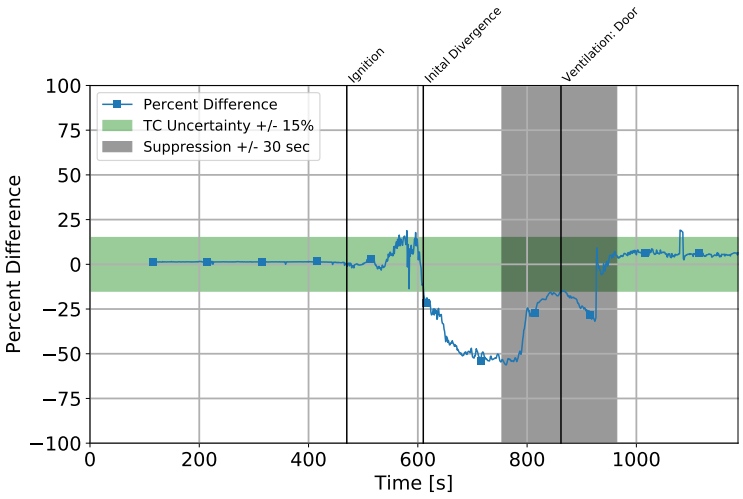

(b) Percent Difference

Figure B.13: Experiment # 1 Living Room TIC vs. TC

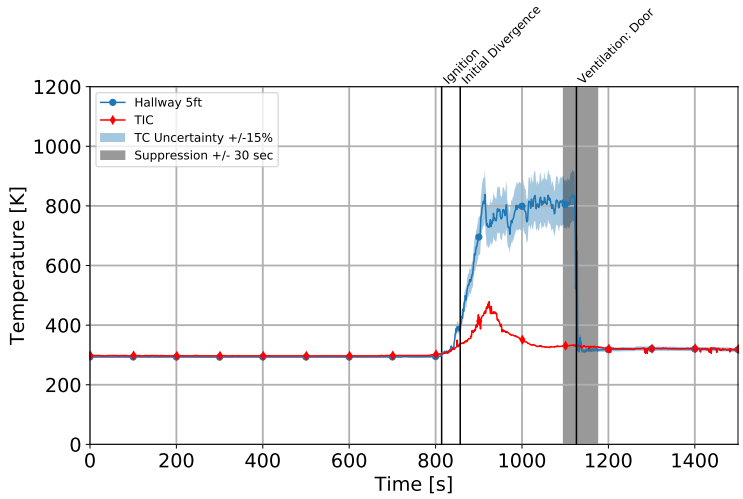

(a) Temperature

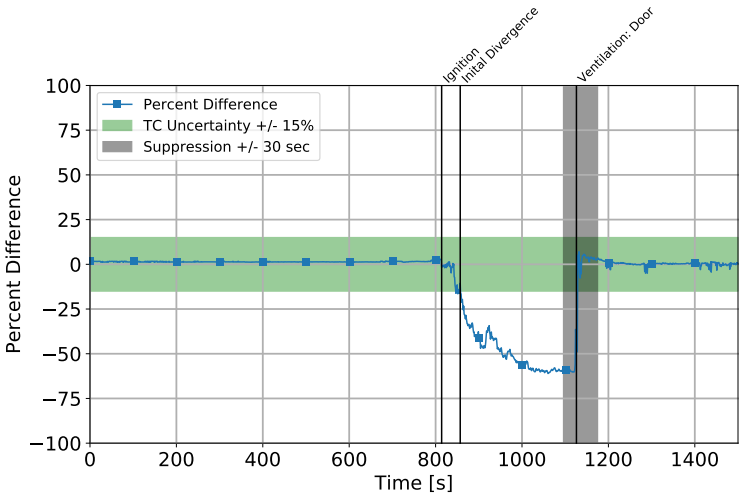

(b) Percent Difference

Figure B.14: Experiment # 7 Living Room TIC vs. TC

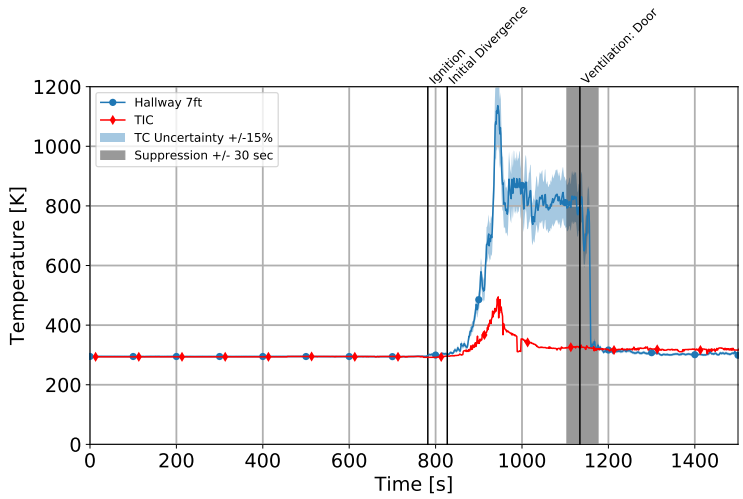

(a) Temperature

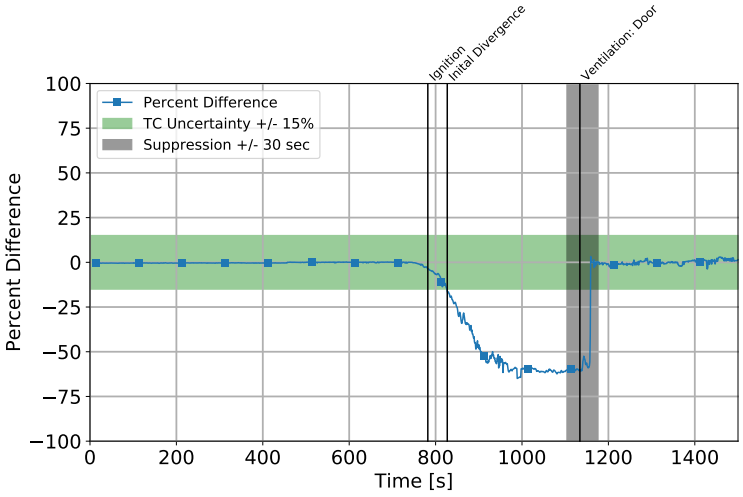

(b) Percent Difference

Figure B.15: Experiment # 9 Living Room TIC vs. TC

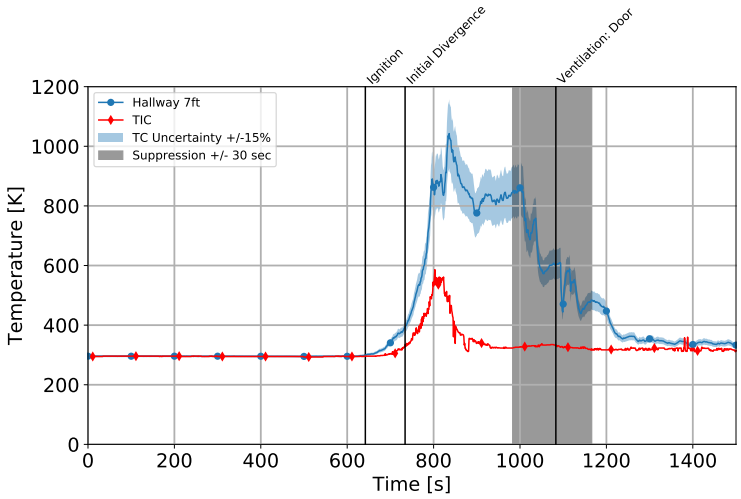

(a) Temperature

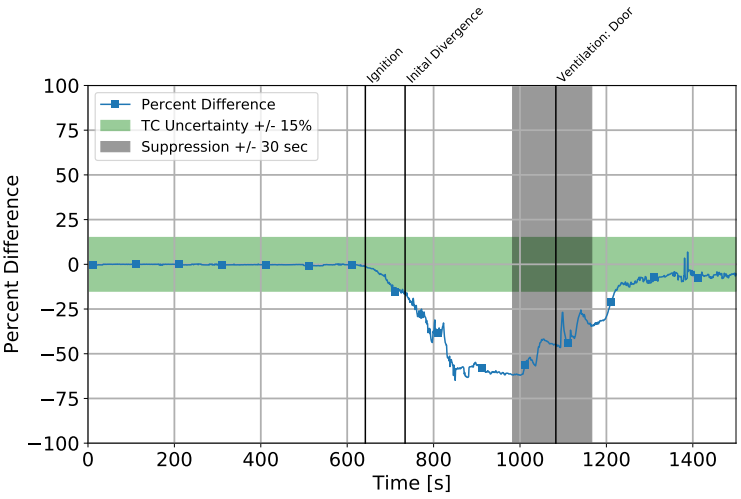

(b) Percent Difference

Figure B.16: Experiment # 11 Living Room TIC vs. TC

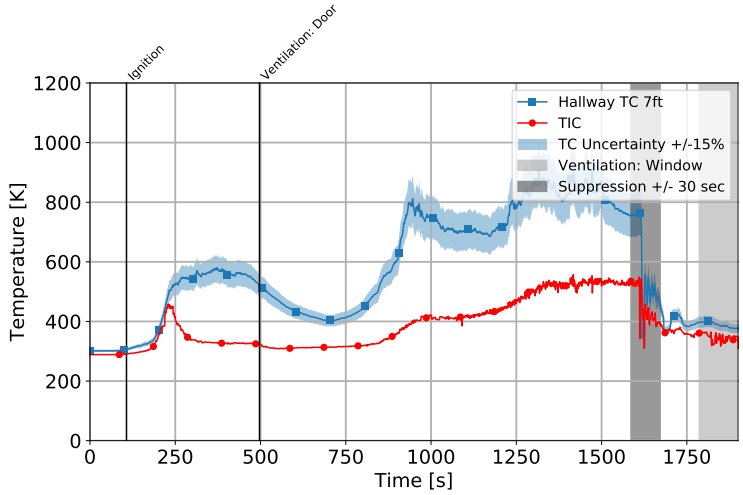

(a) Temperature

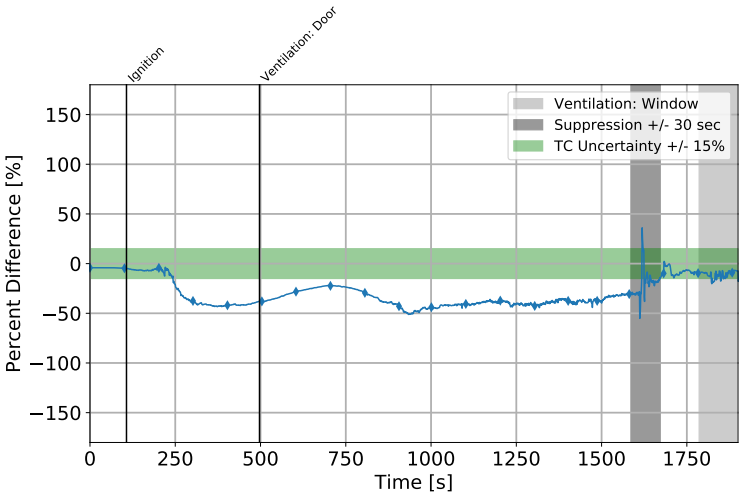

(b) Percent Difference

Figure B.17: Experiment # 1 Hallway TIC vs. TC

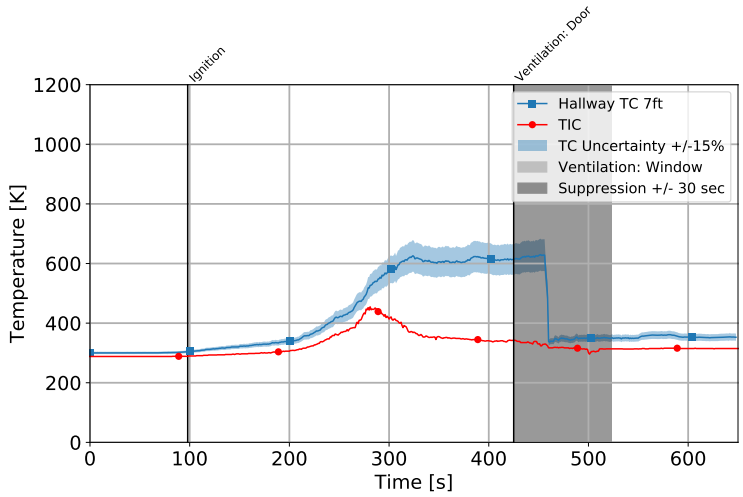

(a) Temperature

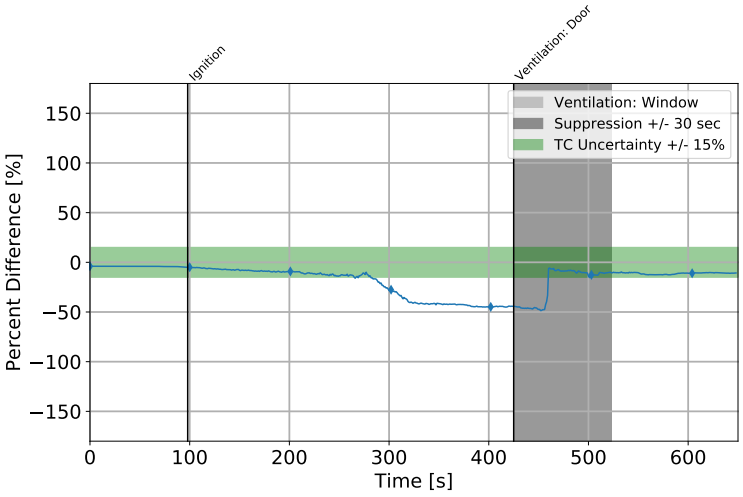

(b) Percent Difference

Figure B.18: Experiment # 2 Hallway TIC vs. TC

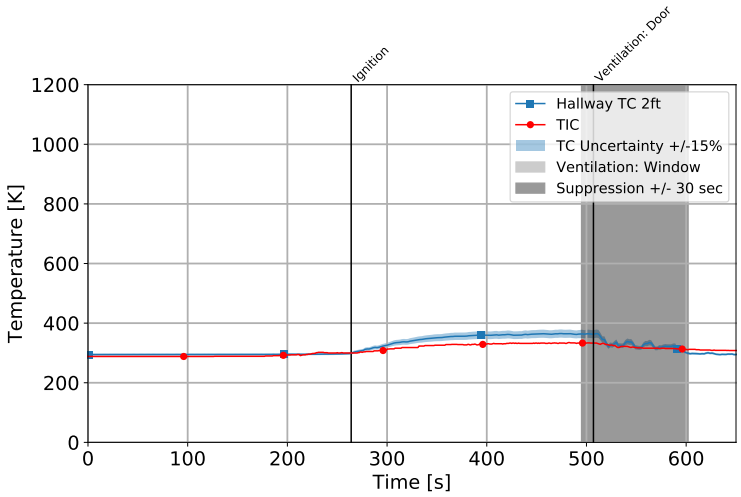

(a) Temperature

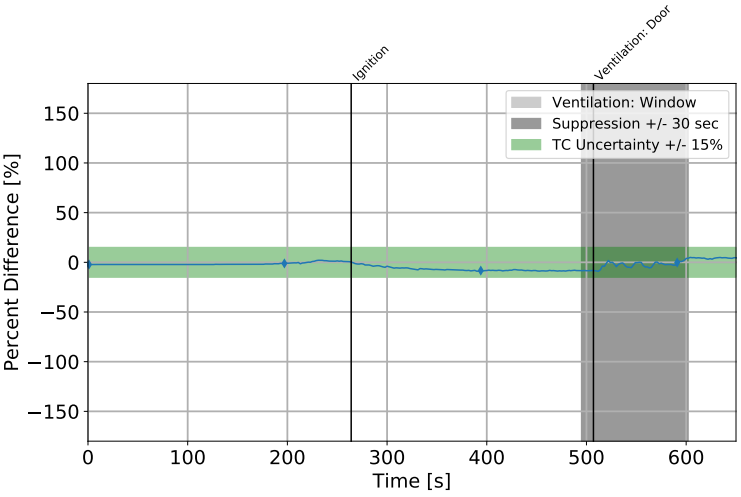

(b) Percent Difference

Figure B.19: Experiment # 3 Hallway TIC vs. TC

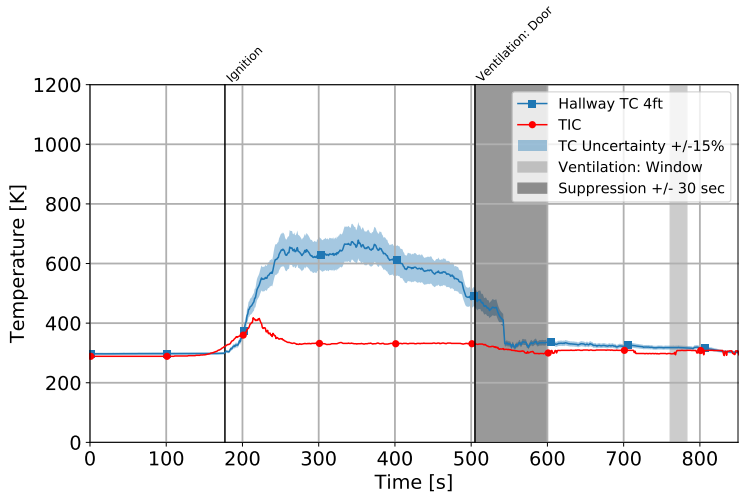

(a) Temperature

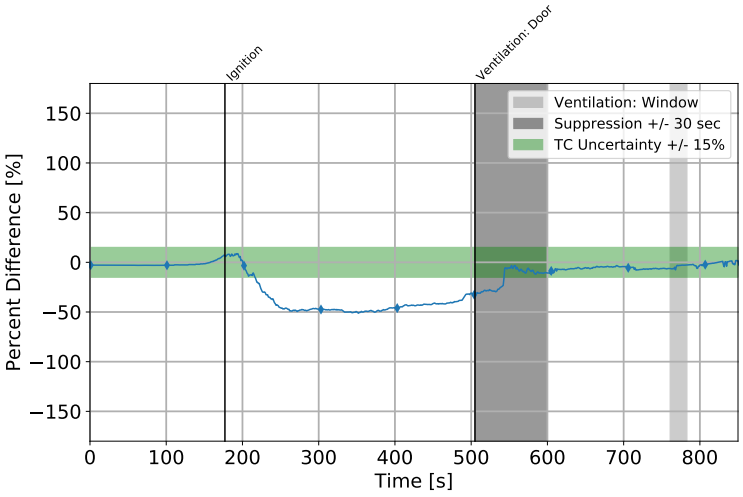

(b) Percent Difference

Figure B.20: Experiment # 4 Hallway TIC vs. TC.

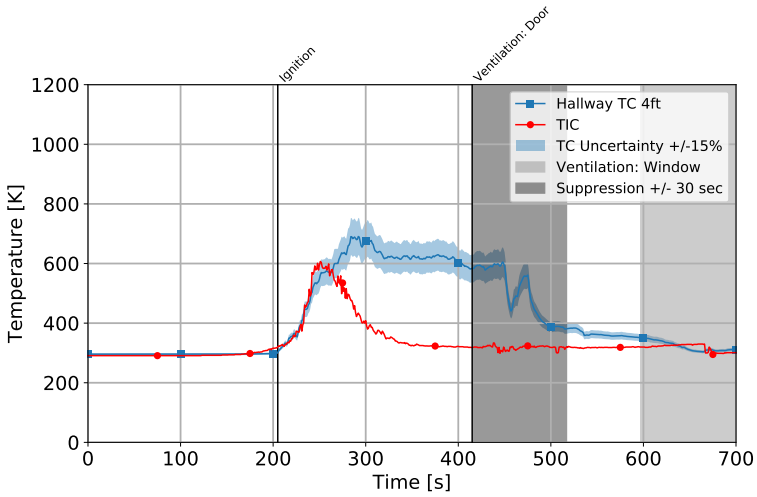

(a) Temperature

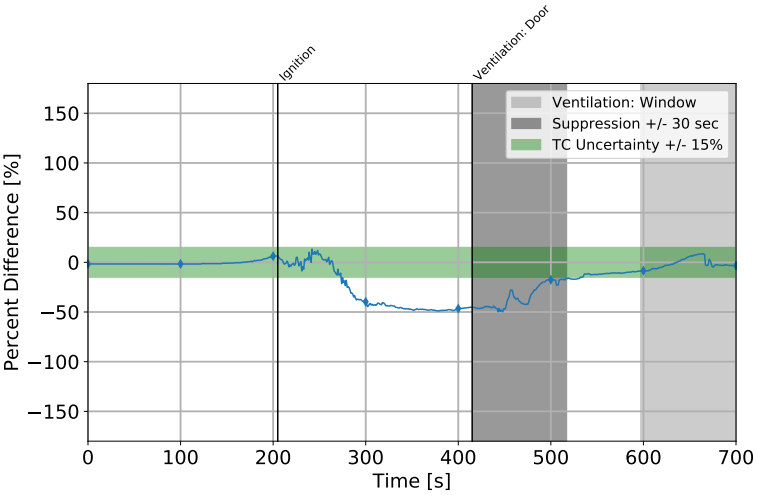

(b) Percent Difference

Figure B.21: Experiment # 5 Hallway TIC vs. TC

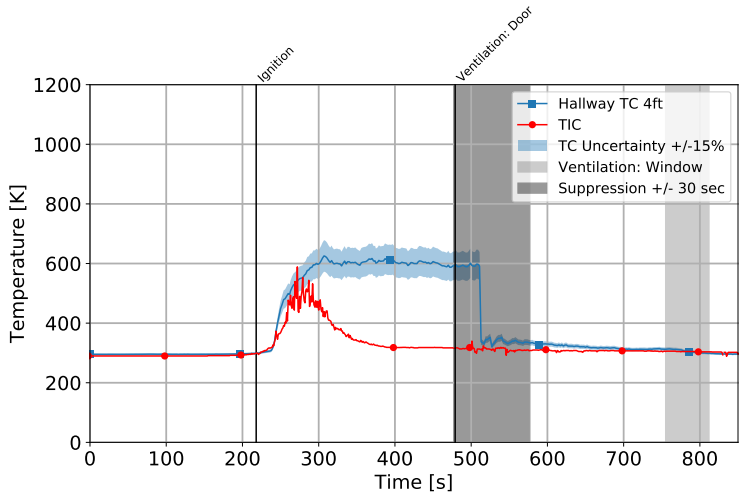

(a) Temperature

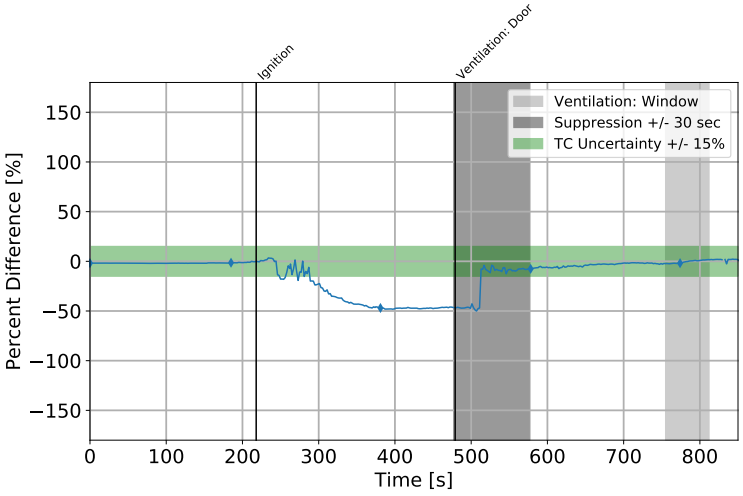

(b) Percent Difference

Figure B.22: Experiment # 6 Hallway TIC vs. TC

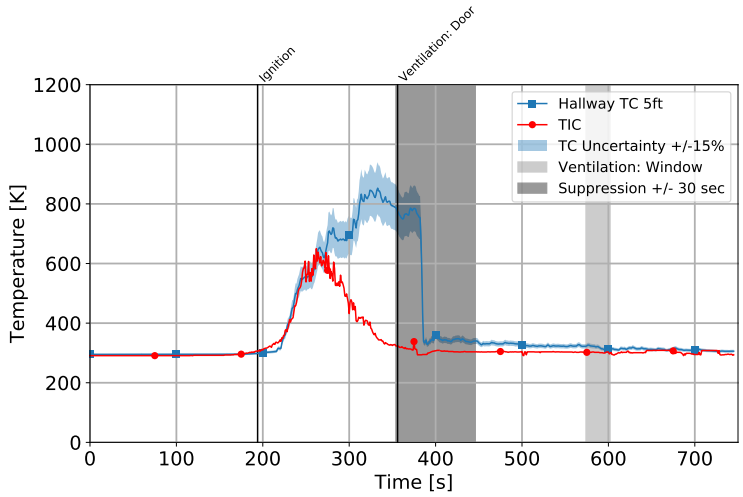

(a) Temperature

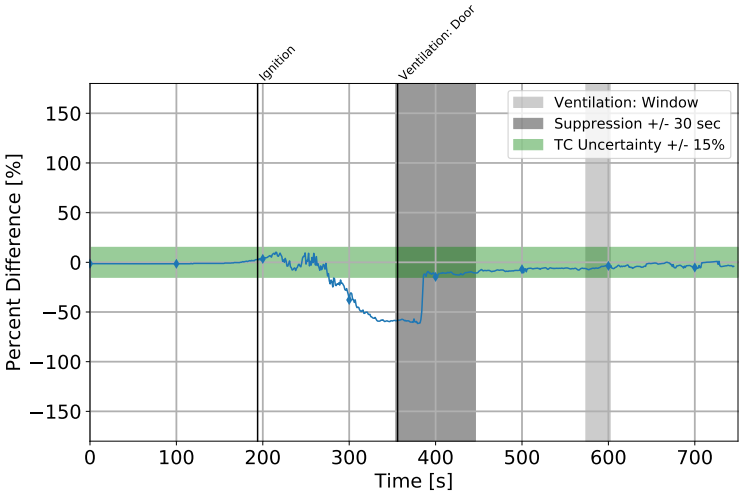

(b) Percent Difference

Figure B.23: Experiment # 7 Hallway TIC vs. TC

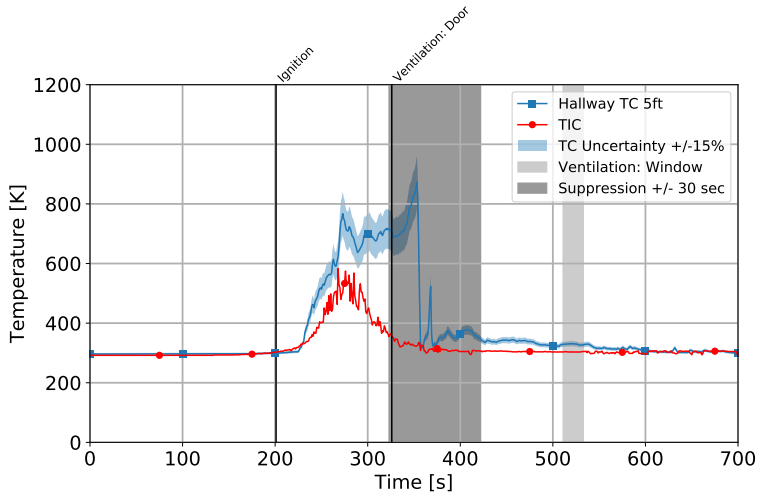

(a) Temperature

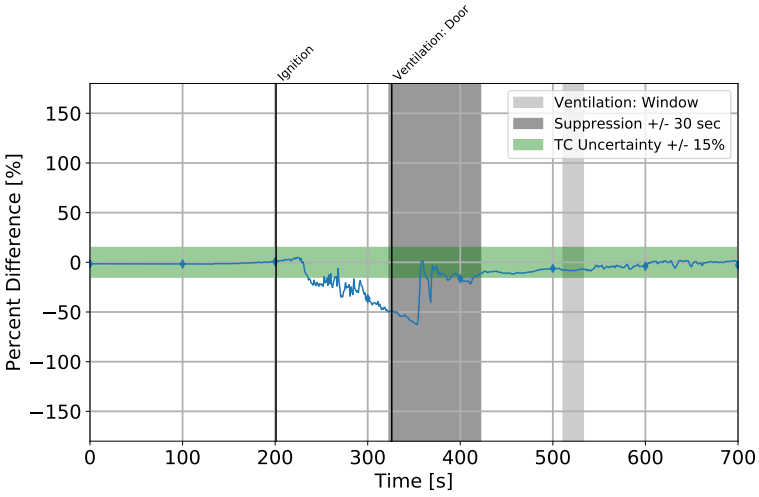

(b) Percent Difference

Figure B.24: Experiment # 8 Hallway TIC vs. TC

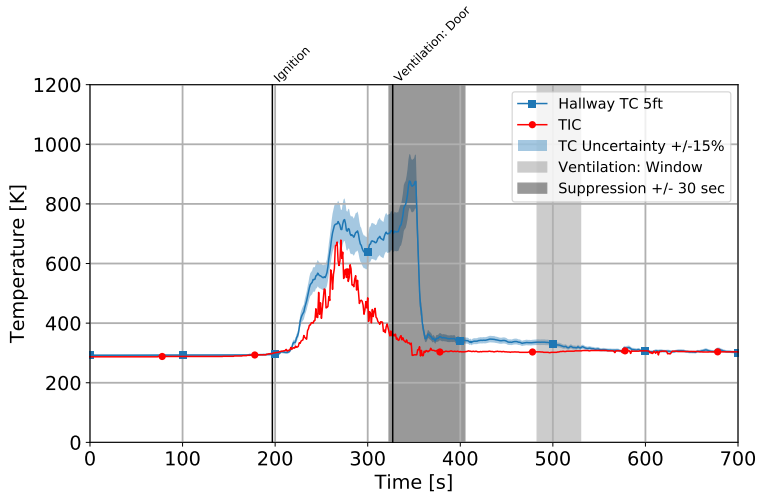

(a) Temperature

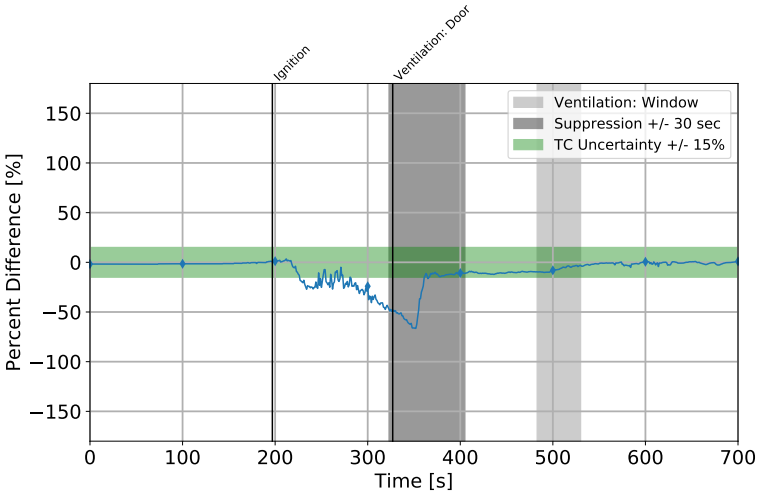

(b) Percent Difference

Figure B.25: Experiment # 9 Hallway TIC vs. TC

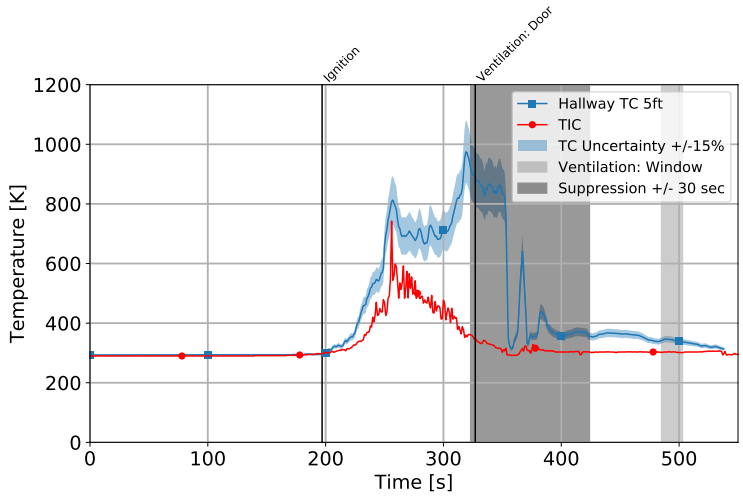

(a) Temperature

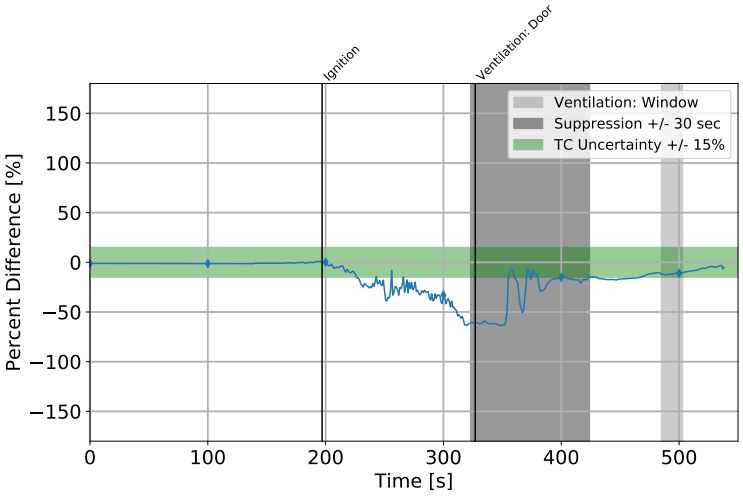

(b) Percent Difference

Figure B.26: Experiment # 10 Hallway TIC vs. TC

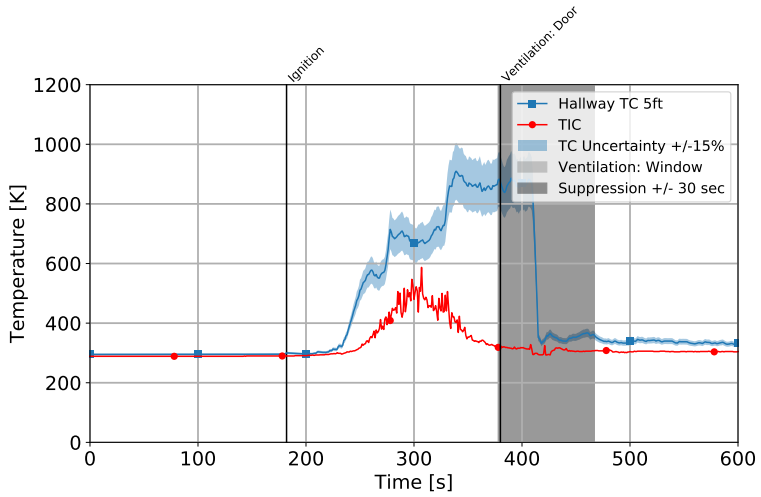

(a) Temperature

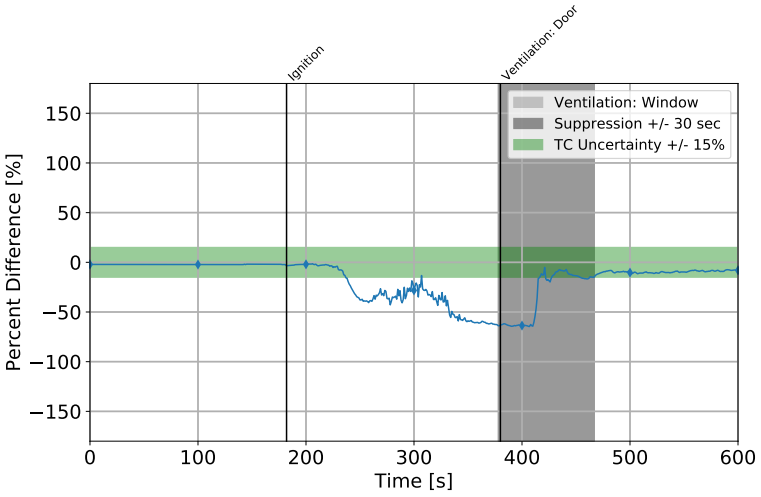

(b) Percent Difference

Figure B.27: Experiment # 11 Hallway TIC vs. TC

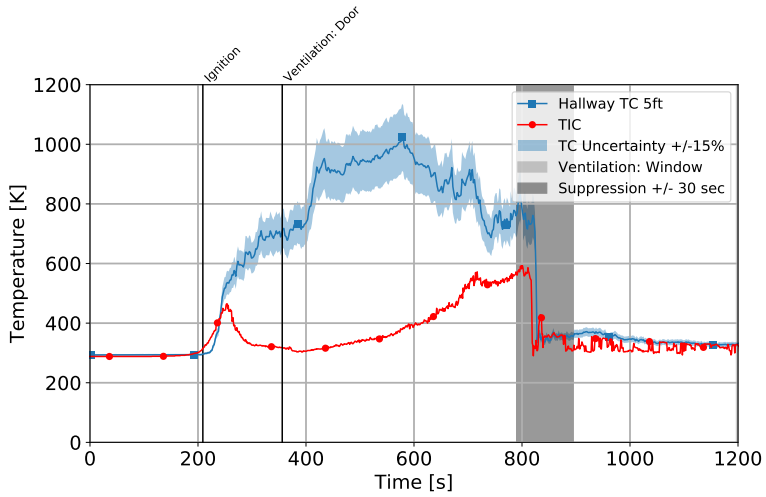

(a) Temperature

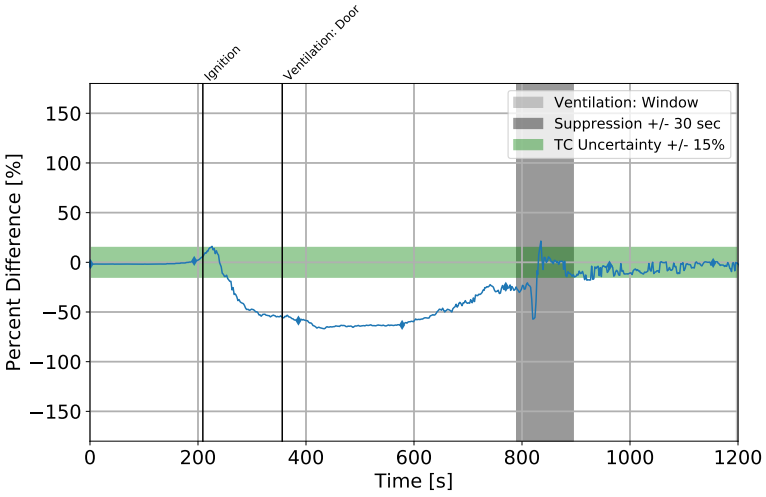

(b) Percent Difference

Figure B.28: Experiment # 12 Hallway TIC vs. TC

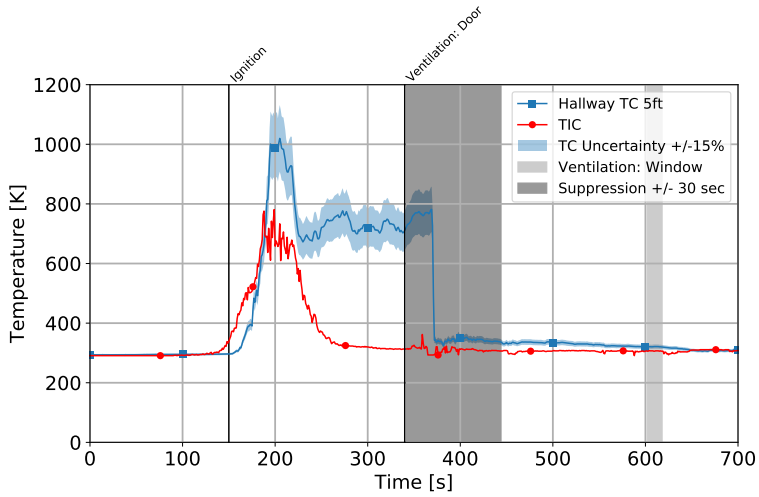

(a) Temperature

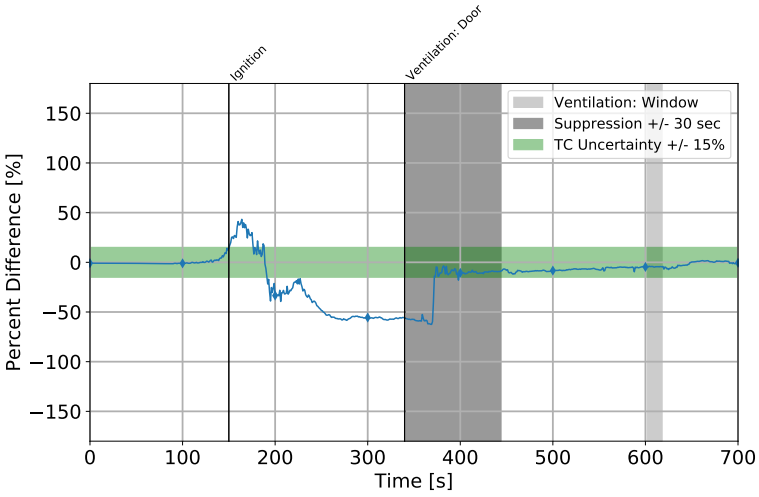

(b) Percent Difference

Figure B.29: Experiment # 13 Hallway TIC vs. TC

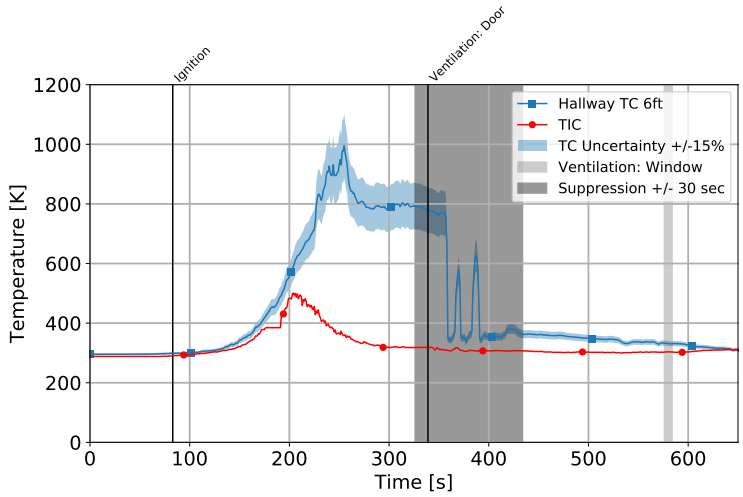

(a) Temperature

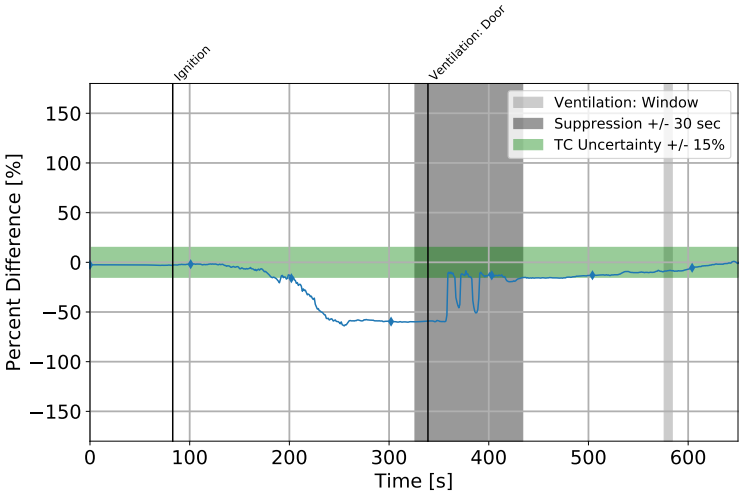

(b) Percent Difference

Figure B.30: Experiment # 15 Hallway TIC vs. TC

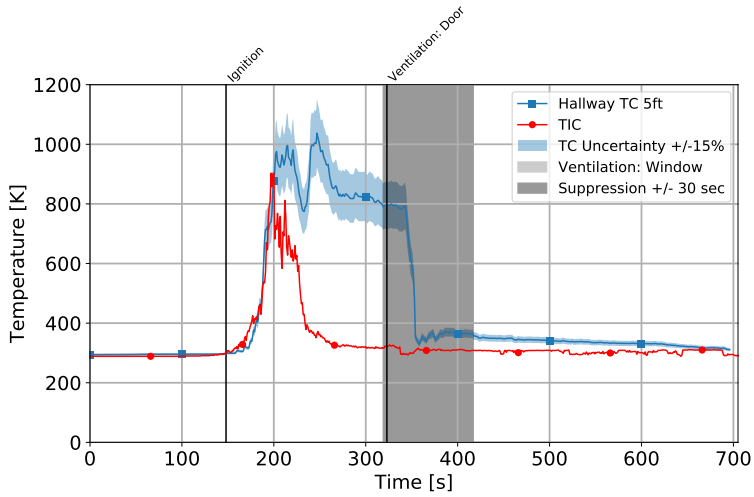

(a) Temperature

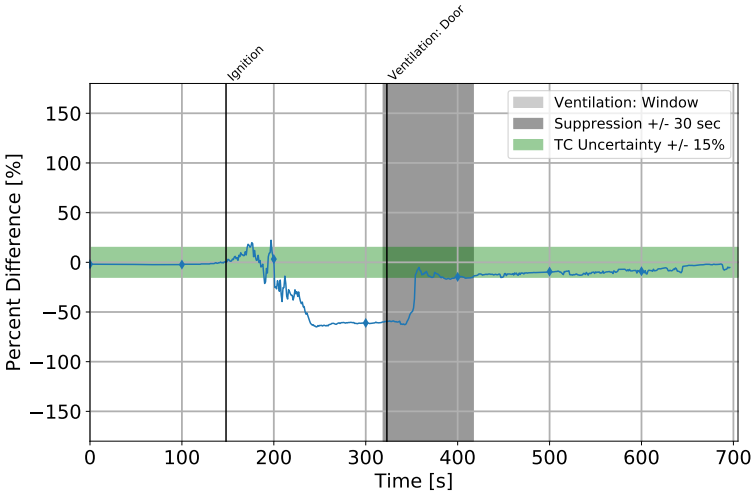

(b) Percent Difference

Figure B.31: Experiment # 16 Hallway TIC vs. TC

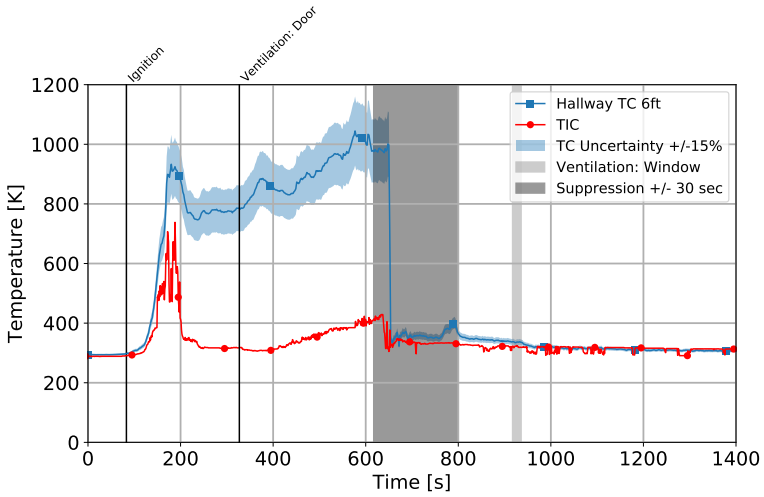

(a) Temperature

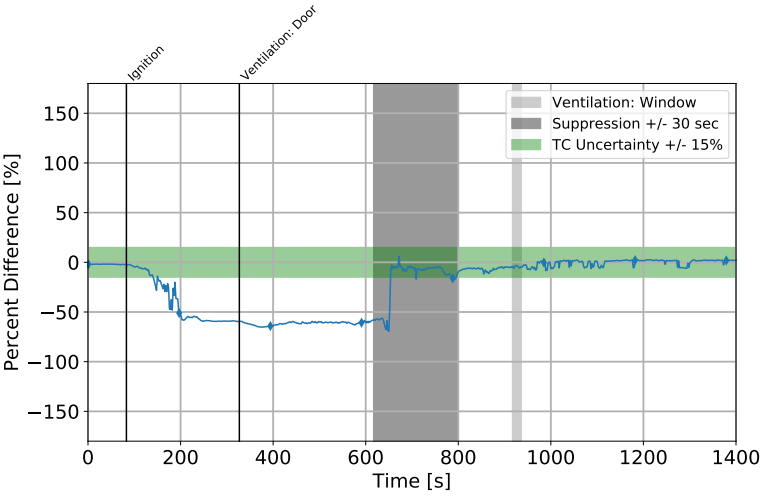

(b) Percent Difference

Figure B.32: Experiment # 17 Hallway TIC vs. TC

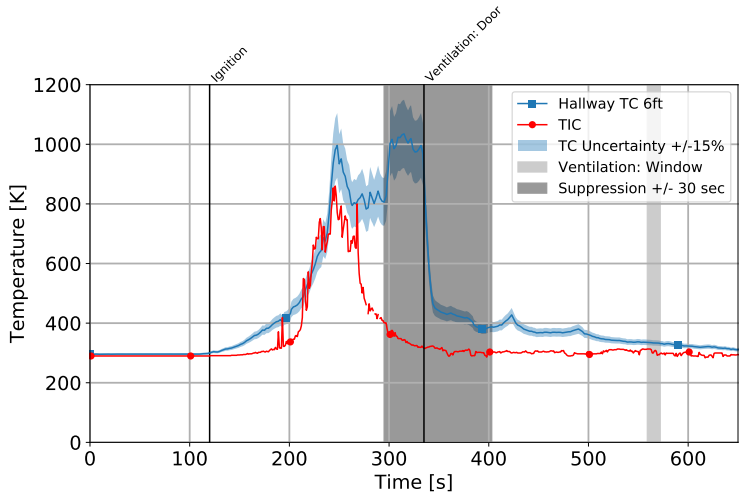

(a) Temperature

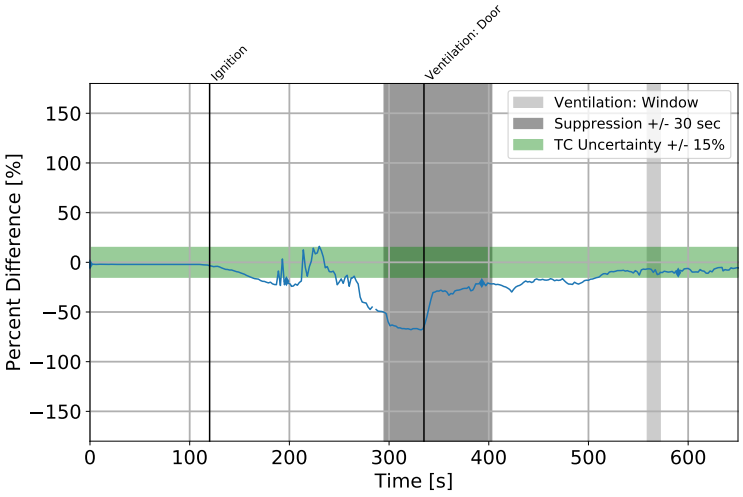

(b) Percent Difference

Figure B.33: Experiment # 18 Hallway TIC vs. TC

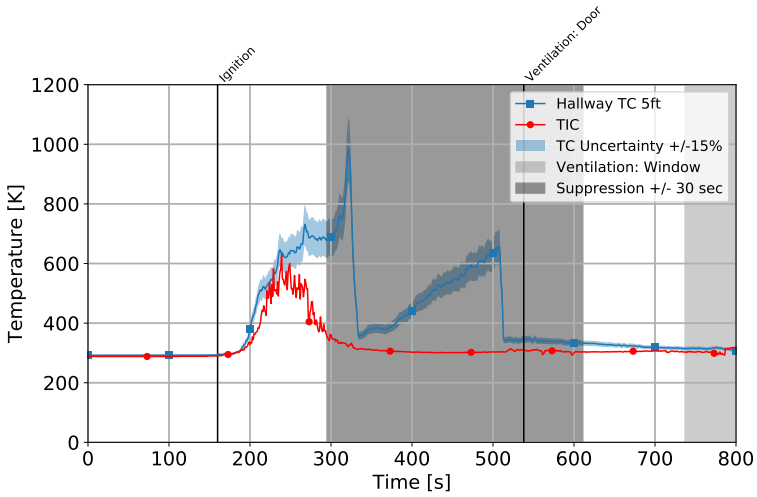

(a) Temperature

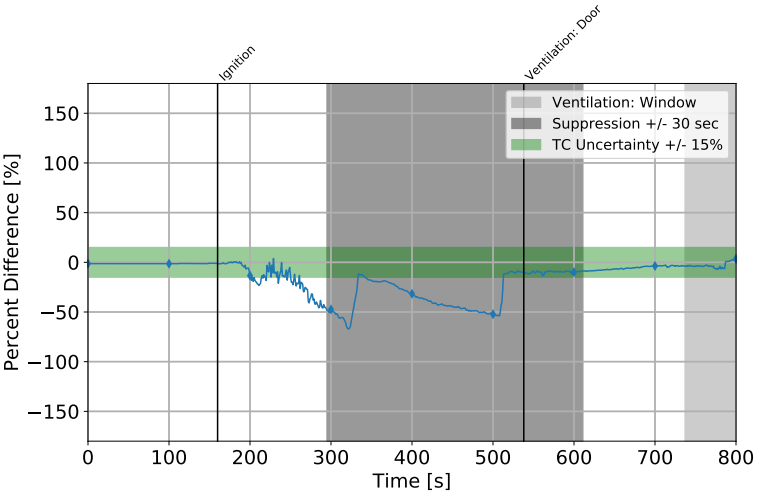

(b) Percent Difference

Figure B.34: Experiment # 19 Hallway TIC vs. TC

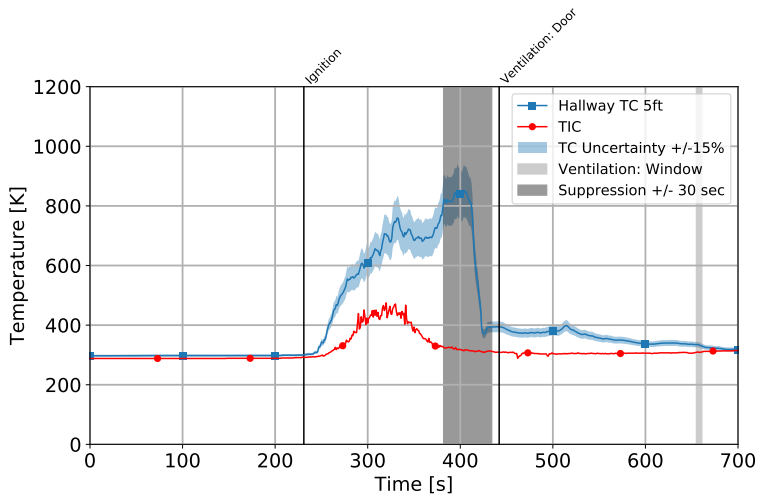

(a) Temperature

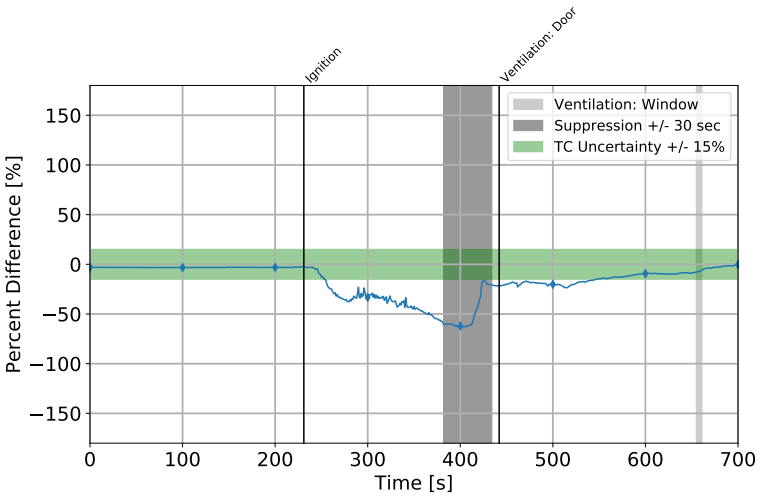

(b) Percent Difference

Figure B.35: Experiment # 20 Hallway TIC vs. TC

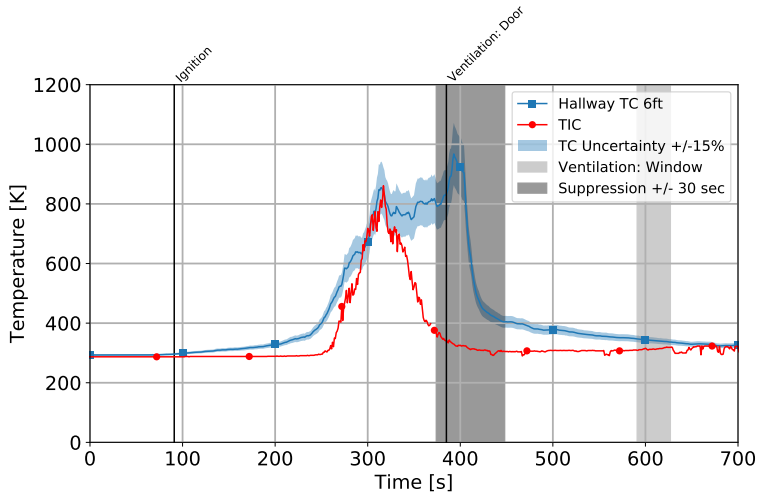

(a) Temperature

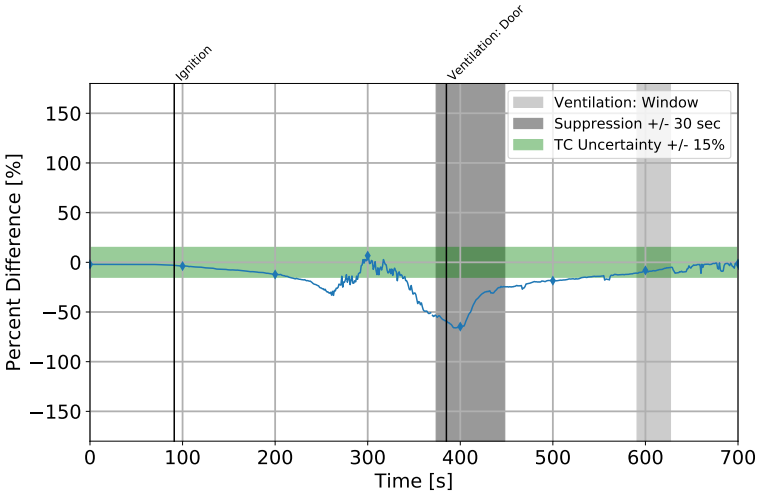

(b) Percent Difference

Figure B.36: Experiment # 21 Hallway TIC vs. TC

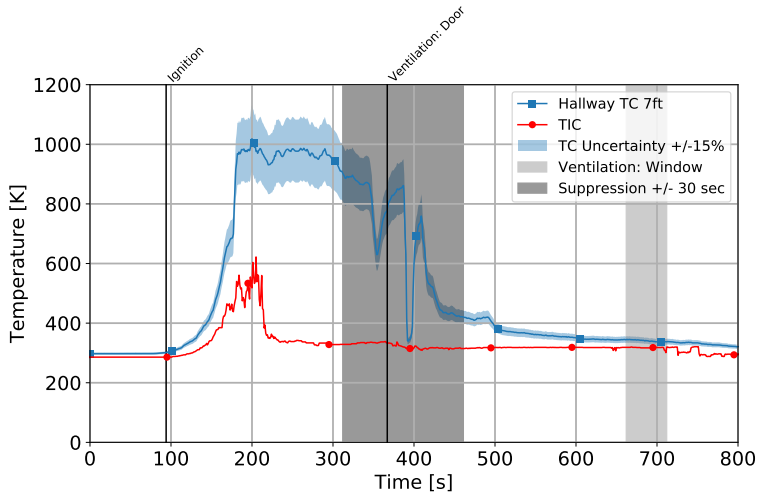

(a) Temperature

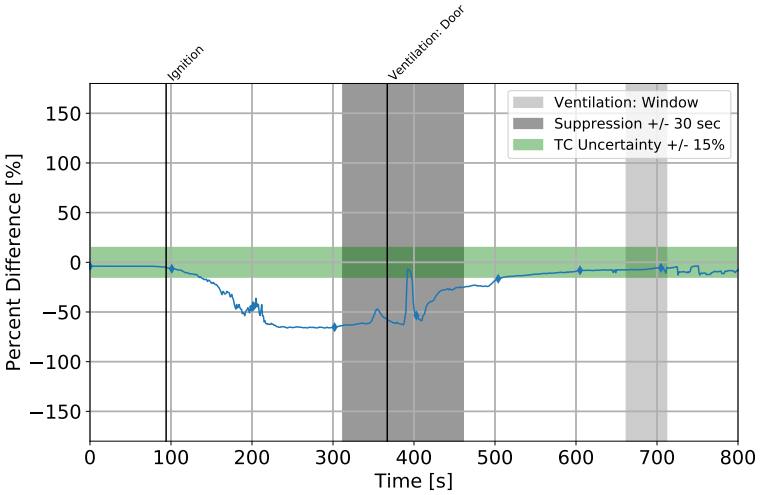

(b) Percent Difference

Figure B.37: Experiment # 22 Hallway TIC vs. TC

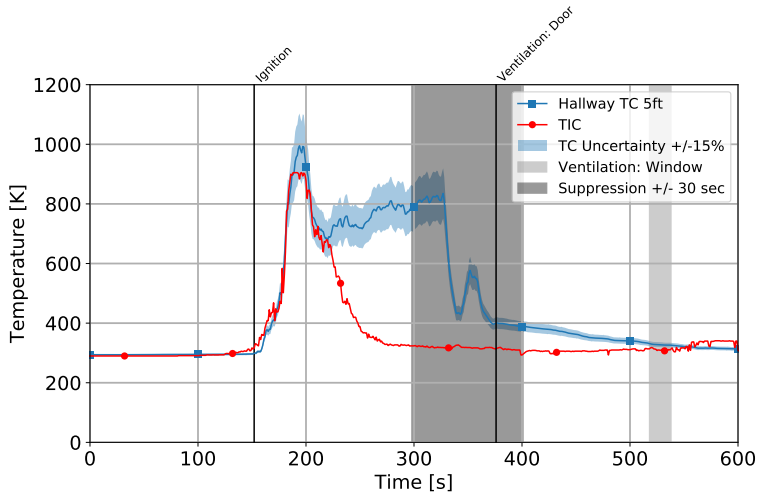

(a) Temperature

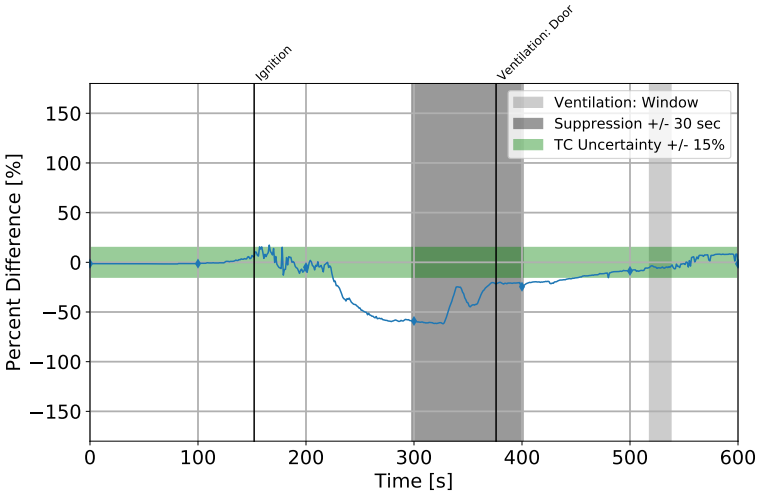

(b) Percent Difference

Figure B.38: Experiment # 24 Hallway TIC vs. TC

Table B.8: Average Percent Difference: FA Hallway TIC

Exp. #	Pre-Ignition	Initial Combustion	Combustion	Post-Suppression
1	-5	-8	-37	-11
2	-5	-10	-40	-12
3	-2	N/A	-7	4
4	-2	-2	-44	-4
5	-1	1	-44	-6
6	-2	-4	-39	-3
7	-1	1	-44	6
8	-2	-10	-34	-5
9	-2	-14	-34	-5
10	-1	-17	-38	-12
11	-3	-20	-50	-10
12	-2	-9	-52	-6
13	-1	24	-46	-5
15	-3	-7	-54	-8
16	-2	-1	-56	-9
17	-2	-8	-58	-2
18	-3	-11	-33	-12
19	-2	-10	-36	-4
20	-4	-6	-38	-13
21	-3	-12	-39	-12
22	-4	-10	-52	-11
24	-1	1	-48	-6

B.5.2 Living Room TIC

Table B.9: Measurement Zone Location: FA Living Room TIC

Exp. #	Approx. Height	Associated TC Tree	Zone Additional Info.
1	1.52 m	5TC	Hallway north wall
2	0.91 m	5TC	Living room north wall / bookcase
3	0.91 m	5TC	Living Room north wall
4	0.61 m	5TC	Living Room bookcase
5	1.22 m	5TC	Living Room bookcase
6	0.91 m	5TC	Living Room north wall
7	0.91 m	5TC	Living Room bookcase
8	0.91 m	5TC	Living Room bookcase
9	0.91 m	5TC	Living Room bookcase
10	0.91 m	5TC	Living Room bookcase
11	0.61 m	5TC	Living Room bookcase
12	0.91 m	5TC	Living Room bookcase
13	0.91 m	5TC	Living Room bookcase
15	0.91 m	5TC	Living Room bookcase
16	0.91 m	5TC	Living Room bookcase
17	0.91 m	5TC	Living Room bookcase
18	0.91 m	5TC	Living Room north wall
19	0.91 m	5TC	Living Room bookcase
20	0.61 m	5TC	Living Room bookcase
21	0.91 m	5TC	Living Room bookcase
22	0.91 m	5TC	Living Room north wall / bookcase
24	0.91 m	5TC	Living Room bookcase

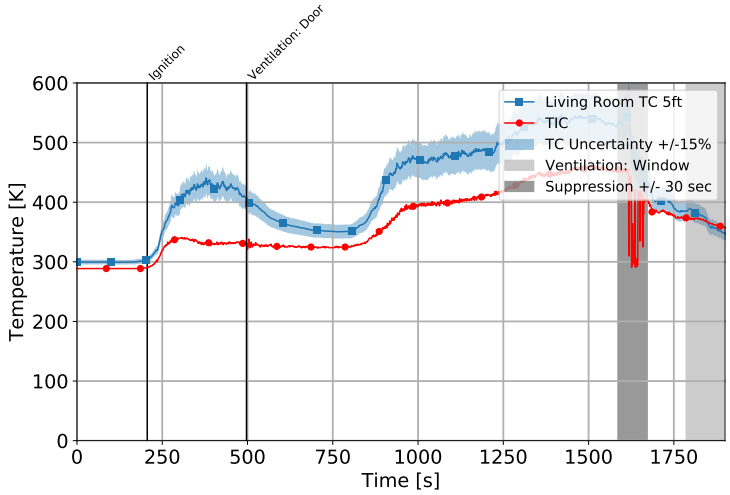

(a) Temperature

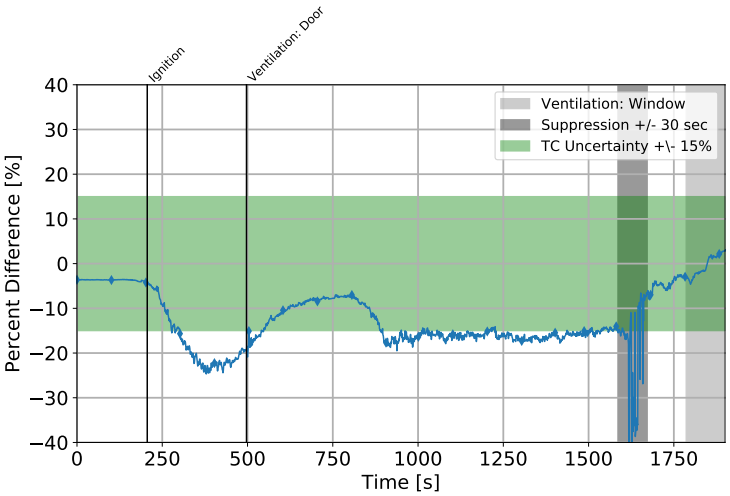

(b) Percent Difference

Figure B.39: Experiment # 1 Living Room TIC vs. TC

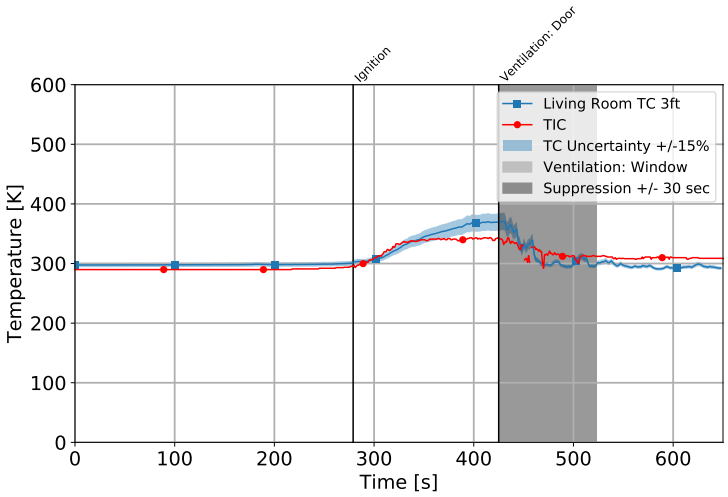

(a) Temperature

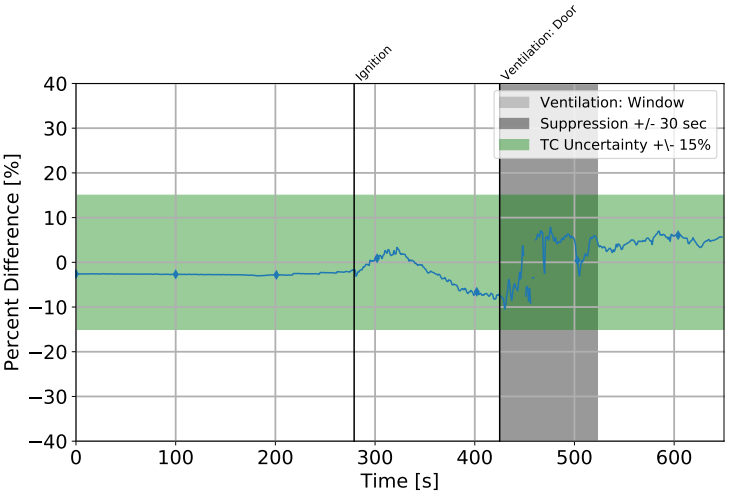

(b) Percent Difference

Figure B.40: Experiment # 2 Living Room TIC vs. TC

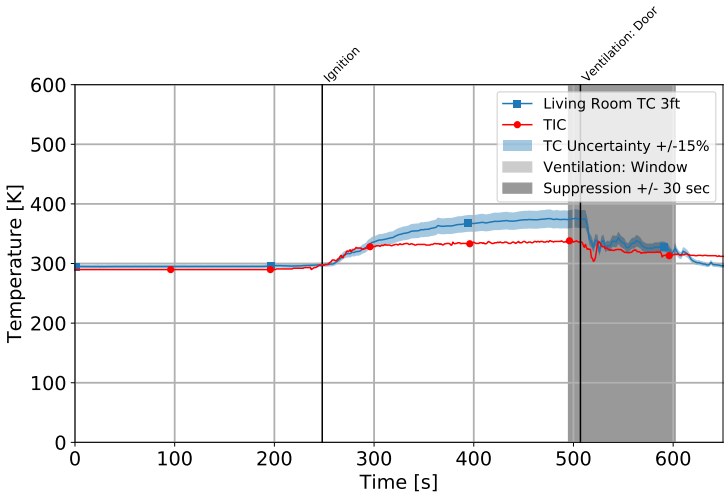

(a) Temperature

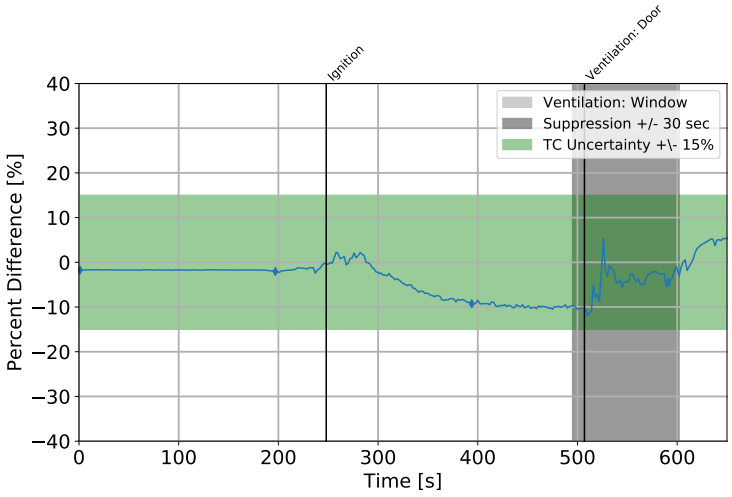

(b) Percent Difference

Figure B.41: Experiment # 3 Living Room TIC vs. TC

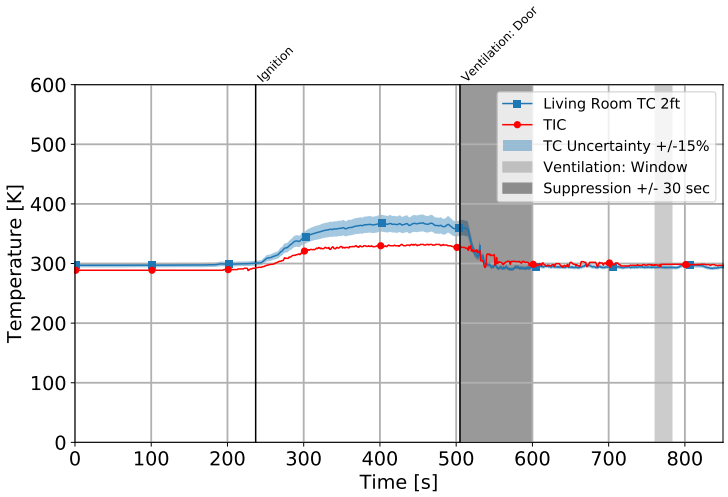

(a) Temperature

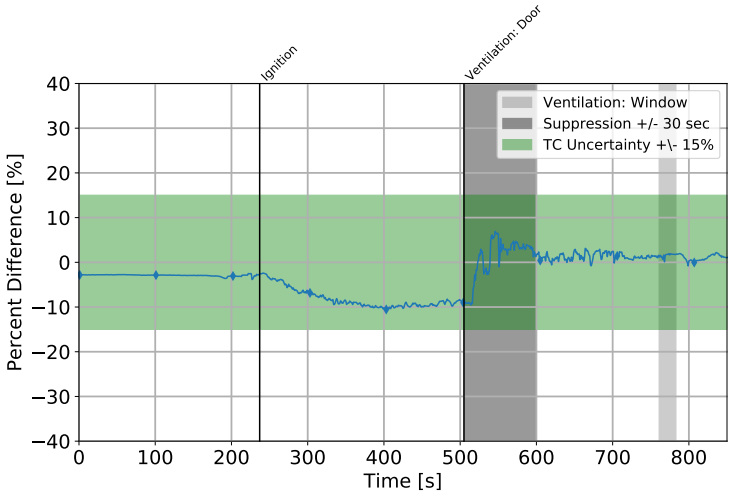

(b) Percent Difference

Figure B.42: Experiment # 4 Living Room TIC vs. TC

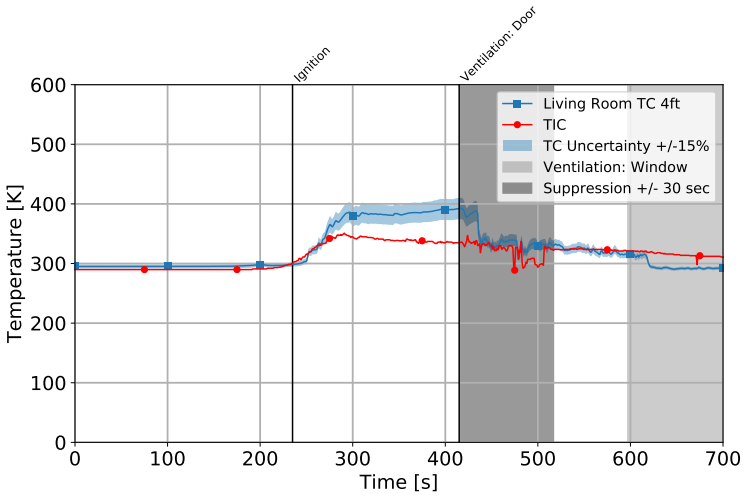

(a) Temperature

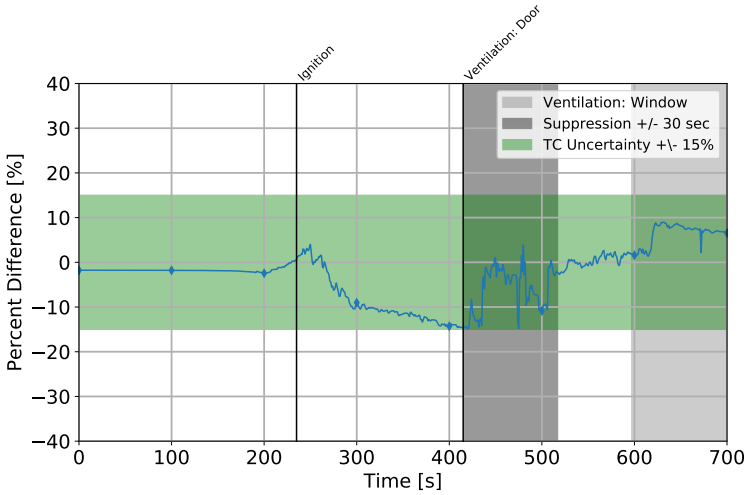

(b) Percent Difference

Figure B.43: Experiment # 5 Living Room TIC vs. TC

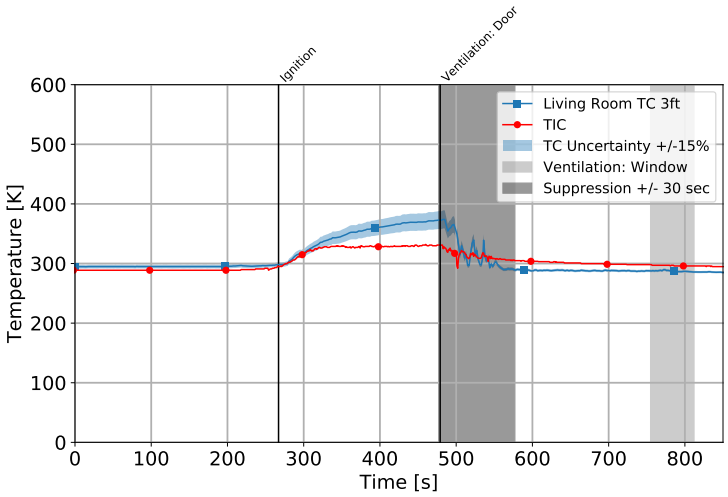

(a) Temperature

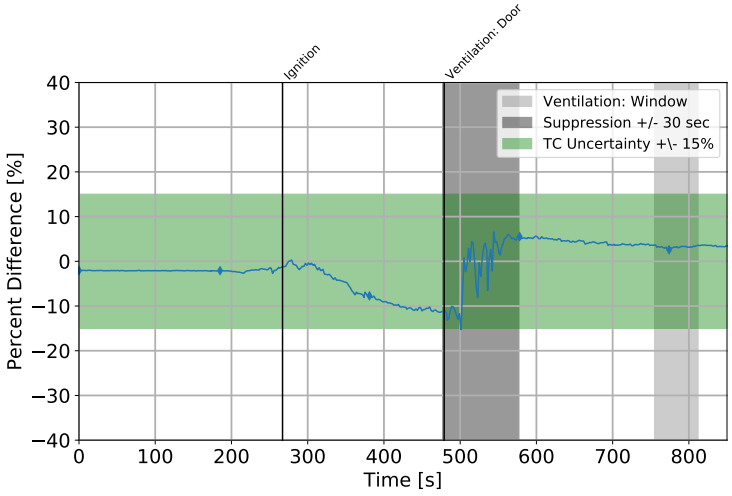

(b) Percent Difference

Figure B.44: Experiment # 6 Living Room TIC vs. TC

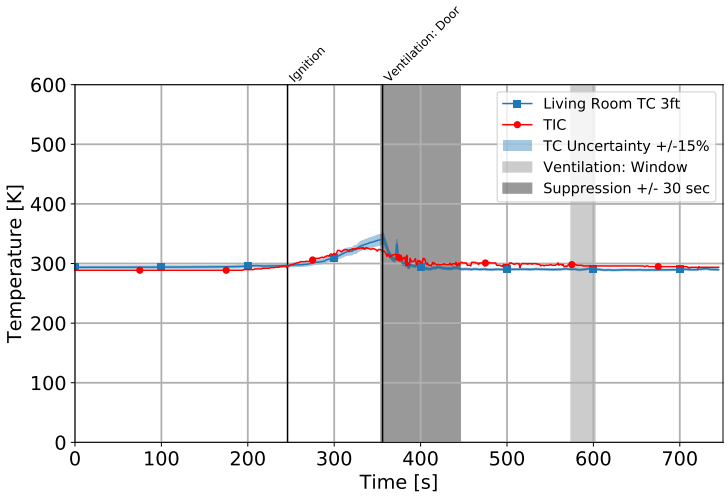

(a) Temperature

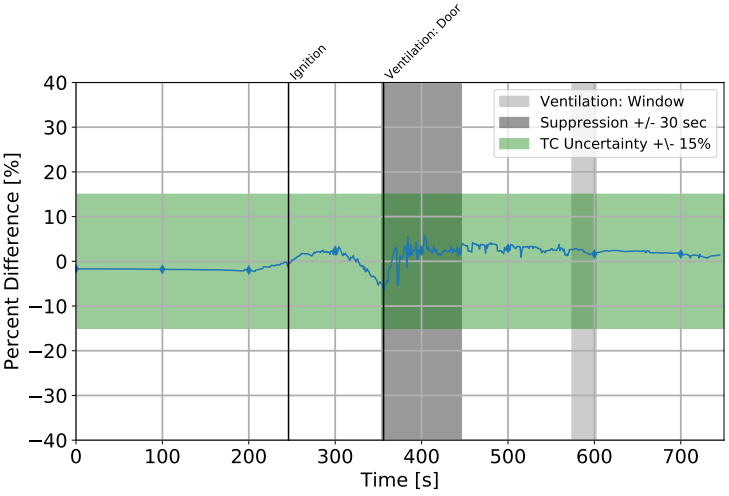

(b) Percent Difference

Figure B.45: Experiment # 7 Living Room TIC vs. TC

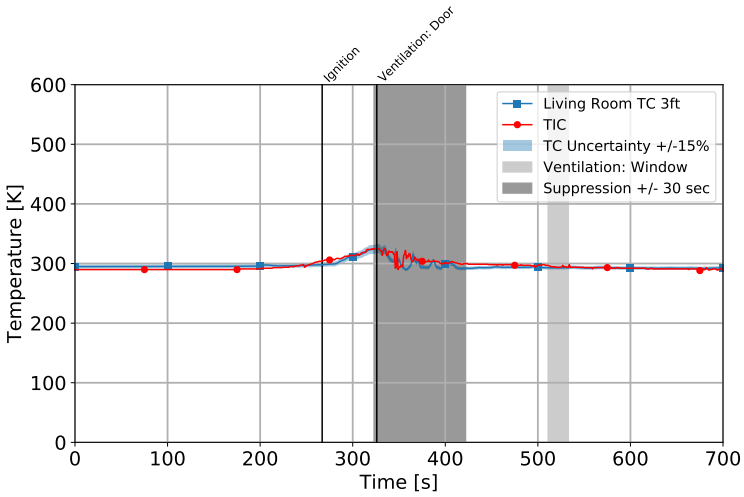

(a) Temperature

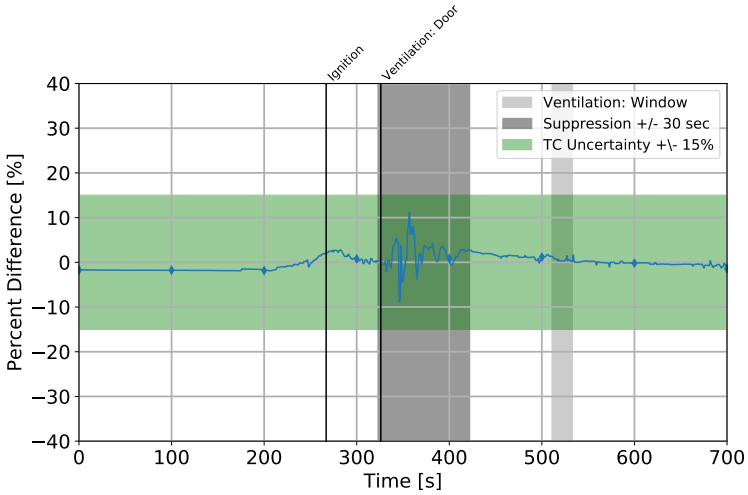

(b) Percent Difference

Figure B.46: Experiment # 8 Living Room TIC vs. TC

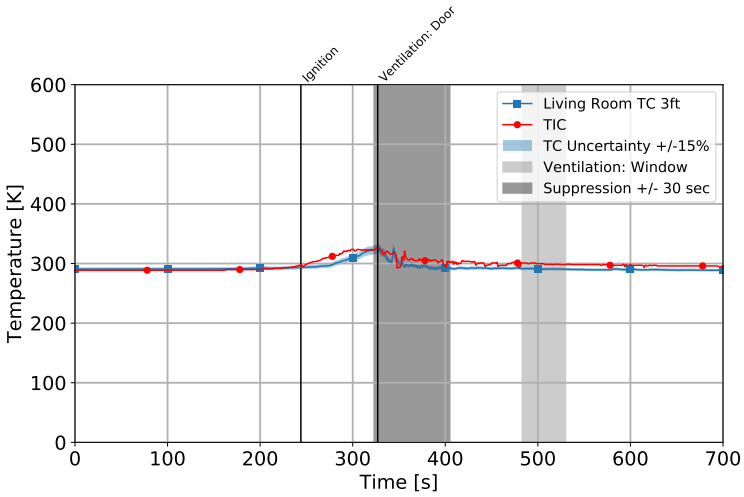

(a) Temperature

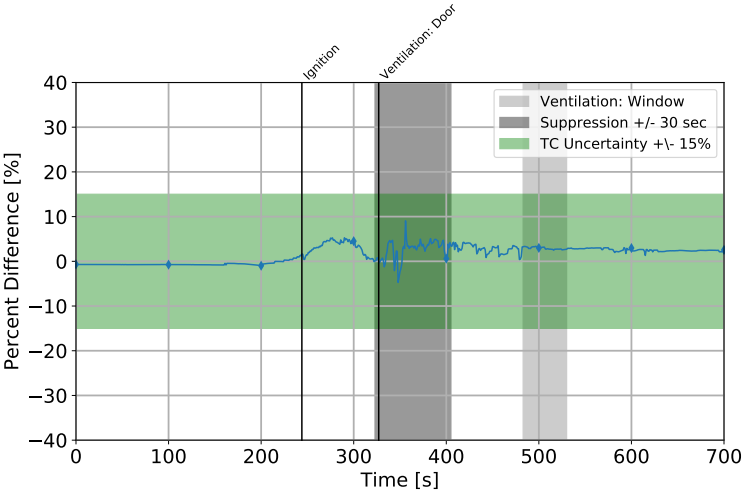

(b) Percent Difference

Figure B.47: Experiment # 9 Living Room TIC vs. TC

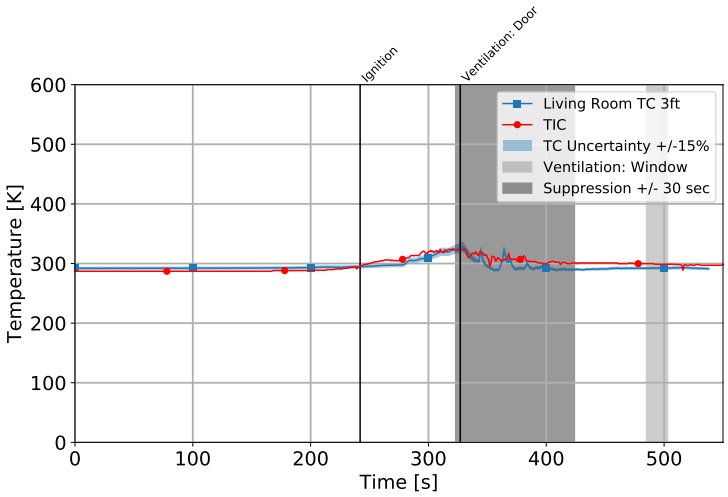

(a) Temperature

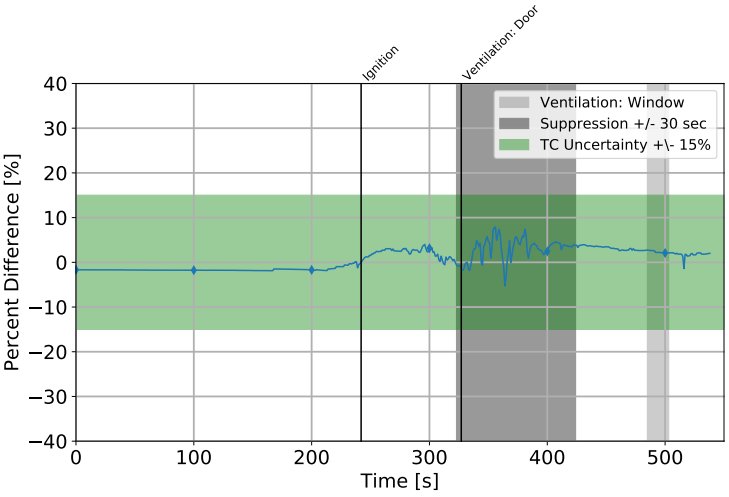

(b) Percent Difference

Figure B.48: Experiment # 10 Living Room TIC vs. TC

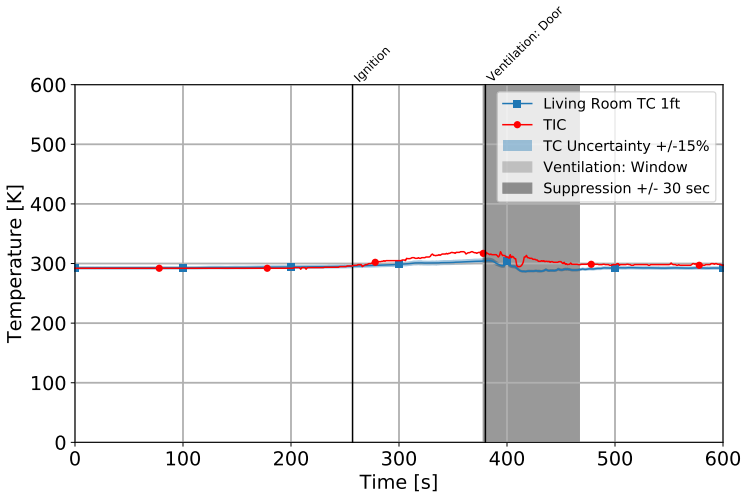

(a) Temperature

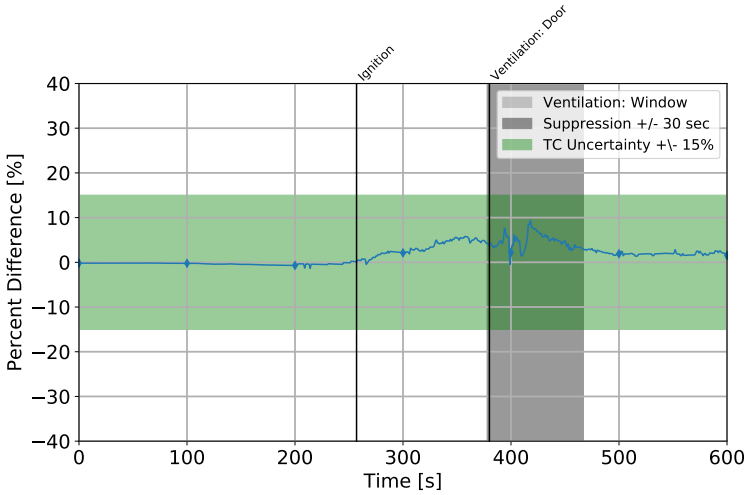

(b) Percent Difference

Figure B.49: Experiment # 11 Living Room TIC vs. TC

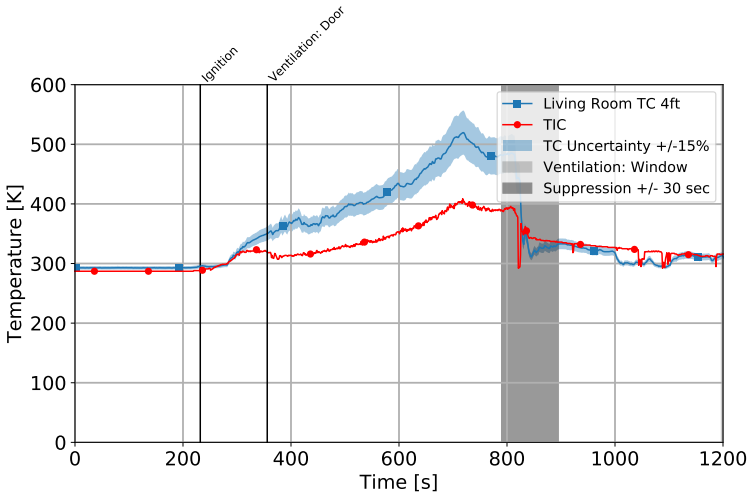

(a) Temperature

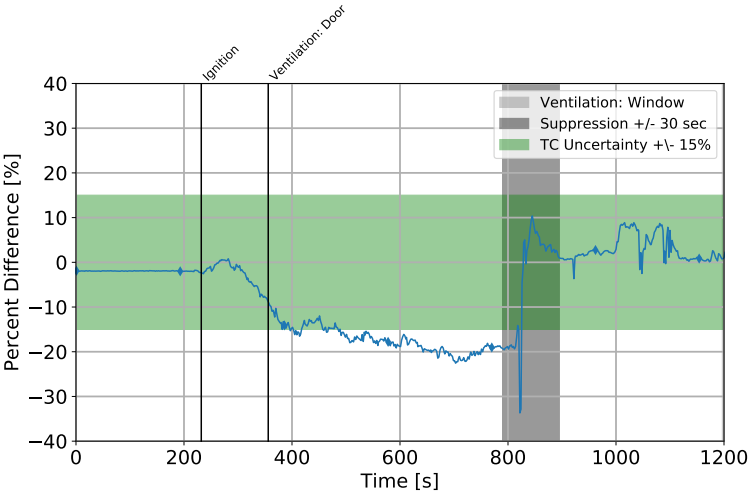

(b) Percent Difference

Figure B.50: Experiment # 12 Living Room TIC vs. TC

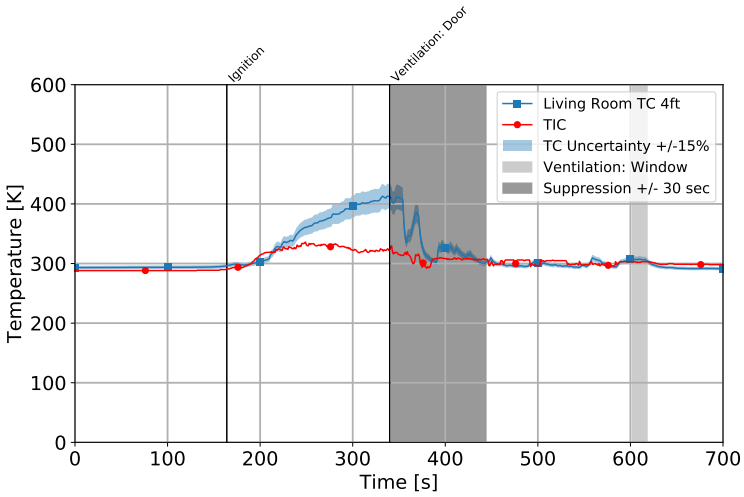

(a) Temperature

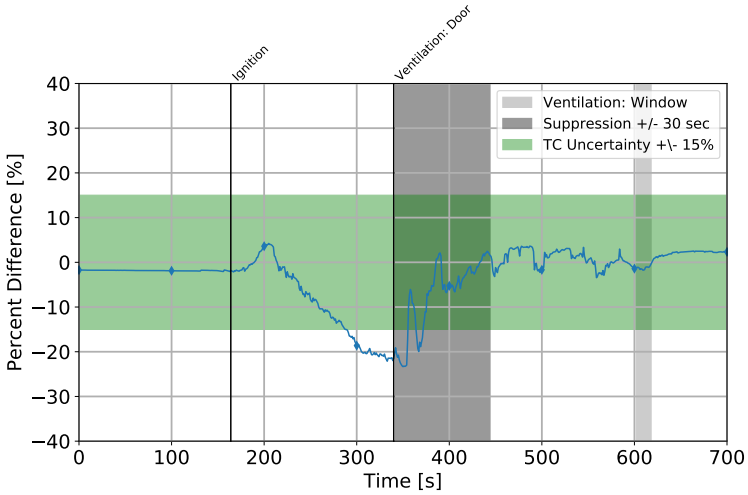

(b) Percent Difference

Figure B.51: Experiment # 13 Living Room TIC vs. TC

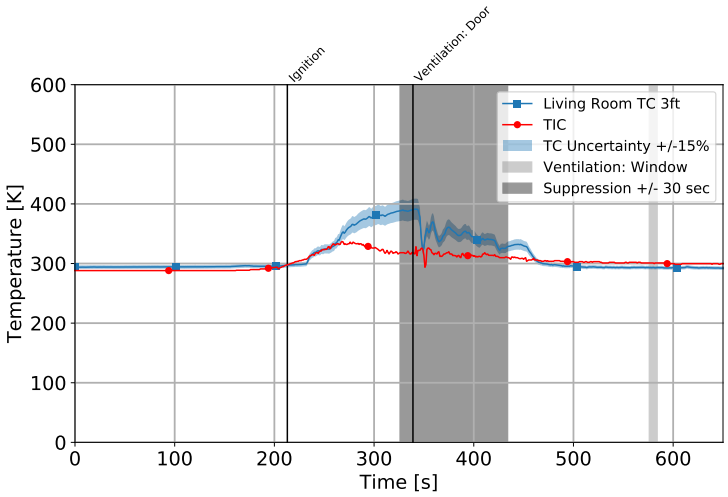

(a) Temperature

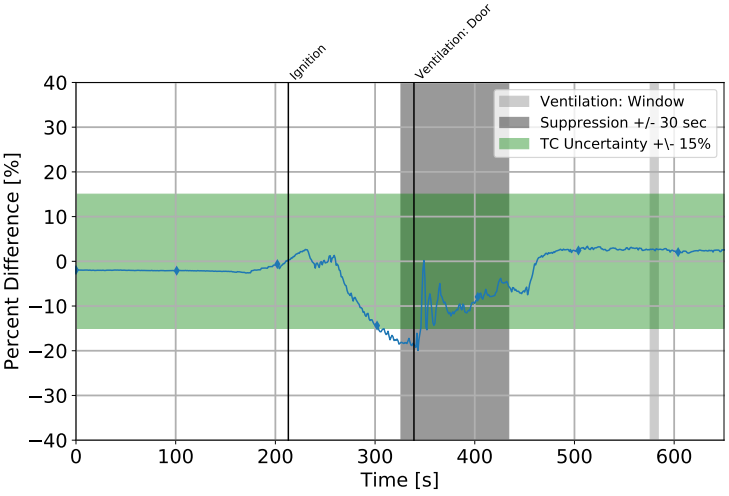

(b) Percent Difference

Figure B.52: Experiment # 15 Living Room TIC vs. TC

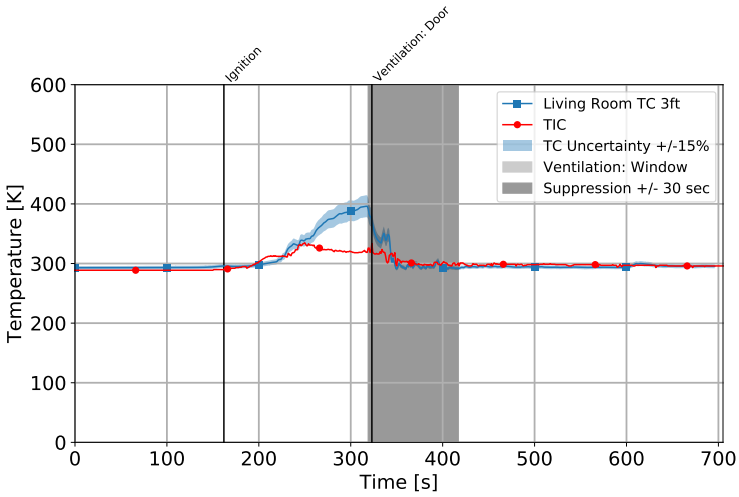

(a) Temperature

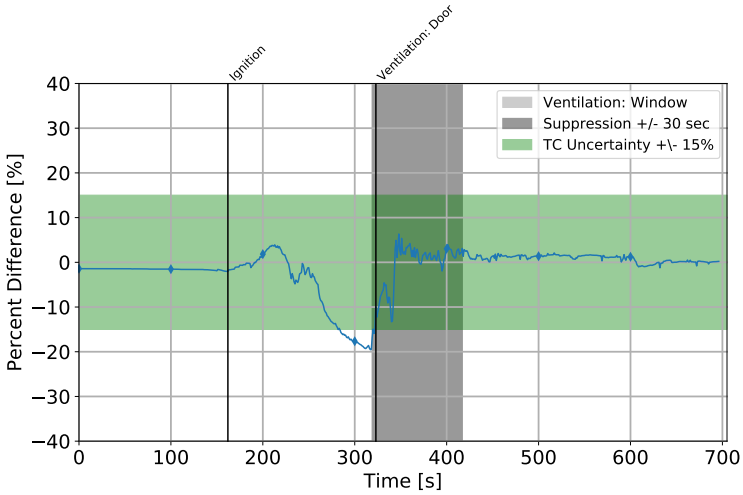

(b) Percent Difference

Figure B.53: Experiment # 16 Living Room TIC vs. TC

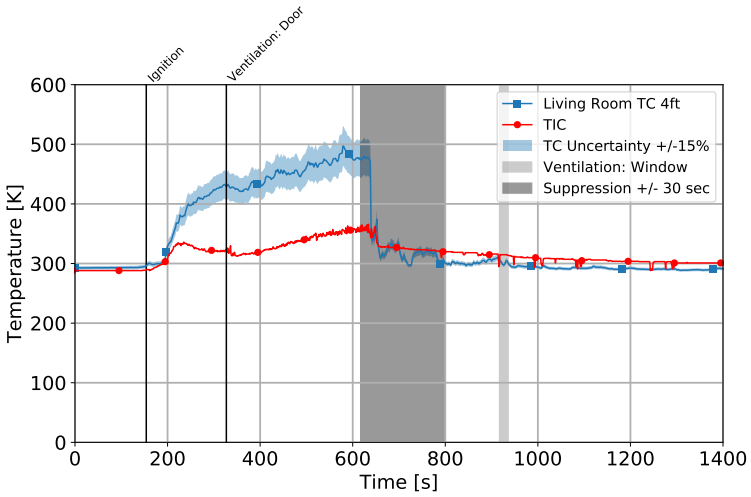

(a) Temperature

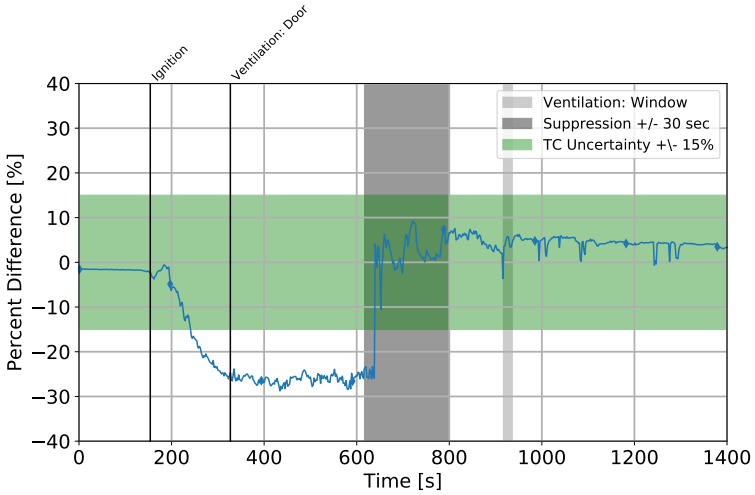

(b) Percent Difference

Figure B.54: Experiment # 17 Living Room TIC vs. TC

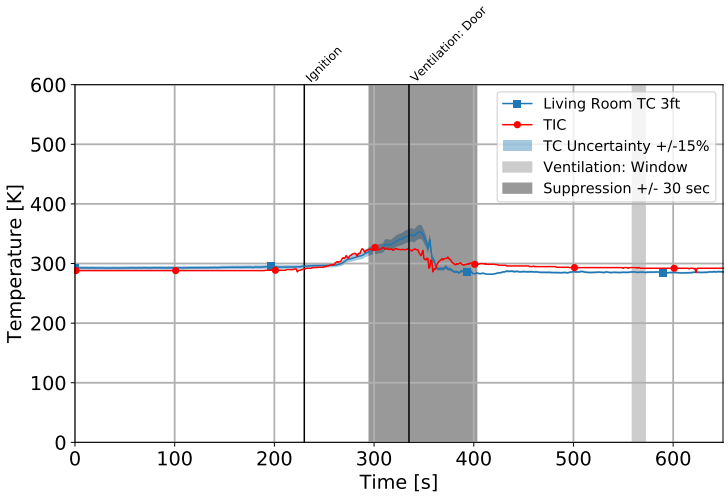

(a) Temperature

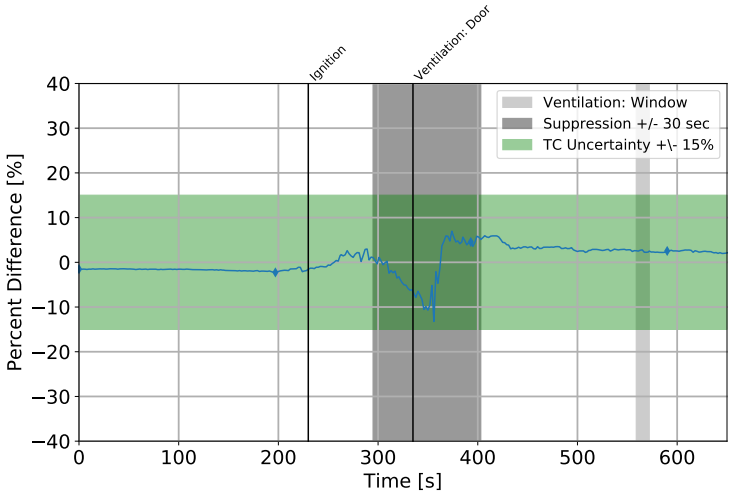

(b) Percent Difference

Figure B.55: Experiment # 18 Living Room TIC vs. TC

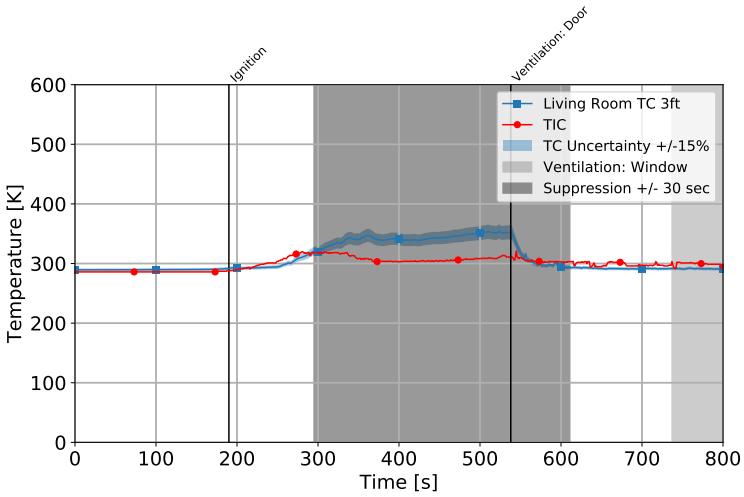

(a) Temperature

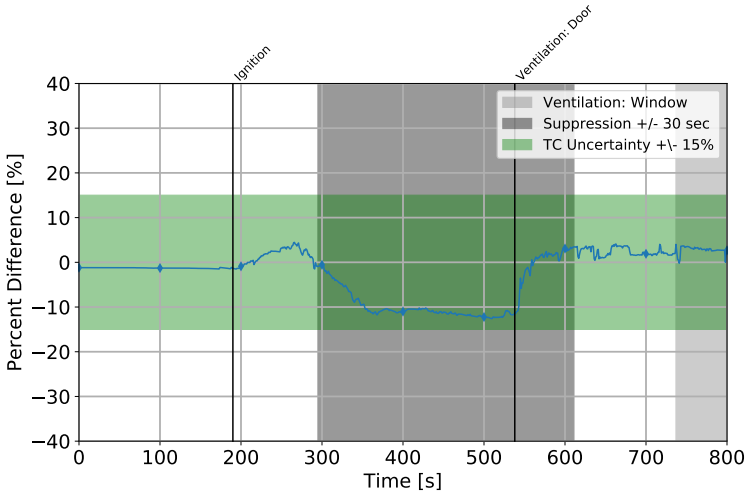

(b) Percent Difference

Figure B.56: Experiment # 19 Living Room TIC vs. TC

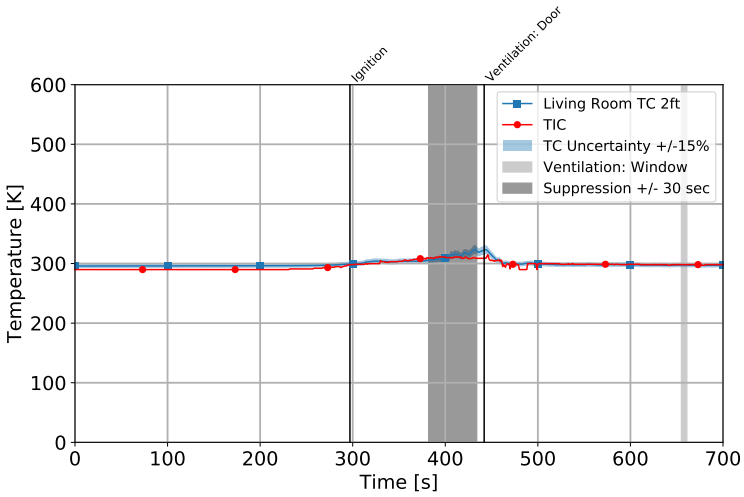

(a) Temperature

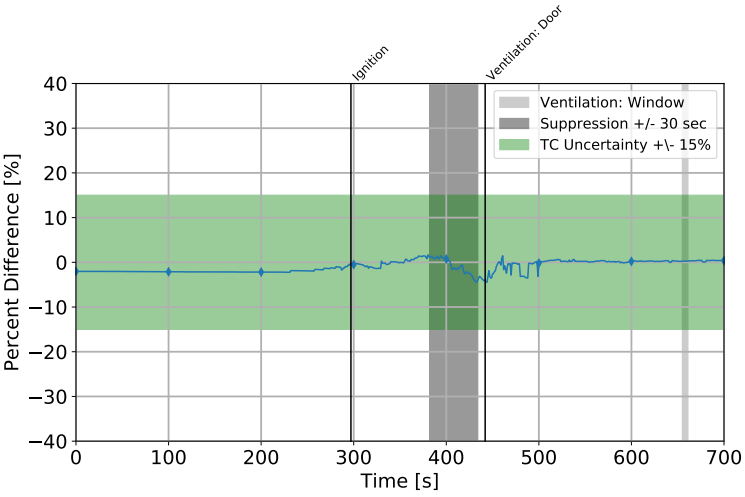

(b) Percent Difference

Figure B.57: Experiment # 20 Living Room TIC vs. TC

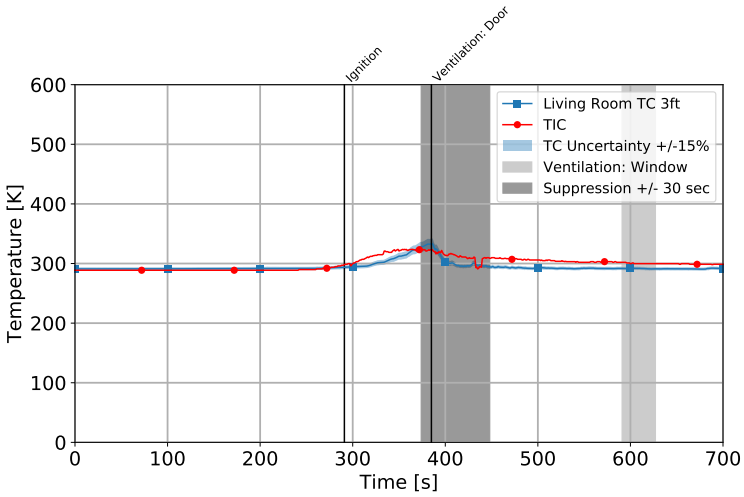

(a) Temperature

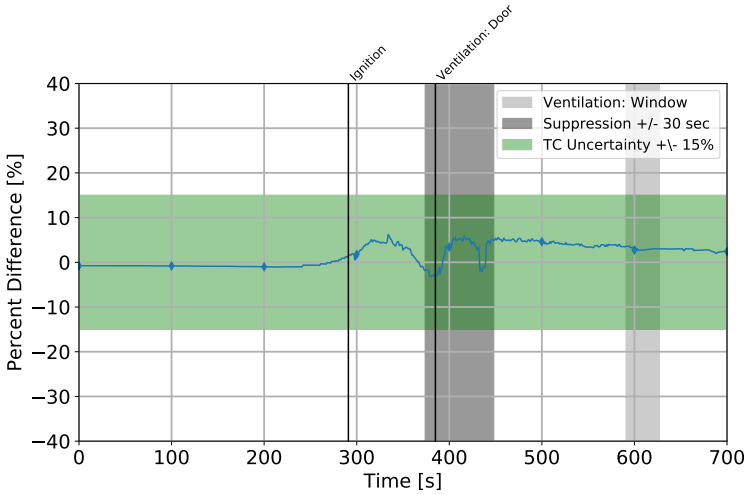

(b) Percent Difference

Figure B.58: Experiment # 21 Living Room TIC vs. TC

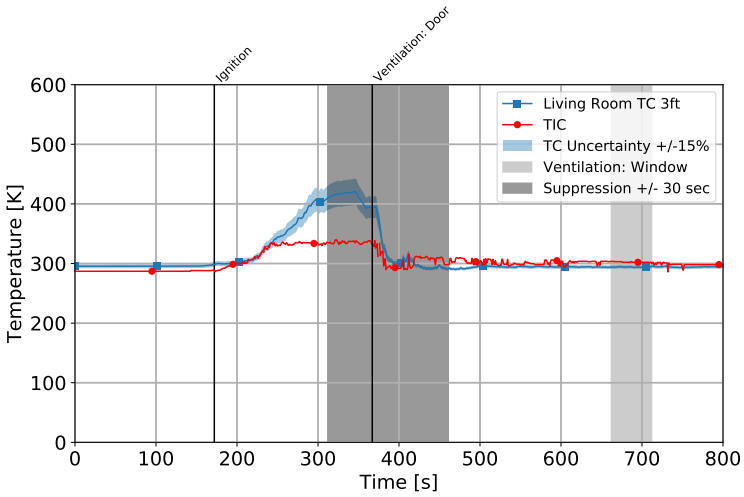

(a) Temperature

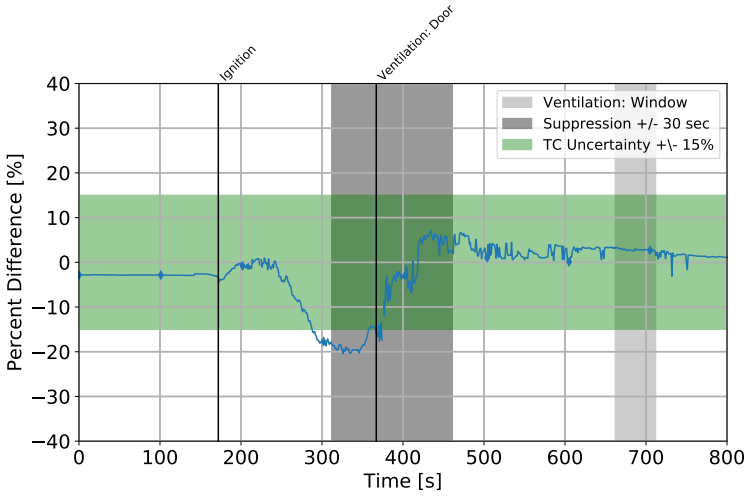

(b) Percent Difference

Figure B.59: Experiment # 22 Living Room TIC vs. TC

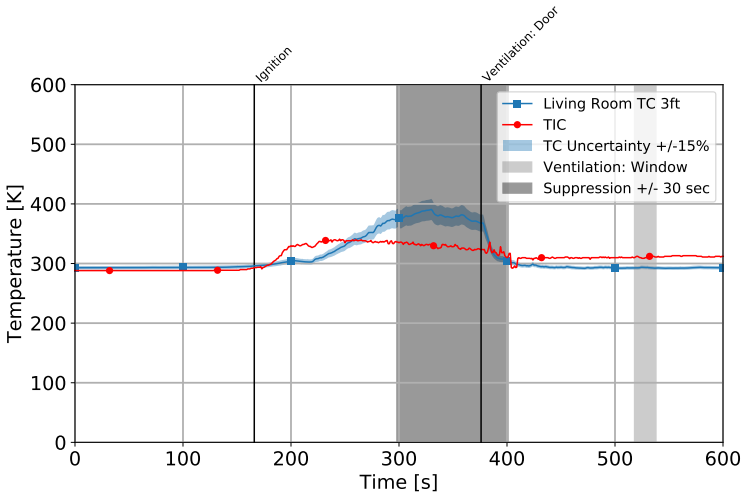

(a) Temperature

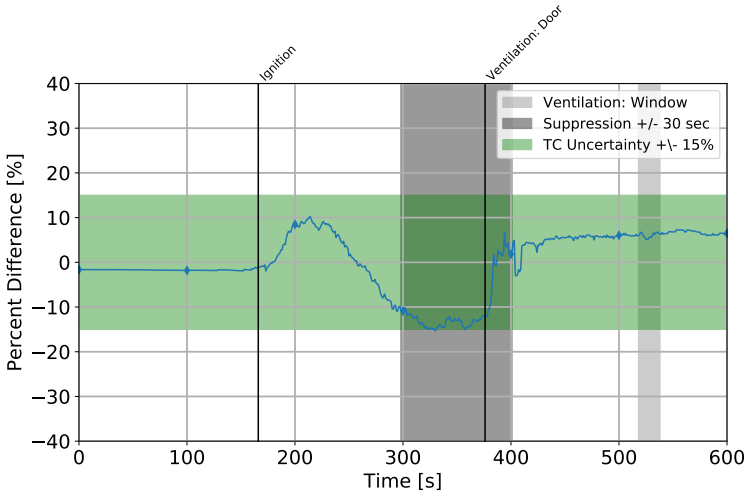

(b) Percent Difference

Figure B.60: Experiment # 24 Living Room TIC vs. TC

Table B.10: Average Percent Difference: FA Living Room TIC

Exp. #	Pre-Ignition	Initial Combustion	Combustion	Post-Suppression
1	-4	-9	-16	-3
2	-3	N/A	-3	-5
3	-2	N/A	-6	5
4	-3	N/A	-9	2
5	-2	N/A	-9	4
6	-3	N/A	-5	-4
7	-2	N/A	-1	3
8	-2	N/A	2	1
9	-1	N/A	4	3
10	-2	N/A	2	3
11	-1	N/A	4	2
12	-2	-4	-18	4
13	-2	-5	-20	2
15	-2	-5	-17	2
16	-2	-3	-18	1
17	-2	-6	-25	5
18	-2	N/A	-1	3
19	-2	N/A	2	3
20	-2	N/A	-1	-1
21	-1	N/A	4	4
22	-3	N/A	-18	3
24	-2	N/A	2	6

Chapter C: Fuel Load Characterization

Table C.1: Fuel Load Heat Release Data

Ignition Location	Peak Heat Release [kW]	Total Energy Released [kJ]	Burn Duration [min:sec]
Left	2.7	693	22:59
Right	4.9	640	21:58
Center	4.6	674	18:34

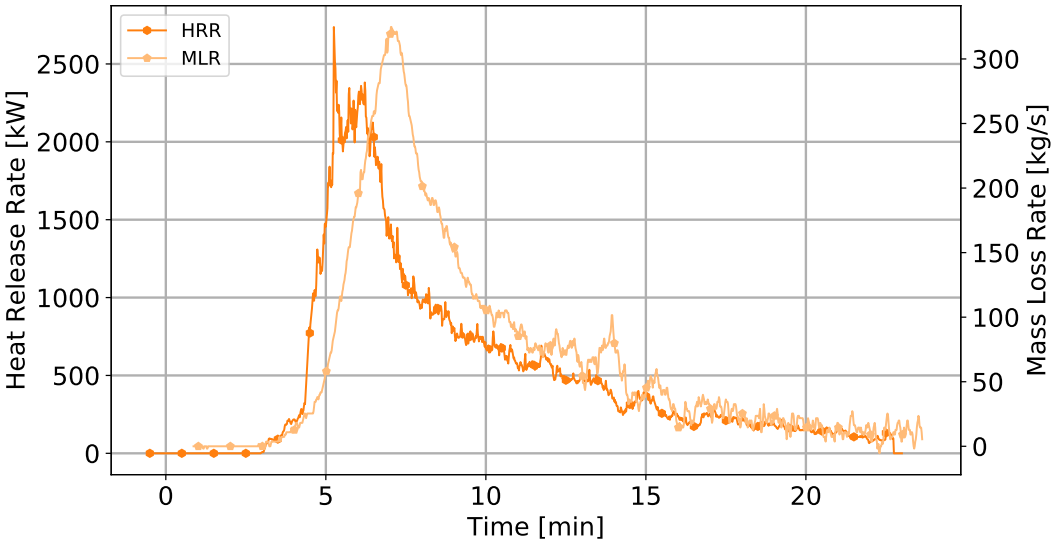

(a) Heat Release Rate & Mass Loss Rate

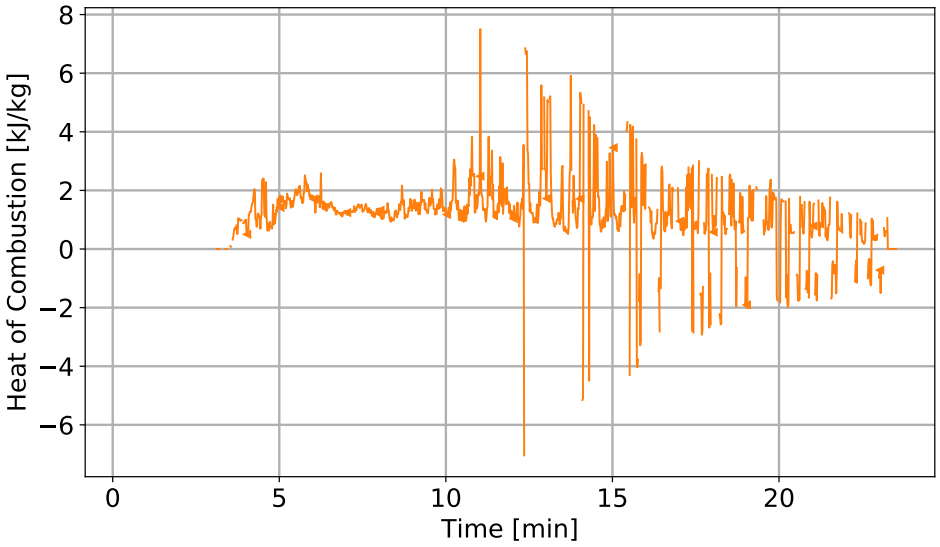

(b) Heat of Combustion

Figure C.1: Left Ignition Fuel Load Characterization

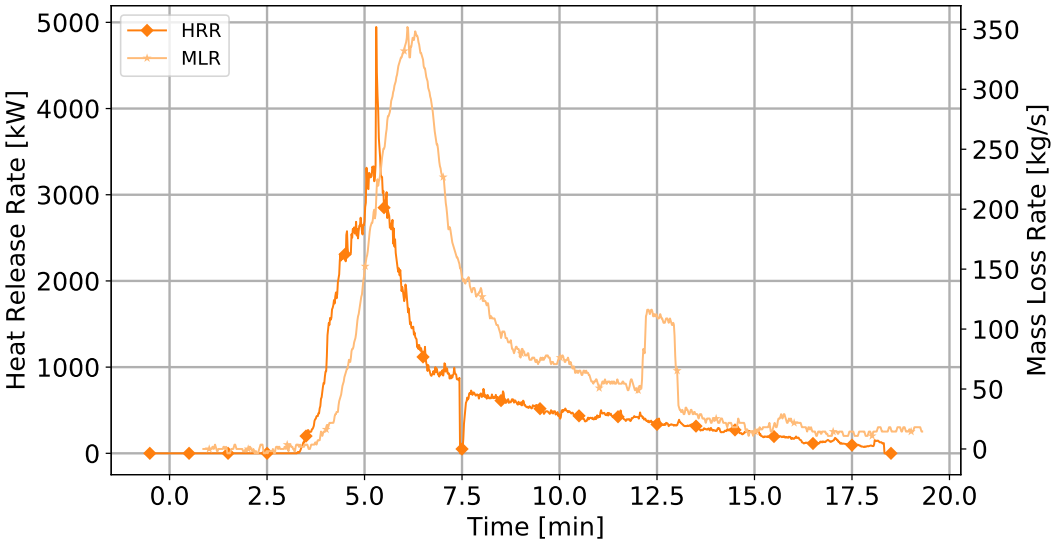

(a) Heat Release Rate & Mass Loss Rate

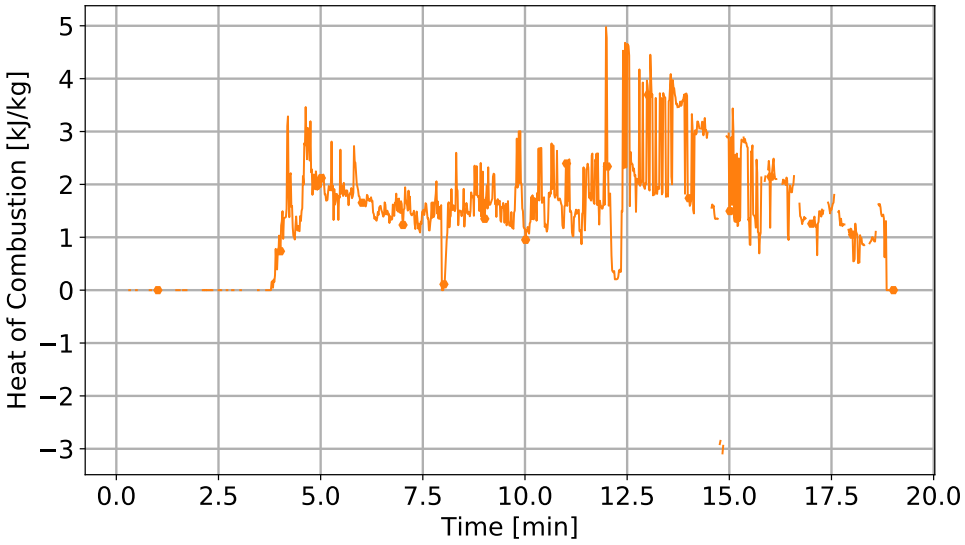

(b) Heat of Combustion

Figure C.2: Right Ignition Fuel Load Characterization

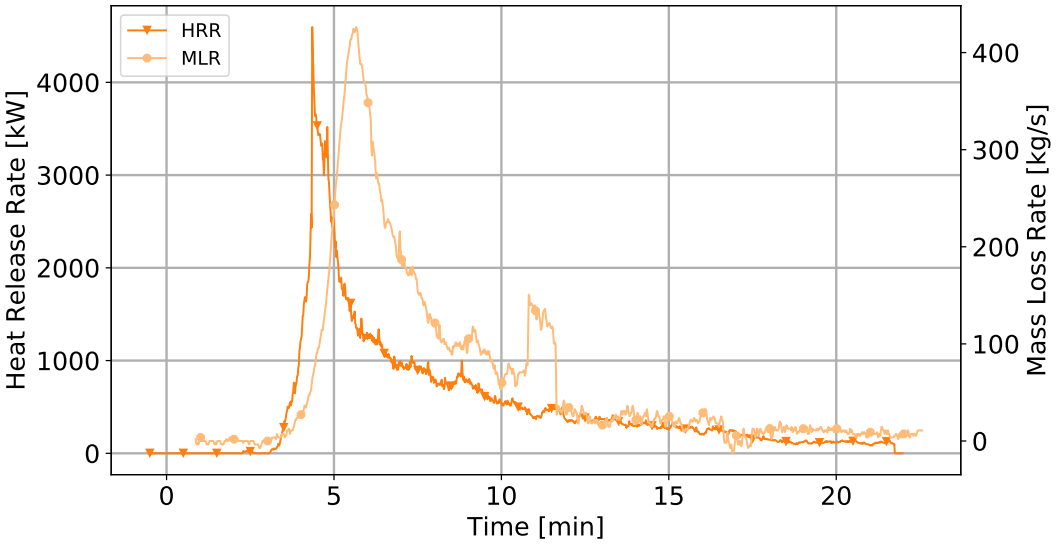

(a) Heat Release Rate & Mass Loss Rate

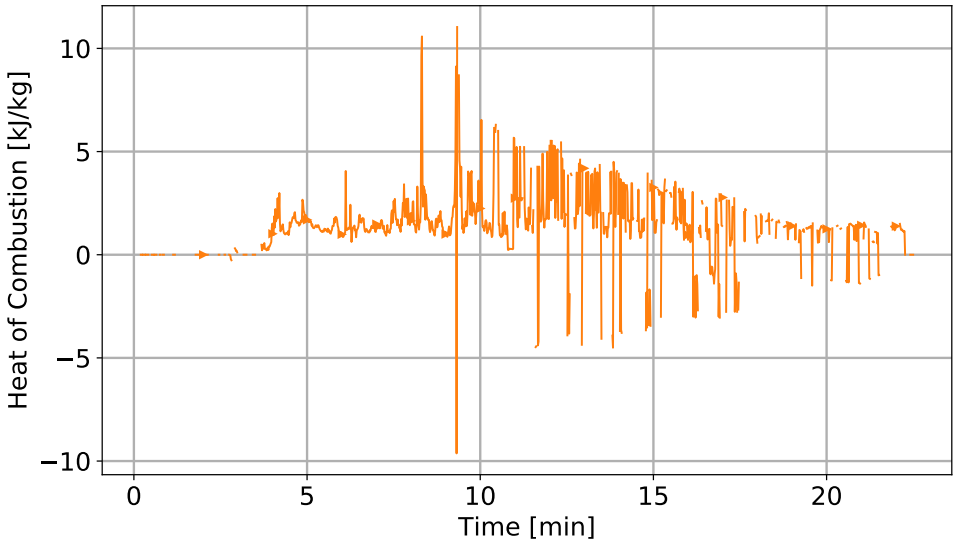

(b) Heat of Combustion

Figure C.3: Center Ignition Fuel Load Characterization

Chapter D: Experimental Results

D.1 Repeatability - Baseline Experiments

First, the temperature data obtained from the wall mounted during two experiments was plotted together along with their associated Type B uncertainties. This was used to verify that the data was initially similar, see Figure D.1.

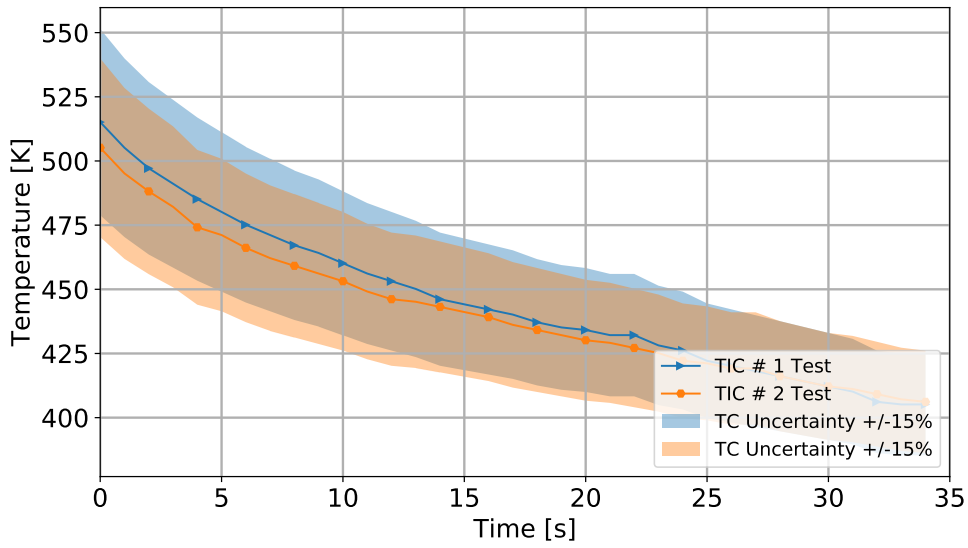

Figure D.1: Temperature measurements for the wall mounted TC during the On-plane 6.10 m TIC # 1 and TIC # 2 experiments. Measurements are accompanied by their associated Type B expanded uncertainty.

Second, the data presented in Figure D.1 was paired together at each time step within the interval. These paired measurements were then plotted together as a scatter plot to ensure evenly distributed data. On this graph the line of perfect agreement and the expanded Type B uncertainty were also indicated. The black line represents the line of perfect agreement indicating what the scatter would look like if the paired measurements were identical. The gray shaded area represents the expanded Type B uncertainty associated with the line of perfect agreement. This indicates that any measurement within this area can not be distinguished from one another due to uncertainty in the measurement itself; therefore, all measurements can be considered identical. Figure D.2 represents this analysis for data presented in Figure D.1.

The red dashed line plotted on the graph is the linear regression line calculated for the paired data. This line was forced through the origin (0,0). This line was used to determine how different the set of paired data was. For when this line falls within the gray shaded area, the data can not be determined as significantly different. When the line falls outside the gray shaded area, the data can be considered as significantly different.

To continue the analysis of agreement between the two data sets, two values were calculated for the set at each time step: intraclass correlation coefficient (ICC) and bias factor (δ). The ICC takes on values between 0, no agreement, to 1, perfect agreement. In order to evaluate the ICC, the following equation was employed:

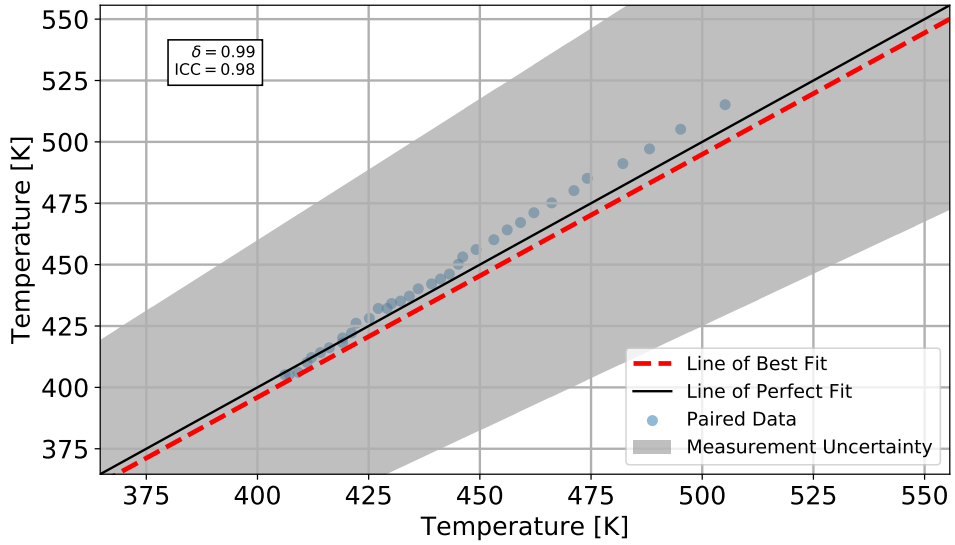

Figure D.2: Scatter plot of temperature measurements obtained from the wall mounted TC during the On-plane 6.10 m TIC # 1 and TIC # 2 experiments. Paired temperatures are plotted as blue circles. The line of perfect agreement is plotted as a black line. The Type B expanded uncertainty for this line is plotted as a gray shaded region. The linear regression line associated with the paired data is plotted as a red dashed line.

$$ICC = \frac{\sigma_a^2 - \sigma_d^2}{\sigma_a^2 + \sigma_d^2 + \frac{2}{n}(n\overline{d}^2 - \sigma_d^2)} \tag{D.1}$$

Where σ_a is the variance between the sum of the pairs, σ_d is the variance between the difference of the pairs, and $\overline{d}$ is the mean of the differences [59]. When calculated, a value greater than 0.5 represents that the majority of the total variance between the paired data is unrelated to the differences between the data.

The bias factor (δ) is a measure of accuracy that describes the relationship

between the paired experiential data and idealized data. It is an indication of the magnitude of the difference between the linear approximation line, red, and the line of perfect agreement, black. The bias factor signifies the relationship between a measurement on the x-axis to its corresponding y-axis measurement on the linear approximation line, expressed by the following equation:

$$y = \delta x \tag{D.2}$$

The bias factor will take on various values; however, values within the range of 0.85 - 1.15 will indicate bias was within the range of the measurement uncertainty. Within this range the temperatures are considered indistinguishable from one another. Values outside of this range indicate that bias was present and that temperatures are significantly different from one another. When bias values are below 1, the x-axis data was on average larger than the y-axis data. Conversely when bias values are greater than 1, the y-axis data was on average larger than x-axis data.

Acceptable ranges of values for both ICC and bias factors were determined to define the level of agree-ability between paired data. Levels of agreeableness were determined as 'highly agreeable', 'agreeable', and 'significantly different'. See Table D.1 for respective ranges.

The ICC and bias values were determined for each paired data set for all experiments mentioned previously. The results are presented in Table D.2.

Table D.1: Levels of Agree-ability: ICC & Bias Factor

Level of Agree-ability	ICC Range	Bias Range	Color Indicator
Highly Agreeable	0.75 - 1.00	0.85 - 1.15	
Agreeable	0.50 - 0.75	0.85 - 1.15	
Significantly Different	ICC $<$ 0.50	0.85 $>$ Bias $>$ 1.15	

Table D.2: Baseline Experiments Repeatability

Experiment	Temperature (x-axis)	Temperature (y-axis)	Overall ICC	Overall Bias
Off-plane: 7.01 m	TIC # 1	TIC # 2	0.90	1.03
	TIC # 3	TIC # 2	0.99	0.99
	TIC # 1	TIC # 3	0.85	1.04
On-plane: 6.10 m	TIC # 1	TIC # 2	0.98	0.99
	TIC # 3	TIC # 2	0.60	0.93
	TIC # 1	TIC # 3	0.70	1.07
On-plane: 4.57 m	TIC # 1	TIC # 2	0.90	1.03
	TIC # 3	TIC # 2	0.99	1.01
	TIC # 1	TIC # 3	0.94	1.02
On-plane: 3.05 m	TIC # 1	TIC # 2	0.74	1.06
	TIC # 3	TIC # 2	0.70	1.06
	TIC # 1	TIC # 3	0.99	0.99
On-plane: 1.52 m	TIC # 1	TIC # 2	0.99	1.01
	TIC # 3	TIC # 2	0.97	1.00
	TIC # 1	TIC # 3	0.97	1.01

D.2 Baseline Experiments

D.2.1 Off-plane Orientation

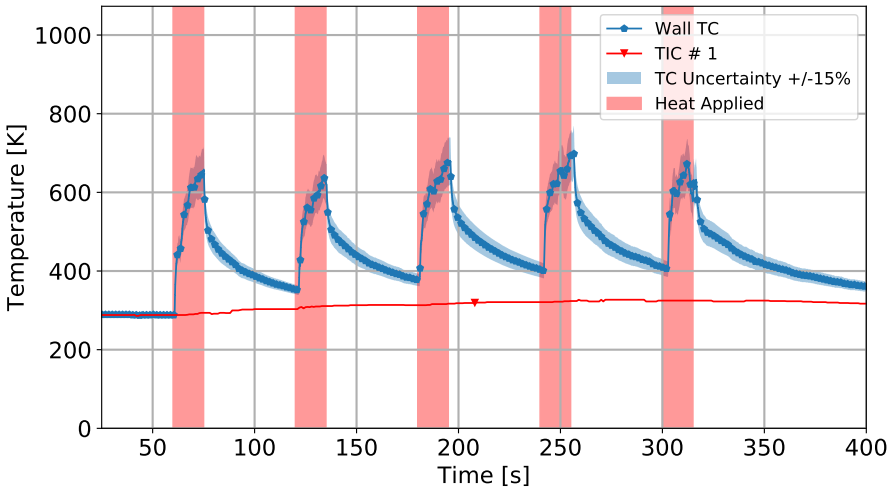

Figure D.3: Off-Plane TIC # 1 vs. TC Temperature

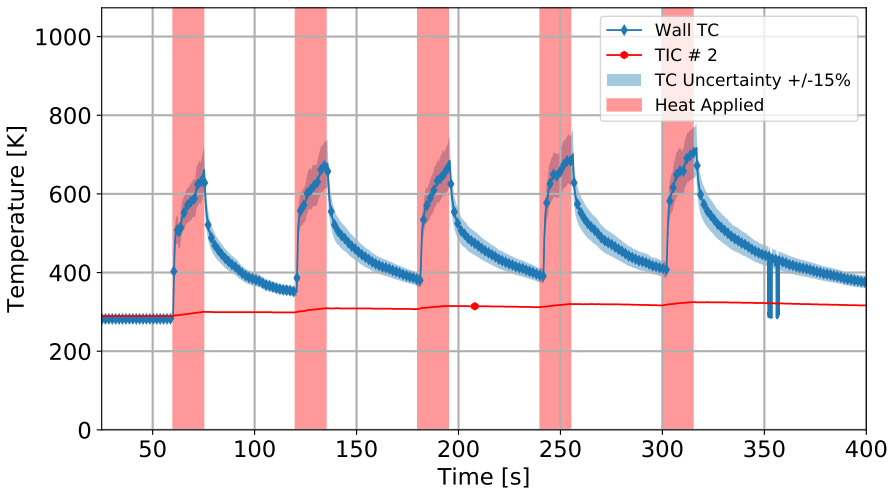

Figure D.4: Off-Plane TIC # 2 vs. TC Temperature

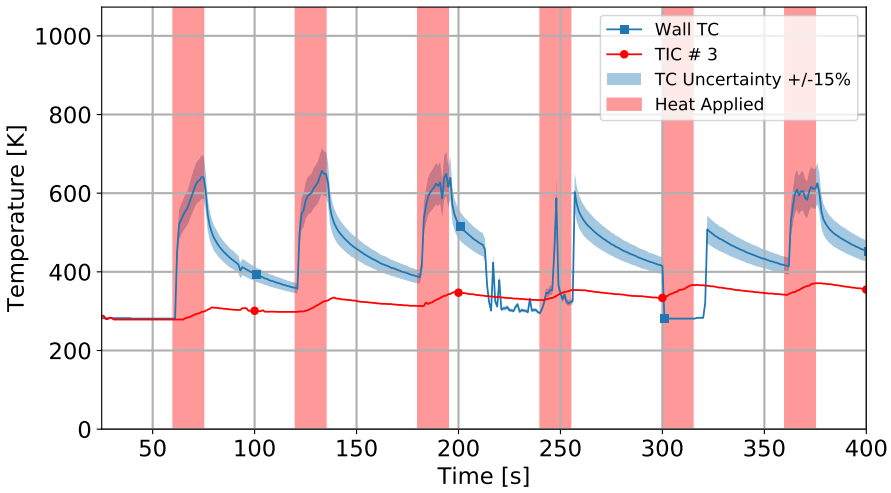

Figure D.5: Off-Plane TIC # 3 vs. TC Temperature

D.2.2 On-plane Orientation

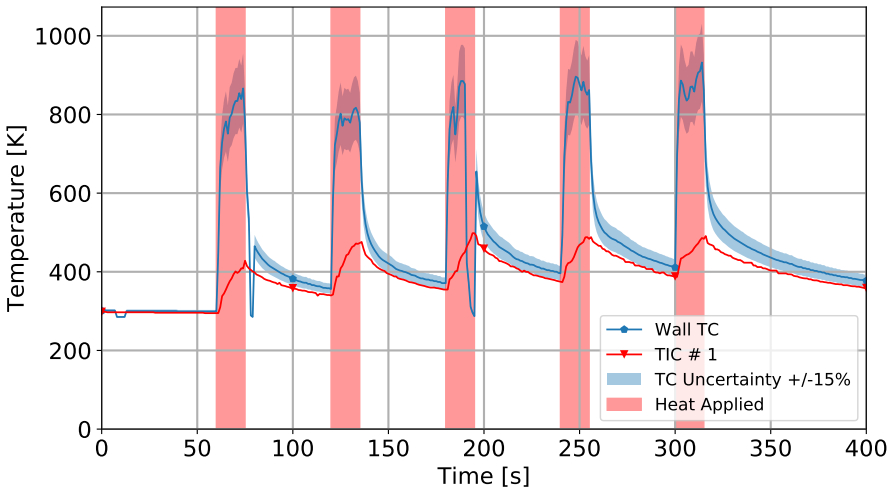

(a) TIC # 1 1.52 m

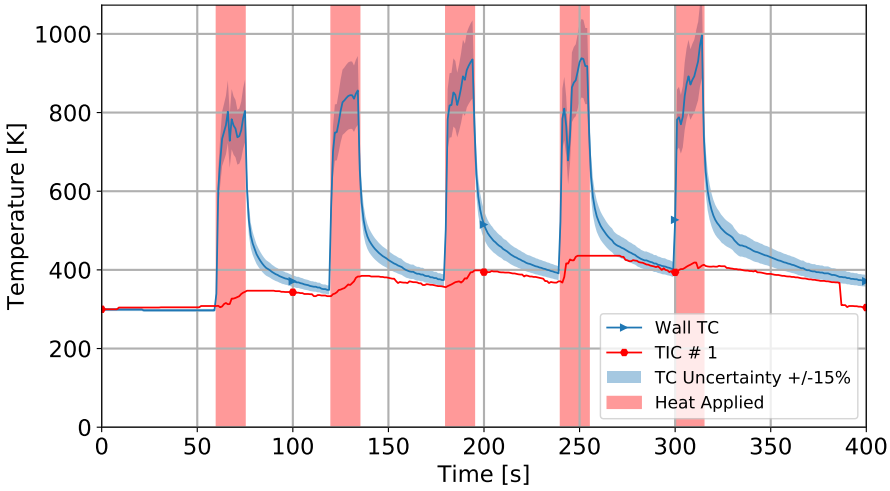

(b) TIC # 1 3.05 m

Figure D.6: On-Plane TIC # 1 vs. TC Temperature

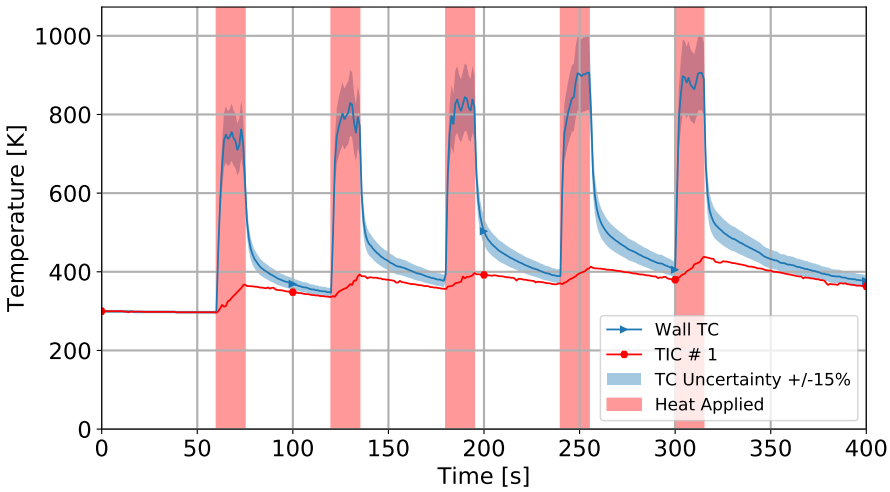

(a) TIC # 1 4.57 m

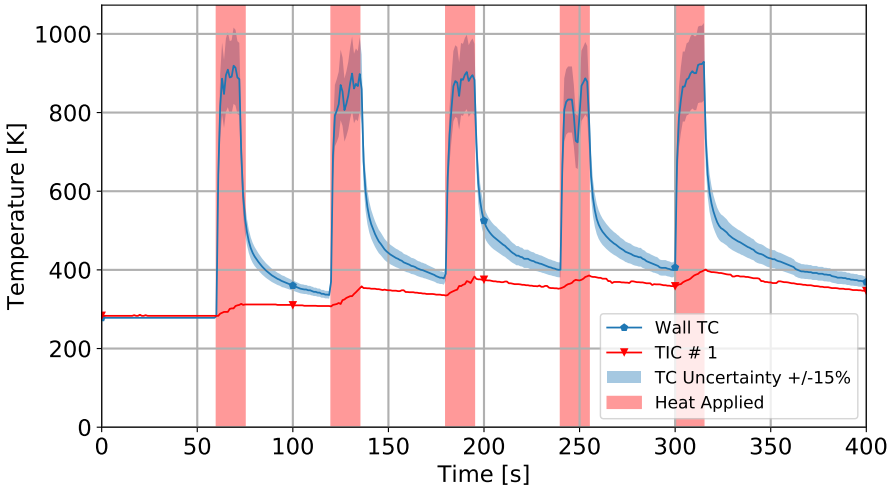

(b) TIC # 1 6.10 m

Figure D.7: On-Plane TIC # 1 vs. TC Temperature

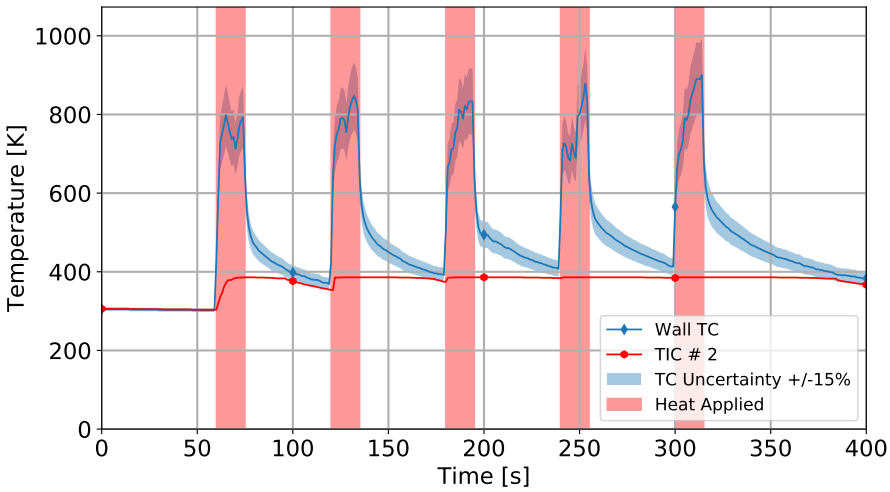

(a) TIC # 2 1.52 m

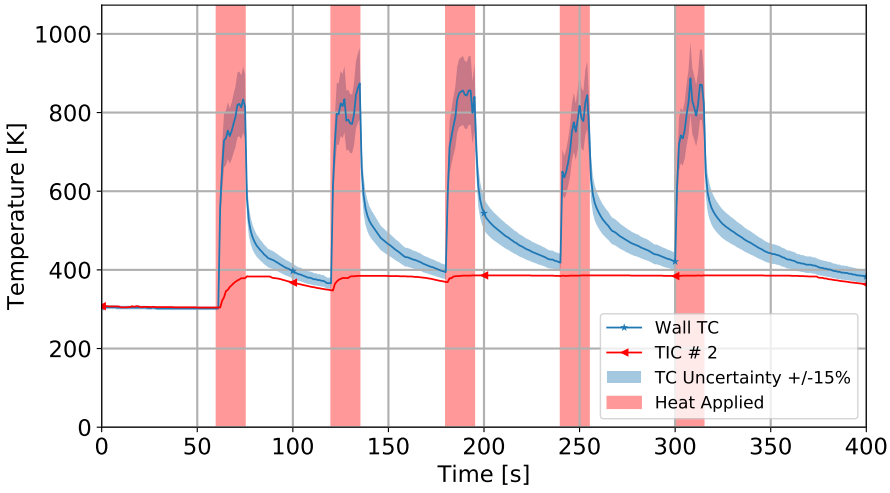

(b) TIC # 2 3.05 m

Figure D.8: On-Plane TIC # 2 vs. TC Temperature

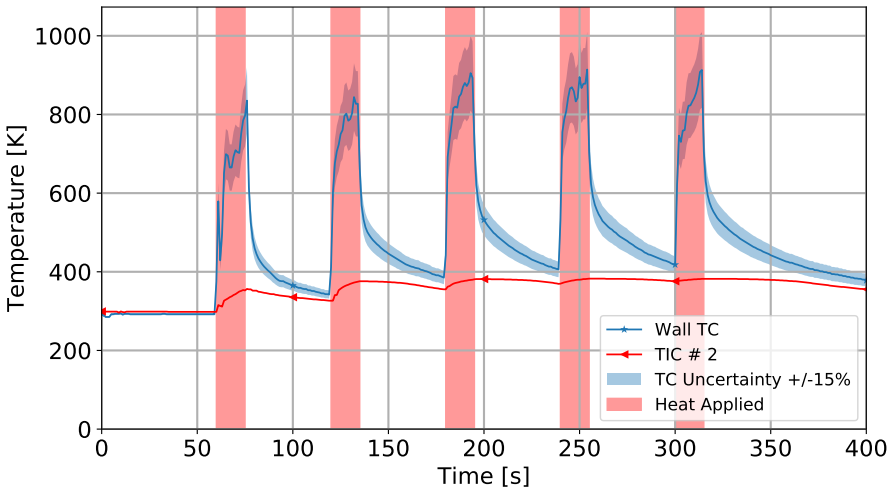

(a) TIC # 2 4.57 m

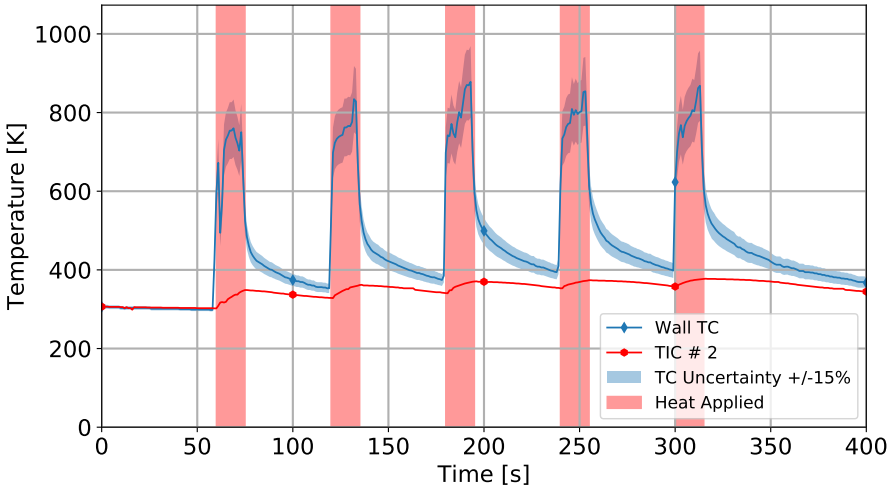

(b) TIC # 2 6.10 m

Figure D.9: On-Plane TIC # 2 vs. TC Temperature

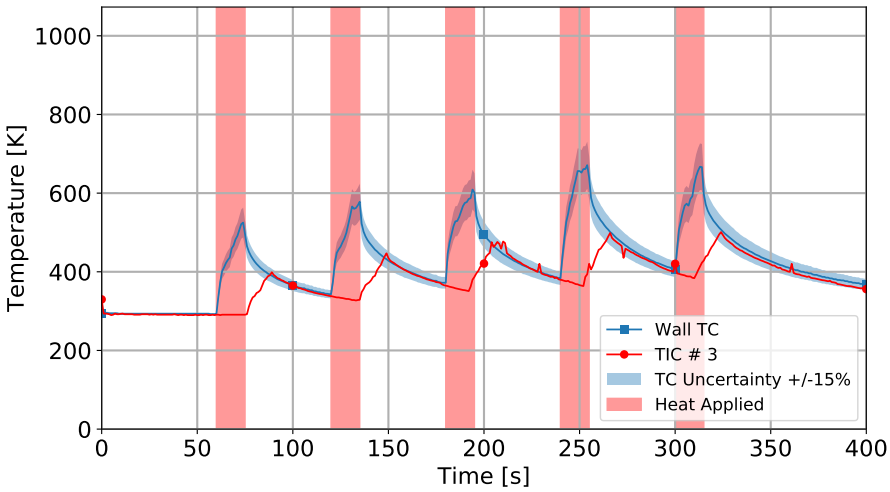

(a) TIC # 3 1.52 m

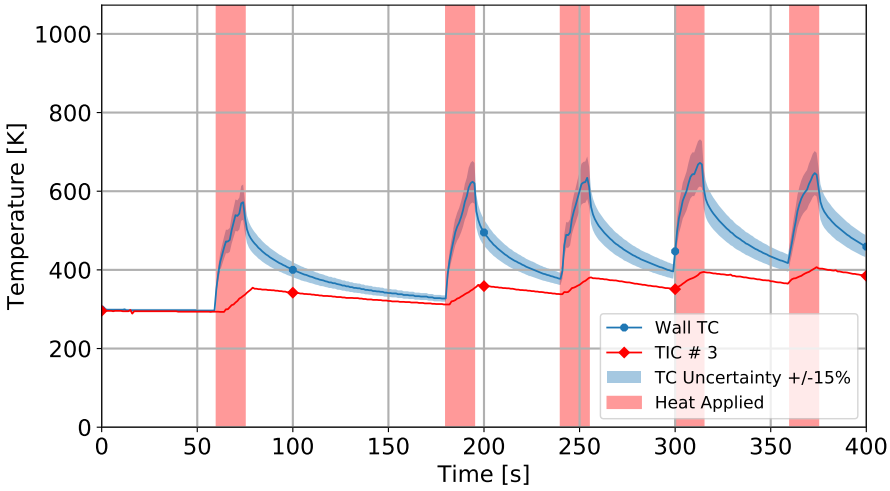

(b) TIC # 3 3.05 m

Figure D.10: On-Plane TIC # 3 vs. TC Temperature

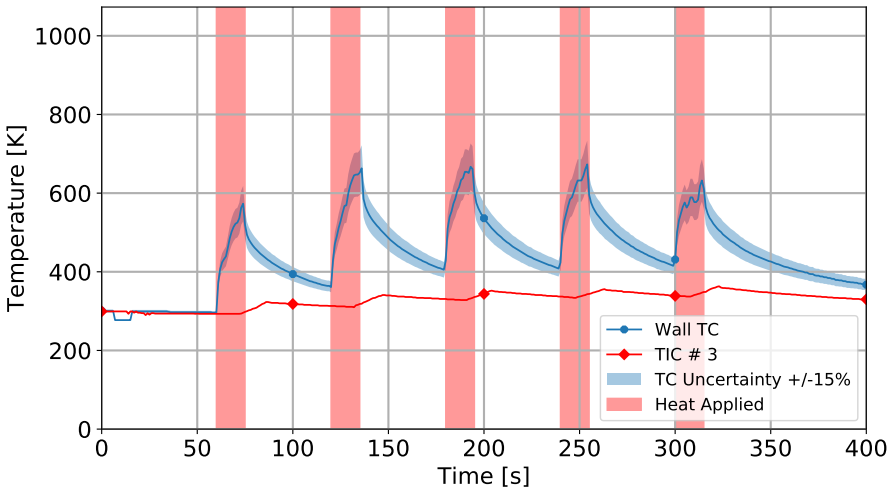

(a) TIC # 3 4.57 m

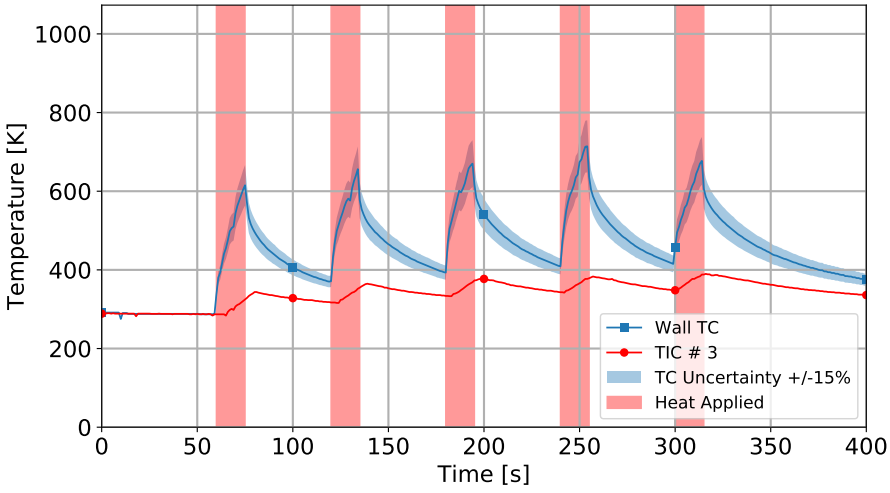

(b) TIC # 3 6.10 m

Figure D.11: On-Plane TIC # 3 vs. TC Temperature

D.3 Room-Scale Fire Experiments

All subsequent graphs have been adjusted to begin at ignition, ignoring any and all background information. The associated times of ventilation and suppression were also adjusted.

D.3.1 Experiment no. 1

Item	Quantity	Initial Weight
Sofa #1	1	48.70 kg
Sofa #2	1	48.95 kg
Carpet	9.75 m^2	13.40 kg
Carpet Padding	9.75 m^2	7.70 kg
Plywood	19.75 m^2	73.60 kg

Table D.3: Room-Scale Fire Experiments: Experiment no. 1 Fuel Load

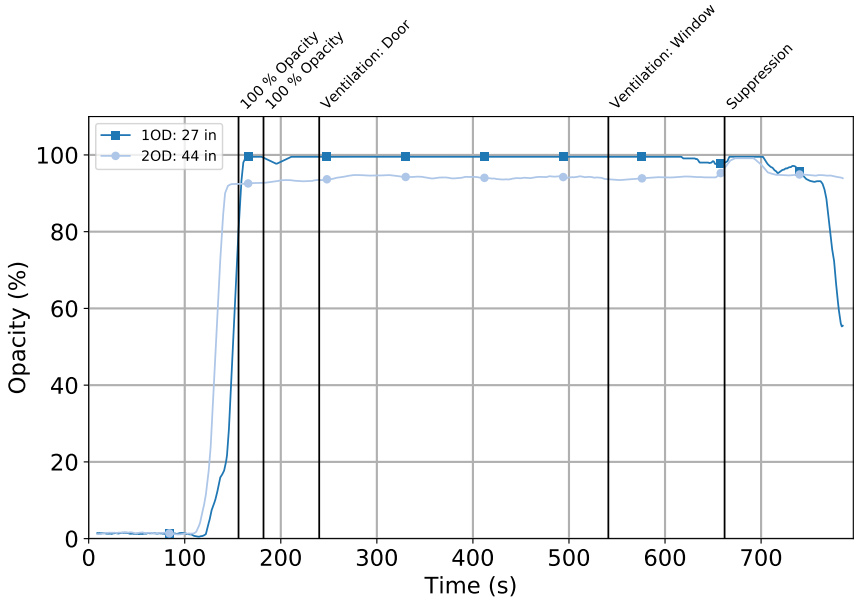

Figure D.12: Opacity during Experiment # 1.

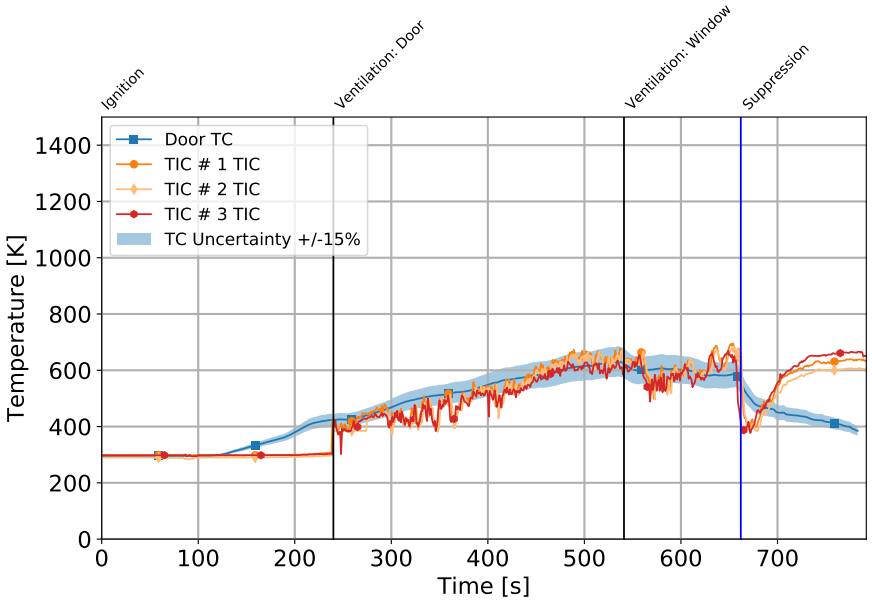

(a) Exterior TIC vs. Inconel TC

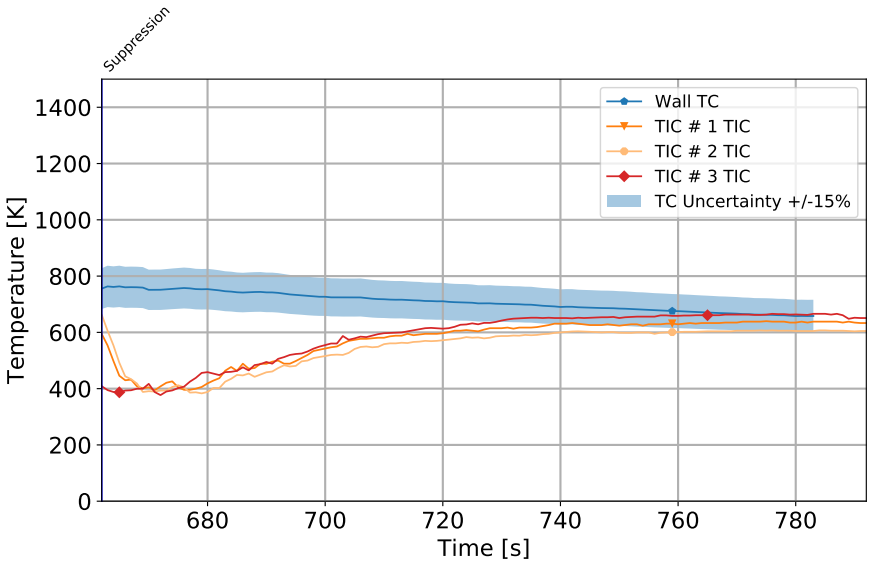

(b) Exterior TIC vs. Wall TC

Figure D.13: Exterior TIC spot temperature measurement results

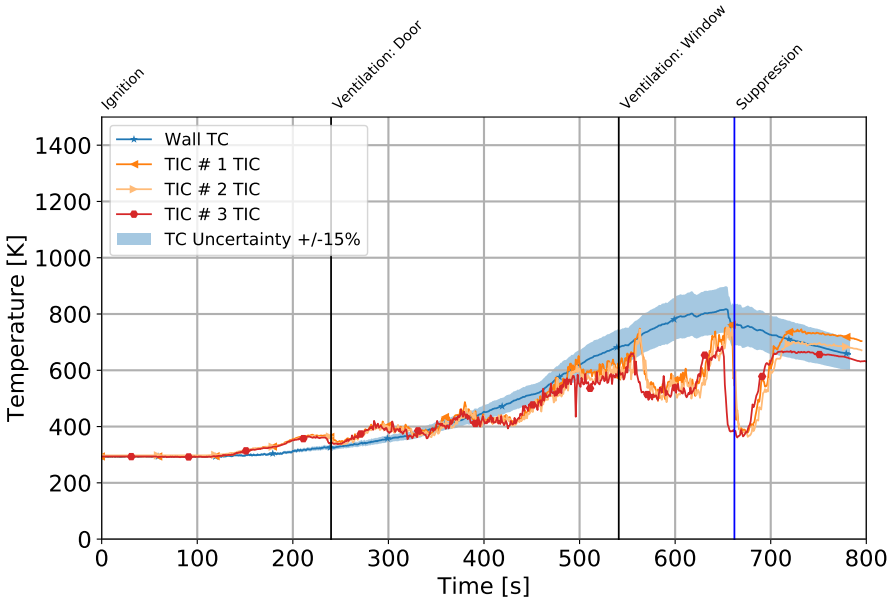

(a) Interior TIC vs. Wall TC

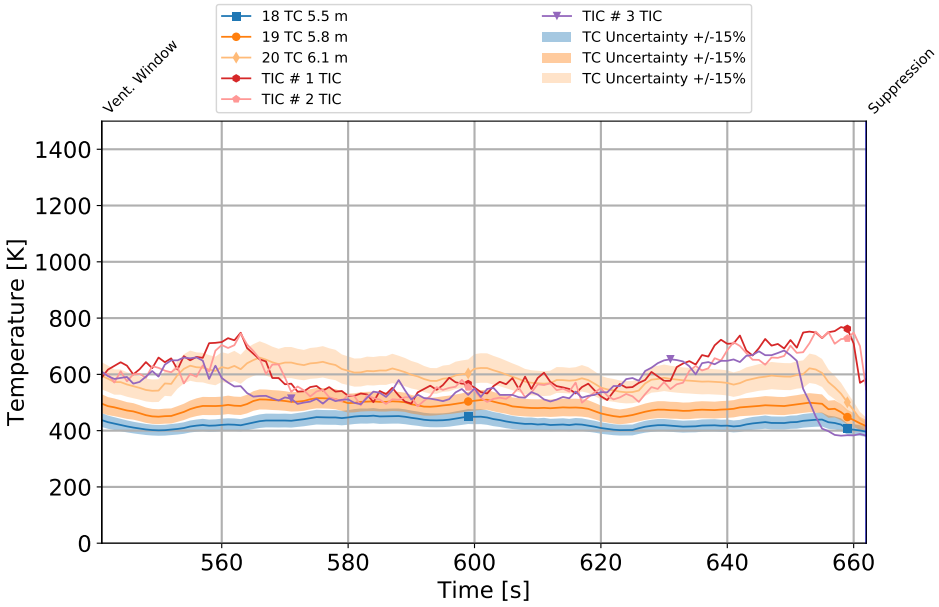

(b) Interior TIC vs. Gas TC

Figure D.14: Interior TIC spot temperature measurement results

D.3.2 Experiment no. 2

Item	Quantity	Initial Weight
Sofa #1	1	49.50 kg
Sofa #2	1	48.95 kg
Carpet	9.75 m^2	12.95 kg
Carpet Padding	9.75 m^2	8.00 kg
Plywood	9.75 m^2	75.45 kg

Table D.4: Room-Scale Fire Experiments: Experiment no. 2 Fuel Load

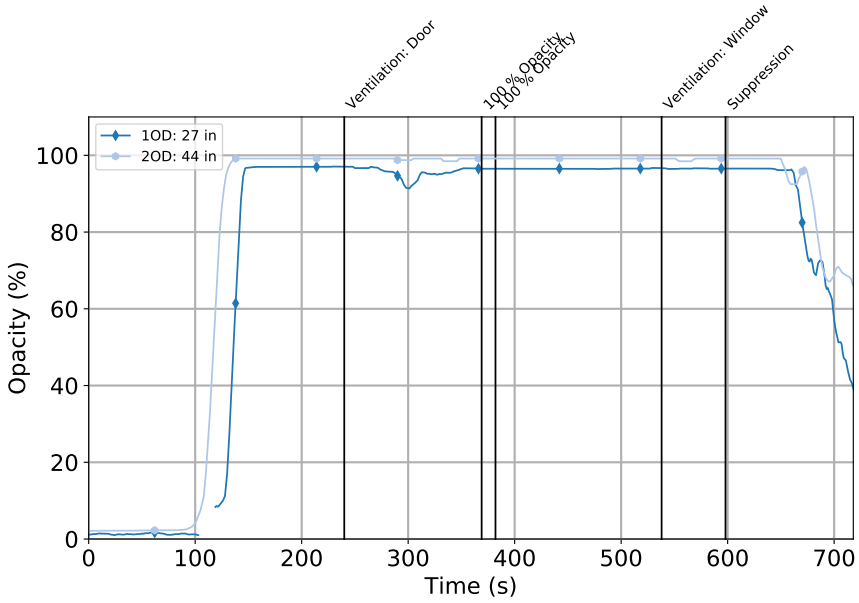

Figure D.15: Opacity during Experiment # 2.

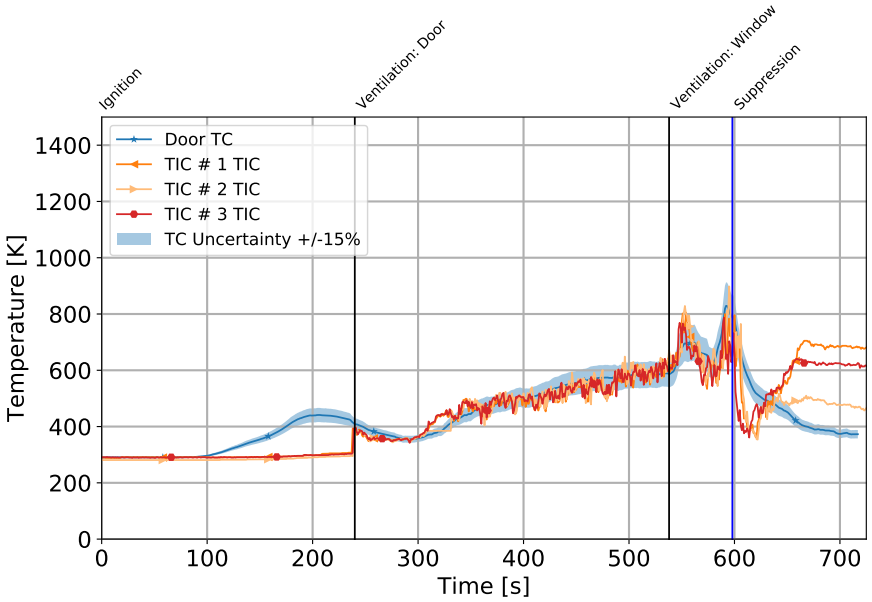

(a) Exterior TIC vs. Inconel TC

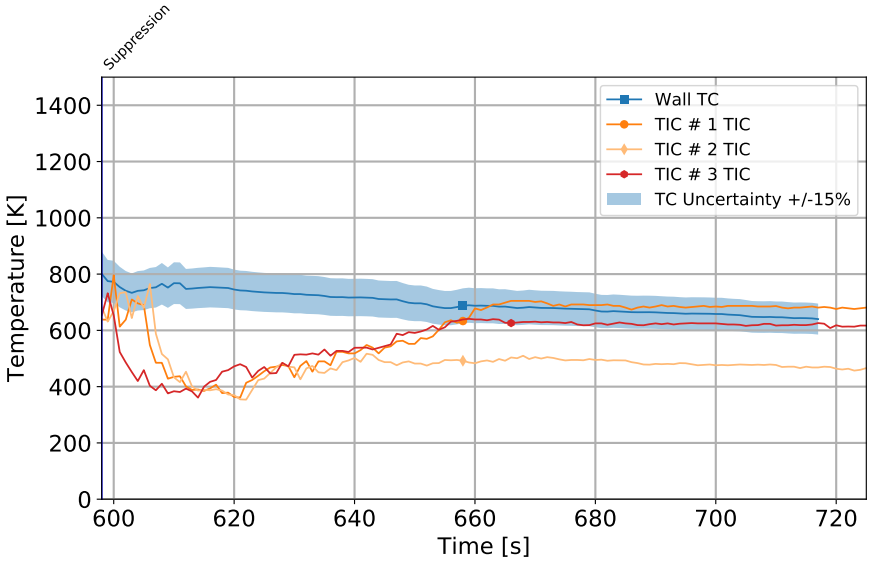

(b) Exterior TIC vs. Wall TC

Figure D.16: Exterior TIC spot temperature measurement results

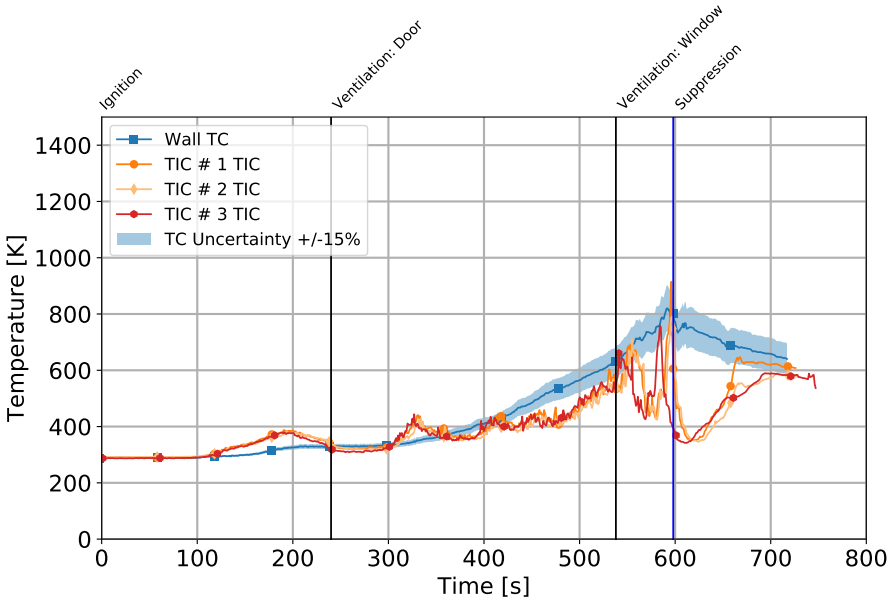

(a) Interior TIC vs. Wall TC

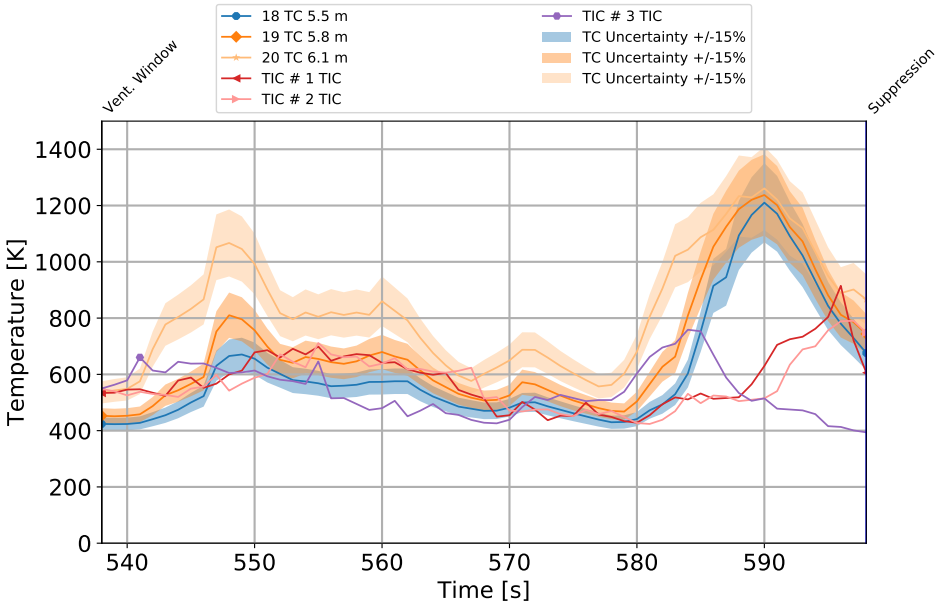

(b) Interior TIC vs. Gas TC

Figure D.17: Interior TIC spot temperature measurement results

D.3.3 Experiment no. 3

Item	Quantity	Initial Weight
Sofa #1	1	52.10 kg
Sofa #2	1	48.85 kg
Carpet	9.75 m^2	12.55 kg
Carpet Padding	9.75 m^2	8.40 kg
Plywood	9.75 m^2	76.60 kg

Table D.5: Room-Scale Fire Experiments: Experiment no. 3 Fuel Load

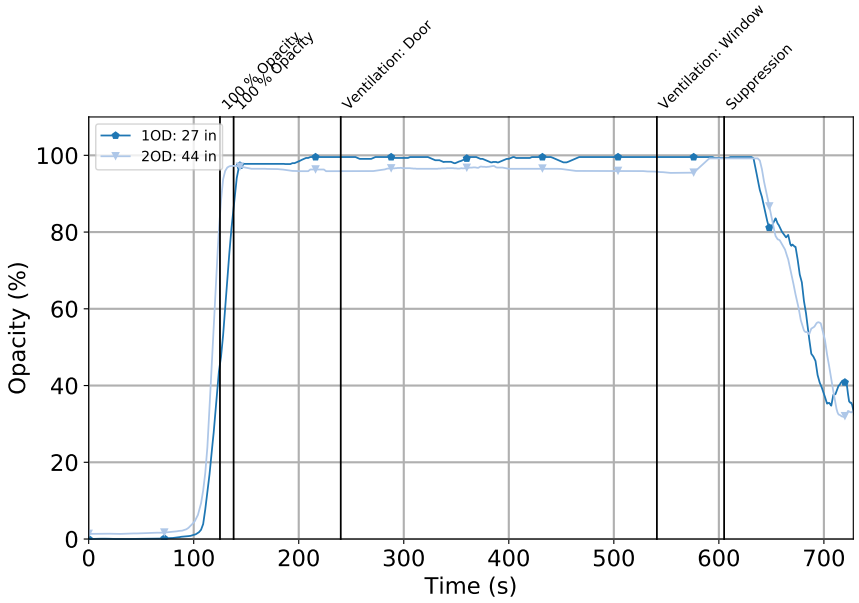

Figure D.18: Opacity during Experiment # 3.

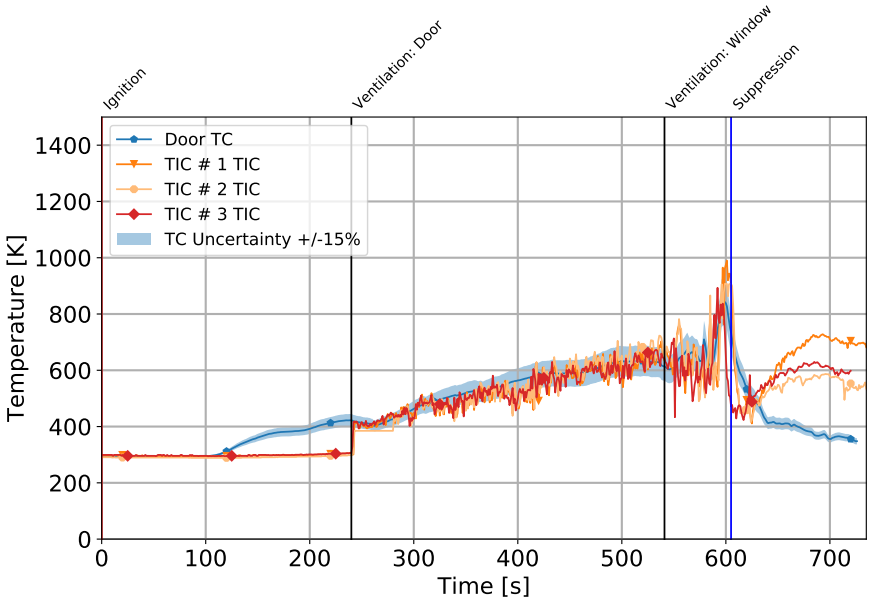

(a) Exterior TIC vs. Inconel TC

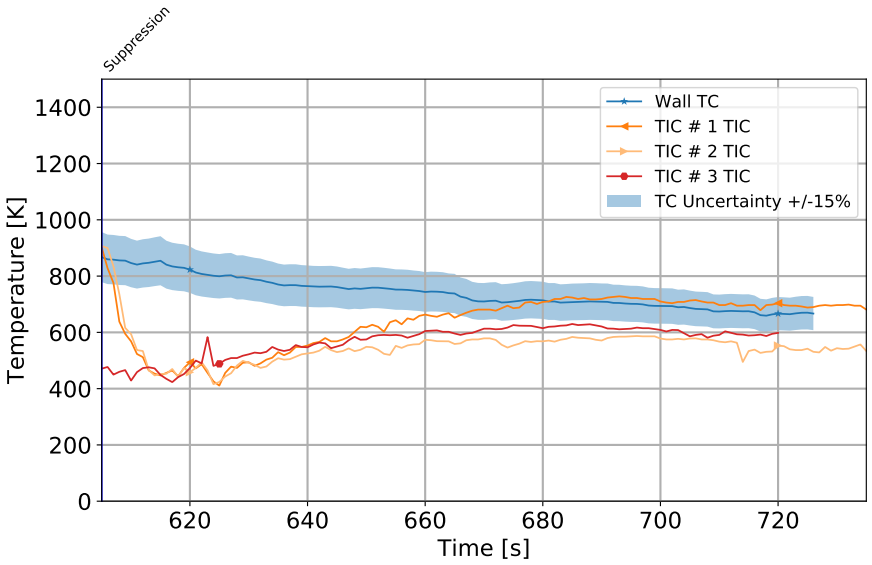

(b) Exterior TIC vs. Wall TC

Figure D.19: Exterior TIC spot temperature measurement results

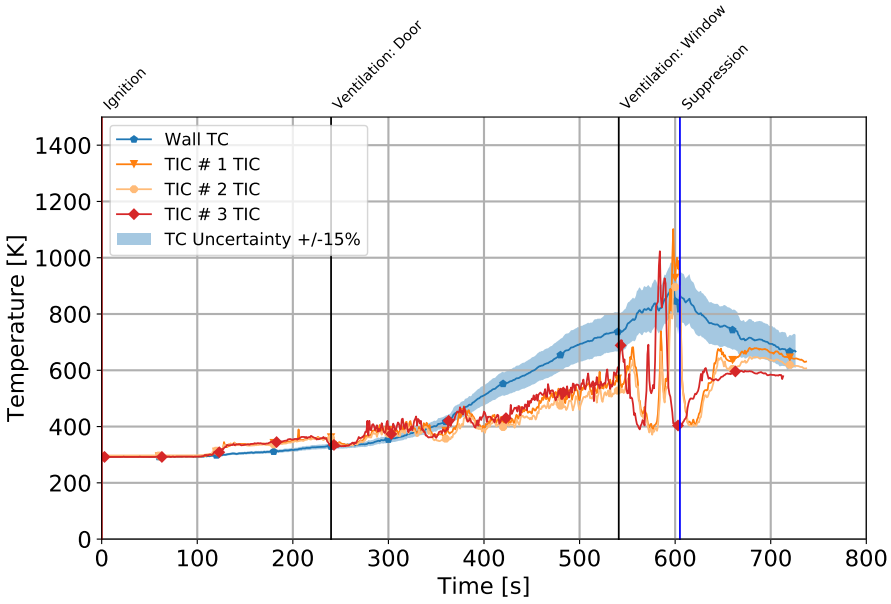

(a) Interior TIC vs. Wall TC

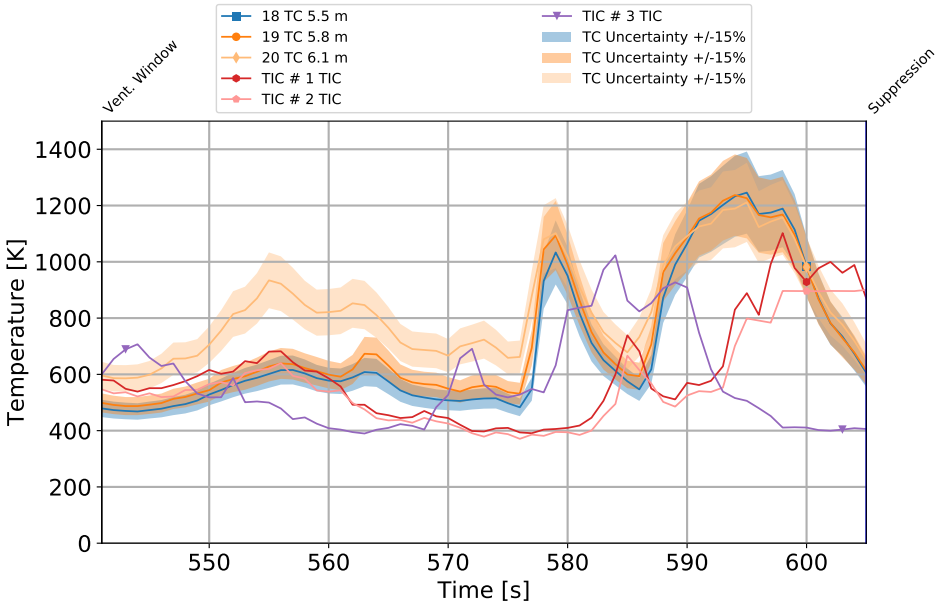

(b) Interior TIC vs. Gas TC

Figure D.20: Interior TIC spot temperature measurement results

D.3.4 Experiment no. 4

Item	Quantity	Initial Weight
Sofa #1	1	49.55 kg
Sofa #2	1	49.25 kg
Carpet	9.75 m^2	12.65 kg
Carpet Padding	9.75 m^2	8.35 kg
Plywood	9.75 m^2	76.55 kg

Table D.6: Room-Scale Fire Experiments: Experiment no. 4 Fuel Load

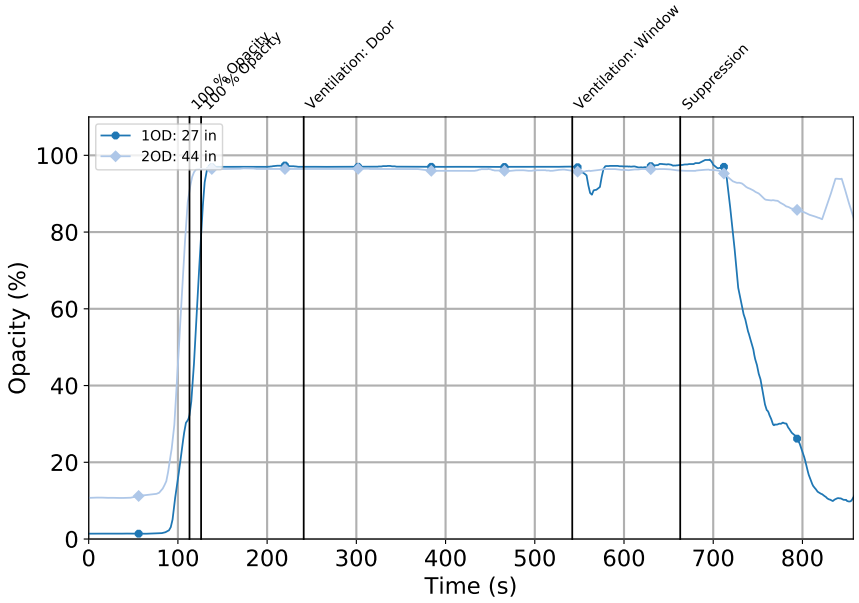

Figure D.21: Opacity during Experiment # 4.

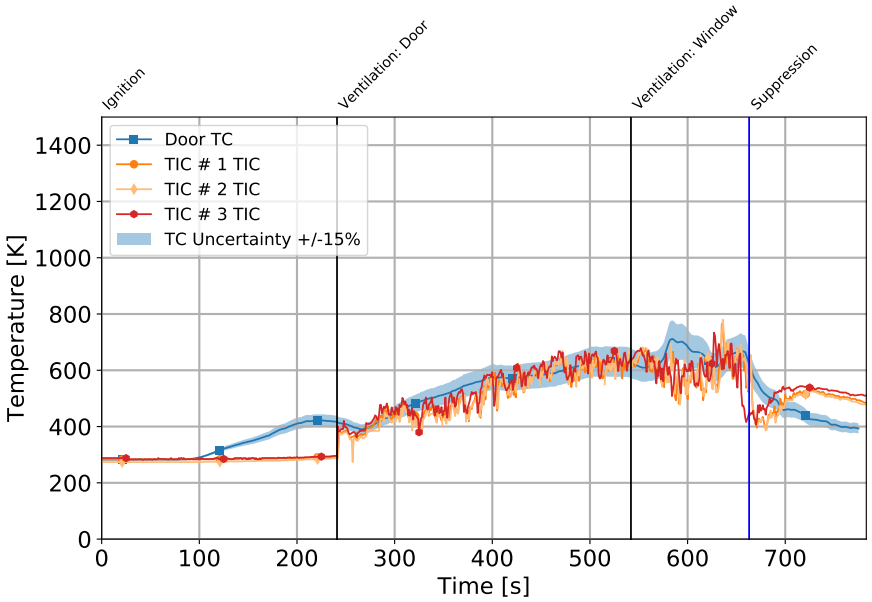

(a) Exterior TIC vs. Inconel TC

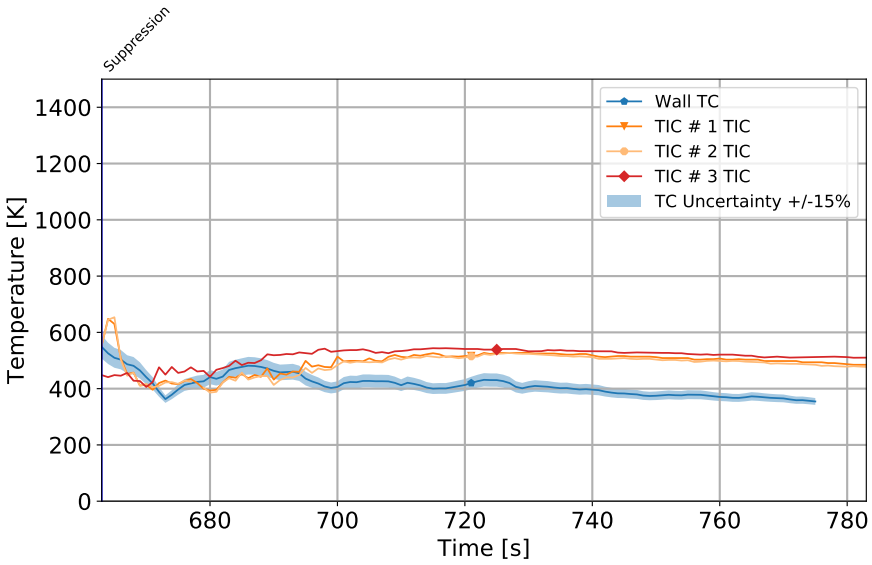

(b) Exterior TIC vs. Wall TC

Figure D.22: Exterior TIC spot temperature measurement results

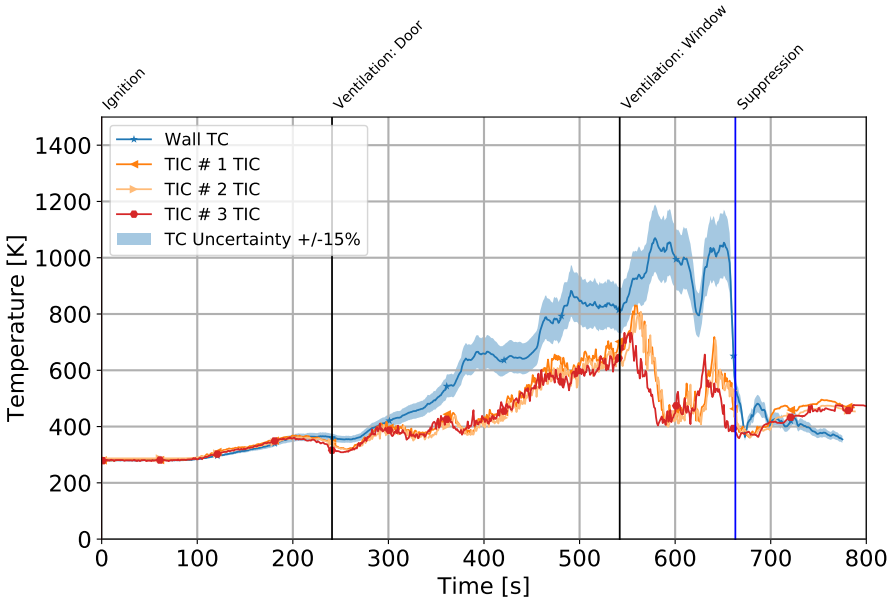

(a) Interior TIC vs. Wall TC

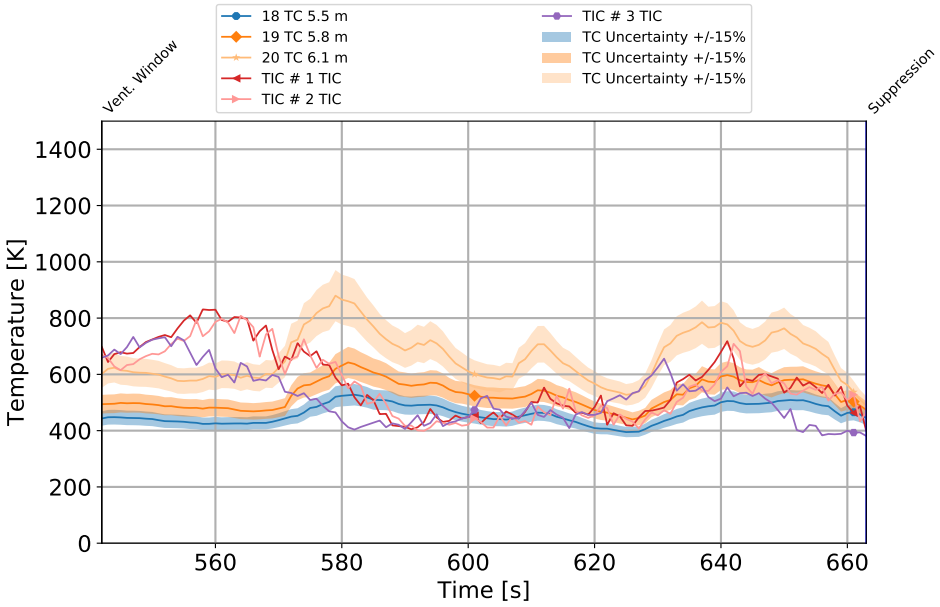

(b) Interior TIC vs. Gas TC

Figure D.23: Interior TIC spot temperature measurement results

Bibliography

[1] William herschel - biography. http://sci.esa.int/jump.cfm?oid=25805, May 2003.

[2] A. Szajewska. Development of the thermal imaging camera (tic) technology. *Procedia Engineering*, pages 1067–1072, December 2017.

[3] Paul W. Kruse and David D. Skatrud. *Uncooled Infrared Imaging Arrays and Systems*, volume 47. Academic Press, San Diego, CA, 1997.

[4] Greg Jakubowski. Thermal imaging cameras help firefighters see through smoke. *Fire Engineering*, 5, November 2010.

[5] AB Turenne. The thermal imaging camera (tic) and the fire service: Versatile use of the tic and its benefits to daily operations. *Fire Engineering*, November 2016.

[6] Six career fire fighters killed in cold-storage and warehouse building fire - massachusetts. Technical report, The National Institute for Occupational Safety and Health, October 2001.

[7] Career fire fighter dies from an out-of-air emergency in an apartment building fire - connecticut. Technical report, The National Institute for Occupational Safety and Health, January 2017.

[8] Two fire fighters die and two fire fighters are injured at multi-occupancy fire with structural collapse - missouri. Technical report, The National Institute for Occupational Safety and Health, July 2017.

[9] Two career fire fighters die in a rapid fire progression while searching for tenants - ohio. Technical report, The National Institute for Occupational Safety and Health, April 2015.

[10] Fire fighter falls through floor and dies at residential structure fire - ohio. Technical report, The National Institute for Occupational Safety and Health, July 2017.

[11] Matthew D. Samuels Mark S. Izydorek, Patrick A. Zeeveld and James P. Smyser. Structural stability of engineered lumber in fire conditions. Technical report, Northbrook, IL, September 2008.

[12] Joseph Willi Robin Zevotek, Keith Stakes. Impact of fire attack utilizing interior and exterior streams on firefighter safety and occupant survival: Full scale experiments. Technical report, UL Firefighter Safety Research Institute, Columbia, MD, December 2017.

[13] Kenneth W. Fent Bo Fernhall Densie L. Smith Gavin P. Horn, Steve Kerber. Interim report: Cardiovascular and chemical exposure risks in modern firefighting. Technical report, IFSI Research, UL FSRI, NIOSH, UIC, September 2015.

[14] AB Turenne. The thermal imaging camera (tic) and the fire service, part ii: Interior operations. *Fire Engineering*, December 2016.

[15] Carl Nix. Risks when using a thermal imaging camera. *Fire Apparatus*, 21, October 2016.

[16] National Fire Protection Association, Quincy, MA. *NFPA 1801, Standard on Thermal Imagers for the Fire Service, First Draft Report*, 2018.

[17] National Fire Protection Association, Quincy, MA. *NFPA 1801, Standard on Thermal Imagers for the Fire Service*, 2018.

[18] Nfpa 1408, standard for training fire service personnel in the operation, care, use, and maintenance of thermal imagers. Technical report, Quincy, MA, 2015.

[19] Andrew Lock Anthony Hamins Francine Amon, Nelson Bryner. Performance metrics for fire fighting thermal imaging cameras – small- and full-scale experiments. Technical report, National Institute for Standards and Technology, Gaithersburg, MD, July 2008.

[20] Andrew Lock Francine Amon. Evaluation of image quality of thermal imagers used by the fire service. Technical report, National Institute for Standards and Technology, February 2009.

[21] Justin Lawrence Rowe. The impact of thermal imaging camera display quality on fire fighter task performance, June 2009.

[22] Paul W. Kruse. *Uncooled Infrared Imaging Arrays, Systems, and Applications*. The International Society for Optical Engineering, Bellingham, WA, 2001.

[23] Jon Guerediaga Laura Vega Julio Molleda Ruben Usamentiaga, Pablo Venegas and Francisco G. Bulnes. Infrared thermography for temperature measurement and non-destructive testing. *Sensors (Basel)*, 14:12305–12348, July 2014.

[24] Avionics Department of the Naval Air Warfare Center Weapons Division. Electronic warfare and radar systems engineering handbook. https://web.archive.org/web/20010913091738/http://ewhdbks.mugu.navy.mil/EO-IR.htm, 2001.

[25] W. Minkina and D. Klecha. Atmospheric transmission coefficient modeling in the infrared for thermovision measurements. *Journal of Sensors and Sensor Systems*, pages 17–23, January 2016.

[26] Shirley P. Cani Robson da Silva Magalhaes Pablo Rodrigues Muniz, Ricardo de Araujo Kalid. Handy method to estimate uncertainty of temperature measurement by infrared thermography. *Optical Engineering*, page 7, July 2014.

[27] Avon Protection. Mi-tic s part of the argus range of thermal imaging cameras. https://www.argusdirect.com/cameras/argus-mi-tic-s-thermal-imager/, 2017.

[28] Bullard. T3x technical specifications. `https://www.bullard.com/uploads/bullard_downloads/TI_T3X_SALESSHEET_AM_EN_LOW_8544.pdf`, 2015.

[29] SAFETEK. Isg elite xr thermal imaging camera. http://www.firetrucks.ca/ProductDetails.asp?ProductCode=ISG-EliteXR, 2017.

[30] Daniel Ostrower. Optical thermal imaging - replacing microbolometer technology an achieving universal deployment. *The Advanced Semiconductor Magazine*, 19, August 2006.

[31] Guo-Gua Gu Ning Liu Xiu-Bao Sui, Qian Chen. Research on the response model of microbolometer. *Chinese Physics B*, 19, March 2010.

[32] Jianjun Lai-Yi Li Hongchen Wang, Xinjian Yi. Fabricating microbolometer array on unplanar readout integrated circuit. *International Journal of Infrared and Millimeter Waves*, 26:751–762, April 2005.

[33] Ray Pini Jermey Huddleston, Alan Symmons. Comparison of the thermal effects on lwir optical designs utilizing different infrared optical mateirals. *Infrared Technology and Applications XL*, 2014.

[34] Knight Optical Ltd. Germanium optical components. https://www.knightoptical.com/stock/optical-components/infrared-optics/germanium-optical-components/, 2014.

[35] Brian Clegg. Vanadium oxides. https://www.chemistryworld.com/podcasts/vanadium-oxides/8838.article, August 2015.

[36] J. Narayan and V.M. Bhosle. Phase transition and critical issues in structure-property correlations of vanadium oxide. *Journal of Applied Physics*, 100, 2006.

[37] Charles Hanson. Ir detectors: Amorphous-silicon bolometers could surpass ir focal-place technologies. April 2011.

[38] Bullard. The new buyer's guide to thermal imaging: Fire service edition. https://www.bullard.com/uploads/bullard_downloads/TI_BUYERSGUIDE_AM_EN_LOW_8560.pdf, 2016.

[39] Vytenis Babrauskas. *Ignition Handbook*. Fire Science Publishers, 2003.

[40] Bullard. Bullard t3x thermal imager user manual. https://www.bullard.com/uploads/bullard_downloads/TI_T3X_USERMANUAL_AM_ENESFR_LOW_60500410818.pdf, 2015.

[41] Avon Protection. Mi-tic user manual. https://www.rosenbauer.com/fileadmin/sharepoint/products/equipment/tics/docs/ARGUS_MI-TIC_user_manual_EN.pdf, May 2016.

[42] Adrian Rosebrock. Recognizing digits with opencv and python. https://www.pyimagesearch.com/2017/02/13/recognizing-digits-with-opencv-and-python/, February 2017.

[43] Adrian Rosebrock. How-to: Python compare two images. https://www.pyimagesearch.com/2014/09/15/python-compare-two-images/, September 2014.

[44] Matthias Lee Samuel Hoffstaetter, Juarex Bochi and Lars Kistner. Project description. https://pypi.org/project/pytesseract/, January 2018.

[45] GitHub. tesseract-ocr. https://github.com/tesseract-ocr/tesseract, 2018.

[46] R.D. Peacock-H.E. Mitler E.L. Johnson P.A. Reneke W.M. Pitts, E. Braun and L.G. Blevins. Temperature uncertainties for bare-bead and aspirated thermocouple measurements in fire environments. *ASTM Special Technical Publication*, 1427:3–15, 2003.

[47] Linda G. Blevins. Behavior of bare and aspirated thermocouples in compartment fires. pages 13–17, 1999.

[48] John Regan Joseph Willi, Keith Stakes and Robing Zevotek. Evaluation of ventilation-controlled fires in l-shaped training props. Technical report, UL Firefighter Safety Research Institute, Columbia, MD, 2019.

[49] Curt H. Liebert and Robert R. Hibbard. Special emittance of soot. Technical report, National Aeronautics and Space Administration, Washington, D.C., February 1970.

[50] Omega. Thermocouple sensors. https://www.omega.com/en-us/resources/thermocouples, August 2018.

[51] Residential Shipping Container Primer (RSCP). History of iso shipping containers. http://www.residentialshippingcontainerprimer.com/ISO2017.

[52] United States Steel Corporation. Benefits of cor ten azp prepainted steel sheet. https://www.ussteel.com/products-solutions/products/cor-ten-azp, 2019.

[53] Ashley Homestore. Darcy sofa. https://www.ashleyfurniturehomestore.com/p/darcy-sofa/7500038.html, 2018.

[54] Home Depot. Carpet sample - viking - color stingray loop 8 in. x 8 in. https://www.homedepot.com/p/TrafficMASTER-Carpet-Sample-Viking-Color-Stingray-Loop-8-in-x-8-in-SH-655633/301961845, 2018.

[55] Daniel Madrzykowski Craig Weinschenk and Paual Courtney. Impact of flashover fire conditions on exposed energized electrical cords and cables. Technical report, Columbia, MD, April 2019.

[56] Barry N. Taylor and Chris E. Kuyatt. Guidelines for evaluating and expressing the uncertainty of nist measurement results. Technical report, National Institute for Standards and Technology, Gaithersburg, MD, September 1994.

[57] NCD Risk Factor Collaboration. A century of trends in adult human height. *eLife*, July 2016.

[58] The Drawing Source. 7 figure drawing proportions to know. https://www.thedrawingsource.com/figure-drawing-proportions.html, 2019.

[59] P.F. Watson and A. Petrie. Method agreement analysis: A review of correct methodology. *Theriogenology*, 73:1167–1179, 2010.